
Appendices to the Approach for Estimating Exposures and Incremental Health Effects from Lead due to Renovation, Repair, and Painting Activities in Public and Commercial Buildings

July 28, 2014

blank
page

Contents

Appendix A. Exterior Analysis Input Variable Values	A-1
Appendix B. Interior Analysis Input Variable Values	B-1
Appendix C. Renovated Building Characteristics	C-1
Appendix D. Renovation Characteristics	D-1
Appendix E. Receptor Building Characteristics	E-1
Appendix F. Soil and Hard Surface Parameters	F-1
Appendix G. AERMOD Variables	G-1
Appendix H. Exterior Emission Rates	H-1
Appendix I. Interior Fraction Emitted	I-1
Appendix J. Dust Model for Exterior Analysis	J-1
Appendix K. Loading to Concentration Conversion	K-1
Appendix L. Estimates of Exposure Factors	L-1
Appendix M. Updates to the Leggett Model	M-1
Appendix N. Background Media Concentrations and Intakes	N-1
Appendix O. Population Biokinetic Variability	O-1
Appendix P. Concentration-Response Curves Supporting Information	P-1
Appendix Q. Approach to estimate universe of P&CBs	Q-1

blank
page

Acronyms and Abbreviations

Acronym / Abbreviation	Stands For
AERMOD	American Meteorological Society (AMS) and the U.S. Environmental Protection Agency (EPA) Regulatory Model Improvement Committee (AERMIC) Model
AIC	Akaike Information Criteria
ASHRAE	American Society of Heating, Refrigerating and Air Conditioning Engineers
BMD	Benchmark Dose
BMDL	Benchmark Dose Level
CBECs	Commercial Buildings Energy Consumption Survey
CBP	County Business Pattern
CBSA	Core Based Statistical Areas
CDC	Center for Disease Control
CDF	Cumulative Distribution Function
COF	Child Occupied Facility
CVDM	Cardiovascular Disease Mortality
DOE	Department of Energy (US Department of)
DOT	Department of Transportation (US Department of)
EFSS	Environmental Field Sampling Study
EPA	Environmental Protection Agency
GFR	Glomerular Filtration Rate
GSA	General Services Administration
GSD	Geometric Standard Deviation
GM	Geometric Mean
HEPA	High Efficiency Particulate Air
HUD	Housing and Urban Development (US Department of)
HVAC	Heating Ventilation and Air Conditioning
IEUBK	Integrated Exposure Uptake Biokinetic Model for lead
IQ	Intelligence Quotient. Also Full Scale Intelligent Quotient (FSIQ)
LBP	Lead Based Paint
LCL	Lower Confidence Level
LEV	Local Exhaust Ventilation
LRRP	Lead Renovation Repair and Painting
MSA	Metropolitan Statistical Areas

Acronym / Abbreviation	Stands For
MSE	Mean Squared Error
NEXHAS	National Human Exposure Assessment Survey
NHANES	National Health and Nutrition Examination Survey
NLCD	National Land Cover Database
NIST	National Institute of Standards and Technology
P&CBs	public and commercial buildings
QCLCD	Quality Controlled Local Climatological Data
PbB	blood lead
RECS	Residential Energy Consumption Survey
SAB	Science Advisory Board
SAMSON	Solar and Meteorological Surface Observational Network
SD	Standard Deviation
SE	Standard Error
UCL	Upper Confidence Level
USGS	United States Geological Survey
VF	Ventilation Factor
TSCA	Toxic Substances Control Act
XRF	X-Ray Fluorescence

blank
page

Appendix A. Exterior Analysis Input Variable Values

Appendix A presents a summary of all inputs used by the exterior Monte Carlo model. All inputs, their values, and the methodology used to calculate the inputs are discussed in detail in the remainder of the Appendices. Table A-1 presents the inputs that are used to define a scenario, while Table A-3 presents the variables used in the Monte Carlo model. The “input 1” and “input 2” columns in Table A-3 correspond to different types of values depending on the distribution type, as shown in Table A-2. For example, input 1 and input 2 are the “mean” and “standard deviation” for a normal distribution and are the “geometric mean” and “geometric standard deviation (GSD)” for lognormal variables. For variables that use a discrete distribution in the Monte Carlo model or that vary by building type, the values and probabilities used are shown in the tables in the remainder of Appendix A.

Table A-1. Scenario-specific inputs.

Input	Input name	Available Inputs	Units
Renovation Activity	RenoScenario	Dry scraping, Wet Scraping, Power sanding without HEPA, Power sanding with HEPA, Heat gun, Needle gun without HEPA, Needle gun with HEPA, Window/door replacement, Trim replacement, Torching, Demolition	n/a
Distance from Renovation	RenoDistance	5, 50, 150, 300, 650, and 800	ft
Size of Renovation	RenoClass	F1T1, F1T2, F1T3, F2T1, F2T2, F2T3, F3T1, F3T2, F3T3	n/a
Vintage of Renovation	RenoVintage	Pre-1930, 1930-1949, 1950-1959, 1960-1979	n/a
Horizontal Containment	HorPlasticOnOff	Present or not present	n/a
Vertical Containment	VertPlasticOnOff	Present or not present	n/a
Receptor Building Types	RecType	Residence, Industrial building, Agricultural building, Public/Commercial building, or School.	n/a
Age Groups	Age	0-10 , 18-49, 50-80	n/a

Table A-2. Key to Definition of “Input 1” and “Input 2” in Table A-3 for Different Distribution Types.

Distribution Type	Input 1	Input 2
Point estimate	Value	N/A
Uniform	Lower Limit	Upper Limit
Normal	Mean	Standard Deviation
Lognormal	Geometric Mean	Geometric Standard Deviation
Discrete	Reference to Table where Values and Probabilities are Presented	N/A

Table A-3. Exterior Analysis Monte Carlo Inputs.

Module	Distribution Type	Parameter	Units	Input 1 (Mean, GM, Point Estimate or Table with Values)	Input 2 (SD, GSD, or N/A)	Upper Bound	Lower Bound	Appendix Describing Input
Reno Bldg	Point	GlassFrac	None	Table A-4	NA	N/A	N/A	Appendix C.1.3
Reno Bldg	Point	NonGlassArea	ft ²	Table A-4	NA	N/A	N/A	Appendix C.1.3
Reno Bldg	Point	WindowDoorArea	ft ²	Table A-4	NA	N/A	N/A	Appendix C.1.4
Reno Bldg	Point	TrimArea	ft ²	Table A-4	NA	N/A	N/A	Appendix C.1.4
Reno Bldg	Point	ContainmentArea	ft ²	Table A-4	NA	N/A	N/A	Appendix C.1.5
Reno Bldg	Lognormal	WallLoadingp1930 (XRF)	g/cm ²	0.00607	2.90	0.0509	0.00072	Appendix C.1.7
Reno Bldg	Lognormal	WallLoading19301949 (XRF)	g/cm ²	0.00377	2.38	0.0214	0.00067	Appendix C.1.7
Reno Bldg	Lognormal	WallLoading19501959 (XRF)	g/cm ²	0.00253	2.30	0.0134	0.00048	Appendix C.1.7
Reno Bldg	Lognormal	WallLoading19601979 (XRF)	g/cm ²	0.00335	2.34	0.0183	0.00061	Appendix C.1.7
Reno	Point	RenoRate	Days	Table A-4	NA	N/A	N/A	Appendix D.1.1
Reno	Point	RenovationDuration	Days	Table A-4	NA	N/A	N/A	Appendix D.1.2
Reno	Point	FracPaintRemoved	None	Table A-5	NA	N/A	N/A	Appendix D.1.2
Reno	Point	FractionAerosolized	None	Table A-5	NA	N/A	N/A	Appendix D.1.4, Appendix A
Reno	Point	FractionBulk	None	Table A-5	NA	N/A	N/A	Appendix D.1.5
Reno	Point	H_Plastic_Eff	None	0.95	NA	N/A	N/A	Appendix D.1.6
Reno	Point	V_Plastic_Eff	None	0.91	NA	N/A	N/A	Appendix D.1.6
Receptor	Discrete	ReceptorVintageResidential	None	Table A-6	NA	N/A	N/A	Appendix E.3
Receptor	Discrete	ReceptorVintageAgricultural	None	Table A-6	NA	N/A	N/A	Appendix E.3
Receptor	Discrete	ReceptorVintageIndustrial	None	Table A-6	NA	N/A	N/A	Appendix E.3
Receptor	Discrete	ReceptorVintageCommercial	None	Table A-6	NA	N/A	N/A	Appendix E.3
Receptor	Discrete	ReceptorVintageSchool	None	Table A-6	NA	N/A	N/A	Appendix E.3

Appendices to the Approach for Estimating Exposures and Incremental Health Effects from Lead due to Renovation, Repair, and Painting Activities in Public and Commercial Buildings

Module	Distribution Type	Parameter	Units	Input 1 (Mean, GM, Point Estimate or Table with Values)	Input 2 (SD, GSD, or N/A)	Upper Bound	Lower Bound	Appendix Describing Input
Receptor	Discrete	ReceptorHtResidential	None	Table A-6	NA	N/A	N/A	Appendix E.4
Receptor	Discrete	ReceptorHtAgricultural	None	Table A-6	NA	N/A	N/A	Appendix E.4
Receptor	Discrete	ReceptorHtIndustrial	None	Table A-6	NA	N/A	N/A	Appendix E.4
Receptor	Discrete	ReceptorHtCommercial	None	Table A-6	NA	N/A	N/A	Appendix E.4
Receptor	Discrete	ReceptorHtSchool	None	Table A-6	NA	N/A	N/A	Appendix E.4
Receptor	Discrete	CeilingHeightResidential	M	Table A-6	NA	N/A	N/A	Appendix E.4
Receptor	Discrete	CeilingHeightAgricultural	M	Table A-6	NA	N/A	N/A	Appendix E.4
Receptor	Discrete	CeilingHeightIndustrial	M	Table A-6	NA	N/A	N/A	Appendix E.4
Receptor	Discrete	CeilingHeightCommercial	M	Table A-6	NA	N/A	N/A	Appendix E.4
Receptor	Discrete	CeilingHeightSchool	M	Table A-6	NA	N/A	N/A	Appendix E.4
Receptor	Lognormal	HouseVolumeResidential	m ³	390.5	2.06	1664.8	91.6	Appendix E.5
Receptor	Lognormal	BldgVolumeAgricultural	m ³	5227	3.14	51459	531	Appendix E.5
Receptor	Lognormal	BldgVolumeIndustrial	m ³	5227	3.14	51459	531	Appendix E.5
Receptor	Lognormal	BldgVolumeCommercial	m ³	1371	3.00	12372	152	Appendix E.5
Receptor	Lognormal	BldgVolumeSchool	m ³	2794	4.20	49206	159	Appendix E.5
Receptor	Normal	AirExchangeRateResidential	hr ⁻¹	0.63	0.65	1.93	0.001	Appendix E.6
Receptor	Normal	AirExchangeRateAgricultural	hr ⁻¹	1.5	0.87	3.24	0.001	Appendix E.6
Receptor	Normal	AirExchangeRateIndustrial	hr ⁻¹	1.5	0.87	3.24	0.001	Appendix E.6
Receptor	Normal	AirExchangeRateCommercial	hr ⁻¹	1.5	0.87	3.24	0.001	Appendix E.6
Receptor	Normal	AirExchangeRateSchool	hr ⁻¹	1.5	0.87	3.24	0.001	Appendix E.6
Receptor	Point	DustModelPenetration	None	1	NA	N/A	N/A	Appendix E.7
Receptor	Point	DustModelResuspension	hr ⁻¹	0.00014	NA	N/A	N/A	Appendix E.9
Receptor	Point	DustModelDeposition	hr ⁻¹	0.65	NA	N/A	N/A	Appendix E.8

Appendices to the Approach for Estimating Exposures and Incremental Health Effects from Lead due to Renovation, Repair, and Painting Activities in Public and Commercial Buildings

Module	Distribution Type	Parameter	Units	Input 1 (Mean, GM, Point Estimate or Table with Values)	Input 2 (SD, GSD, or N/A)	Upper Bound	Lower Bound	Appendix Describing Input
Receptor	Lognormal	PartTrackRateResidential	g/day	0.61	2.52	3.85	0.096	Appendix E.10
Receptor	Lognormal	PartTrackRateAgricultural	g/day	1.79	2.52	11.254	0.279	Appendix E.10
Receptor	Lognormal	PartTrackRateIndustrial	g/day	1.79	2.52	11.254	0.279	Appendix E.10
Receptor	Lognormal	PartTrackRateCommercial	g/day	62.0	2.52	390.5	9.7	Appendix E.10
Receptor	Lognormal	PartTrackRateSchool	g/day	29.9	2.52	188.4	4.7	Appendix E.10
Receptor	Discrete	MatFrac	None	0.13 or 0	NA	N/A	N/A	Appendix E.
Receptor	Discrete	PctCarpetResidential	None	Table A-7	NA	N/A	N/A	Appendix E.12
Receptor	Discrete	PctCarpetAgricultural	None	Table A-7	NA	N/A	N/A	Appendix E.12
Receptor	Discrete	PctCarpetIndustrial	None	Table A-7	NA	N/A	N/A	Appendix E.12
Receptor	Discrete	PctCarpetCommercial	None	Table A-7	NA	N/A	N/A	Appendix E.12
Receptor	Discrete	PctCarpetSchool	None		NA	N/A	N/A	Appendix E.12

Appendices to the Approach for Estimating Exposures and Incremental Health Effects from Lead due to Renovation, Repair, and Painting Activities in Public and Commercial Buildings

Module	Distribution Type	Parameter	Units	Input 1 (Mean, GM, Point Estimate or Table with Values)	Input 2 (SD, GSD, or N/A)	Upper Bound	Lower Bound	Appendix Describing Input
				Table A-7				
Receptor	Discrete	CleanFreqResidential	None	Table A-7	NA	N/A	N/A	Appendix E.13
Receptor	Discrete	CleanFreqAgricultural	None	Table A-7	NA	N/A	N/A	Appendix E.13
Receptor	Discrete	CleanFreqIndustrial	None	Table A-7	NA	N/A	N/A	Appendix E.13
Receptor	Discrete	CleanFreqCommercial	None	Table A-7	NA	N/A	N/A	Appendix E.13
Receptor	Discrete	CleanFreqSchool	None	Table A-7	NA	N/A	N/A	Appendix E.13
Receptor	Point	FloorCleanSlope	None	0.113	NA	N/A	N/A	Appendix E.14

Appendices to the Approach for Estimating Exposures and Incremental Health Effects from Lead due to Renovation, Repair, and Painting Activities in Public and Commercial Buildings

Module	Distribution Type	Parameter	Units	Input 1 (Mean, GM, Point Estimate or Table with Values)	Input 2 (SD, GSD, or N/A)	Upper Bound	Lower Bound	Appendix Describing Input
Receptor	Point	FloorCleanInt	None	-0.5546	NA	N/A	N/A	Appendix E.14
Receptor	Point	CarpetCleanSlope	None	-0.4296	NA	N/A	N/A	Appendix E.14
Receptor	Point	CarpetCleanInt	None	0.6584	NA	N/A	N/A	Appendix E.14
Receptor	Point	FloorCleanEffMin	None	0.06	NA	N/A	N/A	Appendix E.14
Receptor	Point	CarpetCleanEffMin	None	0.15	NA	N/A	N/A	Appendix E.14
Soil	Point	RainFreq	Days	Table A-8	NA	N/A	N/A	Appendix F.1
Soil	Point	TrackInRainEffHardSurface	None	0.5	NA	N/A	N/A	Appendix F.2
Soil	Point	TrackInRainEffSoil	None	0	NA	N/A	N/A	Appendix F.2
Soil	Point	SoilDensity	g/m ³	2600000	NA	N/A	N/A	Appendix F.3
Soil	Point	TrackInDepthHardSurface	mm	1	NA	N/A	N/A	Appendix F.4
Soil	Point	TrackInDepthSoil	cm	1.5	NA	N/A	N/A	Appendix F.4
Soil	Point	TrackInPorosityHardSurface	None	0.2	NA	N/A	N/A	Appendix F.5
Soil	Point	TrackInPorositySoil	None	0.2	NA	N/A	N/A	Appendix F.5
Air	Discrete	MetRegion	None	Table A-8	NA	N/A	N/A	Appendix G.1
Air	Point	ParticleSize	µm	Table A-9	NA	N/A	N/A	Appendix G.3
Air	Point	ParticleDensity	g/cm ³	2	NA	N/A	N/A	Appendix G.3
Air	Equation	ObstructAdjust	None	Table A-10	NA	N/A	N/A	Appendix G.5
Load Conc	Point	LoadingConcenMean	None	0.881	NA	N/A	N/A	Appendix K.
Load Conc	Point	LoadingConcenSlope	None	0.421	NA	N/A	N/A	0
Load Conc	Point	LoadingConcenInt	None	5.145	NA	N/A	N/A	Appendix K.
Load Conc	Point	LoadingConcenDF	None	1643	NA	N/A	N/A	0
Load Conc	Point	LoadingConcenErrorVar	None	0.544	NA	N/A	N/A	Appendix K.
Load Conc	Point	LoadingConcenIntSE	None	0.0182	NA	N/A	N/A	Appendix K.

Appendices to the Approach for Estimating Exposures and Incremental Health Effects from Lead due to Renovation, Repair, and Painting Activities in Public and Commercial Buildings

Module	Distribution Type	Parameter	Units	Input 1 (Mean, GM, Point Estimate or Table with Values)	Input 2 (SD, GSD, or N/A)	Upper Bound	Lower Bound	Appendix Describing Input
Load Conc	Point	LoadingConcenSlopeSE	None	0.0094	NA	N/A	N/A	Appendix K.
Load Conc	Point	LoadingConcenT	None	1.961	NA	N/A	N/A	Appendix K.
Activity	Discrete	TimeSpentValues	None	Table A-11	NA	N/A	N/A	Appendix L.1
Activity	Uniform	TimeSinceLastReno	Years	0	4.2	N/A	N/A	Appendix L.1
Activity	Discrete	AgeProb	None	Table A-12	NA	N/A	N/A	Appendix L.1
Activity	Point	MaternalPbB	µg/dL	0.747	NA	N/A	N/A	Appendix O
Bckground	Lognormal	BgAirConc	µg/m ³	0.02	5.52	0.61	0.0007	Appendix N.1
Bckground	Point	BgSoilConcIndustrial	µg/g	197.3	NA	N/A	N/A	Appendix N.1
Bckground	Point	BgSoilConcCommercial	µg/g	49.97	NA	N/A	N/A	Appendix N.1
Bckground	Lognormal	BgSoilConcResidentialp1930	µg/g	367.4	3.53	4569.8	29.5	Appendix N.1
Bckground	Lognormal	BgSoilConcResidential19301949	µg/g	144.1	3.69	1958.3	10.6	Appendix N.1
Bckground	Lognormal	BgSoilConcResidential19501959	µg/g	79.6	3.77	1131.3	5.6	Appendix N.1
Bckground	Lognormal	BgSoilConcResidential19601979	µg/g	24.2	3.29	261.4	2.2	Appendix N.1
Bckground	Lognormal	BgSoilConcResidentialp1979	µg/g	15.8	2.32	85.3	2.9	Appendix N.1
Bckground	Lognormal	BgSoilConcAgricultural	µg/g	17.1	1.75	52.4	5.6	Appendix N.1
Bckground	Lognormal	BgSoilConcSchool	µg/g	28.0	3.00	252	3.1	Appendix N.1
Bckground	Lognormal	BgDustLoadResidentialp1930	µg/ft ²	3.97	4.76	89.81	0.18	Appendix N.1
Bckground	Lognormal	BgDustLoadResidential19301949	µg/ft ²	1.94	7.76	116.80	0.03	Appendix N.1
Bckground	Lognormal	BgDustLoadResidential19501959	µg/ft ²	1.14	2.65	7.97	0.16	Appendix N.1
Bckground	Lognormal	BgDustLoadResidential19601979	µg/ft ²	0.79	4.25	14.27	0.04	Appendix N.1
Bckground	Lognormal	BgDustLoadResidentialp1979	µg/ft ²	0.49	3.38	5.55	0.04	Appendix N.1
Bckground	Lognormal	BgDustLoadNonResidential	µg/ft ²	0.80	2.25	5.00	0.13	Appendix N.1

Appendices to the Approach for Estimating Exposures and Incremental Health Effects from Lead due to Renovation, Repair, and Painting Activities in Public and Commercial Buildings

Module	Distribution Type	Parameter	Units	Input 1 (Mean, GM, Point Estimate or Table with Values)	Input 2 (SD, GSD, or N/A)	Upper Bound	Lower Bound	Appendix Describing Input
Bckground	Discrete	Leggett_Background_Intakes	µg/day	Appendix N.1	NA	N/A	N/A	Appendix N.1
Bckground	Discrete	Leggett_Background_PbB	µg/dL	Appendix N.1	NA	N/A	N/A	Appendix N.1
Blood Lead	Point	Exposure Factors for Intake	various	Appendix L.4	NA	N/A	N/A	Appendix L4
Blood Lead	Point	PbB_GSD	None	1.9	NA	N/A	N/A	Appendix O

Table A-4. Characteristics of the Renovated Building Size.

Building ID ¹	Fraction of Surface Area that is Glass ²	Component Surface Areas			Renovation Durations		Containment Area
		Non-glass building surface area (ft ²) ²	Window & door surface area (ft ²) ³	Trim surface area (ft ²) ³	Duration, replace windows and doors (days) ⁴	Duration, other activities (days) ⁴	Area inside containment (ft ²) ⁵
F1T1	0.12	1,266	171	155	2	0.5	1,840
F1T2	0.13	2,502	354	321	4	1	3,280
F1T3	0.14	4,972	621	633	8	2	6,160
F2T1	0.15	2,439	280	323	4	1	1,840
F2T2	0.18	4,726	623	701	7	2	3,280
F2T3	0.18	9,451	1,146	1,381	12	4	6,160
F3T1	0.14	3,706	351	457	6	1.5	1,840
F3T2	0.17	7,177	799	1,000	12	3	3,280
F3T3	0.26	19,198	3,053	3,776	36	9	9,040

¹Building sizes were calculated from CBECS data (US EIA, 2003),

²Glass surface area was calculated from CBECS micro-data (USE EIA, 2003)

³Window, door, and trim areas were calculated using methodology provided by EPA

⁴Durations were calculated using rate of removal from RSMears (Mossman and Plotner, 2009) and (Capouch, 2011)

⁵Containment area does not include the area of the renovation building itself.

Table A-5. Activity-specific fraction of paint removed, aerosolized, and remaining as bulk.

Renovation Activity	Fraction of Paint Removed (<i>FracRem</i>)	Fraction of Paint Aerosolized (<i>AerosolFrac</i>) ¹	Fraction of Paint Emitted as Bulk Particulate (<i>PartDebFrac</i>) ²
Power Sanding	0.15	0.248	0.051
Needle Gun	0.15	0.244	0.055
Torching	0.15	0.180	0.056
High Heat Gun	0.15	0.081	0.056
Low Heat Gun	0.15	0.077	0.059
Dry Scrape	0.15	0.070	0.060
Window/Door Replacement	0.15	0.069	0.060
Trim Replacement	0.15	0.070	0.060
Demolition	1.0	0.009	0.060

¹US EPA, 2007a and Farfel *et al.*, 2003

²Lee and Domanski, 1999

³Choe *et al.*, 2000

Table A-6. Receptor Building Characteristics with Probabilities or Distributions

Receptor Type	AERMO D Type	Cumulative Probabilities for Vintage					Cumulative Probabilities for Height (stories)			Ceil. Ht. (m)	Building Volume (m ³)	
		Pre-1930	1930 to 1949	1950 to 1959	1960 to 1979	Post to 1979	1	2	3		GM	GSD
Agricultural	Rural	0.07	0.12	0.18	0.41	1.00	1	0	0	8.53	5227	1.94
Industrial	Urban	0.07	0.12	0.18	0.41	1.00	1	0	0	8.53	5227	1.94
Commercial / Government	Urban	0.13	0.22	0.31	0.61	1.00	0.64	0.89	1.00	2.74	1371	2.25
Schools	Urban	0.05	0.14	0.30	0.61	1.00	0.73	0.88	1.00	3.35	2794	1.86
Residences	Urban	0.10	0.17	0.29	0.57	1.00	0.58	0.89	1.00	2.44	391	2.06

Table A-7. Receptor Cleaning Frequency, Carpet, Air Exchange Rate, and Track-in Rate with Probabilities or Distributions

Receptor Type	Cumulative Probabilities for Cleaning Frequency					Cumulative Probabilities for Percent Carpet		AER (hr ⁻¹)		Particulate Tracking Rate (g/day)	
	Every working day (5 days/week)	Every third day	Every week (1 day/week)	Every other week (1 day/2 weeks)	Every fourth week (1 day/4 weeks)	All Carpet	All Floor	Mean	SD	Mean	SD
Agricultural	0.1	0.3	0.7	0.9	1.0	0.08	1.0	1.5	0.87	1.77	2.52
Industrial	0.2	0.6	0.8	0.9	1.0	0.08	1.0	1.5	0.87	1.77	2.52
Commercial/Government	0.2	0.6	0.8	0.9	1.0	0.45	1.0	1.5	0.87	61.49	2.52
Schools	0.4	0.6	0.8	0.9	1.0	0.27	1.0	1.5	0.87	29.67	2.52
Residences	0.1	0.3	0.7	0.9	1.0	0.52	1.0	0.63	0.65	0.61	2.52

Table A-8. Meteorological Characteristics

Model Index	Region	Region Name	Inland or Coastal	Location (Surface Station)	Location (Upper-air Station)	Cumulative Probability Based on Population in Each Region	Number of days between rain events (days)
M1	1	East North Central	Inland	Iowa City IA	Davenport IA	0.08	9
M2	2	Northeast	Inland	Pittsburgh PA	Township PA	0.18	7
M3			Coastal	Camp Springs MD	Sterling VA	0.28	7
M4	3	Northwest	Inland	Idaho Falls ID	Riverton WY	0.3	8
M5			Coastal	Everett WA	Salem OR	0.32	8
M6	4	South	Inland	Topeka KS	Topeka KS	0.39	13
M7			Coastal	Lake Charles LA	Lake Charles LA	0.46	13
M8	5	Southeast	Inland	Atlanta GA	Peachtree City GA	0.55	7
M9			Coastal	New River NC	Morehead City NC	0.64	7
M10	6	Southwest	Inland	Grand Junction CO	Denver CO	0.69	16
M11	7	West	Inland	Las Vegas NV	Flagstaff AZ	0.755	22
M12			Coastal	Point Mugu CA	Vandenberg AFB CA	0.82	22
M13	8	West North Central	Inland	Sioux Falls SD	Omaha NE	0.84	14
M14	9	Central	Inland	Rockford IL	Davenport IA	1	7

Table A-9. Particle Size Distribution Used in AERMOD Modeling.

Size Class	Cumulative Probability in Size Class
< 2.5 μm	0.02
2.5 – 10 μm	0.74
10 – 20 μm	1

Table A-10. Summary statistics for the custom distribution for the obstruction adjustment.

	Minimum	5 th Percentile	Mean	95 th Percentile	Maximum
Adjustment factor	0.10	0.70	1	1.32	5.3

Table A-11. Cumulative Distributions for Time Spent (Fraction of the Week) in Different Building Types for Each Age Range.

Building Type	Cumulative Probability	Age Range			
		0-<5	5-<17	18-<49	50-80
Residence	0.05	0.58	0.52	0.41	0.46
	0.10	0.65	0.57	0.47	0.52
	0.25	0.79	0.66	0.55	0.61
	0.52	0.90	0.79	0.68	0.81
	0.75	0.98	0.92	0.86	0.94
	0.90	1.00	0.99	0.96	1.00
	0.95	1.00	1.00	1.00	1.00
	1	1.00	1.00	1.00	1.00
Agricultural	0.05	0.01	0.02	0.01	0.01
	0.10	0.01	0.02	0.01	0.02
	0.25	0.02	0.04	0.04	0.03
	0.52	0.05	0.07	0.13	0.10
	0.75	0.08	0.14	0.36	0.20
	0.90	0.10	0.18	0.49	0.34
	0.95	0.13	0.19	0.54	0.36
	1	0.13	0.31	0.67	0.65

Building Type	Cumulative Probability	Age Range			
		0-<5	5-<17	18-<49	50-80
Industrial	0.05	0.01	0.01	0.01	0.01
	0.10	0.01	0.01	0.02	0.02
	0.25	0.01	0.01	0.17	0.14
	0.52	0.01	0.03	0.34	0.34
	0.75	0.02	0.14	0.38	0.38
	0.90	0.02	0.19	0.44	0.42
	0.95	0.02	0.33	0.47	0.46
	1	0.02	0.33	0.53	0.57
Commercial/ Government	0.05	0.01	0.01	0.01	0.02
	0.10	0.01	0.01	0.03	0.03
	0.25	0.03	0.04	0.07	0.06
	0.52	0.06	0.08	0.19	0.14
	0.75	0.10	0.14	0.36	0.31
	0.90	0.16	0.22	0.43	0.40
	0.95	0.20	0.27	0.47	0.44
	1	0.33	0.43	0.60	0.55
School	0.05	0.03	0.08	0.01	0.01
	0.10	0.07	0.13	0.00	0.01
	0.25	0.14	0.22	0.03	0.04
	0.52	0.24	0.27	0.11	0.09
	0.75	0.35	0.30	0.27	0.28
	0.90	0.40	0.34	0.34	0.35
	0.95	0.41	0.38	0.38	0.38
	1	0.46	0.44	0.51	0.44

Table A-12. Cumulative Probabilities for Each Age Range

Age 0-10		Age 18-<50		Age 50-80	
Age	Cumulative Probability	Age	Cumulative Probability	Age	Cumulative Probability
0	0.08	18	0.03	50	0.053
1	0.17	19	0.07	51	0.101
2	0.26	20	0.10	52	0.150
3	0.35	21	0.14	53	0.198
4	0.45	22	0.17	54	0.245
5	0.54	23	0.20	55	0.293
6	0.63	24	0.23	56	0.338
7	0.72	25	0.26	57	0.381
8	0.81	26	0.29	58	0.424
9	0.91	27	0.32	59	0.464
10	1.00	28	0.35	60	0.507
		29	0.38	61	0.545
		30	0.42	62	0.583
		31	0.45	63	0.622
		32	0.48	64	0.657
		33	0.51	65	0.690
		34	0.53	66	0.719
		35	0.56	67	0.747
		36	0.59	68	0.774
		37	0.62	69	0.800
		38	0.65	70	0.824
		39	0.68	71	0.846
		40	0.72	72	0.867
		41	0.75	73	0.887
		42	0.78	74	0.906
		43	0.81	75	0.924
		44	0.84	76	0.941
		45	0.87	77	0.956
		46	0.90	78	0.971
		47	0.93	79	0.986
		48	0.97	80	1.000
		49	1.00		

A.1. References for Appendix A

Capouch S. (2011). Personal Communication by email between Heidi Hubbard of ICF International and Scott Capouch, Construction Project Manager and Professional Engineer with 10 years of experience, of US NIEHS. Title of email: Lead Paint Removal – estimating info. February 2, 2011.

Choe K; Trunov M; Grinshpun S; Willeke K; Harney J; Trakumas S; Mainelis G; Bornschein R; Clark S; Friedman W. (2000). Particle settling after lead-based paint abatement work and clearance waiting period. *American Industrial Hygiene Association Journal* 61: 798-807.

Farfel M; Orlova A; Lees P; Rohde C; Ashley P; Chisolm J. (2003). A study of urban housing demolitions as sources of lead in ambient dust: demolition practices and exterior dust fall. *Environmental Health Perspectives* 111(1128-1234).

Lee and Domanski. (1999). Development of pollutant release estimates due to abrasive blasting for lead paint removal from New York City department of transportation steel bridges, Pittsburg, PA, Air and Waste Management Association.

Mossman M; Plotner S; Babbitt C; Baker T; Balboni B, Eds. (2009). *RSMMeans Facilities Construction Cost Data*.

US Energy Information Administration. (2003) Commercial Building Energy Consumption Survey (CBECS). Available online at:
http://www.eia.gov/emeu/cbecs/cbecs2003/public_use_2003/cbecs_pudata2003.html

US EPA. (2007a). Draft final report on characterization of dust lead levels after renovation, repair, and painting activities. Prepared for EPA's Office of Pollution Prevention and Toxics (OPPT). Available online at: <http://www.epa.gov/lead/pubs/duststudy01-23-07.pdf>

Appendix B. Interior Analysis Input Variable Values

Appendix B presents a summary of all inputs used by the interior Monte Carlo model. All inputs, their values, and the methodology used to calculate the inputs are discussed in detail in the remainder of the Appendices. Table B-1 presents the inputs that are used to define a scenario, while Table B-3 presents the variables used in the Monte Carlo model. The “input 1” and “input 2” columns in Table B-3 correspond to different types of values depending on the distribution type, as shown in Table B-2. For example, input 1 and input 2 are the “mean” and “standard deviation” for a normal distribution and are the “geometric mean” and “geometric standard deviation” for lognormal variables. For variables that use a discrete distribution in the Monte Carlo model or that vary by building type, the values and probabilities used are shown in the tables in the remainder of Appendix B.

Table B-1. Scenario-specific inputs.

Input	Input name	Available Inputs	Units
Renovation Activity	RenoScenario	Dry scraping, Wet Scraping, Door Planing without HEPA, Door Planing with HEPA, Heat gun, Window Removal, Cabinet Removal, Cut outs, Demolition	n/a
Building Use Type	BldgUse	1, 2, 3, 4, or 5	n/a
Room Sizes and Configurations	RoomSize	2 to 4 different sizes for each building use type	ft ²
Carpeting in Renovated Rooms	Carpet	Present or Not Present	n/a
Rooms Renovated	RoomsRen	Combinations of Room 1, Room 2, and/or Room 3	n/a
Location of Exposed Person in Building	Loc	Work room in work area, work room outside work area, adjacent room	n/a
Intensity of Renovation Job	JobIntens	5%, 25%, 50%, or 100%	n/a
Fraction of Paint Removed	FracPaint	15%, 50%, or 100%	n/a
Vintage of Renovation	RenoVintage	Pre-1930, 1930-1949, 1950-1959, 1960-1979	n/a
Horizontal Containment	HorPlasticOnOff	Present or not present	n/a
Vertical Containment	VertPlasticOnOff	Present or not present	n/a
Cleaning Type	CleanType	Baseline or specialized	n/a
Age Groups	Age	0-10, 18-49, 50-80	n/a

Table B-2. Key to Definition of Variables by Distribution Type.

Distribution Type	Input 1	Input 2
Point estimate	Value	N/A
Uniform	Lower Limit	Upper Limit
Normal	Mean	Standard Deviation
Lognormal	Geometric Mean	Geometric Standard Deviation
Discrete	Reference to Table where Values and Probabilities are Presented	N/A

Table B-3. Interior Analysis Monte Carlo Inputs.

Module	Distribution Type	Parameter	Units	Input 1 (Mean, GM, Point Estimate or Table with Values)	Input 2 (SD, GSD, or N/A)	Upper Bound	Lower Bound	Appendix Describing Input
Reno Bldg	Point	CeilingHeightBldg1	ft	Table B-4	NA	N/A	N/A	Appendix C.2.3
Reno Bldg	Point	CeilingHeightBldg2	ft	Table B-4	NA	N/A	N/A	Appendix C.2.3
Reno Bldg	Point	CeilingHeightBldg3	ft	Table B-4	NA	N/A	N/A	Appendix C.2.3
Reno Bldg	Point	CeilingHeightBldg4	ft	Table B-4	NA	N/A	N/A	Appendix C.2.3
Reno Bldg	Point	CeilingHeightBldg5	ft	Table B-4	NA	N/A	N/A	Appendix C.2.3
Reno Bldg	Point	FloorAreaBldg	ft	Mapped to exterior building types, then use Table B-5	NA	N/A	N/A	Appendix C.1.2
Reno Bldg	Point	GlassFrac	None	Table B-4	NA	N/A	N/A	Appendix C.2.5
Reno Bldg	Point	CabinetFrac	None	Table B-4	NA	N/A	N/A	Appendix C.2.6
Reno Bldg	Lognormal	WallLoadingp1930	g/cm ²	0.00630	2.5932	0.00094	0.0424	Appendix C.2.8
Reno Bldg	Lognormal	WallLoading19301949	g/cm ²	0.00334	2.6347	0.00048	0.0232	Appendix C.2.8
Reno Bldg	Lognormal	WallLoading19501959	g/cm ²	0.00314	2.4725	0.00051	0.0192	Appendix C.2.8
Reno Bldg	Lognormal	WallLoading19601979	g/cm ²	0.00366	2.6982	0.00050	0.0266	Appendix C.2.8
Reno Bldg	Point	JobArea	ft ²	10 ft out from wall	NA	N/A	N/A	Appendix D.2.3
Reno Bldg	Point	RoomInRoomThreshold	None	Room size of at least 3800 ft, job	NA	N/A	N/A	Appendix D.2.3

Appendices to the Approach for Estimating Exposures and Incremental Health Effects from Lead due to Renovation, Repair, and Painting Activities in Public and Commercial Buildings

Module	Distribution Type	Parameter	Units	Input 1 (Mean, GM, Point Estimate or Table with Values)	Input 2 (SD, GSD, or N/A)	Upper Bound	Lower Bound	Appendix Describing Input
				area no more than 5% of room				
Reno	Point	FractionEmitted	None	Table B-6	NA	N/A	N/A	Appendix D.2.7
Reno	Point	HEPAEfficiency	None	90%	NA	N/A	N/A	Appendix D.2.8
Reno	Point	DustGeneratingRate	ft ² /hr	Table B-6	NA	N/A	N/A	Appendix D
Reno	Point	RestofRenovationMultiplier	None	Table B-6	NA	N/A	N/A	Appendix D
Reno	Point	RuleCleaningEfficiency	None	Table B-7	NA	N/A	N/A	Appendix D.2.8
Reno	Point	HorizontalPlasticEfficiency	None	Table B-7	NA	N/A	N/A	Appendix D.2.8
Reno	Point	AdjacentRoomFactor, No Vertical Plastic	None	0.0057	NA	N/A	N/A	Appendix D.2.8
Reno	Point	AdjacentRoomFactor, With Vertical Plastic	None	0.0045	NA	N/A	N/A	Appendix D.2.8
Reno	Point	Sill Factor	None	3.86	NA	N/A	N/A	Appendix D.2.9
Reno	Point	PercentExposureSill	None	1%	NA	N/A	N/A	Appendix D.2.9
Receptor	Lognormal	PartTrackRate	g/day	Table B-4	NA	N/A	N/A	Appendix E.10
Receptor	Discrete	MatFrac	None	0.13 or 0	NA	N/A	N/A	Appendix E.
Receptor	Point	FloorCleanInt	None	-0.5546	NA	N/A	N/A	Appendix E.14
Receptor	Point	CarpetCleanSlope	None	-0.4296	NA	N/A	N/A	Appendix E.14
Receptor	Point	FloorCleanEffMin	None	0.06	NA	N/A	N/A	Appendix E.14
Receptor	Discrete	CleaningFreq	None		NA	N/A	N/A	Appendix E.14

Appendices to the Approach for Estimating Exposures and Incremental Health Effects from Lead due to Renovation, Repair, and Painting Activities in Public and Commercial Buildings

Module	Distribution Type	Parameter	Units	Input 1 (Mean, GM, Point Estimate or Table with Values)	Input 2 (SD, GSD, or N/A)	Upper Bound	Lower Bound	Appendix Describing Input
				Table B-8				
Load Conc	Point	LoadingConcenMean	None	0.881	NA	N/A	N/A	0
Load Conc	Point	LoadingConcenSlope	None	0.421	NA	N/A	N/A	0
Load Conc	Point	LoadingConcenInt	None	5.145	NA	N/A	N/A	0
Load Conc	Point	LoadingConcenDF	None	1643	NA	N/A	N/A	0
Load Conc	Point	LoadingConcenErrorVar	None	0.544	NA	N/A	N/A	0
Load Conc	Point	LoadingConcenIntSE	None	0.0182	NA	N/A	N/A	0
Load Conc	Point	LoadingConcenSlopeSE	None	0.0094	NA	N/A	N/A	0
Load Conc	Point	LoadingConcenT	None	1.961	NA	N/A	N/A	0
Activity	Discrete	TimeSpentValues	None	Table B-9	NA	N/A	N/A	Appendix L.1
Activity	Uniform	TimeSinceLastReno	Months	1, 5, 10, 15, 20, 25, 30, 40 or 50	N/A	N/A	N/A	Appendix L.3
Activity	Discrete	AgeProb	None	Table A-12	NA	N/A	N/A	Appendix L.1
Activity	Point	MaternalPbB	µg/dL	0.747	NA	N/A	N/A	Appendix 0
Bckground	Lognormal	BgDustLoad	µg/ft ²	0.8	2.5	5	0.13	Appendix N.1
Bckground	Discrete	Leggett_Background_Intakes	µg/day	Appendix N.4	NA	N/A	N/A	Appendix N.4
Bckground	Discrete	Leggett_Background_PbB	µg/dL	Appendix N.4	NA	N/A	N/A	Appendix N.4
Blood Lead	Point	PbB_GSD	None	1.9	NA	N/A	N/A	Main Document
Blood	Point	Exposure Factors for Intake	various	Appendix	NA	N/A	N/A	Appendix L4

Appendices to the Approach for Estimating Exposures and Incremental Health Effects from Lead due to Renovation, Repair, and Painting Activities in Public and Commercial Buildings

Module	Distribution Type	Parameter	Units	Input 1 (Mean, GM, Point Estimate or Table with Values)	Input 2 (SD, GSD, or N/A)	Upper Bound	Lower Bound	Appendix Describing Input
Lead				L.4				

Table B-4. Interior Analysis Renovated Building Variables.

Building Types	Room Size 1 (ft2)	Room Size 2 (ft2)	Room Size 3 (ft2)	Room Size 4 (ft2)	Ave. Perc. Glass	Percent of Wall that is Cabinet	Ceiling Height	Track In Rate GM (g/day)	Track In Rate GSD
1 Office, outpatient healthcare, and public order/safety	60	200	600	3900	20%	13%	9	15.45	2.52
2 Warehouse, food sales, religious worship, and public assembly	200	9100	N/A		20%	45%	28	0.52	2.52
3 Food service, service, strip shopping mall, enclosed mall, and retail other than mall	1800	3800	8400	N/A	20%	13%	28	100.79	2.52
4 Education	200	1300	12200	N/A	20%	13%	20	29.91	2.52
5 Lodging, Nursing, inpatient health care, and laboratory	300	1300	6200	N/A	20%	13%	11	28.44	2.52

Table B-5. Mapping Interior Buildings to Exterior Building Sizes.

Building Types	F1T1	F2T1	F3T1	F1T2	F2T2	F3T2	F1T3	F2T3	F3T3
Floor Area (ft ²)	1,296	5,184	20,736	2,592	10,368	41,472	3,888	15,552	139,968
Cumulative Probability For each Interior Building Type									
1 Office, outpatient healthcare, and public order/safety	0.25	0.38	0.50	0.63	0.75	0.82	0.88	0.95	1.00
2 Warehouse, food sales, religious worship, and public assembly	0.05	0.25	0.38	0.50	0.75	0.82	0.88	0.95	1.00
3 Food service, service, strip shopping mall, enclosed mall, and retail other than mall	0.05	0.25	0.38	0.50	0.75	0.82	0.88	0.95	1.00
4 Education	0.05	0.25	0.38	0.50	0.58	0.67	0.75	0.95	1.00
5 Lodging, Nursing, inpatient health care, and laboratory	0.05	0.12	0.18	0.25	0.38	0.50	0.62	0.75	1.00

Table B-6. Interior Analysis Renovation Activity Parameters.

Activity type	Fraction of Paint That Remains as Lead Dust	Rate of "dust generating" phase in ft ² /hr	Rest of Renovation Multiplier
Window, Saw	0.2137	42	0.5
Door Planing	0.1118	45	15
Heat Gun Plaster	0.0572	45	15
Dry Scrape	0.0380	45	15
Window, No Saw	0.0155	42	0.5
Heat Gun Wood	0.0119	45	15
Door Planing, with HEPA	0.0112	45	15
Cutouts	0.0056	45	2
Cabinet/Shelf Removal	0.0030	45	2
Demolition	0.0031	45	0.5

Table B-7. Interior Analysis Control Option Efficiencies.

Control Option	Horizontal Plastic / Rule Cleaning Efficiency
Specialized Cleaning with Horizontal Plastic	0.993
Base Cleaning with Horizontal Plastic	0.956
Specialized Cleaning with No Horizontal Plastic	0.975
Baseline Cleaning with No Horizontal Plastic	0.943

Table B-8. Interior Analysis Distribution of Cleaning Frequencies

Building Type	Every working day (5 days/week)	Every third day (approx) (2 days/week)	Every week (1 day/week)	Every other week (1 day/2 weeks)	Every fourth week (1 day/4 weeks)
1 Office, outpatient healthcare, and public order/safety	0.2	0.6	0.8	0.9	1.0
2 Warehouse, food sales, religious worship, and public assembly	0.2	0.6	0.8	0.9	1.0
3 Food service, service, strip shopping mall, enclosed mall, and retail other than mall	0.4	0.6	0.8	0.9	1.0
4 Education	0.4	0.6	0.8	0.9	1.0
5 Lodging, Nursing, inpatient health care, and laboratory	0.4	0.6	0.8	0.9	1.0

Table B-9. Cumulative Distributions for Time Spent (Fraction of the Week) in Different Building Types for Each Age Range.

Building Type	Cumulative Probability	Age Range			
		0-<5	5-<18	18-<50	50-80
1 Office, outpatient healthcare, and public order/safety	0.05	0.01	0.01	0.01	0.01
	0.10	0.01	0.01	0.03	0.02
	0.25	0.01	0.01	0.16	0.08
	0.52	0.02	0.03	0.32	0.25
	0.75	0.04	0.08	0.36	0.35
	0.90	0.07	0.18	0.41	0.40
	0.95	0.12	0.35	0.44	0.43
	1	0.12	0.42	0.53	0.50
2 Warehouse, food sales, religious worship, and public assembly	0.05	0.01	0.01	0.01	0.01
	0.10	0.01	0.01	0.01	0.01
	0.25	0.02	0.04	0.02	0.02
	0.52	0.05	0.08	0.05	0.05
	0.75	0.10	0.13	0.14	0.10
	0.90	0.12	0.19	0.34	0.19
	0.95	0.12	0.23	0.39	0.30
	1	0.12	0.34	0.49	0.42

Appendices to the Approach for Estimating Exposures and Incremental Health Effects from Lead due to Renovation, Repair, and Painting Activities in Public and Commercial Buildings

Building Type	Cumulative Probability	Age Range			
		0-<5	5-<18	18-<50	50-80
3 Food service, service, strip shopping mall, enclosed mall, and retail other than mall	0.05	0.01	0.01	0.01	0.01
	0.10	0.01	0.01	0.01	0.01
	0.25	0.02	0.02	0.03	0.03
	0.52	0.04	0.05	0.05	0.05
	0.75	0.07	0.09	0.11	0.08
	0.90	0.12	0.16	0.22	0.15
	0.95	0.12	0.21	0.33	0.20
	1	0.12	0.32	0.47	0.38
4 Education	0.05	0.01	0.08	0.01	0.01
	0.10	0.04	0.13	0.01	0.01
	0.25	0.11	0.21	0.03	0.04
	0.52	0.12	0.27	0.13	0.09
	0.75	0.12	0.30	0.28	0.28
	0.90	0.12	0.33	0.34	0.35
	0.95	0.12	0.38	0.39	0.38
	1	0.12	0.43	0.49	0.45
5 Lodging, Nursing, inpatient health care, and laboratory	0.05	0.01	0.01	0.01	0.01
	0.10	0.02	0.02	0.02	0.02
	0.25	0.02	0.03	0.04	0.03
	0.52	0.04	0.06	0.10	0.06
	0.75	0.07	0.21	0.34	0.16
	0.90	0.12	0.36	0.43	0.34
	0.95	0.12	0.42	0.50	0.40
	1	0.12	0.56	0.63	0.56

Appendix C. Renovated Building Characteristics

Appendix C includes information for how the renovated building characteristics were determined for the Approach. Each section includes information about the selected data source and how (if at all) the data were processed to estimate point estimates or distributions for the Monte Carlo model.

C.1. Exteriors

In this Approach, the modeled characterization of lead emitted from renovation activities is dependent upon how the renovation building is characterized, which includes specifying its size (both the total building size and the size of different components), height, and vintage. These variables in turn are used to estimate the amount of paint on the building and the lead content of that paint. This section describes the methodology used to select the building characteristics in this Approach.

C.1.1. Building Block Approach

To capture the emissions from a range of building sizes, a unit-based Approach was developed that characterized emissions from a specified amount of surface area on a renovated building. Then, each building is modeled as though one section (or “block”) of the building is undergoing renovation at a time, with the renovation proceeding around the perimeter of the building. This method accounts for the fact that renovations are typically performed on finite sections of a building at a given time rather than on the entire surface area of the building at once.

In this Approach, the renovation block area was constructed to represent the typical wall surface area disturbed by a four-person crew in two hours when performing paint removal jobs. Each renovated building is assumed to have a square footprint, and the total square footage of a side of the building is broken up into incremental numbers of these renovation blocks. The building was also assumed to have windows (applied in the modeling as a fraction of the block that is glass) estimated based on CBECS and to have doors every 32.8 ft (10 m) around the perimeter of the building on the first floor.

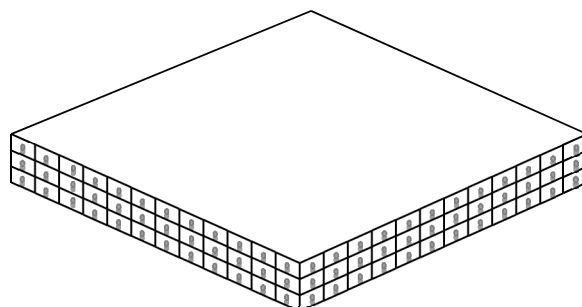


Figure C-1. Largest renovation building with renovation blocks and point sources.

In this Approach, a separate fate and transport model run (see Appendix 2.3) is needed for each activity that has a different job rate. Job rates were collected for each activity from the RSMMeans construction cost manual, a guide that provides typical crew output (e.g., in square feet per day) for different renovation activities. (see Appendix C). Using the block approach above standardizes the rate of renovation for the paint removal and trim/door activities and greatly reduces the required number of fate and transport model simulations. The variability and uncertainty associated with these rates is recognized.

For the purposes of the exterior renovation Approach, the use type of the renovated building is not needed. It is assumed that only the exterior attributes of the building are necessary. However, when the Approach models both exterior and interior renovation activities simultaneously, the renovated building is treated as both a “renovated” and “receptor” building, and the use type is incorporated for track in back into the same P&CB, as described in Section 4 of the Approach document.

C.1.2. Building Sizes

The renovated building size definitions were determined using the Commercial Building Energy Consumption Survey (CBECS) data (US EIA, 2003), a survey that represents the entire US commercial building stock. CBECS presents the overall building square footage based on building size (in eight bins) and number of floors in the building (in five bins). The size bins ranged from “1,000 to 5,000 sf” to “Over 500,000 sf.” The metadata which included information about malls was used for the analysis.

The number of floors were presented as “one”, “two”, “three”, “four to ten”, and “above 10.” It was estimated from these data that 67 percent of commercial buildings in the US are 1 story, 22 percent are two stories, and 11 percent are more than two stories. Based on these estimates, three building height bins were selected to represent the commercial building stock: “one”, “two”, and “three and above.”

To account for skewness of the dataset, a lognormal distribution was fit to the binned CBECS data separately for each of these three height categories, and a “small”, “medium”, and “large” building footprint was estimated for each of the height bins. The analysis proceeded in the following steps:

1. For the one story buildings, the upper bound of each CBECS size bin was noted. For “Over 500,000 sf”, no maximum value was available to use as an upper bound. Thus, the upper bound was set to a maximum of 1,000,000 square feet. Subsequent sensitivity analysis indicated the predictions were not heavily dependent on this number.
2. The cumulative probability was estimated for each size bin. This probability was found by finding the percentage of total buildings in the bin and performing a cumulative sum of the probabilities for that bin and all lower bins.
3. An initial geometric mean and geometric standard deviation were assigned to the overall distribution across bins. The Excel® function “lognormdist” was used to find the cumulative probability in the Lognormal corresponding to the upper bound in each bin.
4. The “Goal Seek” Excel® function was used to adjust the geometric mean and geometric standard deviation until the sum of the squares of the errors between the actual and modeled cumulative probabilities across the bins was minimized.
5. This final geometric mean and geometric standard deviation pair was used to simulate 1,000 values. The means were taken in each tertile, and were used as the renovation building sizes.
6. The analysis was repeated for the two-story and three-and-above-story buildings.

This gave a total of nine different renovation building sizes. These building footprints were then rounded to the nearest size that created an even number of renovation “blocks”.

Buildings that are taller than 3 stories are likely to have lower concentrations of lead due to larger ventilation factors, when compared to shorter buildings. However, taller buildings may transport lead longer distances due to fewer obstructions and prevailing meteorological conditions between the renovated building and the receptor building. Taller buildings, as well as potential future CBECS data, could be considered in the future.

C.1.3. Percent Glass

The fraction of the building that is glass was estimated using CBECS microdata (US EIA, 2003). This dataset presents data for individual buildings, including the size, number of stories, percent glass, and sampling weights used to make the data set representative of US commercial building stock. The CBECS data were mapped to the nine building sizes, as described in Appendix C.1.2. From these data, an average percent glass was found for each building size. The weights from the CBECS survey were included to ensure the means were nationally representative.

Table C-1. Characteristics of the Renovated Building Size.

Building ID	Fraction of Surface Area that is Glass ²
F1T1	0.12
F1T2	0.13
F1T3	0.14
F2T1	0.15
F2T2	0.18
F2T3	0.18
F3T1	0.14
F3T2	0.17
F3T3	0.26

The percent glass used for interiors (Appendix C.2.5) is different than that used for exteriors. In interiors, the percent glass is analyzed by different building types of all sizes, where variation proves to be small. For the exterior analysis, percent glass is analyzed not by building type but by building size, as shown here.

C.1.4. Size of Renovated Building Components

Three renovation activities (trim removal, four wall window/door replacement, and one wall window/door replacement) are performed on specific building components rather than on the entire exterior painted surface area. Thus, emissions for these activities could not be estimated based solely on the total surface area of the walls of the building. Instead, the surface area of these building components had to be estimated, as described below.

The area comprised of window frame trim was estimated by assuming that a typical window is 3.2 ft by 3.2 ft and has a 0.3 ft wide frame around the exterior. The total number of windows was estimated by dividing the area that was glass (determined by multiplying the exterior surface area of the building by the percent glass) by the area of each window (10.24 ft²) and rounding to the nearest whole number. The number of windows was multiplied by the area of frame associated with each window (4.20 ft²) to calculate the total area of window trim.

Doors were assumed to be located every 32.8 ft (10 m) around the perimeter of the building on the first floor. Each door was assumed to be 6.6 ft x 3.0 ft with a 0.3 ft wide trim on three sides. The area of

other trim, not associated with windows and doors, was set equal to that of window and door trim plus an additional 5 percent of the non-glass exterior surface area of the wall.

A summary of the values selected for each of the nine building types is provided in Table C-2.

Table C-2. The parameters of buildings modeled with varying size of disturbance.

Building ID ¹	Building footprint (sf)	# of Stories	Non-glass building surface area (sf)	Window & door surface area (sf)	Trim surface area (sf)	Total # of blocks
F1T1	1,296	1	1,268	171	155	8
F1T2	5,184	1	2,504	354	321	16
F1T3	20,736	1	4,974	621	633	32
F2T1	1,296	2	2,429	284	326	16
F2T2	5,184	2	4,943	535	623	32
F2T3	20,736	2	9,429	1,155	1,389	64
F3T1	1,296	3	3,701	351	457	24
F3T2	5,184	3	6,874	925	1,111	48
F3T3	46,656	3	17,533	3,738	4,377	144

¹F1 = Floor 1, T1 = Tertile 1

C.1.5. Containment Area

The containment area captures the area covered by horizontal plastic (if used) and the distance from the building to the vertical plastic (if used). The Approach assumes that horizontal plastic is placed 10 ft out from the job wall. This distance was selected based on inspection of the Dust Study data. Typically, lead dust loadings tended to drop to at least 2% of their value just next to the wall at a distance of 10 ft. If vertical plastic is used, it is assumed that the plastic is 10 ft from the job wall. Using the total building footprint area and the assumption that the building is square, the containment area is calculated using the building wall lengths and the assumption of 10 ft linear feet out from the job wall.

C.1.6. Vintage of the Renovated Building

The concentration of lead in the exterior paint of a building was assumed to be a function of the age of the building. This assumption is based on the fact that the concentration of lead in paint has decreased with time, particularly leading up to and following the ban on lead paint in residential structures in 1978. Buildings that were built in 1979 to present were not modeled due to the assumption that few, if any, of these building would contain lead-based paint. However, the number of newer buildings that may contain lead based paint is unknown. Four vintage bins were considered for the renovated building: Pre-1930, 1930-1949, 1950-1959, and 1960-1979, which is consistent with the vintage bins used in the benefits analysis performed in support of the residential Lead Renovation, Repair and Painting (LRRP) rule.

C.1.7. Amount of Lead in the Paint on the Building

X-Ray Fluorescence (XRF) measurements provide empirical data about the amount of lead on the walls of buildings of various vintages. In general, XRF techniques quantify lead mass per unit area through multiple layers of paint on the wall. For the Approach, the XRF distributions for the four oldest vintages were estimated from the HUD National Housing Survey (US EPA, 1998a). In the HUD report, Table 2 provides descriptive statistics. The geometric mean for exterior components was used directly from the report; the geometric standard deviation was estimated using the reported mean and geometric mean. The geometric mean, geometric standard deviation, and average lead content in paint (all vintages) are shown in Table C-3 below.

Table C-3. Lead XRF measurements by vintage for exterior analysis.

Renovation vintage bin	XRF Loadings (g/cm ²)		
	Geometric mean	Geometric standard deviation	Average
Pre-1930	0.00607	2.90	0.01068
1930-1949	0.00377	2.38	0.00549
1950-1959	0.00253	2.30	0.00358
1960-1979 ¹	0.00331	2.34	0.0048

¹This vintage bin contains data from houses from 1960-1978, but it is considered representative of the 1960-1979 bin.

The geometric mean loading from the Pre-1930 vintage results in an estimate of 19.6 percent lead in the paint. This estimate can be compared to sources which indicated that before 1940, paints were often 10 and sometimes up to 50 percent lead (NDHHS, 2011).

The lead content in the paint and the density of particles are solved using the equations:

$$\frac{XRF \times WallPaintCov \times UnitConv}{PaintLayers \times PaintDens} = frac$$

$$PaintDens = frac \times DensityPb + (1 - frac) \times DensityRest$$

<i>XRF</i>	=	the XRF-measured amount of lead on the wall (g/cm ² wall)
<i>WallPaintCov</i>	=	the amount of area covered by a single gallon of paint (ft ² /gallon)
<i>UnitConv</i>	=	a conversion factor to convert from gallons to cm ³ and from cm ² to ft ²
<i>PaintLayers</i>	=	the number of layers of paint on the wall
<i>PaintDens</i>	=	the density of the paint (g paint/cm ³ paint)

<i>frac</i>	=	the fraction of paint which is lead by weight (unitless)
<i>DensityPb</i>	=	the density of lead (g/cm ³)
<i>DensityRest</i>	=	the density of the rest of the paint (other than lead) (g/cm ³)

All of the equation variables above were assumed to be fixed, aside from the XRF measurements. According to the EPA Wall Paint Exposure Model (USEPA 2001), the typical coverage of paint (*WallPaintCov*) is 400 ft²/gallon or 0.0025 gallons per ft². The density of lead is 11.3 g/cm³, and the density of the rest of the paint is assumed to be 1 g/cm³.

C.2. Interiors

In this Approach, the modeled characterization of lead emitted from renovation activities is dependent upon how the renovation building is characterized, which includes specifying its use, room sizes, height, and vintage. These variables in turn are used to estimate the amount of paint on the building and the lead content of that paint. This section describes the methodology used to select the building characteristics in the Approach.

C.2.1. The Building Use Type

As discussed in Section 5.1.1 of the main report, the use type of a building will affect key attributes of both the building itself and the time people spend in the building per day. For example, a large warehouse will have one or two larger spaces with multiple smaller rooms, and individuals will visit infrequently. In contrast, hotels will have numerous small rooms, and individuals may stay for days or months at a time.

The CBECS survey provides information about the number of buildings in the U.S. in different use categories, as shown in

Table C-4. These CBECS categories were mapped to 5 assessment categories for this Approach, where CBECS categories were grouped according to layouts, room sizes, and expected time spent patterns. A total of 5 assessment categories were chosen to ensure adequate coverage of different building types but also to balance the resource needs of the Monte Carlo analysis.

Table C-4. CBECS Buildings and Mapped Assessment Categories

CBECS Category	DOE Categories	Assessment Categories
Office	Small Office Medium Office Large Office	1. Office, outpatient healthcare, and public order/safety
Outpatient health care	Outpatient Healthcare	
Public order and safety		
Non-refrigerated warehouse	Warehouse	2. Warehouse, food sales, religious worship, and public assembly
Refrigerated warehouse		
Food sales	Supermarket	
Religious worship	None	
Public assembly	None	
Food service	Quick Service Restaurant Full Service Restaurant	3. Food service, service, strip shopping mall, enclosed mall, and retail other than mall
Service	None	
Strip shopping mall	Strip Mall	
Enclosed mall	None	
Retail other than mall	Stand-alone Retail	
Education	Secondary School	4. Education
Lodging	Small Hotel Large Hotel	5. Lodging, Nursing, inpatient health care, and laboratory
Nursing	None	
Inpatient health care	Hospital	
Laboratory	None	
Other	None	None
Vacant	None	

C.2.2. Room Sizes

Table C-5 presents the representative room sizes for five types of model buildings. To develop these estimates, we began with 14 DOE Reference Buildings (Deru et al 2011). The DOE data provided the size and frequency of each type of zone within the Reference Buildings. In most cases, a zone was synonymous with room; however, we determined that some zones needed to be combined to form one room. For example, Stand-Alone Retail was composed of five zones. It was our judgment that four of the five zones would likely exist in a single room. Accordingly, we combined the Core Retail, Point of Sale, Front Retail, and Front Entry zones into one Core Retail zone. Similarly, we determined that some zones needed to be subdivided into multiple rooms. For example, zones used as offices were much larger than the average office size according to other sources (IFMA 2010) (Miller 2012). To address this, we divided the area of the office zones by the average office size to determine the number of concurrent rooms within an office zone. In addition, we determined that some zones needed to be eliminated. We removed from our data zones representing a building's entire basement, zones that were not climate controlled, and zones with zero occupancy, meaning that individuals do not occupy those spaces.

Some of the sizes of the DOE reference buildings appeared to be considerably larger than the average sized buildings observed in the CBECS data. In particular, the Warehouse, Supermarket, and Stand-Alone Retail DOE reference buildings all had rooms larger than the average sized building of that type according to CBECS. We adjusted the sizes of these buildings and their rooms so that the size of the building after the adjustments matched the size of the average building of that type in CBECS. The sizes of single large rooms were adjusted downward and when there were multiple smaller rooms the number of rooms was adjusted downward. For example, the DOE warehouse building had 14.3 offices that were 178 square feet, 1 bulk storage room that was 34,497 square feet and one fine storage room that was 14,998 square feet. This implies a building size of 52,040 square feet when the average warehouse building size according to the CBECS data is only 21,603 square feet, 42 percent of the DOE reference building size. Thus, we adjusted the size of the two large rooms by multiplying their square footage by 42% and adjusted the number of offices downward by 41.5%. Thus, the new building had 5.9 offices that were 178 square feet, 1 bulk storage room that was 14,319 square feet and one fine storage room that was 6,226 square feet.

After making the adjustments to the data described above, we calculated the prevalence of rooms by size for 5 categories of model buildings. To calculate these prevalence rates, each room within the DOE model building was weighted according to the weight assigned by DOE for that zone and each DOE building was weighted according to their frequency in the CBECS. Cut-points used to group the rooms into 2-4 size bins for each of the 5 model building categories were selected based on a visual inspection of the data so that no group represented less than 2 percent of the rooms in that model building (for example, the rooms in rows shaded the same color in were grouped together). Within each of these groups, the weighted average room size was calculated and rounded to the nearest 10ft² for room sizes below 100ft² and to the nearest 100ft² for rooms greater than 100ft². The resulting room sizes and room frequencies are shown in

Table C-5.

Table C-5. Room Sizes For Each Assessment Building Category

Model Buildings	Room Size (ft ²)	Percentage Weight	
		Within Model Building	Within All Buildings
1 Office, outpatient healthcare, and public order/safety	60	2%	1%
	200	89%	53%
	600	5%	3%
	3,900	4%	2%
2 Warehouse, food sales, religious worship, and public assembly	200	72%	4%
	9,100	28%	1%
3 Food service, service, strip shopping mall, enclosed mall, and retail other than mall	1,800	72%	4%
	3,800	18%	1%
	8,400	11%	1%
4 Education	200	42%	7%
	1,300	54%	9%
	12,200	3%	1%
5 Lodging, Nursing, inpatient health care, and laboratory	300	80%	11%
	1,300	16%	2%
	6,200	4%	1%

C.2.3. Designing Three-Room Renovation Units

We can limit our modeling to three-room renovation units by making the simplifying assumption that exposures to individuals in rooms adjacent to more than 2 renovated rooms is equivalent to the exposures to individuals in rooms adjacent to 2 renovated rooms.

A renovation project might involve disturbing LBP in multiple rooms that are also adjacent to other rooms. The exposure model is designed to account for this by modeling the exposure in each affected room as a separate scenario. For example, consider a 5 room renovation in a hotel that can be represented by the configuration below in Table C-7.

Table C-6: Example Configuration for 5 Room Hotel Renovation

(rooms sharing walls are adjacent)

Room A (not renovated)	Room B (not renovated)	Room C (renovated)	Room D (renovated)	Room E (renovated)	Room F (renovated)	Room G (renovated)	Room H (not renovated)	Room I (not renovated)
---------------------------	---------------------------	-----------------------	-----------------------	-----------------------	-----------------------	-----------------------	---------------------------	---------------------------

We represented this renovation with 7 configurations of 3 rooms (see Table C-7). The exposure was modeled for individuals in Room 2 only. For example, although Room C appears in three different rows below in Table C-8, the exposures to the individuals in room C are only modeled in the second row.

Thus, this approach allows us to use a three room renovation configuration to model a renovation that involves any number of rooms.

Table C-7: Example of 5 Room Hotel Renovation Represented by Three-Room Configurations

Room 1 (room adjacent to where occupants are)	Room 2 (room with occupants)	Room 3 (room adjacent to where occupants are)
Room A (not renovated)	Room B (not renovated)	Room C (renovated)
Room B (not renovated)	Room C (renovated)	Room D (renovated)
Room C (renovated)	Room D (renovated)	Room E (renovated)
Room D (renovated)	Room E (renovated)	Room F (renovated)
Room E (renovated)	Room F (renovated)	Room G (renovated)
Room F (renovated)	Room G (renovated)	Room H (not renovated)
Room G (renovated)	Room H (not renovated)	Room I (not renovated)

C.2.4. Ceiling Height

The ceiling heights for each building type were estimated using the DOE reference buildings. For each building type in a given Approach building category, the reference buildings had a range of ceiling heights. Values corresponding to main rooms were favored over values in rooms deemed to have fewer occupants (e.g., for a quick service restaurant, the dining room and kitchen ceiling heights were favored over the “attic” ceiling height). A representative ceiling height was then chosen for each building category, as shown in Table C-8. Because the DOE buildings do not include either agricultural or industrial buildings, a representative value from a warehouse was used instead.

Table C-8. Ceiling Heights For Each Assessment Building Category

Building Category	Ceiling Height (ft)
1 (Office, outpatient healthcare, Public Order and Safety)	9
2 (Warehouses, Food Sales, Religious Worship, Public Assembly)	28
3 (Food Service, Service, Strip Mall, Retail)	28
4 (Education)	20
5 (Lodging, Nursing, Inpatient Health Care, Lab)	11

C.2.5. Percent Glass

The percent glass is a variable collected from the CBECs. An analysis was conducted to determine if the percent glass varied by building type. Only slight variation was found as all buildings reported approximately 20% glass surfaces. Percentages were derived by combining CBECs categories to match each of the Approach building categories. Then, the adjusted weight variable was used to estimate the nationally-representative fraction of glass in each Approach category. Percent glass as analyzed by building category for the interiors analysis differs slightly from percent glass as analyzed by building size for the exteriors analysis.

Table C-9. Percent Glass for Each Approach Interior Building Category

Building Category	Sum of Percent Glass Weight* ADJWEIGHT	Sum of ADJWeight	Average Percent Glass
0 (Vacant, Other)	49,175	252,552	19.5%
1 (Office, outpatient healthcare, Public Order and Safety)	205,167	1,015,125	20.2%
2 (Warehouses, Food Sales, Religious Worship, Public Assembly)	291,045	1,469,782	19.8%
3 (Food Service, Service, Strip Mall, Retail)	300,137	1,576,039	19.0%
4 (Education)	79,684	385,923	20.6%
5 (Lodging, Nursing, Inpatient Health Care, Lab)	28,839	159,329	18.1%

C.2.6. Amount of Shelving

The one data source found that quantifies the amount of shelving in a public building is from the Child Care Center Survey data (HUD 2003). Using the raw data, entries were separated into “wall” and “cabinet” categories. “Built in cabinets” were counted as “cabinets”; all other data types were not. The total wall area and cabinet area reported for each room (of each childcare center) were calculated. Where both a cabinet and wall area existed for the same room, the cabinet to wall ratio was estimated (N=102). The area of all cabinets and walls were used in the calculation, regardless of whether they tested positive for lead or not. The resulting statistics are shown below in Table C-10. The standard deviation is larger than the mean, indicating significant variability in this variable within the data. Should additional data become available regarding the amount of shelving by building type, EPA could make different assumptions. The generic high and medium estimates derived below may not best represent the variability within a given building category.

Table C-10 Estimated Percentage of Interior Wall that is Cabinet/Shelf in Child Care Centers

Statistic	Cabinet to Wall Ratio
MIN	0.3%
MAX	96.6%
MEAN	13.1%
STD	16.1%

In order to estimate the amount of shelving in each room of each example building, buildings were mapped to specific cabinet “bins” defined using the CCC data:

- “High incidence of cabinetry/shelving”: use the mean plus two standard deviations from the CCC data, or 45%
- “Medium incidence of cabinetry/shelving”: use the mean from the CCC data, or 13%
- “Low incidence of cabinetry/shelving”: use the mean minus two standard deviations from the CCC data, or 0%.

The mappings and values are shown in Table C-11.

Table C-11 Estimated Percentage of Interior Wall that is Cabinet/Shelf in Approach Building Categories

Building Types	Cabinet/Shelf Category	Percent of Wall that is Cabinet
1 Office, outpatient healthcare, and public order/safety	Medium	13%
2 Warehouse, food sales, religious worship, and public assembly	High	45%
3 Food service, service, strip shopping mall, enclosed mall, and retail other than mall	Medium	13%
4 Education	Medium	13%
5 Lodging, Nursing, inpatient health care, and laboratory	Medium	13%

C.2.7. Vintage of the Renovated Building

The concentration of lead in the exterior paint of a building was assumed to be a function of the age of the building. This assumption is based on the fact that the concentration of lead in paint has decreased with time, particularly leading up to and following the ban on lead paint in residential structures in 1978. Four vintage bins were considered for the renovated building: Pre-1930, 1930-1949, 1950-1959, and

1960-1979, which is consistent with the vintage bins used in the benefits analysis performed in support of the residential Lead Renovation, Repair and Painting (LRRP) rule.

C.2.8. Amount of Lead in the Paint in the Building

The distributions for the amount of lead in the paint for interior components were estimated as described in Section C.1.8, but the interior analysis used the interior component estimates for the HUD data source (US EPA, 1998a), Table 2, as shown in Table C-12.

Table C-12. Lead XRF measurements by vintage for interior analysis.

Renovation vintage bin	XRF Loadings (g/cm ²)		
	Geometric mean	Geometric standard deviation	Average
Pre-1930	0.00630	2.59	0.00992
1930-1949	0.00334	2.63	0.00534
1950-1959	0.00314	2.47	0.00473
1960-1979 ¹	0.00366	2.70	0.00599

¹This vintage bin contains data from houses from 1960-1978, but it is considered representative of the 1960-1979 bin.

C.3. References for Appendix C:

U.S. Department of Housing and Urban Development (HUD). 2003. First National Environmental Health Survey of Childcare Centers.”

Deru et al (2011). U.S. Department of Energy Commercial Reference Building Models of the National Building Stock. Technical Report National Renewable Energy Laboratory. TP-5500-46861

IFMA, (2010), *Space and Project Management Benchmarks: IFMA Research Report #34*. NDHHS 2011

Miller, Norm, (2012), *Estimating Office Space per Worker*. Draft Report.

US EIA (2003) Commercial Building Energy Consumption Survey (CBECS). Available online at: http://www.eia.gov/emeu/cbecs/cbecs2003/public_use_2003/cbecs_pudata2003.html

US EPA. (1998a). Risk analysis to support standards for lead in paint, dust, and soil. Appendix G: Health effects associated with exposure to lead and internal lead doses in humans. (Report No. EPA 747-R-97-006). Washington, DC: US Environmental Protection Agency, Office of Pollution Prevention and Toxics. Available online at: <http://www.epa.gov/lead/pubs/toc.pdf>.

US EPA. (2001). Wall Paint Exposure Model Version 3.2 Users Guide. Washington, DC: US Environmental Protection Agency, Office of Pollution Prevention and Toxics (OPPT). Available online at: <http://www.epa.gov/opptintr/exposure/pubs/wpemman.pdf>.

Appendix D. Renovation Characteristics

Appendix D includes information for how the renovation job characteristics were determined for the Approach. Each section includes information about the selected data source and how (if at all) the data were processed to estimate point estimates or distributions for the Monte Carlo model.

D.1. Exteriors

In this Approach, the transport of lead downwind from the renovated building is determined by both the amount of lead emitted and the time over which the lead is emitted. The variables describing these two variables include the rate of renovation, the fraction of paint removed as both aerosol and bulk during the activity, and the efficacy of any containment options employed.

D.1.1. Rate of Renovation

Two different sources were considered to determine the rate of renovation for each of the renovation activities. The Dust Study (US EPA, 2007a), which is used to estimate the fraction of paint emitted in each job (see Appendix H), reported the area of the wall and the associated job duration for each experiment. Rates of renovation for each renovation activity type were estimated based on these data, as shown in Table D-1. For activities with more than one experiment in the Dust Study, the standard deviation is also provided. In general, the standard deviations are large and indicate large variations in the rates of removal, in part stemming from the small number of experiments performed. In addition, three activities had only a single experiment and as a result are subject to large uncertainty.

Owing to these large uncertainties, the RSMeans Facilities Construction Cost Manual (Mossman and Plotner, 2009) was used as an alternative to determine the average rate of lead paint removal. For the paint removal activities, RSMeans reports that surface preparation for a one person crew is 86 ft² per day for aluminum siding, steel siding, and gypsum board. RSMeans does not provide information on typical crew sizes. In lieu of reported data, personal communication with a professional engineer at the National Institute of Environmental Health Sciences, who is an expert in the field of construction project management, estimated that a typical crew for a commercial or public exterior renovation consists of approximately four workers (Capouch, personal communication, 2011). The actual crew size may vary by building or job type. Additional information on this variable would help inform the rate of renovation for exterior renovation activities with larger crews working at a faster rate and smaller crews working at a lower rate. This translates to approximately 344 ft² per hour for the four person

crew assumed in the AERMOD modeling. This rate was rounded to 360 ft² per hour to ensure each of the modeled building panels could be finished within an increment of one day.

Table D-1. Comparison of Dust Study and RSMMeans removal rates

	Dust Study Removal Rates (ft ² /hr)			RSMMeans Removal Rates	RSMMeans Removal Rates For a 4 Person Crew in an 8 hour day (ft ² /hr)	RSMMeans Removal Rates For a 4 Person Crew in an 8 hour day (ft ² /day)	Approach Removal Rates (ft ² /day)
	No. Of Experiments (N)	Mean	Standard Deviation				
Power Sanding	2	54	5	86 ft ² /day	43	344	360
Needle Gun	1	3	N/A	86 ft ² / day	43	344	360
Torching	2	35	2	86 ft ² / day	43	344	360
High Heat Gun	1	6	N/A	86 ft ² / day	43	344	360
Low Heat Gun	1	18	N/A	86 ft ² / day	43	344	360
Dry Scrape	4	154	46	86 ft ² / day	43	344	360
Replace Exterior Door	2	32	7	84 ft ² / day	42	336	360
Trim Replacement	2	96	119	64 ft/ day	16	128	180
Demolition	N/A			900 ft ³ / day	38	300	360

The trim removal rate was taken for the RSMMeans estimate for “Trim”, which gives a value of 64 ft/day. To estimate the square footage for a 4 person crew, it was assumed that the trim had a width of 6 inches and the RSMMeans value was multiplied by 4*0.5=2. This yielded an estimate of 128 ft²/day. This value was rounded to 180 ft² per day to ensure the modeled building panel could be finished within an increment of half a day.

For door removal, a value of 84 ft²/day was taken from the RSMMeans manual. Assuming a four person crew, this yields 336 ft²/day. Again, this value was rounded to 360 ft²/day to ensure a single building block could be renovated in increments of whole days.

Finally, the demolition rate was taken from the RSMMeans with a value of 900 ft³/day. To convert to ft²/day, it was assumed that the walls were 4 inches thick, giving a value of 300 ft²/day. This value was rounded to 360 ft²/day to ensure a single building block could be renovated in increments of whole days.

D.1.2. Job Duration

For each building size, the total job duration can be calculated using the number of blocks on the building, the fraction of the block being renovated, and rate of renovation. The Approach assumes that the crew works an 8 hour shift each day during the day and does not work at night. Then,

$$JobDuration = NumBlock \times BlockSize \times ComponentFrac \times RenoRate \times 8 \text{ hours}$$

where:

<i>JobDuration</i>	=	total duration of the renovation job (days)
<i>NumBlock</i>	=	the number of “blocks” in the building being renovated
<i>BlockSize</i>	=	the size of each building block (ft ²)
<i>ComponentFrac</i>	=	the fraction of the building block that is made up of the component being renovated (e.g., trim) (ft ²)
<i>RenoRate</i>	=	the surface area that can be renovated by a four person crew in an hour

In order to simplify the estimation of the job durations and limit the total number of AERMOD simulations, similar renovation rates were set equal (as discussed above in Section D.1.2) and a block was defined as the area from which a crew could prepare the painted surface in 2 hours, as discussed in Section C.1.1.

D.1.3. Fraction of Paint Removed

For the modeling Approach, a representative surface preparation fraction is used for all the different possible substrate types and removal methods. This fraction was estimated using information in the RSMMeans manual (Mossman and Plotner 2009). RSMMeans indicates that full removal of all exterior lead paint by a four person crew can be performed at a rate of 45 square feet per hour, while surface preparation rates vary between 240 (wood shingles) and 344 (aluminum siding, steel siding, and gypsum board) square feet per hour for different substrates. To estimate the fraction removed during surface preparation, it was assumed that removing a certain mass of paint can be done at a constant rate, but the surface preparation takes less time because less total paint is removed compared with total lead remediation. Thus, the surface preparation rates were divided by the lead removal rate to estimate the fraction of paint removed during surface preparation. This yielded a range of 13 to 19%. A representative value of 15% was selected for the modeling Approach. Because this value is expected to vary across

different substrates and removal methods, the selection of this value introduces uncertainty in the modeling Approach.

D.1.4. Fraction of Paint Emitted As Aerosol By Activity

The fraction of paint emitted as an aerosol was estimated using several different data sources. The primary data source is EPA's Dust Study (US EPA, 2007a), which is the most comprehensive study of lead dust generation by renovation activities to date. Other data sources were used to supplement the Dust Study as noted in each subsection below in order to include additional exterior renovation activity types.

D.1.4.1. Jobs Included in the Dust Study

The Dust Study was used to characterize the fraction of lead on the wall that is emitted from the eight exterior renovation activities studied in the report: paint removal by dry scraping, power sanding, torching, use of heat guns, and use of a needle gun, and replacement of exterior doors and trim (US EPA 2007a). In the Approach, particles may be either bulk particles that are larger and remain closer to the renovated building or aerosol particles that are in the size class that can be transported away from the renovated building. Using the Dust Study data, the fraction of removed paint that becomes aerosolized is estimated for each of these activities, as described in Appendix H.

After the activities were processed, emission fractions for both the interior Dust Study experiments and the exterior Dust Study experiment were combined. Because the Dust Study used vertical plastic to encase the job area, the conditions were likely similar to interior jobs. And, because the emission fraction calculations take into account differences in the amount of lead in paint in interior and exterior building environments, the experiments were deemed similar enough that they could be combined across the interior and exterior experiments to estimate an overall fraction. Thus, the power sanding (exterior) and door planing (interior) experiments were combined and the geometric mean across all the different experiments was used to describe a "sanding" emission fraction. Similarly, the geometric mean was taken across the experiments for all other activity types as well.

In addition, the heat gun experiments for both interior and exterior experiments were also combined. The interior calculations revealed that the emission fraction from heat gun activities performed on plaster substrates was considerably higher than the fraction for activities performed on wood substrates. Thus, heat gun experiments were divided into separate plaster and wood activities and the geometric mean across the interior and exterior experiments across each was used for the emission fractions. In the Monte Carlo model, these two different substrate types were sampled assuming equal probability of occurrence to get health effect estimates for a generic heat gun activity.

D.1.4.2. Jobs that Include Local Ventilation (HEPA filters)

In addition to the jobs examined in the Dust Study, the Approach also considers activities where the use of local ventilation (e.g., a HEPA filter) may reduce the emission of lead dust. The Battelle 2009 memo entitled “Effectiveness of Power Tool Shrouds to Reduce Dust Dispersion (DRAFT)” provides a summary of references found during a 2009 literature search that measured the reduction in airborne dust levels or exposure levels after implementation of HEPA filters for a variety of sawing, sanding, and grinding activities. The studies looked at effectiveness when a variety of different surfaces were disturbed, with many studies looking at grinding concrete or mortar. Most of these activities are expected to produce small (e.g., < PM_{2.5}) particles similar to the power sanding, door planing, and needle gun activities in the Dust Study.

The results are fairly consistent, with most results showing efficiencies in the low 90% range. In particular, one study that looked at cut off saws in the construction industry (Thorpe et al 1999). found efficiencies of 90%. Figure D-1 summarizes the findings by study, where the lowest efficiency captured in the study is chosen as representative. The green bar shows the Thorpe et al. study. Based on this range, 90% is deemed an appropriate efficiency for power sanding, door planing, and needle gun activities. This is not at the high end of the range but instead is chosen to be representative of efficiency during actual (rather than hypothetical “best”) use of the LEV equipment.

Some of the studies also looked at implementation of wet techniques compared to dry techniques and found a similar efficiency, so 90% is also deemed appropriate for wet activities.

In order to include these activities that include local ventilation, the estimated emission fraction was -multiplied by (1-efficiency) = 0.10.

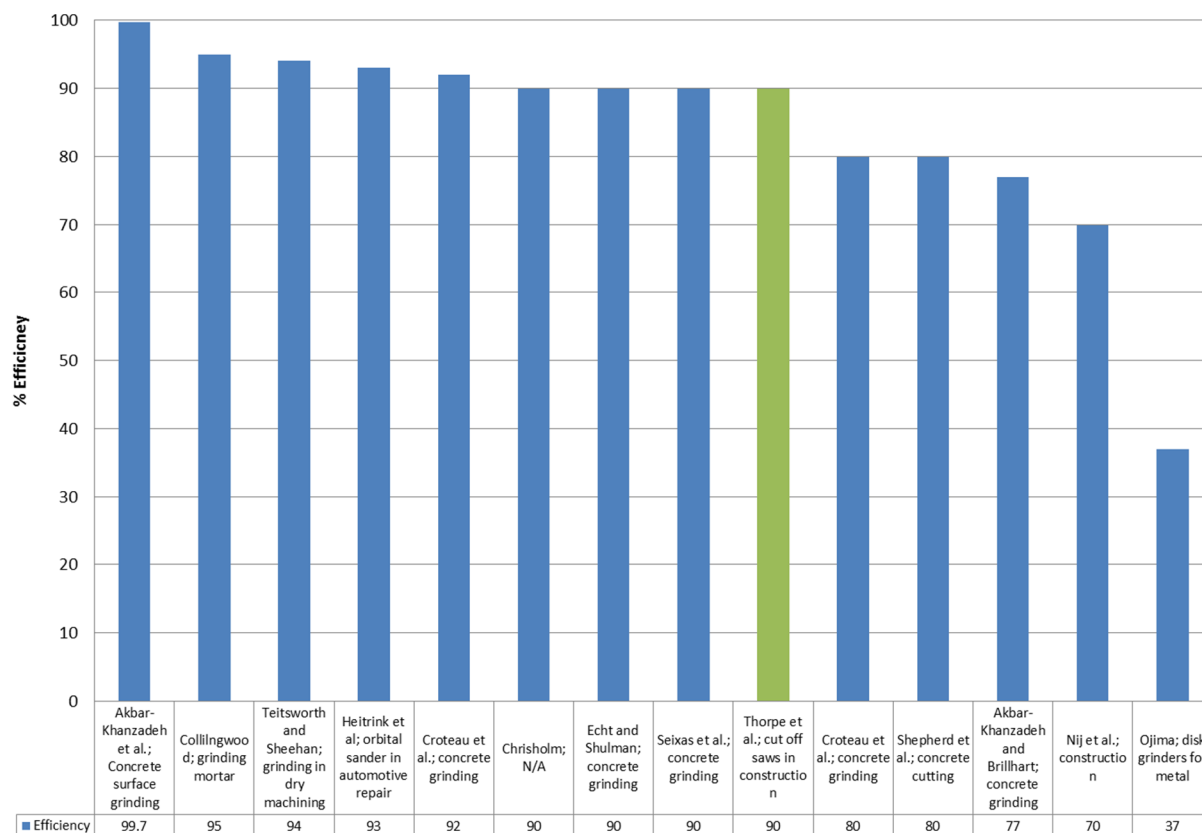


Figure D-1. Summary of HEPA Efficiency Data in the Literature

D.1.4.3. Demolition

Demolition of building walls was not one of the renovation activities included in the Dust Study. However, the literature review report submitted to EPA on January 21, 2011 included sources that measured dust emission from demolition activities. Two studies, Beck *et al.* (2003) and Stefani *et al.* (2005), measured dust generation from the implosion of large structures that were not expected to be analogous to small scale demolition of building walls. Mucha *et al.* (2009) collected dust samples near sites where the demolition of homes was occurring. However, they did not provide information on the size of the demolitions or the proximity of the samplers to the demolition, so it was not possible to calculate an emission rate.

Farfel *et al.* (2003) tracked the lead dust fall rate as measured at 10 m from the renovation during the demolition of two blocks of row houses in Baltimore. In a subsequent paper (Farfel *et al.*, 2005), levels of settled lead dust collected 100 m from demolition sites were measured before, immediately after, and 1 month after demolition were presented.

By subtracting the pre-demolition lead dust level from the measurement taken immediately post-demolition, it was possible to determine the lead dust loading that was attributed to the

demolition. Farfel *et al.* (2003) provides detailed information on the demolition itself, including the vintage of the rowhouses (pre-1950), the dates of the demolitions (10/27/99 and 4/19/2000), the duration (8 hrs), the size (40 m x 50 m, 38 m x 46 m), number of houses demolished (26, 27), and concentration of lead in the paint on the row houses (ranging from below detect to above the limit of quantification, 9.9 mg/cm².)

Because measurements at only 10 m and 100 m were available, the methodology used to calculate emissions for the Dust Study activities could not be applied. Instead, AERMOD was used to estimate an emission rate which would give loading values consistent with the measured values. An AERMOD run was conducted with a unit emission rate which characterized the source using the averaged source data provided by Farfel *et al.* (2003) and meteorological data from <http://www.weatherunderground.com> for the dates of the demolition. Receptors were placed 10 m and 100 m downwind of the demolitions. The hourly deposition rate was calculated at both 10 m and 100 m distances downwind, and these values were summed in time to estimate the cumulative loading after nine hours (eight hours of demolition plus one hour of settling time) to be consistent with measurement methodology in Farfel *et al.* (2003).

The values calculated with the AERMOD run were compared to the Farfel *et al.* (2003) values to back-calculate the emission rates. It was determined that the values measured at 10 m from the renovation were likely much too low. Because 10 m is in the near-field range, particularly considering the extremely large source, it is likely that there is a large amount of variability in these numbers. Because only a limited number of measurements were collected, it was determined that the emission rate based on the 100 m data was more reliable.

The values calculated with AERMOD gave the emission rate in units of mg of lead per second consistent with the demolition of the row houses. However, for a building of different size with a different demolition rate and total square footage and with different lead content in the paint, the lead emission rate per second will be different. The rate of demolition of the row houses was determined by estimating the exterior wall surface area of the row houses using data provided in Farfel *et al.* (2003.) This was estimated at 7,818 m² for the average surface area of building demolished (averaged across the two different demolition events.) The total duration of demolition was 8 hrs, yielding a rate of exterior wall demolition of 2.92 ft²/s. Dividing the lead dust emission rate in mg/s by the demolition rate in ft²/s, results in a lead dust emission rate in units of mg/ft² exterior wall.

The lead loadings measured on different row houses varied widely, as such, the geometric mean lead loading for houses built between 1930 and 1949, 3.77 mg/cm², was used. (The determination of the geometric mean wall lead loadings by building vintage is discussed in Appendix 2.1.1.4.) By dividing the amount of lead emitted, on a per square foot basis, by the

amount of lead on the wall, on a per square foot basis, the aerosol fraction of lead emitted was estimated to be 0.009.

D.1.4.4. Summary and Benchmarking of Results

The resulting fractions of paint emitted as aerosol for each renovation activity is presented in Table D-2. Lee and Domanski (1999) examined the release of lead and abrasives during sandblasting operations to remove lead paint from bridges. They estimated that 9 percent of the lead on the bridge could be released as aerosol due to sandblasting. The emission fractions in this Approach tend to be on the order of this estimate. Power sanding without HEPA, needle gun without HEPA, and torching all predict emission fractions higher than 9%. Overall, the Lee and Domanski (1999) study compares favorably with the magnitudes of the emission fractions estimated here.

Table D-2. Fraction of paint on the wall which is emitted as aerosolized particulate.

Job Type	Fraction of Paint Aerosolized
Power Sanding, without HEPA	0.112
Power Sanding, with HEPA*	0.011
Needle Gun, without HEPA	0.244
Needle Gun, with HEPA*	0.024
Torching	0.180
Heat Gun, Plaster	0.057
Heat Gun, Wood	0.012
Dry Scrape	0.038
Wet Scrape*	0.0038
Window/Door Replacement	0.069
Trim Replacement	0.070
Demolition	0.009

*These emission fractions are estimated using efficiencies applied to the activity above them, as discussed in Section D.1.6

D.1.5. Fraction of Paint Emitted as Particulate Debris by Activity

Small particulate removed during the renovation will be emitted as aerosolized particles. Larger bulk particles will fall to ground during the renovation. The bulk particles themselves, however, may have a wide range of sizes. The largest of these, referred to here as “bulk debris,” are easily seen and picked up, and these will likely be removed during post-job clean-up. In contrast, smaller bulk particles, referred to here as “particulate debris,” will be more difficult to see and clean. Particulate debris may remain on the ground after the job and be available for tracking indoors, depending on the use of horizontal plastic and the efficiency of the plastic in trapping the particulate.

Lee and Domanski (1999) evaluated the removal of lead paint from bridges due to sandblasting and the subsequent release of particles. They estimated that 9 percent of the lead in the paint on the bridge could be released as aerosolized particles. In addition, of the bulk material generated, an additional 6 percent would have an aerodynamic diameter less than 50 μm .

In this Approach it was assumed that the amount of particulate debris available for track-in corresponded to this “less than 50 μm ” size class. In the absence of further information about this fraction in other paint removal activities, the 6 percent value was applied to all the renovation activities. To estimate the fraction of total paint on the wall released as particulate debris, the following equation was used:

$$PartDebFrac = (1 - AerosolFrac) \times 0.06$$

where:

PartDebFrac = fraction of paint on the wall emitted as particulate debris
AerosolFrac = fraction of paint on the wall emitted as aerosol

The final particulate debris fractions by renovation activity are shown in Table D-3.

Table D-3. Fraction of paint on the wall which is emitted as bulk particulate.

Job Type	Fraction of Paint Emitted As Particulate Debris
Power Sanding, without HEPA	0.0593
Power Sanding, with HEPA	0.0533
Needle Gun, without HEPA	0.0585
Needle Gun, with HEPA	0.0454
Torching	0.0492
Heat Gun, Plaster	0.0566
Heat Gun, Wood	0.0593
Dry Scrape	0.0577
Wet Scrape	0.0598
Window/Door Replacement	0.0559
Trim Replacement	0.0558
Demolition	0.0595

D.1.6. Containment Efficiencies

As discussed in the main Approach document, both horizontal and vertical plastic were included as exposure control options. To estimate the horizontal containment efficiency, the Dust Study data for each activity type were used to find the ratio of the loading under the plastic to the loading on top of the plastic, as shown in Table D-4. An average across all activities, or an efficiency of 0.95, was used as a representative horizontal plastic efficiency.

Table D-4. Horizontal containment efficiency.

Renovation Activity	Loading on top of plastic ($\mu\text{g}/\text{ft}^2$)	Loading underneath plastic ($\mu\text{g}/\text{ft}^2$)	Efficiency
Door Replacement	32653	32	0.999
Trim Replacement	44474	648	0.985
Dry Scrape	12004	89	0.992
Needle Gun	7713	270	0.966
High Heat Gun	37431	3149	0.922
Power Sanding	111388	4896	0.957
Torching ¹	5447	8565	0.388
Low Heat Gun	18000	388	0.978

¹Torching data were assumed to be anomalous and not included in calculations.

As discussed in the main document, fewer data were available to calculate the efficiency of dust captured by vertical containment. Iyiegbuniwe *et al.* (2006) presented data for the efficiency of containments used during bridge de-leading by abrasive blasting and found an efficiency of 91% for lead particles. In the absence of additional data, this value was used for the vertical containment efficiency for all renovation activities.

D.2. Interiors

In this Approach, the exposure to lead emitted during interior renovation activities are characterized by the amount of lead emitted, the area over which the lead spreads, and the amount of time the lead loading remains elevated. The variables describing these two variables include floor area in the job area, the fraction of paint removed, the overall building size, the rate of renovation, the fraction of removed paint that remains as lead dust, the efficiencies of any control options used to mitigate the dust, and the relative exposure from floors versus window sills.

D.2.1. Job Intensity

The job intensity describes the fraction of the wall surface area (painting jobs and cutouts jobs), the fraction of the cabinets/shelves (cabinet removal jobs), or the fraction of the windows (window replacement jobs) in the room that are affected by the renovation.

For all jobs, a low, middle, and high intensity were selected. For painting, cabinetry, and windows, representative values of 15%, 50%, and 100% are the representative intensity values. In addition, a very low case was added for painting to account for jobs that just require small paint removal and touch up work within a larger room. For this case, a value of 5% was selected.

For cutouts, it was more difficult to determine what an appropriate intensity range would be. The Approach assumes this activity covers renovation activities involving electrical receptacles and lighting fixtures as well as larger jobs involving creating new windows/doors or performing HVAC work. An internet and literature search was conducted to find construction standards for light fixtures, thermostats, wall outlets, plumbing access, HVAC ductwork, windows, and doors. Very little information on construction standards for these indoor construction additions was found.

However, standards from the International Code Council and the U.S. Government GSA present minimum requirements and provide some guidance that was used to inform the Approach assumptions. Based on the information found for lighting and power receptacle requirements, calculations were made to estimate the fraction of total wall square footage needed to rewire or relight a room. The estimates for lighting are assumed to capture the fraction of the ceiling area, but they are converted to an equivalent wall area for ease of implementation in the Approach. For lighting, the fraction is between 0.004% to 0.2% using the GSA ranges of required power density and the example lighting fixture sizes found in an internet search. For receptacles placed every 6 ft (a conservative assumption based on requirements for a GSA “communication room”), the fraction of wall is 0.2%. Thus, cutouts for installing electrical outlets or ceiling lighting are expected to be less than 1% of the total wall area. Extensive information on cutout sizes for HVAC work could not be found, so an upper range of 10% of wall space was assumed. Comparing this range (< 1% to 10%) with the intensities for the other jobs, the assumption was made that the cutout intensities were 1/10 of the intensities in the other activities. This yielded low, middle, and high estimates of 1.5%, 5%, and 10%.

The range of intensities are shown in Table D-5 In the Approach, renovation scenarios may include one or more job activity types. For the purposes of calculating the fraction of components disturbed during the renovation, the assumption was made that the entire job was either “low”, “middle”, or “high”. For painting jobs only, the “very low” option was also included.

Table D-5. Job Intensities Describing Fraction of Room Components Disturbed During Renovation

Activity Type	Very Low	Low	Middle	High
Paint removal	5%	15%	50%	100%
Cabinetry/shelves	N/A	15%	50%	100%
Cutouts	N/A	1.5%	5%	10%

D.2.2. The Fraction of Paint Removed

In addition to the intensity (fraction of wall area affected), the paint removal jobs also need the fraction of paint layers on the wall that are removed during the renovation. In preparing to paint, the crew may only prepare the surface by removing the degraded top layers of paint or they may remove the paint down to the substrate. To represent surface preparation, a fraction removed of 15% was selected based on the analysis described in Appendix D.1.3. In addition, paint removal fractions of 50% and 100% were included for each paint removal renovation job to cover the range of expected removal fractions.

D.2.3. The Job Area and Exposure for Different Occupants

Within the room being renovated, the effective job floor area over which the lead dust spreads may be equal either the entire room (for smaller rooms and larger jobs) or only a portion of the room (for larger rooms and smaller jobs). To estimate the effective spread of the lead dust, the Dust Study data were examined. As described in Appendix I, experiments where the job area could be identified were used to estimate regression equations. These equations describe the exponential decrease in lead loading with distance from the job wall. These regression equations were examined to find the typical distance where the renovation-related lead loadings reach 5% of their value just next to the job wall. Based on this analysis, a representative value of 10 ft was selected to describe the length of a job out from the wall.

Then, for each renovated room size, the job area was estimated using the following equation, which calculates the floor area in the job area assuming the length of the room is twice the width and making sure not to double count corners:

$$JobArea = intensity \times jobwidth \left(6 \times \sqrt{\frac{RoomArea}{2}} - 4 \times jobwidth \right)$$

where:

- JobArea* = Floor area next to the job walls over which the lead dust spreads
- intensity* = The fraction of the room components being renovated
- jobwidth* = The length of the job area out from the job wall
- RoomArea* = The area of the room being renovated

After estimating this job area, the job area was compared with the overall room area for the different room sizes and job intensities in the interior analysis, as shown in Table D-6. For the job area to be considered different from the room area, a threshold of 3% was applied to the ratios. In these cases, it was deemed reasonable that the job could be thought of as an isolated “room within a room” compared with the remainder of the room area. Based on this threshold, in any cases where the job intensity was 5% and the room size was greater than or equal to 3800 ft², the job size was considered to be smaller than the room size and the activity was treated as a “room within a room” scenario (as shown with the shading in Table D-6). Actual conditions where a “room within a room” scenario would be present are unknown, but could be adjusted at a later time if additional information should become available suggesting either a higher or a lower threshold (i.e. 2%, 4%, 6%, 8%, or 10%).

Table D-6. Comparison of Job Size to Floor Size

Room Floor Area (ft ²)	Room Width (ft)	Room Length (ft)	Job Size 5%	Ratio Job to Floor Size	Job Size 25%	Ratio Job to Floor Size	Job Size 50%	Ratio Job to Floor Size
60	5.5	11.0	3.0	5.0%	15.0	25.0%	30.0	50.0%
200	10.0	20.0	10.0	5.0%	50.0	25.0%	100.0	50.0%
300	12.2	24.5	16.7	5.6%	83.7	27.9%	167.4	55.8%
600	17.3	34.6	32.0	5.3%	159.8	26.6%	319.6	53.3%
1,300	25.5	51.0	56.5	4.3%	282.4	21.7%	564.9	43.5%
1,800	30.0	60.0	70.0	3.9%	350.0	19.4%	700.0	38.9%
3,800	43.6	87.2	110.8	2.9%	553.8	14.6%	1107.7	29.1%
3,900	44.2	88.3	112.5	2.9%	562.4	14.4%	1124.8	28.8%
6,200	55.7	111.4	147.0	2.4%	735.2	11.9%	1470.3	23.7%
8,400	64.8	129.6	174.4	2.1%	872.1	10.4%	1744.2	20.8%
9,100	67.5	134.9	182.4	2.0%	911.8	10.0%	1823.6	20.0%
12,200	78.1	156.2	214.3	1.8%	1071.5	8.8%	2143.1	17.6%

For these “room within a room” scenarios, exposure was estimated for two different theoretical occupants, as shown in the right panel of Figure D-2; in some cases, some occupants will be in

the actual job area (either during or after the renovation event), so exposure is estimated using the lead dust emitted divided by the job area.

$$Lead\ Loading_{job\ area\ occupant} = \frac{LeadEmitted}{JobArea}$$

Equation D-1

Other occupants may be in the remainder of the room and have a relatively small interaction with the renovated-related lead dust. In these cases, the rest of the room is treated as if it were an adjacent room, so these occupants are exposed to the lead dust emitted divided by the rest of the room area and multiplied by the “adjacent factor”.

$$Lead\ Loading_{rest-of-room\ occupant} = \frac{LeadEmitted}{RestofRoomArea} \times AdjFactor$$

Equation D-2

In cases where the job area is the full room area (left panel of Figure D-2), exposure for only a single work room occupant is estimated:

$$Lead\ Loading_{work\ room\ occupant} = \frac{LeadEmitted}{RoomArea}$$

Equation D-3

The location of occupants included in the Approach are:

- In work room, allowed in workspace throughout renovation- exposure begins at the beginning of renovation activity
- In work room, not allowed in workspace throughout renovation- exposure begins after the renovation activity
- In an adjacent room- exposure begins at the beginning of renovation activity

Loadings are estimated for each occupant location in a particular renovated building scenario.

$$Lead\ Loading_{adjacent\ room\ occupant} = \frac{LeadEmitted}{AdjacentRoomArea} \times AdjFactor$$

Equation D-4

The full range of exposed occupants is shown in

Table D-7.

Table D-7. Different Room Occupants During Dust-Generating Phase

Allowed in work area during renovation ?	Work room occupants		Adjacent occupants
	Work area = room area	Work area <> Room Area	
Allowed	- Work room occupant EQ D3	- Job area occupant EQ D-1 - Rest of room occupant EQ D-2	Adjacent occupant EQ D-4
Not Allowed	- Work room occupant Exposure = 0	- Job area occupant Exposure = 0 - Rest of room occupant EQ D-2	



Figure D-2. Diagram of work area with the renovated room.

D.2.4. Mapping Interior Building Types to Exterior Buildings

The exterior analysis covers receptors downwind from a renovated building. However, the exterior renovation can also affect occupants of the renovated building itself. If interior and exterior renovations are going on simultaneously, the occupants may be exposed to lead dust levels elevated by both exterior and interior renovations.

Thus, each interior scenario is simulated three ways:

- Assuming no exterior job is happening simultaneously,
- Assuming a “low” exterior job is happening simultaneously, and
- Assuming a “high” exterior job is happening simultaneously.

For jobs where an exterior renovation is happening, the contribution is added in two different ways:

- The renovation-only dust loading value estimated from an exterior simulation is added in to the post-renovation loadings after the interior job, and
- The track-in of renovation-only soil lead is included throughout the remainder of the interior simulation.

Thus, representative low and high soil and dust levels are needed to represent these exterior jobs. A subset of the full exterior simulations were examined and the 25th and 75th percentile values at the 0ft receptor were calculated to represent these low and high estimates, as shown in Table D-8.

Table D-8. Representative Exterior Renovation-Only Dust and Soil Values for Use in the Interior Analysis

Low (25 th percentile)		High (75 th percentile)	
Dust (µg/ft ²)	Soil (µg/g)	Dust (µg/ft ²)	Soil (µg/g)
6.3	3.9	62.9	27.5

As in the exterior analysis dust model, the track-in loading contribution is estimated as

$$TrackingLoading_{Pb} = \frac{PbSoilConcen \times TrackingRate \times (1 - MatFrac)}{BuildingArea}$$

where:

- TrackingLoading* = accumulation of tracked-in lead loading on the floor in a day (µg/ft²-day)
- PbSoilConcen* = concentration of lead in the tracked-in soil (µg/g)
- TrackingRate* = rate at which particulate is deposited on front mats (g/day)
- MatFrac* = fraction of total tracked material which is deposited on the front mat (as opposed to the remainder of the house)
(unitless)

BuildingArea = the total floor area of the building over which the lead is tracked (ft²)

In order to implement this equation, the total building square footage is needed; however, for the interior Approach, only three rooms of a building are modeled at a time based on the assumption used for this modeling approach that lead dust does not travel further than one room away from the renovated room.

To estimate the total building square footages, the interior building types were mapped to the exterior building model sizes (F1T1, F1T2, F1T3, F2T1, F2T2, F2T3, F3T1, F3T2, or F3T3). The CBECs data (US EIA, 2003) were used to estimate the fraction of total buildings in each building category that were in each size class. Then, these probabilities were cumulative summed to get the cumulative probability distribution, as shown in *Table D-9*. In the Monte Carlo code, a random number is used to select a building size for each building type for each iteration where an exterior job is included.

Table D-9. Probability Distribution for Interior Building Types Mapped to Exterior Building Sizes

Buildings that use Layout	Cumulative Probability								
	F1T1	F2T1	F3T1	F1T2	F2T2	F3T2	F1T3	F2T3	F3T3
SIZE (total floor area in ft²)	1,296	5,184	20,736	2,592	10,368	41,472	3,888	15,552	139,968
1 Office, outpatient healthcare, and public order/safety	0.25	0.38	0.50	0.63	0.75	0.82	0.88	0.95	1.00
2 Warehouse, food sales, religious worship, and public assembly	0.05	0.25	0.38	0.50	0.75	0.82	0.88	0.95	1.00
3 Food service, service, strip shopping mall, enclosed mall, and retail other than mall	0.05	0.25	0.38	0.50	0.75	0.82	0.88	0.95	1.00
4 Education	0.05	0.25	0.38	0.50	0.58	0.67	0.75	0.95	1.00
5 Lodging, Nursing, inpatient health care, and laboratory	0.05	0.12	0.18	0.25	0.38	0.50	0.62	0.75	1.00

D.2.5. Rate of Renovation – Dust Generating Phase

As discussed in Appendix D.1.2, the RSMean Facilities Construction Cost Manual (Mossman and Plotner, 2009) was used to determine the average rates for the renovation activities. The interior analysis utilizes the same surface preparation, window removal, and demolition as used in the exterior analysis. The values are repeated in Table D-10.

Additional activity rates are needed for the interior analysis. For the cabinet/shelf removal activity, the RSMean “minor building deconstruction, kitchen cabinets” entry was used. This

value is 18 linear feet for a 2 person crew per day. Assuming 3 ft high cabinets, this corresponds to a rate of 108 ft²/day.

For the cutouts activity, the RSMMeans “receptacle and switch plates, electrical demolition, remove” entries were averaged. The units in RSMMeans are “output per day” assuming one worker. Assuming the average receptacle is 0.12 ft², this gives an average rate of 4.1 ft²/day for a two person crew.

Table D-10. Rates of Dust-Generating Phase in Interior Analysis

Activity Type	Rate for a Four Person Crew (ft ² /day)
Paint removal	360
Window Removal	336
Cabinet/shelf removal	108
Cutouts	4
Demolition	360

The duration of each activity is then estimated as:

$$Duration_{DustGenerating} = \frac{ComponentArea \times Intensity}{Rate}$$

where:

- Duration_{DustGenerating}* = Duration of the dust-generating phase of the renovation (days)
- ComponentArea* = The area of the component being renovated (wall, cabinet, or window)
- Intensity* = The fraction of the room components being renovated
- Rate* = The rate of renovation (ft²/day)

After the duration is estimated for each separate room and each separate renovation activity, they are summed to give the total duration for the job.

D.2.6. Rate of Renovation – Rest of Renovation Phase

After the dust-generating phase is complete, the Approach assumes the crew proceeds with the rest of the renovation, including painting, installation, etc. To estimate the rest of renovation duration, for each activity, the dust-generating activity was paired with a complementary rest-of-renovation activity from RSMMeans.

For paint removal, RSMMeans interior Paintings and Coatings activities were averaged to get a rate of 1,340 ft²/day for one worker. This gives a corresponding estimate of 5,360 ft²/day for a four person crew.

For windows, the RSMMeans entries for “Windows, replacement” were averaged to give an estimate of 7.2 windows per day for a two person crew. Assuming a window size of 10.24 ft² as in other parts of the Approach, this gives a total of 148 ft²/day for a four person crew.

For cutouts, the RSMMeans entries for installation of “Receptacle Devices” were averaged to give a value of 9.0 receptacles per day for a one person crew. Again assuming a square footage of 0.21 ft² for each receptacle, this gives an estimate of 4.3 ft²/day for a four person crew.

For cabinets, the RSMMeans entries for “Custom Cabinets” were averaged to give a value of twenty cabinets per day for a two person crew. Using the accompanying cabinet dimensions in the RSMMeans entries, this gave an average rate of 239 ft²/day for a four person crew.

For demolition, a general “rebuild” activity rate was estimated using all the other rest-of-renovation rates averaged with additional RSMMeans entries for “Framing” (373 ft²/hr) and “Drywall installation” (70 ft²/hr). Averaging all the rates gave an overall estimate of 1,776 ft²/day for a four person crew.

Each dust-generating and rest-of-renovation activity with the corresponding estimate rates is shown in Table D-11. The rest-of renovation rates were divided by the dust-generating rates and rounded to yield the final “divisor” in the table. To estimate the rest-of-renovation duration, the dust-generating duration is divided by this number:

$$Duration_{RestofRenovation} = \frac{Duration_{DustGenerating}}{Divisor_{Activity}}$$

where:

- $Duration_{RestofRenovation}$ = Duration of the rest-of-renovation phase of the renovation (days)
- $Duration_{DustGenerating}$ = Duration of the dust-generating phase of the renovation (days)
- $Divisor_{Activity}$ = The activity-specific divisor to relate the two durations

As with the dust-generating durations, the rest-of-renovation durations are estimated separately for each room and each activity and then summed to give the total duration.

Table D-11. Rates of Rest-of-Renovation Phase in Interior Analysis

Dust-Generating Activity Type	Rate for a Four Person Crew (ft ² /day)	Rest-of-Renovation Activity Type	Rate for a Four Person Crew (ft ² /day)	Divisor for Rest-of-Renovation Duration
Paint removal	360	Painting	5,360	15
Window Removal	336	Window Installation	148	0.5
Cabinet/shelf removal	108	Cabinet Installation	239	2
Cutouts	4	Receptacle Installation	4	1
Demolition	360	Rebuilding	1,776	5

D.2.7. Fraction of Paint Emitted

The fraction of paint emitted as lead-containing dust was estimated using several different data sources. The primary data source is EPA’s Dust Study (US EPA, 2007a), which is the most comprehensive study of lead dust generation by renovation activities to date. Other data sources were used to supplement the Dust Study, as noted in the subsections below, in order to include additional interior renovation activity types.

D.2.7.1. Jobs Included in the Dust Study

The Dust Study was used to characterize the fraction of lead on the wall that is emitted from the six interior renovation activities studied in the report: paint removal by dry scraping, door planing, and use of heat guns; window removal; cabinet removal, and cut outs (US EPA 2007a). Using the Dust Study data, the fraction of removed paint that remains as small floor dust particulate is estimated for each of these activities, as described in Appendix I.

After the activities were processed, emission fractions for both the interior Dust Study experiments and the exterior Dust Study experiment were combined. Because the Dust Study used vertical plastic to encase the job area, the conditions were likely similar to interior jobs. And, because the emission fraction calculations take into account differences in the amount of lead in paint in interior and exterior building environments, the experiments were deemed similar enough that they could be combined across the interior and exterior experiments to estimate an overall fraction. Thus, the power sanding (exterior) and door planing (interior) experiments were combined and the geometric mean across all the different experiments was used to describe a “sanding” emission fraction. Similarly, the geometric mean was taken across the experiments for all other activity types as well.

In addition, the heat gun experiments for both interior and exterior experiments were also combined. The interior calculations revealed that the emission fraction from heat gun activities performed on plaster substrates was considerably higher than the fraction for activities

performed on wood substrates. Thus, heat gun experiments were divided into separate plaster and wood activities and the geometric mean across the interior and exterior experiments across each was used for the emission fractions. In the Monte Carlo model, these two different substrate types were sampled assuming equal probability of occurrence to get health effect estimates for a generic heat gun activity.

Finally, inspection of the window removal experiments revealed a bimodal pattern, with a group of high emitting experiments and a group of lower emitting experiments. Based on the experiment notes provided in the Dust Study, the higher emitting experiments used saws to remove the window, while the lower emitting experiments used a crowbar or other method to remove the window. Thus, the activity was broken into two separate activities: window, with saw and window, no saw. In the Monte Carlo model, each was assumed to occur with equal probability in a given window removal iteration.

D.2.7.2. Jobs that Include Local Ventilation (HEPA filters)

In addition to the jobs examined in the Dust Study, the Approach also considers activities where the use of local ventilation (e.g., a HEPA filter) may reduce the emission of lead dust. As described in Appendix D.1.4.2, a HEPA efficiency of 0.9 was used in the Approach. In the interior analysis, it was applied to the door planing activity.

D.2.7.3. Demolition

Demolition of building walls was not one of the renovation activities included in the Dust Study. However, the EFSS documents renovation activities performed in houses and the associated loadings (US EPA 1998). The report provides nearly all the information needed to estimate the fraction of emitted paint that lands as small dust particulate. As stated in the report, the demolition experiments were part of the Controlled Experimentally Designed (CED) experiments that were completed in row houses in Baltimore and single-family dwellings in Denver. The EFSS measured both the personal air monitoring concentrations of the workers and the floor loadings after the experiment was completed. Then, an exponential distribution of the loading away from the demolished wall as a function of distance was estimated, and the resulting equations was used to estimate the total amount of lead within 6 feet of the wall.

This equation was then further adjusted in the EFSS report so that it represents the loading from a standardized work area within the room where demolition experiments were conducted. The average amount of lead in the surface substrate in the demolished rooms was also specified in $\mu\text{g}/\text{cm}^2$. So, then, to get the fraction released as:

$$frac_{emitted} = \frac{Loading \times WorkArea}{WallArea \times XRF} \times UnitConv$$

where:

$frac_{emitted}$	=	The fraction of paint removed from the wall that remains on the floor as small dust particles
$Loading$	=	The average lead dust loading on the floor ($\mu\text{g}/\text{ft}^2$)
$WorkArea$	=	The work-area of the renovated room (ft^2)
$WallArea$	=	The wall area of the renovated room (ft^2)
XRF	=	The mass of lead on the wall per unit area ($\mu\text{g}/\text{cm}^2$)
$UnitConv$	=	A term to convert from cm^2 to ft^2

Unfortunately, the EFSS does not provide detailed information about the definition of the “unit” room or about how exactly the conversion was done from experimental results to results for loadings presented in table 8C-10. Thus, the “ $WorkArea$ ” and “ $WallArea$ ” variables are not directly available in the EFSS. The loadings shown in 8C-3, and estimated in EFSS Table 8C-10 are representative of the six foot gradient work area adjacent to the demolition activity.

It was also assumed that the rooms where the demolition activities took place were typical residential rooms with 8 foot ceilings of rectangular shape, 14 feet wide by 28 feet long. In determining the fraction emitted, the same answer is calculated whether you assume the 14 foot wall or the 28 foot wall was demolished.

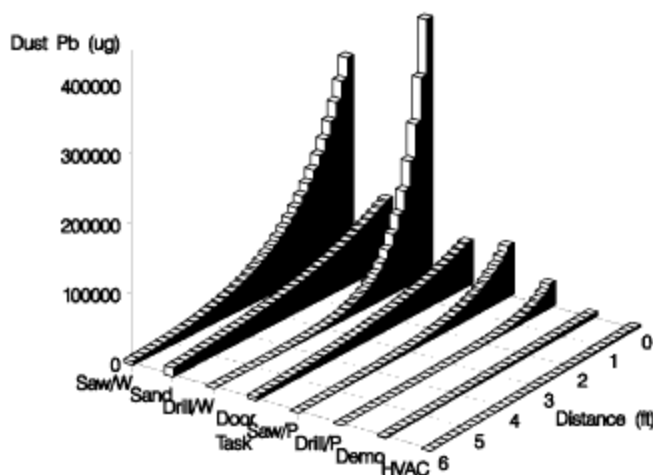


Figure 8C-3. Estimated Lead Fallout Gradient in Settled Dust from 0 to 6 Feet Away from the Edge of the Activity Space

Figure D-3. Copy of EFSS Figure 8C-3 showing the lead dust emitted as a function of distance from the wall for each activity.

Variable	Value for 14 ft Wall	Value for 28 ft Wall	Source
<i>Loading</i>	3,250 $\mu\text{g}/\text{ft}^2$	3,250 $\mu\text{g}/\text{ft}^2$	EFSS Table 8C-10, converting to $\mu\text{g}/\text{ft}^2$
<i>Work Area</i>	84 ft^2	168 ft^2	84 ft^2 = 14 ft. multiplied by 6 ft. 168 ft^2 = 28 ft. multiplied by 6 ft.
<i>Wall Area</i>	104,048 cm^2	208,096 cm^2	104,048 cm^2 = 14 ft multiplied by 8 ft multiplied by 929 cm^2/ft^2 208,096 cm^2 = 14 ft multiplied by 8 ft multiplied by 929 cm^2/ft^2
<i>XRF</i>	840 $\mu\text{g}/\text{cm}^2$	840 $\mu\text{g}/\text{cm}^2$	Geometric Mean from EFSS Table 8C-11
<i>frac_{emitted}</i>	0.0031	0.0031	Equation

So, the estimated fraction of lead on a wall that is emitted as lead dust when the wall is demolished is 0.0031 (or 0.31%).

D.2.7.4. Summary and Benchmarking of Results

The resulting fractions of removed paint that remain on the floor as lead dust for all the interior activities are shown in Table D-12. Activities using a saw or power sander emit the most lead dust, while demolition and cutout jobs emit the least.

Table D-12. Fraction of paint removed that remains as small dust particulate.

Job Type	Fraction of Paint Aerosolized
Window, With Saw	0.2137
Door Planing, without HEPA	0.1118
Heat Gun, Plaster	0.0572
Dry Scrape	0.0380
Window, No Saw	0.0155
Heat Gun, Wood	0.0119
Door Planing, with HEPA	0.0112
Cutouts	0.0056
Cabinet Removal	0.0030
Demolition	0.0031

As mentioned above, the different experiments in the Dust Study (US EPA 2007a) were aggregated for a single activity type by taking the geometric mean across all experiment types. As a quality assurance step, these geometric means were used to try to back-calculate the loading in each room. Then, the estimated loading was compared with the mean measured loading and the range of measured loadings in the room.

Figure D-4 shows the actual loadings versus the predicted loadings for the interior Dust Study experiments. Owing to the wide spread in the values, the graph is shown in log scale. The graph reveals there is no systematic bias between the predicted and experimental loadings. The overall R^2 (estimated using the raw data and not using a natural log transformation) is 0.61. In addition, of the 60 interior experiments, 50 of the predicted mean loadings lay within the overall range of loadings captured in the different sample trays for each experiment. The remaining 10 were examined, but no single reason was apparent for the over or under prediction of the loadings as they were spread across different types of renovation activities and experiment conditions. Overall, this quality assurance step indicated the estimated emission fractions were reasonable and appropriate based on the jobs performed in the Dust Study.

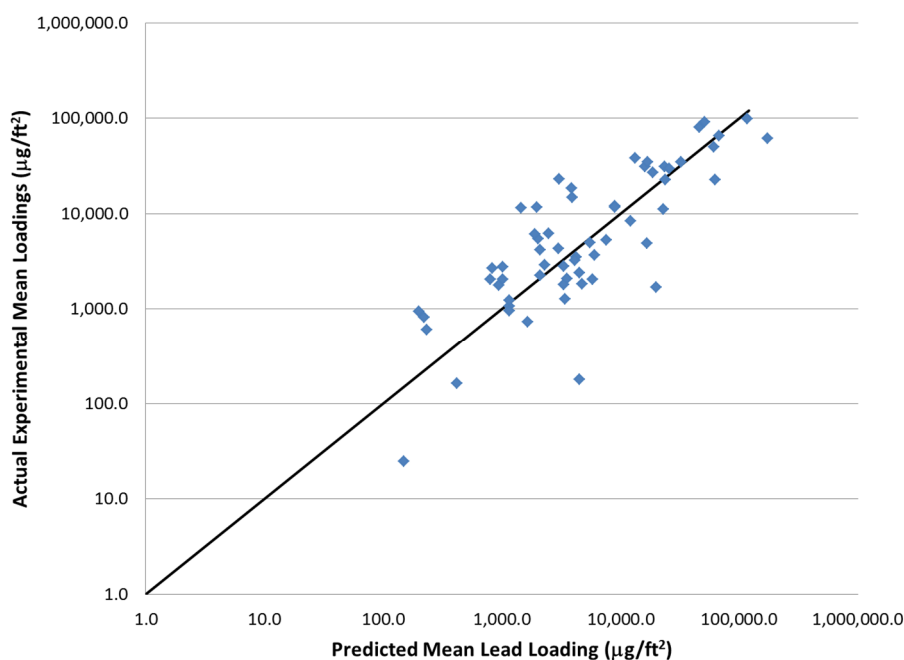


Figure D-4. Actual Experimental Mean Loadings from the Dust Study as a Function of the Predicted Mean Loadings using the Geometric Mean Estimates of Fraction Emitted, Log-log scale

D.2.8. Containment Efficiencies

The Dust Study (US EPA 2007a) considered three different control options to mitigate the occupant exposure to lead dust:

- Horizontal plastic in the work room, covering the floor and removed after the renovation job,
- Vertical plastic over the doorways in the work room, isolating the room from the remainder of the building, and
- Wet mop cleaning with an additional verification step to ensure lead dust was removed to acceptable levels.

These different activities were grouped into four different options:

1. Verification cleaning with horizontal and vertical plastic,
2. Non-Verification cleaning with horizontal and vertical plastic, and
3. Verification cleaning without horizontal or vertical plastic,
4. Non-Verification cleaning without horizontal or vertical plastic.

In the Approach, horizontal and vertical plastic are isolated from each other by assuming that horizontal plastic only affects the work room and vertical plastic only affects the adjacent room. In addition, the cleaning step only affects the work room. Thus, control efficiencies for both the work room and adjacent room need to be calculated for each of the four Dust Study control options. By comparing across two different options, the Approach can isolate the effects from either verification cleaning, horizontal plastic, or vertical plastic.

D.2.8.1. Work Room Control Option Efficiencies

To estimate the work room control option efficiencies, the “post work” and “post cleaning” room-average lead loading results from the Dust Study were compared for each experiment. The post cleaning value represents the value after the room has been cleaned (non-verification or verification cleaning) and the horizontal plastic has been removed (if present). The ratio of the “post cleaning” and “post work” values gives an efficiency factor for the cleaning (mitigation) step for each experiment.

In addition to this data source, an additional data source was located. Grinshpun et al. (2002) looked at different control options after different renovation activities in a chamber study. The authors were contacted and the original data from the experiments were obtained. Air concentrations were continuously measured in a small chamber after doors containing lead based paint were either sanded for dry scraped. Air concentration values were converted to approximate loading values using the equation:

$$FloorLoad \approx AirConc \times DepRate \times ExpDuration \times CeilHeight \times UnitConv$$

where:

$FLOORLOAD_{Pb}$	= Floor lead loading at the end of the experiment ($\mu\text{g}/\text{m}^2$)
$INAIRCONC_{Pb}$	= indoor concentration of lead in air during experiment ($\mu\text{g}/\text{m}^3$)
$DustDep$	= deposition rate (h^{-1})
$ExperimentDuration$	= duration in hours of the experiment (h)
$CeilingHeight$	= height of the ceiling in the renovated room (m)

To estimate the deposition rate, a data source including both air concentrations and dust loadings was used to optimize the depositions for different activity types. The Dust Study air concentrations were used to estimate the dust loadings using the above equations. For each activity type, the depositions were then optimized to give the least mean square error between the predicted and actual mean floor loadings. This gave depositions of 0.09 hr^{-1} for sanding activities and 4 hr^{-1} for scraping activities.

These values were applied to the Grinshpun experiments and the loadings were estimated. Estimated loadings agreed well with measured loadings taken at the corresponding time step. Then, the control options were mapped to the closest Dust Study control option, and the Grinshpun et al. (2002) efficiencies were estimated.

Finally, the geometric mean across the different efficiencies for each control option for the aggregated Grinshpun et al. and Dust Study data were estimated. This gave final control option efficiencies shown in Table D-13. All the different work practice activities provide high efficiencies (>94%), although these efficiencies are applied to very large post-work loading values. Thus, even small differences in the efficiency factors can lead to large differences in exposure after the renovation job is complete.

Table D-13. Work Room Control Option Efficiencies.

Control Option	Efficiency
Verification cleaning with horizontal plastic	0.993
Baseline cleaning with horizontal plastic	0.956
Verification cleaning without horizontal plastic	0.975
Baseline cleaning without horizontal plastic	0.943

D.2.8.2. Adjacent Room Control Option Multipliers

For the adjacent room control options, only the Dust Study (US EPA 2007a) data were used. In this case, the post-work values in the “observation room” and the work room were compared. The ratio was estimated for each experiment in each Dust Study control option and then the average across the experiments was calculated for each control option. Because the ratio was estimated before any cleaning practice was performed, the difference between verification and non-verification cleaning in the work room had no effect. Thus, the final ratios were estimated by taking the geometric mean across control options 1 and 2 (both with vertical plastic) and control options 3 and 4 (both without vertical plastic). The resulting adjustment factors, summarized in Table D-14, are applied to the post-work work room loadings to estimate the associated adjacent room loadings.

Table D-14. Adjacent Room Adjustment Factors

Control Option	Efficiency
With vertical plastic	0.0045
Without vertical plastic	0.0047

D.2.9. Exposure from Window Sills

In the Dust Study, samples were taken both on the floor and on the window sill after renovation experiments (US EPA 2007a). The window sills loadings tended to be much higher than the floor loadings, suggesting exposure to the window sills should be included in the exposure analysis.

First, the ratio between the sill loading and the floor loading in the post-work experiment phase was estimated for each Dust Study experiment. The average across all the different experiments gave a multiplier of 3.86. Thus, in the Approach, the sill loadings are estimated by multiplying the rest-of-renovation loadings by 3.86.

No literature exists describing the relative ingestion from window sills versus floor dust for either children or adults. In lieu of this information, the estimated ratio between the typical window sill surface area and the floor area of public and commercial buildings was used. Assuming that the room is 20% glass (see Appendix C.2.5) and that the windows are of constant height, then the windows extend over 20% of the perimeter. Assuming 4” sills and varying the overall square footage of the room from 200 to 10,000 ft², the sill to floor ratio is between 0.2% and 2%. Thus, a representative value of 1% was selected, and it was assumed the exposure ratio between sill and floor is the same as the ratio in square footage. Thus, the total loading exposure is estimated as:

$$Loading_{exp\ ave} = frac_{floor} \times Loading_{floor} + frac_{sill} \times Loading_{sill}$$

$$Loading_{exp\ ave} = 0.99 \times Loading_{floor} + 0.01 \times 3.86 \times Loading_{floor}$$

where:

$Loading_{exp\ ave}$	= Average lead dust loading the person is exposed to in the renovated building ($\mu\text{g}/\text{ft}^2$)
$Loading_{floor}$	= Lead loading on the floor in the renovated building ($\mu\text{g}/\text{ft}^2$)
$Loading_{sill}$	= Lead loading on the window sills in the renovated building ($\mu\text{g}/\text{ft}^2$)
$frac_{floor}$	= The fraction of the ingestion of dust that is from floors
$frac_{sill}$	= The fraction of the ingestion of dust that is from sills

D.3. References for Appendix D

- Beck C; Geyh A; Srinivasa A; Breyse P; Eggleston P; Buckley T. (2003). The impact of a building implosion on airborne particulate matter in an Urban community. *Journal of the Air and Waste Management Association* 54(10): 1256-1264.
- Capouch S. (2011). Personal Communication by email between Heidi Hubbard of ICF International and Scott Capouch, Construction Project Manager and Professional Engineer with 10 years of experience, of US NIEHS. Title of email: Lead Paint Removal – estimating info. February 2, 2011.
- Farfel M; Orlova A; Lees P; Rohde C; Ashley P; Chisolm J. (2003). A study of urban housing demolitions as sources of lead in ambient dust: demolition practices and exterior dust fall. *Environmental Health Perspectives* 111(1128-1234).
- Farfel M; Orlova A; Lees P; Rohde C; Ashley P; Chisolm Jr. J. (2005). A study of urban housing demolition as a source of lead in ambient dust on sidewalks, streets, and alleys. *Environ Res* 99(2): 204-213.
- Grinshpun et al (2002). Efficiency of Final Cleaning for Lead-Based Paint Abatement in Indoor Environments. *Applied Occupational and Environmental Hygiene*. Volume 17. Issue 3.
- Iyegbuniwe E; Conroy L; Scheff P. (2006). Emission factors development for the control of lead and other metals during bridge paint removal. *Environmental Informatics* 4:244-261.
- Lee and Domanski. (1999). Development of pollutant release estimates due to abrasive blasting for lead paint removal from New York City department of transportation steel bridges, Pittsburg, PA, *Air and Waste Management Association*.

Mossman M; Plotner S; Babbitt C; Baker T; Balboni B, Eds. (2009). RSMMeans Facilities Construction Cost Data.

Mucha A; Stites N; Evens A; MacRoy P (2009). Lead dustfall from demolition of scattered site family housing: Developing a sampling methodology. *Environmental Research* 109(143-148).

Thorpe et al 1999. Measurements of the effectiveness of dust control on cut-off saws used in the construction industry. *Ann Occup Hyg* 43 (7): 443-456.

US EIA (2003) Commercial Building Energy Consumption Survey (CBECS). Available online at: http://www.eia.gov/emeu/cbecs/cbecs2003/public_use_2003/cbecs_pudata2003.html

US EPA. (1998). Risk analysis to support standards for lead in paint, dust, and soil. Appendix G: Health effects associated with exposure to lead and internal lead doses in humans. (Report No. EPA 747-R-97-006). Washington, DC: US Environmental Protection Agency, Office of Pollution Prevention and Toxics. Available online at: <http://www.epa.gov/lead/pubs/toc.pdf>.

US EPA. (2007a). Draft Final Report on Characterization of Dust Lead Levels After Renovation, Repair, Painting Activities. Prepared for EPA's Office of Pollution Prevention and Toxics (OPPT). Available at: <http://www.epa.gov/lead/pubs/duststudy01-23-07.pdf>

Appendix E. Receptor Building Characteristics

The dust model required inputs which were either sampled or which used central tendency estimates, depending on the available data and on the expected sensitivity of the model results on each parameter. The variable values/distributions are discussed further below.

E.1. Receptor Distances

For the exterior analysis, the receptors were assumed to be at a series of distances from the renovated building. Initial scoping runs were done with receptors spaced at 50 ft, 100 ft, 150 ft, 200 ft, 300 ft, 450 ft, 650 ft, 900 ft, 1250 ft, and 3500 ft. Inspection of results indicated very low air, soil, and dust concentrations at distances past 650 ft. For this Approach, a representative set of distances were set at 0ft, 50 ft, 150 ft, 300 ft, 650 ft, and 800 ft. The 0 ft receptor was added as a representation of the impacts on interior dust on the renovated building itself; in the model runs, it was set at a nominal distance of 5 ft from the building perimeter.

E.2. Receptor Types

For the exterior analysis, the receptor types need to cover all P&CBs, child-occupied facilities, and residences that might be located near a renovated building. For the exterior analysis, the buildings were broken into categories based on expected building size and characteristics of the amount of time spent in the building. Buildings need to be included whether they are likely to have lead based paint or not, since these receptor buildings are not the source of the renovation-related lead dust. The chosen categories included:

- Agricultural buildings
- Industrial buildings
- Commercial/Governmental buildings
- Schools, and
- Residences

For interiors, the renovated and receptor buildings are the same building. The selection of building types for that analysis is discussed in Appendix C.2.1.

E.3. Receptor Vintage

The vintage of the receptor building helps determine the background air, dust, and soil values to use in conjunction with the renovation-derived lead media. In this Approach, the background air, dust, and soil values are constant across all the public and commercial buildings owing to a general scarcity of more detailed information in the literature. Thus, the receptor vintage is only

needed for the residential receptors. For those receptors, the Residential Energy Consumption Survey (RECS) was used to estimate the proportion of U.S. homes in each of the analysis vintage bins. In estimating the proportion in each bin, the sample weights provided in the survey were incorporated to ensure the distribution is nationally representative. The resulting cumulative distribution function is shown in Table E-1.

Table E-1. Residential Building Vintage Cumulative Distribution

Cumulative Probabilities for Residential Vintage				
Pre-1930	1930 to 1949	1950 to 1959	1960 to 1979	Post-1979
0.10	0.17	0.29	0.57	1.00

E.4. Receptor Ceiling Height and Building Height

For the exterior analysis, the receptor building ceiling height is needed for the indoor dust model, while the building height is needed to select the appropriate AERMOD run from the choice of three different receptor heights. To select the ceiling heights, the NIST CONTAM example buildings were used. For each building type, the example buildings were used to find a representative ceiling heights; because the example buildings do not cover agricultural or industrial buildings, warehouses were used as a proxy.

The number of stories was estimated using the DOE 2005 Residential Energy Consumption Survey (RECS) (US EIA, 2005) for residences and from the DOE 2003 Commercial Building Energy Consumption Survey (CBECS) (US EIA, 2003) for the public and commercial buildings. The surveys provide information about the numbers of buildings in different story bins. The sample weights were used to estimate the proportion of buildings that are 1 story, 2 stories, or 3 or more stories. The resulting ceiling heights and distribution for number of stories are shown in Table E-2.

Table E-2. Receptor Ceiling Heights and Distribution of Number of Stories

Receptor Type	Ceil. Ht. (m)	Cumulative Probabilities for Height (stories)		
		1	2	3
Agricultural	8.53	1	0	0
Industrial	8.53	1	0	0
Commercial / Government	2.74	0.64	0.89	1.00
Schools	3.35	0.73	0.88	1.00
Residences	2.44	0.58	0.89	1.00

E.5. Receptor Volume

The receptor volume (needed only for the exterior analysis) was taken from the DOE 2005 Residential Energy Consumption Survey (RECS) (US EIA, 2005) for residences and from the DOE 2003 Commercial Building Energy Consumption Survey (CBECS) (US EIA, 2003) for the public and commercial buildings. For CBECS, the different CBECS building types were mapped to the analysis building types as shown in Table E-3. CBECS does not separately report building parameters for agricultural or industrial buildings, so warehouses were used as a proxy for those two building types.

Table E-3. Mapping from Exterior Approach Building Categories to CBECS Categories

ICF Categories	CBECS Categories
Agricultural and Industrial	'05'='Nonrefrigerated warehouse'
	'11'='Refrigerated warehouse'
	'91'='Other'
Schools	'14'='Education'
Commercial/Governmental	'02'='Office'
	'04'='Laboratory'
	'06'='Food sales'
	'07'='Public order and safety'
	'08'='Outpatient health care'
	'12'='Religious worship'
	'13'='Public assembly'
	'15'='Food service'
	'16'='Inpatient health care'
	'17'='Nursing'
	'18'='Lodging'
	'23'='Strip shopping mall'
	'24'='Enclosed mall'
'25'='Retail other than mall'	
'26'='Service'	

The survey reports the square footages, and these were multiplied by the ceiling heights in DOE 2005 Residential Energy Consumption Survey (RECS) (US EIA, 2005) for residences and from the DOE 2003 Commercial Building Energy Consumption Survey (CBECS) (US EIA, 2003) for the public and commercial buildings. The surveys provide information about the numbers of buildings in different story bins. The sample weights were used to estimate the proportion of

buildings that are 1 story, 2 stories, or 3 or more stories. The resulting ceiling heights and distribution for number of stories are shown in Table E-2.

Table E-2 and converted to cubic meters to estimate the volumes. The sample weights in each survey were used when estimating the geometric mean and geometric standard deviation for each building type to ensure the distributions are nationally representative. The resulting volume distributions are shown in Table E-4

Table E-4. Receptor Building Characteristics with Probabilities or Distributions

Receptor Type	Building Volume (m ³)	
	GM	GSD
Agricultural	5227	1.94
Industrial	5227	1.94
Commercial / Government	1371	2.25
Schools	2794	1.86
Residences	391	2.06

E.6. Air Exchange Rate

A literature search was conducted to find appropriate air exchange rates for different types of public and commercial buildings; a few sources were located that provided information, as shown below in Table E-5. However, the IMC and ASHRAE ventilation standards were rejected because they reported in units based on occupancy, a variable that is not captured in the Approach. All other sources were based on small sample sizes or were based on modeling rather than measurements. For this reason, the values from the EPA Exposure Factors Handbook for “non-residential buildings” were used for all the public and commercial building types (industrial, agricultural, commercial/governmental, and schools) while the values from the EPA Exposure Factors Handbook for “residential buildings” was used for residences (US EPA 2011). These values are shaded in Table E-5. For consistency across the two categories, the mean and standard deviation were used to estimate a normal distribution (as opposed to using the geometric mean and geometric standard deviation to estimate a lognormal distribution for residences).

Table E-5. Sources Considered for the Air Exchange Rates

Source	Building Category	N	Mean	StDev	GM	GSD	Range
US EPA 2011 Exposure Factors Handbook (based on Turk et al., 1987)	Non-residential buildings		1.5	0.87			
US EPA 2011 Exposure Factors Handbook	Residential buildings		0.63	0.65	0.46	2.25	
Turk et al 1987	Educational	7	1.9				0.8 to 3.0
	Office (<100k sf)	8	1.5				0.3 to 4.1
	Office (>100k sf)	14	1.8				0.7 to 3.6
	Library	3	0.6				0.3 to 1.0
	Multiuse	53	1.4				0.6 to 1.9
	Commercial (all)	40	1.5	0.87			0.3 to 4.1
EPA BASE Study	Office buildings	100	1.8	2.1			
Fradella et al., 2005	Warehouse	4					0.6 to 2.8
IMC Standards Findings are reported in L/s/person	Educational classroom		15				
	Public assembly space or theatre		15				
	General or office conference room		20				
	Office building office		20				
	Hotel, motel, resort		15				
ASHRAE Standards Findings are reported as minimum cfm/person	Education		7.5-10				
	Office		5				
	Retail		7.5				
	Hotel		5				
	Public assembly		7.5-10				

E.7. Penetration Efficiency

The penetration efficiency has been modeled for particles of various size classes and has been measured in a few field studies to be less than one (e.g., Dockery and Spengler, 1981; Freed *et al.*, 1983; Liu and Nazaroff, 2001). However, unlike the above studies, in a field study that simultaneously controlled for penetration and deposition, the penetration efficiency (P) was found to be near 1 for all size classes (Thatcher and Layton, 1995); a similar result was also

reported for PM_{2.5} for homes in California (Ozkaynak *et al.* , 1996). Thus, the penetration efficiency (*P*) was set to 1 for the mechanistic model.

E.8. Deposition Rate

The deposition rate (*DustModelDep*) was set to 0.65 h⁻¹ based on information in the Exposure Factors Handbook (USEPA, 1997) based on a paper by Wallace (1996). The value for PM₁₀ was selected, as most of the suspended particulate in the home is expected to fall within this size range. The resuspension rate (*A*) of 1.4 x 10⁻⁴ s⁻¹ was taken from values calculated from Thatcher and Layton (1995) for particles between 5 μm and 10 μm.

E.9. Resuspension Rate

The resuspension rate (*R*) varies strongly according to what activity is being undertaken in the home. Resuspension rates during periods where humans are still or absent are lower than during periods of human activity. Vacuuming, in particular, introduces much higher resuspension. For the Approach model, an intermediate value was taken from values calculated in Layton and Beamer (2009) for homes in the NHEXAS Midwest region (1.4 x 10⁻⁴ h⁻¹). This value incorporates the increased resuspension rate during an episode when one person was walking through the room.

E.10. Particulate Tracking Rate

E.10.1. Residences

The particulate tracking term represents the mass of dust being tracked into a building during a day from all occupants who enter the building. For residences, this number was estimated from Von Lindern *et al.* (2003), who measured the amount of particulate deposited on front mats in 276 houses in two locations near the Bunker Hill Superfund Site. The lead levels reported in the paper are expected to be high-end and are not expected to represent general population exposures. However, the assumption is made that the rate of accumulation of dust (as opposed to the lead in the dust) on doormats is not strongly affected by the location and can be used to represent track-in to the receptor locations.

A distribution was developed by combining the data in the two locations in the 1998 site-wide analysis (their Table 4, number 4) and assuming the sample mat was 0.318 m² (as reported in Thatcher and Layton, 1995 for a similar type of analysis). The geometric mean and geometric standard deviation were estimated for the pooled data to be 0.0789 g/day and 2.52, respectively. Since this represents the amount of lead that remained on the doormat in the study, it was divided by the estimated fraction of dirt that remains on a doormat (see Appendix E.11) to get a final distribution with geometric mean and geometric standard deviation 0.61

g/day and 2.52, respectively. The tracking rate was sampled as part of the Monte Carlo analysis with a lognormal distribution.

E.10.2. Public and Commercial Buildings

This track in rate in residences was scaled to other types of P&CB using information inferred about the number of people per household within the 276 homes, how often those individuals entered their home on a given day, and how many people enter a typical P&CB:

$$TrackingRate_{P\&CB} = \frac{TrackingRate_{Residence} \times NumEntries_{P\&CB}}{NumEntries_{Residence}}$$

where:

$TrackingRate_{P\&CB}$	=	Tracking rate into a public and commercial building (g/day)
$TrackingRate_{Residence}$	=	Tracking rate into residences (g/day)
$NumEntries_{P\&CB}$	=	Number of people entering the public and commercial building each day
$NumEntries_{Residence}$	=	Number of people entering the residence each day

Limited information is available within the Von Lindern et al 2003 study on the activity patterns of individuals living within those homes. Information on the number of people per household and the number of times they entered their home per day was estimated from other data sources. The homes were sampled in 1998 from the towns of Smelterville, ID and Kellogg, ID. The American Community Survey has information on the number of people per household for all cities and towns in the United States. However, this information was not collected in 1998. Census data for 1990, 2000, and 2010 on the number of people per household in the State of Idaho is also available. This information is consistent with what is reported in Von Lindern et al 2003, that approximately 84% of the households had less than 3 adults living in the household, and approximately 26% of the households had more than 3 adults. Homes with and without children were sampled, so the number of people per household rather than the number of people per family was chosen as a more appropriate metric. Information from these five data sources were averaged together an average value of 2.48 people per household was chosen, as shown in Table E-6.

Table E-6. Estimates of Numer of People Per Household in Smelterville and Kellogg, ID

Data Source	People Per Household
ACS Smelterville, ID 2008-2013	1.97
ACS Kellogg, ID 2008-2013	2.29
Idaho US Census 2010 people per household	2.66
Idaho US Census 2000 people per household	2.69
Idaho US Census 1990 people per household	2.79
Average	2.48

Information on real-time activity patterns of people and how they move into and out of buildings is limited. Traditional activity pattern data shows how long individuals spend in different microenvironments based on self-reported questionnaires. One study using real-time GPS monitors found a difference in exposures for a full time worker who left and entered their home one time per day, and a stay-at-home parent who left and returned to their home two times per day. (Dons et al 2011). Another study monitored 265 elderly home owners, and found that they left and re-entered their homes an average of 2 times per day over 33 months. (Kaye et al 2011). For this analysis, it was assumed that each occupant of the residences enters and leaves the residence twice a day, so the total number of entries is

$$NumEntries_{Residence} = 2.48 \times 2 = 4.96$$

Then, the estimates were made for the number of entries into public and commercial buildings of different use types. The methodologies are based on a 2010 U.S. Department of Energy (DOE) report analyzing door-opening frequency, *Energy Saving Impact of ASHRAE 90.1 Vestibule Requirements: Modeling of Air Infiltration Through Door Openings* (Cho et al., 2010). The number of times a PnCB is entered is estimated to be half of the door-opening frequency.

Table E-7 presents the door-opening frequency per day for each building type. Building sizes are calculated using the Commercial Buildings Energy Consumption Survey (CBECS). Peak frequencies (persons per hour) are obtained directly from field data or are derived from building occupancy estimates. For retail and strip mall stores, customers are assumed to use the entrance door two times within 1 hour (once when they enter and once when they leave). Therefore, the door-opening frequency during peak hours is twice the occupancy. For all other building types, people are assumed to stay longer than 1 hour in the building, and so the peak door-opening frequency is equal to the number of occupants. It is assumed that off-peak frequency (per hour) is one-tenth of the value during the peak hour for all buildings except for restaurants and hospitals, which do not use peak and off-peak hours in their frequency calculations. A schedule of peak and off-peak operating hours for each building was derived

from *Energy Saving Impact of ASHRAE 90.1 Vestibule Requirements: Modeling of Air Infiltration Through Door Openings* (Cho et al., 2010).

The average daily door-opening frequency is the sum of the frequency for all peak building hours and the frequency for all off-peak building hours each day. Because the door-opening schedule differs for weekdays and weekends for some buildings, the average door-opening frequency is also weighted by day of the week.

Table E-8 presents estimates for the frequency of entries per day, which are assumed to be half of the total door-opening frequency, for each exposure group. A building's average frequency of entries per square foot per day is weighted by its relative prevalence within an exposure group, and scaled up to the average building size for the group to estimate average entries per day for each exposure group, with the exception of exposure group 2. For exposure group 2, a building's entries per day is estimated without scaling because the size of industrial and agricultural buildings is unknown. The derivation of the inputs used to estimate entries for each P&CB is described in more detail below.

E.10.2.1. Office

The number of workers for small office, medium office, large office, and warehouse buildings are based on the Commercial Buildings Energy Consumption Survey (CBECS) data by the Energy Information Administration (EIA) (EIA, 2003).

E.10.2.2. Quick-Service and Sit-down Restaurant

The number of customers visiting quick-service and sit-down restaurants is derived from a field study by Claar et al (1985). Claar et al. (1985) reports an average of 898 daily customers for quick service restaurants and 284 daily customers for sit-down restaurants. For quick-service restaurants, it is assumed that half of the customers will use the drive-through. Therefore, an estimated 449 customers ($898/2$) visit quick-service restaurants and 284 ($568/2$) customers visit sit-down restaurants daily. If customers enter once and leave once per visit, the door-opening frequency for customers is 898 for quick-service and 568 for sit-down restaurants.

According to the Bureau of Labor Statistics Quarterly Census of Employment and Wages, the average number of employees per establishment is 15.37 for limited-service restaurants and 20.36 for full-service restaurants (BLS, 2013b; BLS, 2013c). If employees enter and leave the restaurant once per day, the door-opening frequency for employees is 30.74 ($15.37 * 2$) and 40.72 ($20.36 * 2$) for quick-service and sit-down restaurants, respectively.

The average door-opening frequency for quick-service and sit-down restaurants is the sum of the frequencies for customers and employees.

E.10.2.3. Strip Mall and Stand-alone Retail

Field data from Yuill (1996) indicate an average door-opening frequency of 153 openings/hour for stand-alone retail stores. If it is assumed that customers do not stay longer than one hour, each customer will use the entrance door two times within one hour. Therefore, occupancy is estimated to be half of the average door-opening frequency: 76.5.

The strip mall is assumed to have the same number of people per entrance zone area as the stand-alone retail store. Based on the DOE retail prototype, the entrance zone area is about 69.8 percent of the total store area (U.S. DOE, 2010). The area occupied per person for stand-alone retail is determined to be 91.4 ft² ($[69.8\% * 10,028 \text{ ft}^2] / 76.5$). Therefore, the occupancy for a stripmall is 177 ($69.8\% * 23,223 \text{ ft}^2 / 91.4$).

E.10.2.4. Secondary School

The number of staff for secondary schools is derived from the CBECES data (EIA, 2003). The national average of teacher-to staff ratio in 2009 was 0.505, and the national average of student to teacher ratio was 15.4 (U.S. Department of Education, 2012a; U.S. Department of Education, 2012b). The number of students is estimated using these two ratios, and the total school occupancy is the sum of the number of students and staff.

E.10.2.5. Small and Large Hotel

Based on the CBECES data, small hotels have an average of 4.82 staff members and 29.7 rooms available, and large hotels have an average of 47.5 staff members and 127 rooms available (EIA, 2003). It is assumed that the hotels have a 65 percent occupancy rate and 1.5 guests stay in each room (American Hotel and Lodging Association, 2007). Therefore, approximately 29.0 guests stay at the small hotel ($29.7 * 65\% * 1.5$) and approximately 124 ($127 * 65\% * 1.5$) stay in the large hotel. The occupancy of small and large hotels is the sum of the number of staff and guests.

E.10.2.6. Hospital

An average of 470 employees work during the main shift for inpatient care facilities (EIA, 2003). Because hospital employees work in shifts, the peak and off-peak operating schedule is not applied. We assume that staff work 8 hour shifts (i.e. three shifts per day) and that the number of staff working the night shift is half the number working the main shift. If each employee enters the hospital once and leaves once per day, then the door-opening frequency for workers is 2350 ($(470 * 2 * 2) + (470 / 2 * 2)$).

An average of 20.82 people are discharged from the hospital per day (U.S. Department of Health and Human Services, 2010). It is assumed that the number of people admitted per day is equal to the number of people discharged per day. Thus, the door-opening frequency for non-ER patients is 41.64 ($20.82 * 2$).

In addition, an average of 68.82 people visit the Emergency Department per day and 58.29 people are discharged daily (U.S. Department of Health and Human Services, 2010). Therefore, 10.53 people per day are admitted to the hospital from the ER. These 10.53 people are assumed to be included in the number of people admitted to the hospital per day; therefore, to avoid double-counting, it is assumed that the number of people who are discharged from the ER is equal to the number of people who enter. Note that these ER discharges are distinct from the 20.82 non-ER discharges. Thus, the door-opening frequency for ER patients is 116.58 ($58.29 * 2$).

The average door-opening frequency for the hospital is the sum of the frequencies for employees, non-ER patients, and ER patients.

E.10.2.7. Outpatient Health Care

The average door-opening frequency is estimated to be 123 openings/hour, based on field data from Yuill (1996).

E.10.2.8. Warehouse- Industrial Buildings

Employee and establishment data for the industrial sector are retrieved from the U.S. Census Bureau 2009 County Business Patterns (CBP) and a report that estimated the universe of P&CB buildings, the methodology of their report is described in Appendix Q (U.S. Census Bureau, 2009). The CBP data indicate 12,879,161 employees in the industrial sector. See Appendix Q for methods that estimated 2,400,604 industrial buildings. Occupancy is therefore 5.36 people per building.

E.10.2.9. Warehouse- Agricultural Building

According to the CBP data, there are 153,829 employees in the agricultural sector (U.S. Census Bureau, 2009). See Appendix Q for methods that estimated 7,877,314 agricultural buildings. Therefore, the occupancy is 0.02 people per building.

E.10.2.10. Supermarket

According to the Food Marketing Institute (FMI), median weekly sales and weekly sales per transaction are \$318,170 and \$35.01, respectively (FMI, 2012). This implies an average of 1,298 customers per day ($[\$318,170/\$35.01]/7$), and .028 customers per square foot per day ($1,298/46,000 \text{ ft}^2$; FMI, 2012). We calculate the customers per day in an 8,314 ft^2 supermarket to be 234.65 ($8,314 \text{ ft}^2 * .028$). Including an average of 10.94 employees entering the building once per day, the total door-opening frequency per day is estimated to be 491.18 ($[(234.65 + 10.94) * 2]$; EIA, 2003).

It should be noted that some estimations in this analysis make use of older data, such as the 1996 field-study by Yuill and the 1985 study by Claar et al. Due to industry changes since the time of data collection, it is possible that the current average occupancy of the buildings differs from the estimates used in this analysis. In addition, the door-opening frequencies for some

buildings are likely to be greater than the estimates listed in Table E-7. This is due to additional visitors that are not included in the peak occupancy count. For example, hospital visitors, apartment visitors, and restaurant food suppliers are not included in occupancy estimates. Furthermore, many large hotels frequently host conventions, conferences, and other events which are not considered in the frequency estimates.

Table E-7. Average Door-Opening Frequency for 16 PnCBs

Building Category ¹	CBECS Average Floor Area (ft ²)	Number of Peak Hours		Number of Off-Peak Hours		Peak Occupancy (persons)	Peak Frequency (persons per hour)	Off-Peak Frequency (persons per hour)	Average Frequency per day	Derivation of Average Frequency
		Week-day	Week-end	Week-day	Week-end					
		(a)	(b)	(c)	(d)					
SOFF	5,951	3	0	10	0	13.39	13.39	1.3393	38.27	$([5 * [(a)(f) + (c)(g)]] + [2 * [(b)(f) + (d)(g)]]) / 7$
MOFF	71,909	3	0	10	0	171.82	171.82	17.1825	490.93	$([5 * [(a)(f) + (c)(g)]] + [2 * [(b)(f) + (d)(g)]]) / 7$
LOFF	655,409	3	0	10	0	1,487.25	1,487.25	148.7249	4,249.28	$([5 * [(a)(f) + (c)(g)]] + [2 * [(b)(f) + (d)(g)]]) / 7$
OUTP	10,409	11	0	2	0	123.00	123.00	12.3000	984.00	$([5 * [(a)(f) + (c)(g)]] + [2 * [(b)(f) + (d)(g)]]) / 7$
WH	21,603	3	0	10	0	10.26	10.26	1.0255	29.30	$([5 * [(a)(f) + (c)(g)]] + [2 * [(b)(f) + (d)(g)]]) / 7$
WH (Ind.)	N/A	3	0	10	0	5.36	5.36	0.5365	15.33	$([5 * [(a)(f) + (c)(g)]] + [2 * [(b)(f) + (d)(g)]]) / 7$
WH (Ag.)	N/A	3	3	10	10	0.02	0.02	0.0020	0.08	$([5 * [(a)(f) + (c)(g)]] + [2 * [(b)(f) + (d)(g)]]) / 7$
SUP	8,314	N/A	N/A	N/A	N/A	N/A	N/A	N/A	491.18	$2 * (((((318,170/35.01)/46,000)/7) * 8314) + 10.94)$
QSR	3,345	N/A	N/A	N/A	N/A	N/A	N/A	N/A	928.74	$(898 * 2/2) + (15.37 * 2)$
FSR	6,585	N/A	N/A	N/A	N/A	N/A	N/A	N/A	608.72	$(284 * 2) + (20.36 * 2)$
SART	10,028	8	8	4	4	76.50	153.00	15.3000	1,285.20	$([5 * [(a)(f) + (c)(g)]] + [2 * [(b)(f) + (d)(g)]]) / 7$
STRIP	23,223	8	8	4	4	177.16	354.33	35.4326	2,976.34	$([5 * [(a)(f) + (c)(g)]] + [2 * [(b)(f) + (d)(g)]]) / 7$
SSCL	37,024	2	0	9	0	235.98	235.98	23.5981	488.82	$([5 * [(a)(f) + (c)(g)]] + [2 * [(b)(f) + (d)(g)]]) / 7$
SHTL	14,990	3	3	13	13	33.77	33.77	3.3768	145.20	$([5 * [(a)(f) + (c)(g)]] + [2 * [(b)(f) + (d)(g)]]) / 7$
LHTL	97,102	3	3	13	13	171.34	171.34	17.1340	736.76	$([5 * [(a)(f) + (c)(g)]] + [2 * [(b)(f) + (d)(g)]]) / 7$
HOS	241,416	N/A	N/A	N/A	N/A	N/A	N/A	N/A	2,513.11	$(471 * 2 * 2) + (471/2 * 2) + (20.82 * 2) + (58.29 * 2)$

¹SOFF — Small Office; MOFF — Medium Office; LOFF — Large Office; HOS — Hospital; WH — Warehouse (Ind.=Industrial; Ag.=Agricultural); SUP — Supermarket; QSR — Quick Service Restaurant; FSR — Fast Service Restaurant; STRIP — Strip Mall; SSCL — Secondary School; OUTP — Outpatient Healthcare; SHTL — Small Hotel; LHTL — Large Hotel; SART — Stand-alone Retail

Note: Values may not calculate exactly due to rounding

Table E-8. Estimated Entries Per Day for Each Building Category

Building Category ¹	CBECS Average Floor Area (ft ²)	Exposure Group	Average Frequency of Entries per ft ² per day	CBECS Building Frequency		Building Weight	Weighted Entries per ft ² per day ²	Weighted CBECS Average Floor Area (ft ²)	Entries per day
				Building Category	Exposure Group				
SOFF	5,951	1	0.003215	756,965	944,624	80.13%	0.008863	14,255	126.3
MOFF	71,909		0.003414	61,875		6.55%			
LOFF	655,409		0.003242	4,965		0.53%			
OUTP	10,409		0.047266	120,819		12.79%			
WH	21,603	2	0.000678	384,012	10,747,915	3.57%	N/A	19,172	4.229
WH (Ind.)	N/A		N/A	2,400,604		22.34%			
WH (Ag.)	N/A		N/A	7,877,314		73.29%			
SUP	8,314		.029539	85,985		0.80%			
QSR	3,345	3	0.138846	78,190	795,451	9.83%	0.067810	12,147	823.7
FSR	6,585		0.046218	161,213		20.27%			
SART	10,028		0.064081	346,625		43.58%			
STRIP	23,223		0.064081	209,423		26.33%			
SSCL	37,024	4	0.006601	68,014	68,014	100.00%	0.006601	37,024	244.4
SHTL	14,990	5	0.004843	69,949	97,447	71.78%	0.004661	49,845	232.4
LHTL	97,102		0.003794	19,607		20.12%			
HOS	241,416		0.005205	7,890		8.10%			

¹SOFF — Small Office; MOFF — Medium Office; LOFF — Large Office; HOS — Hospital; WH — Warehouse (Ind.=Industrial; Ag.=Agricultural); SUP — Supermarket; QSR — Quick Service Restaurant; FSR — Fast Service Restaurant; STRIP — Strip Mall; SSCL — Secondary School; OUTP — Outpatient Healthcare; SHTL — Small Hotel; LHTL — Large Hotel; SART — Stand-alone Retail

²For exposure group 2, weighted entries per ft² per day cannot be calculated because the size of industrial and agricultural buildings is unknown.

Note: Values may not calculate exactly due to rounding

Based on the above information, the residential particulate track-in rate distribution was scaled for each of the analysis public and commercial building types. The final distributions are shown in Table E-9.

Table E-9. Particulate Tracking Rate for Analysis Receptor Types

Analysis	Receptor Type	Geometric Mean (g/day)	Geometric Standard Deviation
Exterior	Agricultural	1.79	2.52
	Industrial	1.79	2.52
	Commercial/Governmental	61.99	2.52
	Schools	29.91	2.52
	Residences	0.61	2.52
Interior	Office, service, outpatient healthcare, and public order/safety	15.45	2.52
	Warehouse, food sales, religious worship, and public assembly	0.52	2.52
	Food service, strip shopping mall, enclosed mall, and retail other than mall	100.79	2.52
	Education	29.91	2.52
	Lodging, Nursing, inpatient health care, and laboratory	28.44	2.52

E.11. Fraction of Dirt Remaining on Floor Mat

Some fraction of dirt tracked into a building will be deposited on a floor mat near the entry way. To estimate this fraction, the Approach uses Thatcher and Layton (1995), which measured the difference between particulate accumulation in tracked and untracked areas in the home as well as the amount on the front mat. The assumption was made that 75 percent of the home will contain tracked dirt, and the other 25 percent consists of corners or other less accessible areas in which people do not walk as frequently. Using this assumption and the information about the amount of mass on the front mat, the tracked areas of the home, and the untracked areas of the home in Thatcher and Layton (1995), an estimated 13 percent of tracked-in mass remains on the front mat and 87 percent is carried into the homes. To account for the variability within the universe of building types, it was assumed that some buildings have floor mats and some do not. In the absence of data for this variable, it was assumed that 50% of all buildings had front mats and 50% did not.

E.12. Percentage of Building that is Carpeted

The percent of a residence that is carpeted was derived from two different data sources. First, data taken from the National Survey of Lead and Allergens in Housing indicate that nearly all

homes (over 90%) had some carpeting or rugs in one or more of the rooms sampled (HUD 2002). The arithmetic mean of the percent of area carpeted was 52% (EPA 2008).

The second method used a typical home layout and estimated upper and lower bounds of typical carpeting based on assigning each room as either carpeted, not carpeted, or having a specific probability of being carpeted. Two methods were used to estimate the overall square footage of a typical home. The first method used the average whole house volume of 492 m³ presented in the EPA 2011 Exposure Factors Handbook (EPA 2011). Estimates for room volumes are available from standard consumer exposure models (EPA 2007), and were scaled up to match the 492 m³ whole house volume. Room volumes were divided by 2.59 meters (assuming 8.5 ft. ceilings) and multiplied by 10.76 to convert from meters squared to feet squared.

The second method used the generic floor plan for a single home presented in EPA's Formaldehyde Indoor Air Model and estimated total square footage within different room types. Both methods assumed that kitchens, bathrooms, and utility rooms are always non-carpeted, that living rooms/dens, bedrooms, and dining rooms are always carpeted, that hallway and stair spaces have a 50% chance of being carpeted, and that storage closets, garages, and attics have a 25% chance of being carpeted. These methods yielded percent carpeting estimates of 57% and 59% (Table E-10), both of which support the estimate derived from HUD National Survey of Lead and Allergens data. In the Approach, residences were represented as being carpeted 52% of the time and hard surface flooring the other 48% of the time.

Table E-10. Estimate of Percent Carpet Using a Typical House Layout

Method 1						
Room Type	Room Volume	Room Size	Number of Rooms	Total Square Footage	Carpet, Non-Carpet, Mix	Percent Carpet
Bedroom	36	150	3	449	Carpet	57%
Living Room, Den	48	199	2	399	Carpet	
Bathroom	18	75	2	150	Non-Carpet	
Laundry Room, Utility Room	20	83	2	166	Non-Carpet	
Dining Room	20	83	1	83	Carpet	
Kitchen	36	150	1	150	Non-Carpet	
Hallway, Stairwells, Closets	70	291	1	291	Mix (Assume 50%)	
Storage Closets, Garage, Attic	86	357	1	357	Mix (Assume 25%)	
	492	n/a	n/a	2044		

Method 2			
Room Type	Square Feet	Carpet, Non-Carpet, Mix	Percent Carpet
Bedrooms (3)	562	Carpet	59%
Living Room (1)	203	Carpet	
Bathroom (2.5)	154	Non-Carpet	
Laundry Room (1)	20	Non-Carpet	
Dining Room (1)	145	Carpet	
Kitchen (1)	150	Non-Carpet	
Hallway (3), Stairwells (1)	109	Mix (Assume 50%)	
Storage Closets (3), Garage (1), Attic (0)	489	Mix (Assume 25%)	
	1832		

For public and commercial buildings, the Commercial Flooring Maintenance Report (Cirpus, 2013) was used. The publisher provided estimates of the percentage of different building types that are carpeted in the United States. These estimates were used to create cumulative distribution functions for the probability a building is carpet or hard surface flooring, as shown in Table E-11. These estimates were obtained for the exterior analysis building types only; in the interior analysis, the carpeting status is treated as a scenario variable, with separate results provided for carpeted and non-carpeted floor types.

Table E-11. Cumulative Probability Distribution For Flooring Type in Public and Commercial Buildings and Residences

Receptor Type	% Carpet		Data Source
	All Carpet	All Floor	
Agricultural	0.08	1	Cirpus 2013
Industrial	0.08	1	Cirpus 2013
Commercial/Governmental	0.45	1	Cirpus 2013
Schools	0.27	1	Cirpus 2013
Residences	0.52	1	HUD 2002

E.13. Cleaning Frequency

Cleaning frequency (*CleanFreq*) represents a particularly sensitive variable, so a literature search was undertaken to identify all readily available data sources for residences and P&CBs.

In residences, there are two sources of data on cleaning frequency reported in the Exposure Factors Handbook (USEPA, 2011). The first is the National Human Activity Pattern Survey. One

of the questions in the follow-up questionnaire for this Survey was the “frequency that floors were swept or vacuumed.” There were 4,663 respondents for this question, although a subset of these respondents comprised young children less than 11. Respondents in the top three age categories (12-17, 18-64, and >64) were believed to better represent individuals who most often clean. Thus, results are broken out by all respondents and respondents over age 11.

Available survey responses were not a specific frequency, but ranges: nearly every day, three to five times a week, once or twice a week, once or twice a month, less often, never, or don’t know. In order to estimate distributions of cleaning frequency from the survey, each of these ranges was represented by a single point estimate in the middle of the range, as shown below in Table 1. For the cases that were unbounded (less often, never, and don’t know), we chose to represent the ranges as “once every two months”, “once every year”, and “not available”, respectively. All individuals for which data were not available were excluded from the analysis. The data from respondents above the age of 11 were used estimate the average, median, and standard deviation values are presented in Table E-13-1.

The second data source on cleaning frequency reported in the Exposure Factors Handbook is the National Usage Survey of Household Cleaning Products. Respondents were asked how frequently they performed various cleaning tasks. Two of the tasks were cleaning bathroom floors and cleaning kitchen floors. These are reasonable surrogates for cleaning frequency of floors. The results are shown in Table E-13-1.

In addition, there are two newer data sources that were not available at the time the 2011 version of the Exposure Factors Handbook was being compiled. The Michigan Department of Community Health initiated a Home-Based Environmental Intervention and Education program for Families with Pediatric Asthma in Michigan. 234 respondents were asked how frequently they vacuumed their child’s bedroom and other rooms of the home at baseline and after a six month intervention. The mean and standard deviation values are reported in Table E-13-1 (Largo et al 2011).

As part of the Study of Use of Products and Exposure Related Behavior (SUPERB) study, California residents were asked questions about their cleaning habits. The population was comprised of two general groups: households with parents of young children and households with older adults. Results were further split based on whether the primary cleaner was a man or a woman. The mean, standard deviation, median, and 90th percentile values are reported in Table E-12 (Moran et al 2012).

Across these four studies, there is a large range of cleaning frequencies in residences. The standard deviations, when available are large compared with the means, indicating significant

variability. The means are also larger than the medians, suggesting a larger percentage of residences may be cleaned more frequently rather than less frequently.

Table E-12. Summary of Cleaning Frequencies from Available Data Sources for Residences. Times per month

Data Source and Activity		Median	Mean	Standard Deviation
Exposure Factors Handbook 2011: NHAPS, adults only, "vacuum"		8	11.4	8.5
Exposure Factors Handbook 2011: National Usage Survey, Clean kitchen or bathroom floor		4	6	
Moran et al 2012., women, houses with young children	Dry Mop hard floors	4	7.2	7.6
	Wet Mop hard floors	4	6.4	8.4
	Sweep Hard floors	12	14.2	11.5
	Vacuum hard floors	4	7.3	6.9
	Vacuum carpet	5	9.0	8.0
Moran et al 2012., women, older adults	Dry Mop hard floors	4	5.4	5.6
	Wet Mop hard floors	4	4.5	5.6
	Sweep Hard floors	4	8.6	8.0
	Vacuum hard floors	4	5.2	5.8
	Vacuum carpet	4	4.7	4.7
Largo et al 2011 Michigan	Vacuuming floor in child's bedroom		3.2	2.1
	Vacuuming floor in other rooms		3.8	1.9

In public and commercial building, sources of cleaning frequency data include the ISSA, the worldwide cleaning industry association, the GSA, and the cleaning schedules from various universities. The information contained in the ISSA's CompuClean calculator suggests that the maximum cleaning frequency of public and commercial building floors would be 260 days per year, every working day, or approximately 5 days per week. This value is generally supported by information available in GSA standard leases, which apply to most government buildings. Other types of buildings, including retail space and warehouses, may be cleaned more or less frequently for various reasons. However, data is generally not available for these types of buildings. Readily available information on cleaning frequency is summarized in Table E-13.

Table E-13. Summary of Cleaning Frequencies from Available Data Sources for Public and Commercial Buildings

Data Source	Narrative	Cleanings per Week
The Carpet and Rug Institute's Carpet Maintenance Guidelines For Commercial Applications	lower traffic areas: vacuum 2 to 3 d/wk	2
The Carpet and Rug Institute's Carpet Maintenance Guidelines For Commercial Applications	high traffic area: vacuum daily	5
GSA Property Managers Book, COF	sweep, mop, or scrub floor; thoroughly vacuum all carpet daily	5
GSA Standard Lease, Section 6-07	sweep, spot vacuum carpets; clean restroom fixtures, floors daily	5
ISSA 540 Cleaning Times As Used in CompuClean v10	Carpet spot cleaning, vacuuming, 260 d/y	5
Purdue University	vacuum carpet, dust mop floors weekly	1
Purdue University	conference rooms: vacuum carpet, dust mop floors weekly	1
Purdue University	libraries: vacuum carpet 2 d/wk	2
Purdue University	Auditoriums: Vacuum 3 d/wk	3
Purdue University	classrooms and conference rooms: daily (mopping floors; spot vacuuming)	5
Purdue University	dust mop floors 2 d/wk; wet mop 1 d/wk	1
Purdue University	vacuum, dust mop floors 3 d/wk	3
Purdue University	Childcare facility: Vacuum and dust mop daily	5
University of Minnesota	vacuum and mop 1 d/wk	1
University of Minnesota	classrooms and conference rooms: vacuum and mop 1 d/wk	1
University of Minnesota	autoscrub, mop public floors daily	5
Kettering University	vacuum, dust/spot mop hard floors in office suites & lounges 2 d/wk	2
Kettering University	general cleaning 5 d/wk (vacuum, mop)	5
Tulane University	daily (mopping floors; spot vacuuming)	5
ISSA 540 Cleaning Times As Used in CompuClean v10 Healthcare	365 days per year	7
ISSA 540 Cleaning Times As Used in CompuClean v10 Lodging	365 days per year	7
Suffield, CT Green Cleaning Program	School: Clean classrooms 3 d/wk	3
Stratford, CT Green Cleaning Program Statement	School: Clean classrooms daily	5
ISSA 540 Cleaning Times As Used in CompuClean v10 Schools	School: 180 d/y	2

An overall range of cleaning frequencies was constructed based on available data and matched to the different building types. To match each one, a central estimate was found using the most commonly reported cleaning frequency for that building type in the literature. Then each

building type was assigned to other surrounding frequency bins according to the approximate range in the literature. In order to complete the distribution, the probability that a given building is in each category must be assigned. These weights were assigned assuming the central frequency had the highest probability and the probabilities tapered linearly in both the lower and higher frequency directions. The distributions are shown in Table E-14.

Table E-14. Cleaning Frequency Distributions by Building Type

Analysis	Receptor Type	Cleaning Frequency				
		Every working day (5 days/week)	Every third day (approx) (2 days/week)	Every week (1 day/week)	Every other week (1 day/2 weeks)	Every fourth week (1 day/4 weeks)
Exterior	Agricultural	0.1	0.3	0.7	0.9	1.0
	Industrial	0.2	0.6	0.8	0.9	1.0
	Commercial/Governmental	0.2	0.6	0.8	0.9	1.0
	Schools	0.4	0.6	0.8	0.9	1.0
	Residences	0.1	0.3	0.7	0.9	1.0
Interior	1 Office, outpatient healthcare, and public order/safety	0.2	0.6	0.8	0.9	1.0
	2 Warehouse, food sales, religious worship, and public assembly	0.2	0.6	0.8	0.9	1.0
	3 Food service, service, strip shopping mall, enclosed mall, and retail other than mall	0.4	0.6	0.8	0.9	1.0
	4 Education	0.4	0.6	0.8	0.9	1.0
	5 Lodging, Nursing, inpatient health care, and laboratory	0.4	0.6	0.8	0.9	1.0

E.14. Cleaning Efficiency

Cleaning efficiency (*CleanEff*) has been found to vary according to the type of flooring (carpeting versus hard floor) and the total amount of lead on the floor. After an exposure event introducing more lead into the environment, the fraction of lead removed from a carpet will depend on the cleaning iteration, with higher efficiencies after the first cleaning iteration and lower efficiencies after multiple iterations due to electrostatic interactions which trap the particles within the carpet. For hard surfaces, the efficiency will depend on the total particle

loading on the floor, with higher efficiencies for higher loadings. Once higher loadings associated with a high exposure event have been cleaned away, the efficiencies associated with routine cleaning are expected to be low. The RRP Approach derived cleaning efficiency equations based on the Clemson Environmental Technologies Laboratory (2001) efficiency data (USEPA, 2008a). For the hard floor equation, the efficiency depends on the loading values (in $\mu\text{g}/\text{ft}^2$) according to the equation:

$$\text{Absolute cleaning efficiency} = 0.113 * \ln(\text{Loading}) - 0.555$$

For the carpet equation, the efficiency depends on the cleaning iteration according to the equation:

$$\text{Absolute cleaning efficiency} = -0.430 * \ln(\text{CleanIteration}) + 0.658$$

These equations are appropriate for high loadings after an interior renovation event. These equations are retained for this modeling effort.

However, because these equations are not applicable for low loadings or for numerous routine cleaning iterations, it is necessary to define a lower limit on the efficiency to prevent predictions of negative efficiencies. A lower limit of 6 percent removal was selected for hard floors (at low loadings) and 15 percent efficiency was set for carpets (after numerous iterations). These values were based on the minimum cleaning efficiency reported for the final round of cleaning in the Clemson data.

E.15. References for Appendix E

American Hotel & Lodging Association. 2007. *The 2007 Lodging Industry Profile*. Washington, DC. Available at: http://www.ahla.com/uploadedFiles/AHLA/Press_Room/Lodging_Industry_Profile/LIP2007.pdf

Cho, H., Gowri, K. and Liu, B. 2010. *Energy Saving Impact of ASHRAE 90.1 Vestibule Requirements: Modeling of Air Infiltration through Door Openings*. U.S. Department of Energy, Pacific Northwest National Laboratory.

Claar, C.N., R.P. Mazzucchi, and J.A. Heidell. 1985. *The Project on Restaurant Energy Performance—End-use Monitoring and Analysis*, PNL-5462, Pacific Northwest National Laboratory, Richland, WA.

Dockery, D; Spengler, J. (1981). Indoor-outdoor relationships of respirable sulfates and particles. *Atmospheric Environment*. 15: 335-343.

- Energy Information Administration (EIA), 2003 Commercial Buildings Energy Consumption Survey. Available at: <http://www.eia.doe.gov/emeu/cbecs/>
- Food Marketing Institute (FMI). 2012, Supermarket Facts: Industry Overview 2012. Accessed February, 2014. Available at <http://www.fmi.org/research-resources/supermarket-facts>.
- Freed J; Chambers T; Christie W; Carpenter C. (1983). Methods for assessing exposure to chemical substances: Volume 2. (Report No. EPA- 560/5-83/015 pp: 70-73.) Washington DC, Environmental Protection Agency, Office of Pollution Prevention and Toxics (OPPT).
- HUD (U.S. Department of Housing and Urban Development). (2002). National Survey of Lead and Allergens in Housing: Final Report, Revision 6. Office of Lead Hazard Control. October 31. Available at: <http://www.hud.gov/offices/lead/techstudies/survey.cfm#natsurvey>
- Largo et al 2011. Healthy Homes University: A home-based environmental intervention and education program for families with Pediatric Asthma in Michigan. Public Health Reports. 2011 Supplement 1. Volume 126 (14-26).
- Layton D; Beamer P. (2009). Migration of contaminated soil and airborne particles to indoordust. *Envir. Science and Technol.* 43: 8199-8205.
- Moran et al 2012. Frequency and longitudinal trends of household care product use. *Atmospheric Environment* 55 (2012) 417-424
- Liu D; Nazaroff W. (2001). Modeling pollutant penetration across building envelopes. *Atmospheric Environment.* 35: 4451-4462.
- Ozkaynak H; Xue J; Spengler J; Wallace L; Pellizzari E; Jenkins P. (1996). Personal exposure to airborne particles and metals: Results from the Particle TEAM Study in Riverside, California. *J.Expo. Anal. Environ. Epidemiol.* 6(1): 57-78.
- Thatcher T; Layton D. (1995). Deposition, resuspension, and penetration of particles within a residence. *Atmospheric Environment.* 29(13): 1487-1497.
- U.S. Census Bureau. 2009. 2009 County Business Patterns. Available at: <http://www.census.gov/econ/cbp/index.html>
- U.S. Bureau of Labor Statistics (BLS). 2012. Occupational Outlook Handbook, 2012-13 Edition. Farmers, Ranchers, and Other Agricultural Managers. Accessed October 18, 2013. Available at: <http://www.bls.gov/ooh/management/farmers-ranchers-and-other-agricultural-managers.htm>

- U.S. Bureau of Labor Statistics (BLS). 2013b. Quarterly Census of Employment and Wages. U.S. total, full-service restaurants, private ownership. Accessed October 18, 2013. Available at: <http://www.bls.gov/cew/>
- U.S. Bureau of Labor Statistics (BLS). 2013c. Quarterly Census of Employment and Wages. U.S. total, limited-service restaurants, private ownership. Accessed October 18, 2013. Available at: <http://www.bls.gov/cew>
- U.S. Department of Education. 2012. National Center for Education Statistics, Digest of Education Statistics 2011, Table 86: Staff employed in public elementary and secondary school systems, by type of assignment and state or jurisdiction: Fall 2009. Accessed September 2013. Available at <http://nces.ed.gov/pubs2012/2012001.pdf>
- U.S. Department of Education. 2012. National Center for Education Statistics, Digest of Education Statistics 2011, Table 71: Teachers, enrollment, and pupil/teacher ratios in public elementary and secondary schools, by state or jurisdiction: Fall 2009. Accessed September 2013. Available at: <http://nces.ed.gov/pubs2012/2012001.pdf>
- U.S. Department of Energy. 2010a. Commercial Prototype Building Models. Accessed September 2013. Available at: http://www.energycodes.gov/development/commercial/90.1_models
- U.S. Department of Energy. 2010b. Commercial Reference Buildings -Supermarkets. Accessed February 2014. Available at: <http://energy.gov/eere/buildings/new-construction-commercial-reference-buildings>
- U.S. Department of Health and Human Services. 2010. Healthcare Cost and Utilization Project. Accessed September 2013. Available at: <http://hcupnet.ahrq.gov/Hcupnet.jsp>
- US EIA. (2005) Residential Energy Consumption Survey (RECS). Available online at: <http://205.254.135.24/consumption/residential/data/2005/>
- US EIA. (2003) Commercial Building Energy Consumption Survey (CBECS). Available online at: http://www.eia.gov/emeu/cbecs/cbecs2003/public_use_2003/cbecs_pudata2003.html
- US EPA 1997. Exposure Factors Handbook. Available online at: <http://cfpub.epa.gov/ncea/cfm/recordisplay.cfm?deid=12464>
- US EPA 2007: E-FAST User Guide. Available online at: <http://cfpub.epa.gov/ncea/risk/recordisplay.cfm?deid=236252>

US EPA 2011. Exposure Factors Handbook. Available online at:

<http://cfpub.epa.gov/ncea/risk/recordisplay.cfm?deid=236252>

von Lindern I; Spalinger S; Bero B; Petrosyan V; von Braun, M. (2003). The influence of soil remediation on lead in house dust. *Sci. Total Environ* 303(1-2): 59-78.

Wallace L. (1996). Indoor particles: a review. *Journal of the Air and Waste Management Association* 46(2): 98-126.

Yuill, G.K. 1996. *Impact of High Use Automatic Doors on Infiltration*. Project 763-TRP, American Society of Heating, Refrigerating and Air-Conditioning Engineers, Inc., Atlanta, GA.

Appendix F. Soil and Hard Surface Parameters

Several soil and hard surface parameters are needed to estimate the soil and hard surface loading concentration time series. The following Appendix details the sources for these parameters.

F.1. Runoff Removal Frequency (*RainFreqDays*)

The runoff removal frequency was needed for each of the nine climate regions. A report by the US DOT and US GS (2010) reports the average number of rain events per year in climate regions in the US, where an event is defined as a rain event resulting in at least 0.1 inches of rain and at least 6 hours between events. The data were digitized using GetData[®] software and 365 days per year was divided by the mean days between events to get the average number of events per year. The 15 climate regions correspond to US EPA “rain zones” and do not exactly match the climate regions. The rain zones were averaged, where appropriate, to approximately map the rain zones to the 9 climate regions. The resulting days between rain events is shown in Table F-1.

Table F-1. Days between rain events

Climate Region Name	Days Between Rain Events (days)
1 (East North Central)	9
2 (Northeast)	7
3 (Northwest)	8
4 (South)	13
5 (Southeast)	7
6 (Southwest)	16
7 (West)	22
8 (West North Central)	14
9 (Central)	7

F.2. Runoff Removal Efficiency (*TrackInRainEff*)

During each rain event, some percentage of the standing dirt on the hard surface will be removed. It was assumed that 50 percent of the dirt layer was removed from the patio during each rain event (Batrone *et al.*, 2010). This does not apply to soil. It was assumed that once present in the soil, lead persists throughout the duration of the exposure event.

F.3. Dust Layer Density (*TrackInDensity*)

McKone *et al.* (2001) report a typical soil density of 2,600 kg/m³. The particles on the hard surface will be a mix of particles from the renovation and soil particles. In the Approach, the hard surface particle density was set equal to the soil density owing to a lack of more specific hard surface data.

F.4. Dust Layer Depth (*TrackInDepth*)

The thickness of the surface soil layer assumed in TRIM.FaTE model simulations performed for EPA OAQPS ranges from 1 cm for non-agricultural soils to 20 cm for tilled agricultural soils (USEPA, 2009a). In order to be adequately conservative, a yard surface soil layer thickness of 1.5 cm was assumed to remain consistent with the methodology used to collect soil samples for comparison to the soil lead hazard standards.

For an outdoor hard surface, the layer thickness represents the thickness of the dirt layer on top of the hard surface. No appropriate value could be identified in the literature. Based on professional judgment, a value of 1 mm was selected for the hard surface layer thickness.

F.5. Dust Layer Porosity (*TrackInPorosity*)

McKone *et al.* provided an estimate for the soil porosity of 20 percent or 0.2. In reality, the dust layer on the hard surface may be more or less porous than the soil. In the absence of further data sources for hard surfaces, the soil value was used in the Approach.

F.6. References for Appendix F

Batroney T; Wadzuk B; Traver, R. (2010) A Parking Deck's First Flush. *Journal of Hydrologic Engineering*, 15(2): 123-128.

McKone T; Bodnear A; Hertwich E. (2001). Development and evaluation of state-specific landscape data sets regional multimedia models. Lawrence Berkeley National Laboratory Report No. LBNL-43722.

US DOT and USGS. (2010). Methods for Development of Planning-Level Estimates of Stormflow at Unmonitored Stream Sites in the Conterminous United States. Office of Project Development and Environmental Review. Publication No. FHWA-HEP-09-005. Washington, DC. Available online at: <http://webdmamrl.er.usgs.gov/g1/FHWA/FHWA-HEP-09-005/FHWA-HEP-09-005.pdf>

U.S. EPA (2009a). Risk and Technology Review (RTR) risk assessment methodologies: For review by the EPA's Science Advisory Board. Case Studies – MACT I petroleum refining sources & portland

cement manufacturing. (Report No. EPA-452/R-09-006.) Research Triangle Park, NC: U.S. Environmental Protection Agency, Office of Air Quality Planning and Standards.

Appendix G. AERMOD Variables

G.1. Meteorology

The methods used to process meteorology data for use in the AERMOD runs of the current analysis are discussed in Appendix G.1.1, while the additional details about the sources of meteorology-related data are discussed in Appendix G.1.2.

G.1.1. Methods for Estimating Meteorological Conditions

To account for the fact that renovation may occur in any part of the country, an analysis was performed to determine sets of meteorological conditions that together would be representative of the entire US. Similar methodology has been used previously for other EPA research, including modeling near roadway pollutants for the Office of Transportation and Air Quality (US EPA, 2011). 14 stations were selected from 9 climate regions in the U.S.

EPA provides guidance for the use of meteorological data for air quality dispersion modeling in Appendix W to 40 CFR Part 51. The guidance specifies that the meteorological data selected should be spatially and temporally representative of the transport and dispersion conditions in the area of concern. The meteorological data used in this public and commercial buildings analysis must be representative of the conditions at the sources considered, yet general enough to represent broad regions. While it would be ideal to formulate an entirely objective procedure for use in evaluating representativeness, no generally accepted analytical or statistical technique is available to determine representativeness of meteorological data (US EPA, 2000). Determining how well a given station represents the encompassing climate region is more difficult than determining how well a station represents a project site. Although various methods could be used for this analysis, the following Approach was chosen.

G.1.1.1. Selecting Representative Stations

As a starting point, the meteorology station(s) for each climate region were selected based on an analysis previously performed (US EPA, 2011). In that 2011 analysis, as discussed in further detail in Appendix G.1.2, 392 active meteorological stations were identified in each climate region. To obtain hourly mixing heights, the (1) hourly surface, (2) twice-daily upper-air, and (3) monthly micrometeorological data were input into the AERMET preprocessor.

Next, the ventilation factor (VF) was calculated for each station. The VF is a combination of wind speed and mixing height that relates pollution dispersion potential to the local setting. More specifically, the VF is defined as the product of a representative wind speed and local mixing height and effectively

represents a measurement of the dispersion flux through an idealized box around a source of pollution. In area per unit time, VF increases with either increasing mixing height or increasing wind speed, thus increasing the idealized volume in which pollutants are allowed to mix and dilute. In US EPA (2011), in order to estimate the VF consistently, all hourly surface wind data were translated to a standard 2-m height by assuming a standard logarithmic wind profile. This corrects measurements made at different heights between stations to a single value to make inter-comparisons between datasets viable. It also establishes a consistent height within the mixing layer to use for comparisons. This height-corrected wind speed was multiplied by the AERMET-determined hourly mixing height, which was taken as the greater of the convective and mechanical mixing height values.

Station representativeness was determined based on the range of VFs at a station relative to that of the encompassing climate region. This method ensures that the selected single station adequately represents the range of dispersive conditions present in the mixing layer in a region. A time series of hourly VFs was developed in US EPA (2011) spanning the full year of hourly records, minus any missing hours, for each station. A small number of stations were not used due to large amounts of missing data. Specific quantiles of the cumulative distribution function (CDF) of each annual VF data series (the 5th, 25th, 50th, 75th, and 95th percentiles) were determined and then averaged for each station, creating a mean and standard deviation in the annual estimate of the 5th, 25th, 50th, 75th, and 95th percentile values of VF for each station.

After each station was processed, the stations in a climate region were aggregated to estimate the means and standard deviations of climate-region-wide 5th, 25th, 50th, 75th, and 95th percentile VFs.

Finally, the quantile data (x_j) from each station in each climate region (g) was individually compared to that of the aggregate of all stations in the region (h), using a χ^2 -type analysis. The station that exhibited the smallest value of χ^2 was taken as representative of the region as a whole. This type of test is used to compare two sets of data to determine whether they are drawn from the same parent distribution. Its application is appropriate in this case because the statistic is being used in a relative sense to compare between subsets of the full distribution.

For the current analysis, the same representative stations identified in US EPA (2011) were used. In addition, for the five climate regions bordering the Pacific or Atlantic Oceans or the Gulf of Mexico, if the selected station was near a coastline, then an additional station was included that was inland, or vice versa. More specifically, the additional station selected in each coastal region (a) was well inland if the first station was coastal (or relatively coastal if the first station was inland), (b) was in a different state from the first station, (c) experienced wind conditions that were significantly different from the first

station, and (d) had high-frequency wind data available for the target period. Note that the χ^2 values were not considered for these additional stations.

Table G-1 shows the selected surface station(s) for each climate region, along with their corresponding upper-air stations and the χ^2 values determined from comparing its CDFs of VF values against the entire climate region's CDFs of VFs. Figure G-1 shows a map of the selected stations. Each of the χ^2 values for the first station selected per region was much less than one, indicating good relative agreement between the sets of VFs. The χ^2 values for four of the five additional selected stations were greater than one, though the χ^2 values were not considered in selecting these additional stations.

G.1.1.2. Processing the Data from the Selected Stations

The 2007 through 2010 data (the analysis period for this project) for these 14 stations were then reprocessed for the purposes of the current dispersion and deposition analyses. The hourly surface meteorological data were re-downloaded in a format friendlier to AERMET than the format used in the above analysis to select the 14 stations (see Appendix G.1.2 for more information). Annual determinations of surface wetness were reevaluated using additional data. Then, several reprocessing methods were used to reduce the number of calm and missing wind values as well as the number of missing mixing height values, increasing the number of hours for which AERMOD can produce dispersion and deposition data.

The first method of replacing calm or missing wind data used the AERMINUTE preprocessor (version 11325 11/21/2011) with one-minute wind observations in order to reduce the number of calm winds compared to the typical hourly wind reports. The source of these one-minute data is discussed in Appendix G.1.2. One input to AERMINUTE is the date on which the ice-free wind sensor (i.e., sonic anemometer) was installed, as the sensitivity of the instrumentation dictates how AERMINUTE processes light wind speeds. Table G-1 provides these installation dates. Note that the Camp Springs, MD station in the Northeast climate region is not an ASOS station, so AERMINUTE was not used for that station. Using AERMINUTE outputs when running AERMET (version 13350; 12/16/2013) significantly reduced the occurrences of calm winds in most of the data, and it also reduced the number of missing wind observations. AERMET was also run using settings that randomized hourly wind direction observations (which are typically reported in tens of degrees) and avoided substitutions of missing cloud cover data (which was known to be coded incorrectly in the version of AERMET being used).

After substitutions of wind data using AERMINUTE, the second method of replacing missing data used methods similar to EPA's guidelines for replacing missing meteorology data, as described in US EPA (1992). The data replacement methods used here generally followed EPA's "objective" steps, but those objective methods do not necessarily replace every instance of missing data – in these cases, EPA

suggests some subjective steps which rely to a large extent on professional judgment. Additional steps were developed for this analysis that identify reasonable replacements for missing data, to the extent that the existing data allows. In general, variables were replaced so that an average of nearby hours is preferred, but otherwise the same hour of day from other neighboring days were used. This method was applied to missing mechanical mixing heights (during non-convective conditions), convective mixing heights (during convective conditions), and temperature data. For wind data, missing values were replaced by first preferring an average of nearby hours, and when that was not successful the average was taken of other nearby hours. The averaging process for wind direction values used the scalar components of the wind vector. Missing convective mixing heights during non-convective hours, mechanical mixing heights during convective hours, and surface heat fluxes (which is the parameter used to determine whether or not the boundary layer is convective) were not replaced.

The resulting wind roses for the 14 selected stations are shown in Figure G-2. Note that wind roses indicate both wind speed and direction, while the VFs used in US EPA (2011) to select the stations only include wind speed. Thus, elements of variation between stations in each region (e.g., wind direction patterns) will occur that are not included in the representativeness determination.

G.1.2. Sources of Meteorological Data for AERMOD

In a previous study (US EPA, 2011), meteorological data were collected from stations around the US and grouped into climate regions. The station data were then analyzed to select one to two stations per climate region. This Appendix gives further details about the sources of the meteorological data used to select the final 14 stations used in the current analysis and then to process the data for those stations for use in this analysis.

G.1.2.1. Surface Meteorological Data for Station Selection

The Quality Controlled Local Climatological Data (QCLCD) dataset used for this analysis is available from NOAA and covers thousands of surface meteorological stations within the US at an hourly resolution and includes all fields necessary for processing in the AERMOD Meteorological Processor (AERMET) and running AERMOD (NOAA, 2011a). However, no pre-existing tools were found capable of translating the QCLCD data into a form AERMET can read. Thus, scripts were developed in-house for US EPA (2011) to translate this QCLCD surface data in both of its formats (the QCLCD data underwent a change in format in June 2007) into the Solar and Meteorological Surface Observational Network (SAMSON) format accepted by AERMET. Some of the differences in fields prior to and subsequent of the format change are noted in the QCLCD update documentation (NOAA, 2011b).

To reduce processing time and meet the objectives of this project, only the 392 stations in the QCLCD dataset that were active during the 2006 through 2010 modeling period and within U.S. Census

urbanized areas were considered. Urbanized areas are defined as densely settled territories that contain 50,000 or more people each (US Census Bureau, 2011). Core-based statistical areas (CBSAs) or metropolitan statistical areas (MSAs) were not considered due to the fact that some CBSAs are MSAs (those containing at least one urbanized areas) while others are not (those containing one urban cluster of at least 10,000 people), and, unlike urbanized areas, CBSAs can contain whole counties (US Census Bureau, 2011). To further reduce processing time, the US EPA (2011) analysis to select stations representative of climate regions covered a three-year time frame (2008 through 2010), although the final processing for use in the current dispersion modeling analysis utilized years 2007 through 2010.

Each of the lower 48 states (except Delaware) and Washington, DC contained at least one of these 392 surface stations. As an example of the distribution, four states (New Hampshire, South Dakota, Vermont, and Wyoming) and Washington, DC, each contained one station, while California contained 48 stations. Each of the nine climate regions contained at least 10 stations – ranging from 10 stations in Climate Region 9 (the Central region, covering the Ohio Valley) to 84 stations in Climate Region 5 (the Southeast region).

An additional input necessary for AERMET execution and for VF calculation is the anemometer height. For ASOS stations, these values were taken from a NOAA dataset (NOAA, 2011d) containing anemometer heights from 2009. Roughly 75 percent of the stations (298) considered here were included in this table. All remaining stations, as well as three stations where the anemometer height was reported as 0 m above ground level, were assumed to be at a standard 10 m height.

G.1.2.2. Surface Meteorological Data for the Current Analysis

When the data for the 14 selected meteorological stations were reprocessed for the purposes of the current analysis, the hourly surface data were redownloaded in Integrated Surface Hourly format (NCDC, 2013b), which works better with AERMET than does the QCLCD data used in the station selection analysis. The one-minute wind data used for the current analysis were obtained from NOAA (NOAA, 2013a).

G.1.2.3. Upper-Air Meteorological Data

Upper-air data was collected for US EPA (2011) from NOAA's ESRL database (NOAA, 2011c). There were approximately 79 upper-air stations in the "lower 48" states active during the 2006 through 2010 period used to select representative stations. The upper-air station network has less coverage than for surface stations. While most states have an upper-air station (some have multiple), nine states do not. Some surface stations are more than 100 km from the nearest upper-air station, and the nearest upper-air station might not have the same geographic and climate characteristics as the surface station. Because of these differences between the surface and upper-air datasets, each surface station was first matched

with its closest upper-air station. Then, each proximate match was scrutinized to be sure that the surface station and upper-air station shared similar geographic and meteorological characteristics. For a surface station that did not share these characteristics with its proximate upper-air station, that upper-air station was replaced with the closest upper-air station that did share these characteristics. For example, a coastal surface station was matched with a coastal upper-air station even if an inland upper-air station was physically closer. This resulted in 59 upper-air stations being matched with the 392 surface stations. This pairing was chosen to appropriately capture regional dispersion characteristics. The same upper-air station data were used for the current analysis.

G.1.2.4. Micrometeorological Data for Station Selection

Surface characteristics surrounding the surface meteorological station are also required for AERMET processing. AERMET requires the land use distributions of the study sites in order to estimate values of three important surface characteristics (surface roughness length, albedo, and Bowen ratio). Surface roughness length contributes to AERMOD's estimations of surface turbulence and boundary layer stability. Albedo affects the amount of solar radiation absorbed by the surface, which affects boundary layer height and stability. The Bowen ratio describes how much surface heat is lost to the boundary layer through conduction and convection versus through evaporation, which affects the height and stability of the convective boundary layer.

AERMOD's land-use preprocessor, AERSURFACE, was used to calculate the distribution of land use types surrounding each station using the 1992 National Land Cover Database (NLCD) (USGS, 2010). In order for AERSURFACE to tailor its calculations for a specific location, it also requires information on the location's climate (i.e., snowiness, season definitions, and aridity). Using NCDC climate normal contour maps, monthly season assignments were made for US EPA (2011) based on median frost/freeze dates and monthly average temperatures, the snowiness assignment was made based on average snow-day data, and aridity was determined using annual average rainfall data. AERSURFACE has the ability to calculate separate surface roughness for a maximum of 12 directional sectors out to a distance of up to 5 km, and these sector roughness values are then assigned to each hour of modeling based on that hour's wind direction. The maximum number of sectors, evenly dispersed, for every station (12 30-degree sectors starting with due North) along with the recommended default distance of 1 km, was used. In the US EPA (2011) analysis, all stations were assumed to have "average" wetness for moisture flux calculations. Each station was also characterized as an airport station in the preliminary analysis, which lowers the surface roughness values for the commercial/industrial/ transportation land cover type (which is otherwise assumed to have higher surface roughness values representative of a developed area with buildings). This is a reasonable assumption because most of the 392 surface stations are at airports. Using all of these data, AERSURFACE used look-up tables to identify the values of the three surface characteristics (see Appendix A of the AERSURFACE User's Guide [USEPA, 2008b]).

G.1.2.5. Micrometeorological Data for the Current Analysis

To use data from the 14 selected station pairs in AERMOD runs, the wetness and airport determinations were revisited to tailor them to the surface station sites. For wetness, the 2007 through 2010 annual rainfall amounts for each station were compared to the climate normal annual rainfall amount from the closest station in the 1981-2010 30-year NCDC climate normal dataset. For a given year, if a station received at least 25 percent more rainfall than the climatological normal, it was processed in AERSURFACE as “wet” for that year; if a station received at least 25 percent less rainfall, it was “dry”; and, otherwise, it was “average”. Each of the 14 selected station pairs was confirmed to be at an airport, and all other settings used in the station selection analysis were unchanged when rerunning AERSURFACE (first version; 01/2008).

Table G-1. Selected surface and paired upper-air stations representing each climate region.

Climate Region	Surface Station							Upper-air Station				Ventilation Factor VF χ^2
	WBAN	Call Sign	Location	Coastal or Inland, with approximate distances to water for coastal	Installation Date of Ice Free Wind Sensor	Latit.	Longit.	WBAN	Location	Latit.	Longit.	
1 (East North Central)	14937	KIOW	Iowa City, IA	Inland	10/20/2005	41.633	-91.543	94982	Davenport, IA	41.6	-90.57	0.098 (smallest in region)
2 (Northeast)	13705	KADW	Camp Springs, MD	Coastal (31 km from Chesapeake Bay, 60 km from Atl. Ocean)	Not ASOS	38.811	-76.867	93734	Sterling, VA	38.98	-77.47	0.149 (smallest in region)
	14762	KAGC	Pittsburgh, PA	Inland	4/3/2007	40.355	-79.922	94823	Township, PA	40.53	-80.23	0.764 (13th smallest of 69 stations in region)
3 (Northwest)	24222	KPAE	Everett, WA	Coastal (4 km from Puget Sound, 50 km from Salish Sea, 180 km from Pac. Ocean)	3/29/2007	47.908	-122.28	24232	Salem OR	44.92	-123.02	0.250 (smallest in region)
	24145	KIDA	Idaho Falls, ID	Inland	1/30/2007	43.516	-112.06	24061	Riverton, WY	43.06	-108.47	16.087 (largest of 21 stations in region)
4 (South)	13920	KFOE	Topeka, KS	Inland	9/7/2006	38.95	-95.664	13996	Topeka, KS	39.07	-95.62	0.273 (smallest in region)
	03937	KLCH	Lake Charles, LA	Coastal (41 km from Gulf of Mexico)	4/19/2007	30.125	-93.228	03937	Lake Charles, LA	30.12	-93.22	2.734 (28th smallest of 59 stations in region)

Appendices to the Approach for Estimating Exposures and Incremental Health Effects from Lead due to Renovation, Repair, and Painting Activities in Public and Commercial Buildings

Climate Region	Surface Station							Upper-air Station				VF χ^2
	WBAN	Call Sign	Location	Coastal or Inland, with approximate distances to water for coastal	Installation Date of Ice Free Wind Sensor	Latit.	Longit.	WBAN	Location	Latit.	Longit.	
5 (Southeast)	93727	KNCA	New River, NC	Coastal (20 km from Atl. Ocean)	Unknown ^a	34.7	-77.433	93768	Morehead City, NC	34.7	-76.8	0.379 (smallest in region)
	13874	KATL	Atlanta, GA	Inland	3/27/2007	33.64	-84.427	53819	Peachtree City, GA	33.35	-84.56	1.396 (24th smallest of 84 stations in region)
6 (Southwest)	23066	KGJT	Grand Junction, CO	Inland	3/13/2007	39.134	-108.538	23062	Denver, CO	39.77	-104.88	0.459 (smallest in region)
7 (West)	93111	KNTD	Point Mugu, CA	Coastal (2 km from Pac. Ocean)	10/1/2007	34.117	-119.110	93214	Vandenberg AFB, CA	34.75	-120.57	0.284 (smallest in region)
	23169	KLAS	Las Vegas, NV	Inland	4/25/2007	36.079	-115.155	53103	Flagstaff, AZ	35.23	-111.82	4.253 (33rd smallest of 52 stations in region)
8 (West North Central)	14944	KFSD	Sioux Falls, SD	Inland	8/22/2006	43.577	-96.754	94980	Omaha, NE	41.32	-96.37	0.377 (smallest in region)
9 (Central)	94822	KRFD	Rockford, IL	Inland	5/22/2007	42.196	-89.093	94982	Davenport, IA	41.6	-90.57	0.127 (smallest in region)

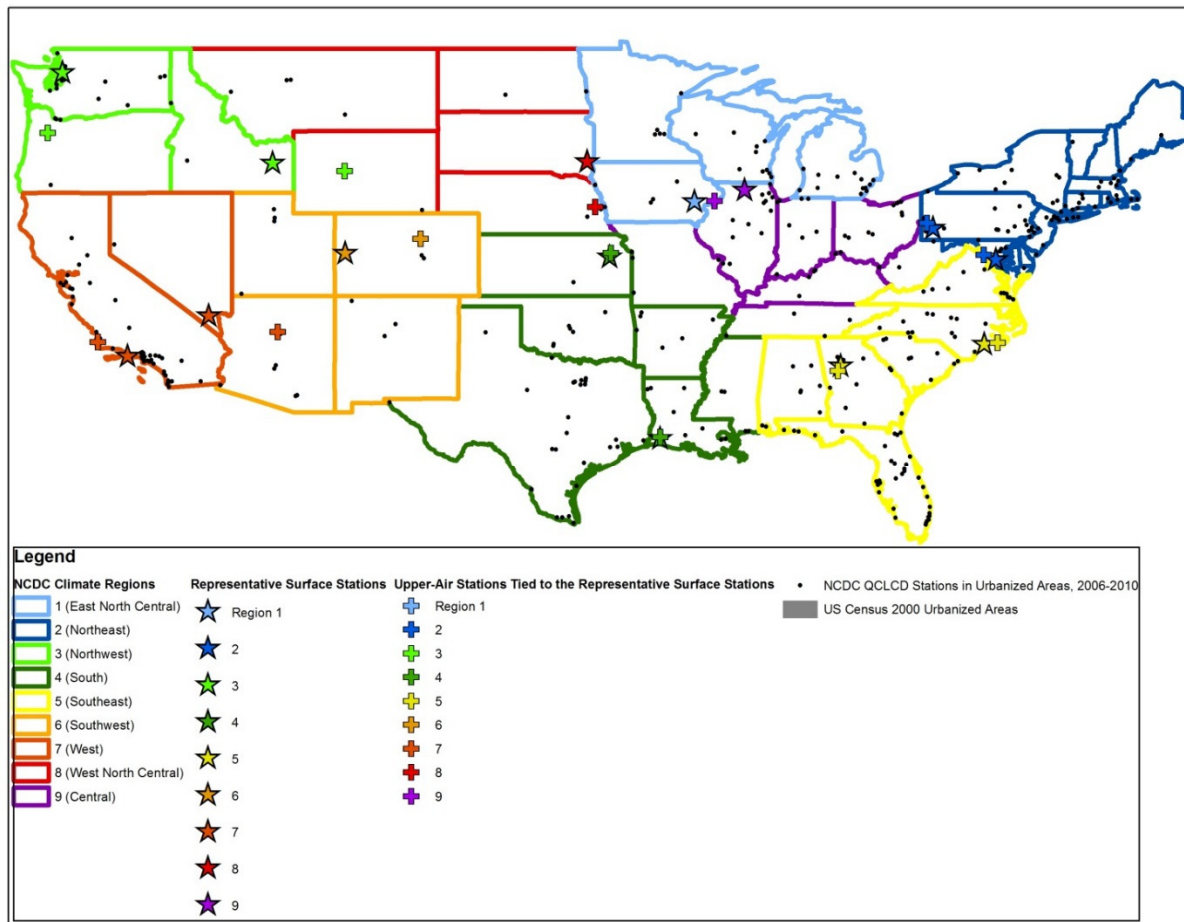


Figure G-1. Map of selected surface and paired upper-air stations representing each climate region.

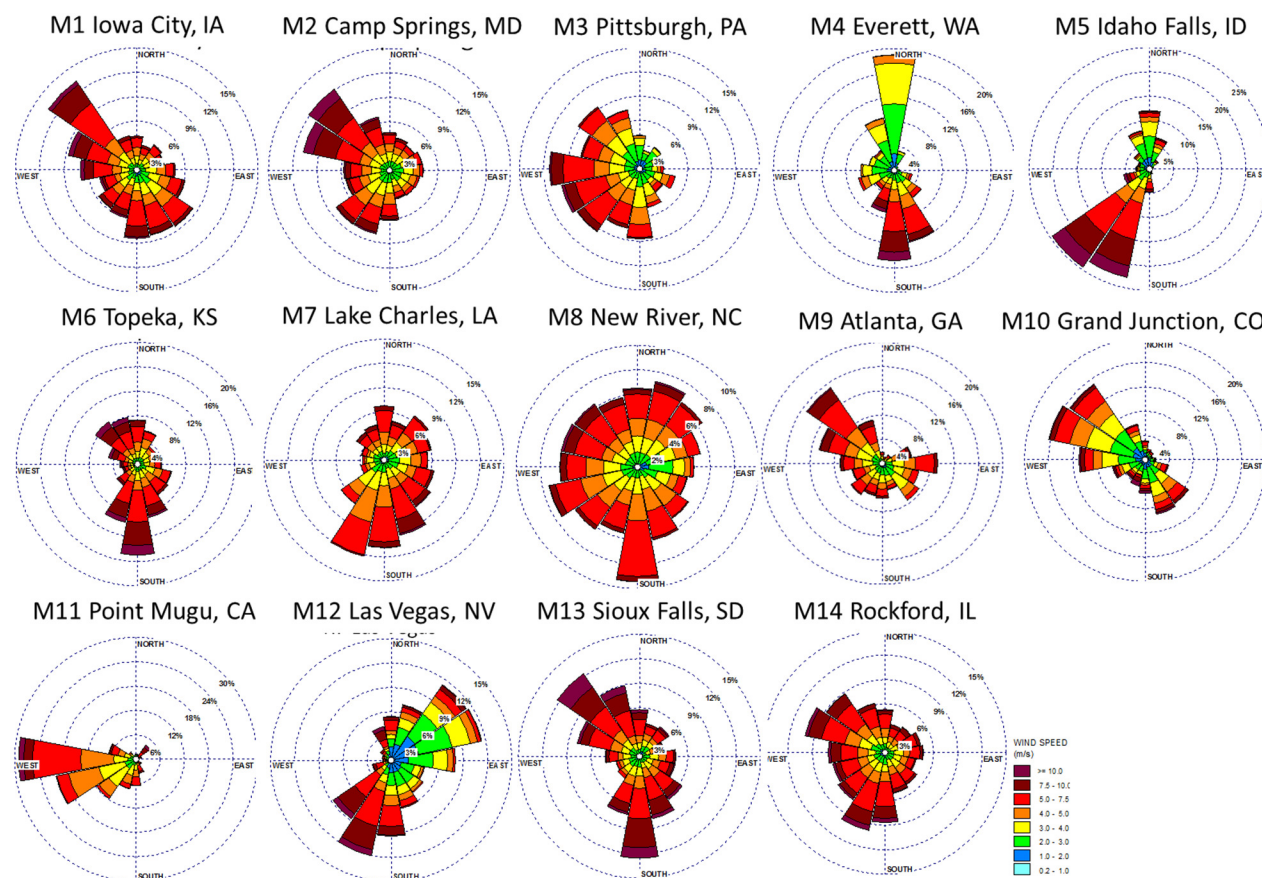


Figure G-2. Wind roses for each selected regionally representative station, 2007-2010.

G.2. Emissions

To account for the fact that renovations may occur during any season, the renovation emission progression around the building blocks was begun four times during a model year, on January 1st, April 1st, July 1st, and October 1st. This progression was also repeated for four different years, each with different meteorological conditions (see below). Then, the air concentrations from each renovation hour for all of the 16 seasons (4 years \times 4 seasons/year) were aligned for each receptor location and averaged to give a central tendency estimate of the air concentrations across the seasons at that location. Then, the time series of these central tendency concentrations were used in the Monte Carlo model.

G.3. Deposition

The size of the particles emitted during the renovation will affect the deposition and air concentrations at each receptor in AERMOD. If the relative mix of particle sizes includes more coarse particles, the

concentrations at the closest receptors will be larger and the concentrations at the farthest receptors will be smaller because the larger particles will tend to deposit closer to the renovated building. AERMOD (version 13350; 12/16/2013), deposition was modeled using AERMOD deposition “method 1” algorithm (USEPA, 2009b), which requires the specification of the fraction of particulate matter in each size category modeled and the density of the particles. Thus, in order to accurately model the emissions due to the full set of renovation activities, different deposition values were used for different renovation activities.

Before the selected size distributions and particle density are discussed, it is noted that the AERMOD modeling is intended to model the particulate containing lead (such as renovation-derived dust) rather than lead itself; then, the emission rates are used to estimate the lead mass emitted as part of that particulate. Thus, the deposition values should be consistent with the emitted lead-containing particulate (assumed primarily to be paint particles) rather than the lead on the particulate.

Three size classes, 2.5, 10, and 20 μm , were selected for all AERMOD runs. Choe *et al.* (2000) measured airborne particulate concentrations when doors with lead paint were dry scraped and dry sanded. They measured the mass fractions in sizes up to 20 μm because their preliminary experiments showed no appreciable mass above 20 μm after the renovation activity. The line corresponding to the 0th hour after abatement in Choe *et al.*'s Figure 3 was digitized using the GetData[®] software program (GetData[®], 2008). Then, the fraction of mass in each of the three size classes was estimated by (1) multiplying each concentration density by the $\text{dlog}(d)$ to get the incremental concentration at that diameter, (2) performing a cumulative sum across all diameters to get the cumulative concentration at each diameter, and (3) identifying the cumulative concentration for each of the three target size classes (2.5, 10, and 20 μm), and (4) finding the incremental concentration in each size bin. For dry scraping, 2 percent was less than 2.5 μm , 72 percent was between 2.5 and 10 μm , and 26 percent was between 10 and 20 μm . For sanding, 4 percent was less than 2.5 μm , 62 percent was between 2.5 and 10 μm , and 34 percent was between 10 and 20 μm . The two different particle size distributions were each run and determine to have less than a 2% effect on air or soil lead concentrations. To reduce the number of AERMOD runs required all activities were modeled using the particle size distribution resulting from dry scraping.

For the particle density, the density was set equal to 2 g/cm^3 to be representative of the density of lead-containing paint. If the released particles consist of building substrate as well as paint, the particle density may be somewhat larger or smaller. In addition, the exact density will depend on the fraction of lead in the paint, which varies by the year the paint was applied and from building to building. Thus, this assumption introduces uncertainty in the modeling. It was not computationally feasible, however, to perform AERMOD runs for every particle density. Early scoping results indicated that AERMOD particle density did not strongly affect the indoor dust loadings.

G.4. Urban/Rural

Each AERMOD modeling run for each combination of renovated building, renovation activity pattern, and meteorology data were run twice – once using AERMOD’s urban setting with an arbitrary population of 1 million people, and once not using the rural setting.

For the Approach, agricultural buildings were modeled with AERMOD’s rural option; all other receptor building types were modeled with AERMOD’s urban option. AERMOD’s urban modeling option parameterizes one of the effects of the urban heat island—the decreased nighttime cooling that creates a “convective-like” nighttime boundary layer with enhanced heating and turbulence compared to an adjacent, nonurban area. Because the renovations occur only during the day and the urban effect occurs primarily at night, the difference between simulated air concentrations using the urban versus rural model setting is expected to be minimal. Early test runs indicated that differences in modeled air concentrations were less than 1 percent in approximately 90 percent of the simulated scenario-days. For the small percentage of scenarios where this distinction does make a difference, EPA could consider additional data sources that describe how often different building types occur in urban or rural locations by adding this as a sampled variable.

Urban areas tend to experience increased daytime surface heating and decreased nighttime surface cooling compared to rural areas. They experience such heating due both to densely distributed human activity and to ground cover and building materials that absorb solar radiation during the day and slowly release it overnight. By contrast, rural areas with natural vegetation cover release daytime heating fairly quickly overnight, allowing rural areas to cool overnight relatively faster than urban areas. These near-surface heating and cooling aspects also affect stability, turbulence, and mixing heights, all of which affect the transport of chemicals in the air. The urban setting in AERMOD parameterizes an urban area’s decreased nighttime cooling by creating a nighttime boundary layer with a taller mixing height and enhanced heating and turbulence compared to an adjacent, non-urban area. The magnitude of these urban effects in AERMOD is partially controlled by a user-input value for urban population.

The urban option is not intended to affect daytime conditions, which in AERMOD is defined as hours when the atmosphere is unstable. However, there can be a sharp and artificial discontinuity in mixing height when daytime begins and the modeled urban effect shuts off, so the fifth AERMOD revision (version 11059, 02/28/2011) implemented a transition period that allows the urban mixing height adjustments to continue until the daytime mixing height becomes taller.

In some simplistic test runs with AERMOD, the urban option and any necessary daytime transition adjustments affected the modeled air concentration and deposition fluxes during approximately 10 percent of hours in the 9am-to-5pm renovation window used in the current analysis. During these

affected times, the urban option increases average air concentrations and deposition fluxes by approximately a factor of 2, though the effect averaged across the whole renovation window is closer to 10 or 20 percent. These simplistic AERMOD test runs and their results should not be interpreted as representative of all urban-setting scenarios or of building renovation activities in particular; the intent was only to show the conditions where the urban setting impacts modeling results, with some notion of magnitude of impact.

G.5. Obstruction Adjustment

The presence of obstructions between the source building and the receptor may either provide an enhancement or protection to the receptor from the renovation-derived lead-containing dust. The windfield will be influenced by the buildings such that emitted dust may be channeled around and over the obstruction building and concentrated in a mixing “rotor” zone on the leeward side of the building. Thus, receptors located near the obstruction might be exposed to either a larger concentration (in the rotor zone) or smaller concentration (outside the rotor zone).

The Approach takes this potential obstruction effect into account. However, it is not feasible quantitatively to model the effects of the infinite number of combinations of sources, obstructions, and receptors. Thus, a distribution of protection/enhancement factors was developed and sampled during the Monte Carlo modeling. These factors are then applied to the AERMOD concentrations to account for potential obstruction effects.

Early scoping results evaluated the effects of 13 obstruction scenarios were modeled using the BPIP-PRIME algorithms in AERMOD to find the greatest protection and enhancement effects introduced by a third building, termed an obstruction, that is located near to both the source and receptor location and disrupts the windfield around the receptor location. These exploratory model runs were performed with a grid of 1,381 downwind receptors, rather than the 160 receptors locations used in the Monte Carlo modeling. It was found that the greatest effect occurred when an obstruction was located very near the source building and angled orthogonally to the source building. In that scenario, the maximum modeled protective factor was approximately 0.1, meaning the resulting air concentrations were 10 percent the level found in the case of no obstruction, and the maximum enhancement factor was approximately 5.3, or 530 percent greater than when no obstruction building was present.

For this analysis, eight additional obstruction scenarios were modeled in an attempt to find the greatest effect of an obstruction. The scenarios including variations on placing the obstruction closer to the source building, elongating the obstruction (i.e., a rectangular, rather than square, configuration), and placing obstructions in series (i.e., more than one obstruction). The protective and enhancement effects produced by the original orthogonal scenario tested for the transport analysis seemed to represent a

ceiling, as the additional tested scenarios produced nearly identical magnitudes of protective and enhancement effects, but did not exceed those found in the original scenario. This is illustrated by the results of three obstruction scenarios presented in Figure G-3.

From the obstruction scenario tests, the following general observations on the effects of obstructions on the modeled air concentration were found:

- For any given hour, the effect of the obstruction is minimal to zero for at least half of the compass directions (i.e., the directions upwind of the source building are not affected by the obstruction).
- For most of the reasonable combinations of source buildings and obstructions, the maximum protection and enhancement factors of an obstruction were not less than 0.1 or greater than 5.3, respectively.
- Among the locations where the obstruction affected modeled air concentrations, the effects were relatively large at relatively few locations and relatively small, that is, near one, at a majority of locations.

Given the above observations, a distribution was developed to describe the expected effect of an obstruction on modeled air concentrations. First, it was assumed that all receptors upwind of the modeled renovation will experience no effect from an obstruction on a given modeling hour. To replicate this, a number of receptors equal to the number modeled downwind but with no obstruction effect (protection/enhancement factor equal to one) were added to the results of each modeling run, resulting in 2,762 reported values. These values were then sorted from smallest to largest for each scenario. The worst case and average of all obstruction cases were plotted, as shown in Figure G-3 and the distributions were described using the following equations:

$$\text{For the 1}^{\text{st}} \text{ to } 32^{\text{nd}} \text{ percentiles: } ObsAdj = 0.15 * \ln(perc) + 1.15$$

$$\text{For the 33}^{\text{rd}} \text{ to } 87^{\text{th}} \text{ percentiles: } ObsAdj = 1$$

$$\text{For the 88}^{\text{th}} \text{ to } 100^{\text{th}} \text{ percentile: } ObsAdj = \exp(perc^{25})$$

where $ObsAdj$ = obstruction adjustment

$Perc$ = percentile of distribution

The obstruction adjustment was also bound by the overall minimum and maximum found experimentally, 0.1 and 5.3, respectively.

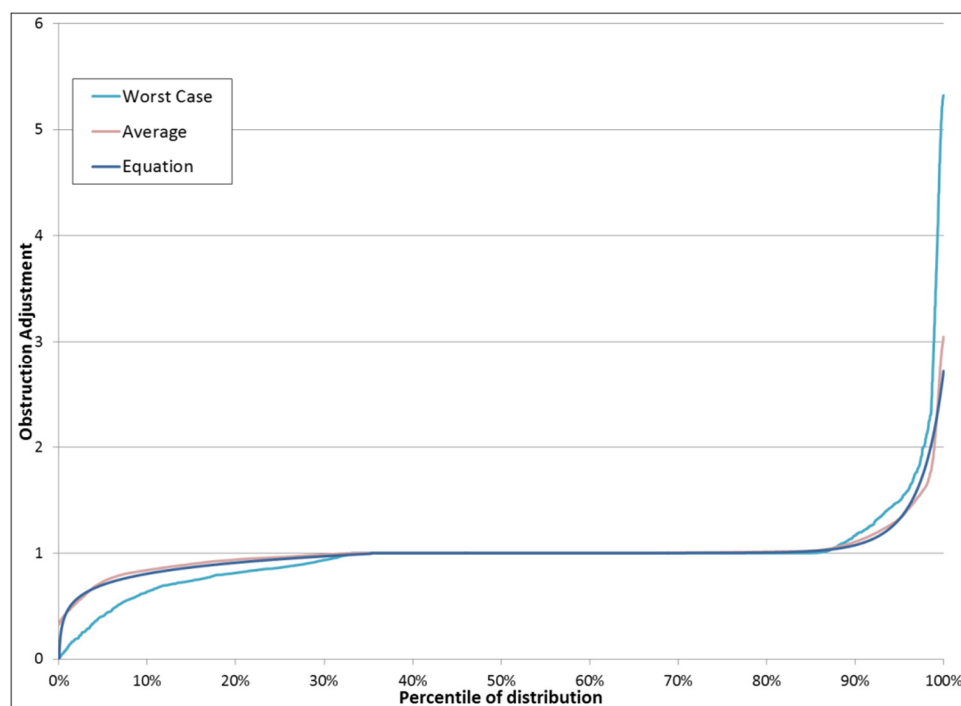


Figure G-3. Distribution used to describe the effect of an obstruction building on air concentrations at a given receptor.

G.6. References for Appendix G

Choe K; Trunov M; Grinshpun S; Willeke K; Harney J; Trakumas S; Mainelis G; Bornschein R; Clark S;

Friedman W. (2000). Particle settling after lead-based paint abatement work and clearance waiting period. *American Industrial Hygiene Association Journal* 61: 798-807.

GetData®. (2008). GetData® Graphic Digitizer. <http://www.getdata-graph-digitizer.com/download.php>

NOAA (2011a). Quality Controlled Local Climatological Data (QCLCD [2.4.4]): Documentation. Effective January, 2005. Available online at: <http://cdo.ncdc.noaa.gov/qclcd/qclcddocumentation.pdf>.

NOAA (2011b). Quality Controlled Local Climatological Data (QCLCD [2.4.4]): Quality Controlled LCD Improvements/Differences/Updates. Available online at: <http://cdo.ncdc.noaa.gov/qclcd/qclcdimprovements.pdf>.

NOAA (2011c). NOAA/ESRL Radiosonde Database. Available online at:http://www.census.gov/geo/www/cob/ua_metadata.html.

NOAA (2011d). National Weather Service Surface Observations Program: Wind Tower Dataset. Availableonline at: <http://www.weather.gov/ops2/Surface/documents/windtower.xls>.

US EPA. (2011). Development of a Microscale “Meta-model” for Estimating Near-road Impacts ofEmissions from Archetypal High-traffic Roads, Contract EP-C-06-094, WA 4-06 Final Report, Prepared for

U.S. EPA, Office of Transportation and Air Quality, by ICF International, September 30, 2011.

Appendix H. Exterior Emission Rates

EPA's Dust Study (US EPA, 2007a) is the most comprehensive study of lead dust generation by renovation activity to date. It was used to characterize the lead-emissions from eight of the exterior renovation activities considered: paint removal by dry scraping, power sanding, torching, use of high and low temperature heat guns, and use of a needle gun; and replacement of exterior doors and trim. An emission rate was estimated for each of these renovation activities using the methodology described below. The ninth activity, demolition, used a different methodology described in Appendix B.10.

To design an analysis framework for estimating lead aerosol emissions due to renovation of a building from the Dust Study, it is necessary to understand the study methodology and the experimental variables captured in the study. Figure H-1 shows the typical layout of an experiment in the Dust Study. The steps of the experiments were generally as follows:

An area of wall (or trim, door, railing, or porch ceiling) was selected and specified as the disturbed area.

The area around the disturbed area was prepared for the experiment. Plastic was placed on the ground and had a specified length along the wall (referred to as the plastic "width" or the "along-wall" direction) and a length perpendicular to the wall (referred to as the plastic "distance from wall" or the "out-from-wall" direction). The plastic included "rule plastic" closer to the job and "beyond rule plastic" further from the job. In addition, vertical plastic was used at the edges of the ground plastic to encase the job and limit horizontal transport of dust outside the job area.

The job was performed and the time needed to completely perform the renovation within the disturbance area was noted.

The dust loading in units of mass of lead per square foot was measured at six different distances from the wall for each experiment. To support the estimation of emission rates, the contractor who collected the data in the Dust Study, Battelle, provided maps for each experiment showing the geometry of the plastic and the placement of the sample trays. This information is not presented in the Dust Study report but is provided in this Appendix in Sections O to H.14.

Either a single experiment or multiple experiments were performed for each activity, with six measurements of surface loading per experiment.

To estimate the fraction of paint on the wall in the Dust Study emitted during a specific activity, it is necessary to estimate the total amount of dust that was removed and introduced into the air during the activity as a fraction of the total amount of paint that was on the wall. The total amount of emitted dust must be estimated from the loading values in the Dust Study by accounting for spatial differences in the loading and integrating the loading over the area of the plastic. In this Approach, the emission calculation is achieved by

1. Along-wall distribution: Performing several conversions on the loading data and estimating an along-wall distribution of dust,
2. Out-from-wall distribution: Generating a regression equation for the loading as a function of distance from the wall to estimate the out-from-wall distribution of dust,
3. Total dust emitted: Integrating the loading on the plastic in the along-wall and out-from-wall directions to estimate the total dust emitted during the job,
4. Total paint on wall: Estimating the total amount of paint originally on the wall before the experiment began, and
5. Emission fraction: Estimating the fraction of paint on the wall that was emitted as aerosol particles.

Each of these steps is described in general terms below. Then, specific details (including the experiment maps) are provided for each experiment in the remainder of the Appendix.

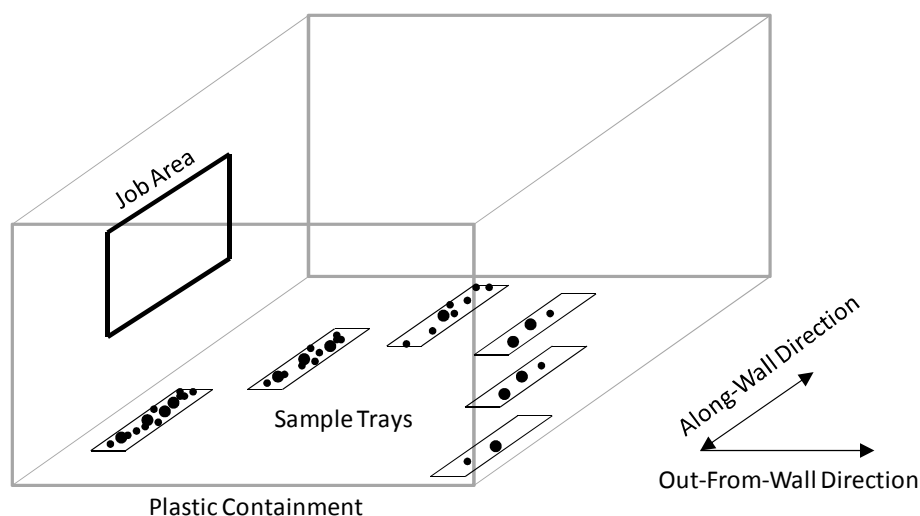


Figure H-1. Schematic of the Dust Study experimental set-up.

H.1. Loading Data Conversions and Along-Wall Distribution of Paint Dust

Because each experiment was performed using different total wall disturbance sizes, the fraction of paint emitted was calculated on a per square foot of disturbed wall basis. Thus, each Dust Study lead loading was divided by the area disturbed in the experiment to get the loading in units of lead mass per square foot of plastic and per square foot of wall disturbed:

$$LeadLoad_{per\ wall\ unit} = \frac{LeadLoad}{AreaDist}$$

where:

$LeadLoad_{per\ wall\ unit}$	=	the total lead loading on the plastic per unit of wall area disturbed ($\mu\text{g}/\text{ft}^2/\text{ft}^2$)
$LeadLoad$	=	the total lead loading on the plastic ($\mu\text{g}/\text{ft}^2$)
$AreaDist$	=	the total wall area disturbed during renovation (ft^2)

In addition, because each experiment was performed on buildings with different compositions of lead within the paint, the fraction emitted was calculated based on the total amount of paint dust emitted rather than the total amount of lead emitted. This conversion assumes that each experiment within an activity should produce nearly uniform amounts of paint dust per square foot disturbed, even though the amount of lead will vary according to the lead content in the paint. To make this conversion, each lead loading was divided by the percentage of lead in the paint specified in the Dust Study to

approximate loadings in units of mass of paint particles per square foot of plastic and per square foot of wall disturbed (see equation below).

$$PaintDustLoad_{per\ wall\ unit} = \frac{LeadLoad_{per\ wall\ unit}}{frac} \times \frac{1}{1000\ \mu g / mg}$$

where:

- $LeadLoad_{per\ wall\ unit}$ = the total lead loading on the plastic per unit of wall area disturbed (mg/ft²/ft²)
- $PaintDustLoad_{per\ wall\ unit}$ = the total paint dust loading on the plastic per unit of wall area disturbed (mg/ft²/ft²)
- $frac$ = the fraction of paint which is lead by weight (unitless)

Note that this conversion assumes that all the emitted particles are paint particles and does not account for the fact that the total emitted dust might include wall substrate particles as well. Thus, the estimated paint dust emission rate will not represent the total dust emitted during the activity but is intended to account for all the lead emitted, assuming that there is lead in the paint but not within the substrate or other disturbed portions of the building.

Next, the along-wall distribution of dust was estimated. Following inspection of the general trends in the Dust Study experiments, it was assumed that the loadings were relatively constant over the width of the job and then tapered linearly to zero at the edge of the ground plastic in the along-wall direction (see Figure H-2). Thus, if measurements were made at locations wider than the job width (for example, Sample X in Figure H-2), these measurements were adjusted using a linear relationship to approximate the loading within the job area (for example, Sample X_{adj} in Figure H-2). In the event that experiment-specific dust distributions differed from this general format, the distribution used is noted in the experiment-specific information in Sections O to H.14.

To make this linear conversion, the following equation was used:

$$PaintDustLoadAdj_{per\ wall\ unit} = \frac{DistPlast}{DistPlast - DistMeasure} PaintDustLoad_{per\ wall\ unit}$$

where:

- $PaintDustLoadAdj_{per\ wall\ unit}$ = the total paint dust loading on the plastic per unit of wall area disturbed adjusted to the level within the job area (mg/ft²/ft²)
- $PaintDustLoad_{per\ wall\ unit}$ = the total paint dust loading on the plastic per unit of wall area disturbed (mg/ft²/ft²)
- $DistPlast$ = the distance between the edge of the job and the

DistMeasure containment plastic (ft)
= the distance between the edge of the job and the
measurement (ft)

All of these distances were calculated from the information in the Dust Study job maps provided by Battelle. Because the dust is measured over discrete areas 1 ft wide, the measurements are assumed to apply to the center of the measurement area. Thus, the loadings were assumed to taper to zero over a distance 1 ft wider than shown in the diagrams. This assumption causes the loadings to fall to zero in the center of the 1 ft box next to the containment plastic. The alternative assumption (loadings going to zero at the center of the box just inside the containment plastic) was not used, since non-zero measurements were available at those locations in the Dust Study.

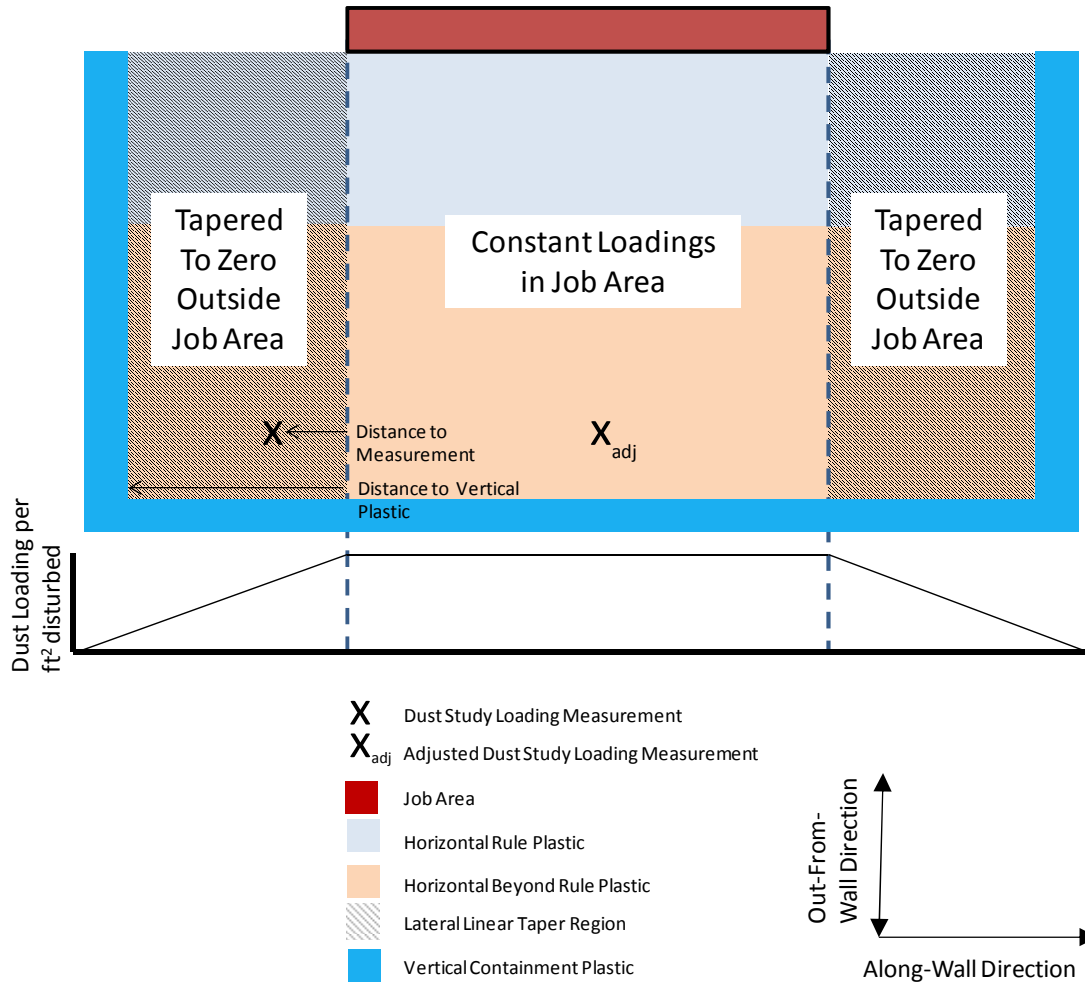


Figure H-2. Schematic of Assumed Along-Wall Distribution of Loading

H.2. Regression of Dust Study Data by Renovation Activity

To estimate the distribution of dust in the out-from-wall direction within the job area, a regression analysis was performed on the *PaintDustLoadAdj_{per wall unit}* values (or the *PaintDustLoad_{per wall unit}* values if no adjustment was necessary because the measurement was made within the job area) at each corresponding distance from the wall with Microsoft Excel® using the following equation for exponential decay:

$$PaintDustRegression = Load_0 \times e^{Shape \times Dist}$$

where:

<i>PaintDustRegression</i>	=	paint dust loading (mg/ft ² /ft ² disturbed)
<i>Load₀</i>	=	loading just below the job at 0 ft (mg/ft ² /ft ² disturbed)
<i>Shape</i>	=	shape of exponential regression (/ft)
<i>Dist</i>	=	distance from renovation activity (ft)

Before performing the regressions, an adjustment was made to account for the presence of large bulk material in the Dust Study. Dust Study samples were collected and reported as “with bulk” and “without bulk”. Owing to the nature of the activities, some of the material removed during the renovation was expected to be too large to be released into the air. However, bulk samples in the Dust Study include samples in which either the particles were too large to be captured in a wipe sample (which should be excluded from this Approach) or where there was too much dust to be collected in a wipe sample (which should be included in this Approach). There is no way to separate these two different types of samples.

Thus, an empirical correction was made to account for the large bulky particles. It was assumed that most of these bulky particles would fall within three ft of the job wall (assuming they fell directly downward). Thus, any bulk samples collected within two ft of the job were excluded from the regression. In addition, any samples designated as “bulk” samples taken at three ft from the renovation wall were also excluded from the regression, since it was assumed that large debris could reach that distance for some of the activities. This correction allowed the samples at further distances (where bulk is assumed to be absent) to define the shape of the regression curve. Comparing the regression parameters both before and after the correction, the power sanding regression coefficients changed very little while the dry scraping coefficients changed dramatically. This trend is as expected and provides some indication that this Approach is appropriate, as power sanding is expected to emit few bulky particles while dry scraping emissions could be dominated by bulky particles.

H.3. Total Amount of Dust Emitted

Once these regression equations were determined, the total amount of dust on the plastic was estimated by combining the along-wall (Appendix H.1) and away-from-wall (Appendix H.2) distributions and integrating to get the total mass. This was done by estimating the mass within the job area, estimating the mass outside the job area, and then adding the two together. For the mass within the job area, the mass was found by integrating the regression expression over the length of the plastic (out-from-wall direction) and multiplying by the width of the job (along-wall direction):

$$MassDust_{inside} = \frac{Load_0}{Shape} \times (e^{Shape \times LenPlast} - 1) \times JobWidth$$

where:

$MassDust_{inside}$	=	paint dust mass on the plastic inside the job area (mg/ft ² disturbed)
$Load_0$	=	loading just below the job at 0 ft (mg/ft ² disturbed)
$Shape$	=	shape of exponential regression (ft ⁻¹)
$LenPlast$	=	length of plastic in the out-from-wall direction (ft)
$JobWidth$	=	the width of the job in the along-wall direction (ft)

For the mass outside the job area, that is, collected on either side of the area disturbed, the mass was found by finding the area within each linear taper region (one on each side) according to the equation:

$$MassDust_{outside \ / \ side} = 0.5 \times \frac{MassDust_{inside}}{JobWidth} \times PlastWidth_{Outside}$$

where:

$MassDust_{outside / side}$	=	paint dust mass on each side of the plastic outside the job area (mg/ft ² disturbed)
$MassDust_{inside}$	=	paint dust mass on the plastic inside the job area (mg/ft ² disturbed)
$JobWidth$	=	the width of the job (ft)
$PlastWidth_{Outside}$	=	the width of the plastic beyond the job on one side only (ft)

The above equation reflects the assumption that in the region outside the job area, the total mass will taper linearly from being equal to that within the job area down to zero at the edge of the plastic.

Finally,

$$MassDust_{total} = MassDust_{inside} + MassDust_{outside \ / \ side} \times Number_{side}$$

where:

$MassDust_{total}$	=	total paint dust mass on the plastic (mg/ft ² disturbed)
$MassDust_{inside}$	=	paint dust mass on the plastic inside the job area (mg/ft ² disturbed)
$MassDust_{outside / side}$	=	paint dust mass on the plastic outside the job area (mg/ft ² disturbed)
$Number_{side}$	=	Number of linear taper areas adjacent to the job area (0, 1, or 2)

H.4. Amount of Paint on the Wall

To estimate the total amount of paint on the wall for each renovation experiment, first the paint density and number of layers of paint were estimated. The average paint density for each activity was estimated for the Dust Study jobs using the fraction of lead in paint according to the equation:

$$\text{PaintDens} = \text{frac} \times \text{DensityPb} + (1 - \text{frac}) \times \text{DensityRest}$$

where:

<i>PaintDens</i>	=	the density of the paint (g paint/cm ³ paint)
<i>frac</i>	=	the fraction of paint which is lead by weight (unitless)
<i>DensityPb</i>	=	the density of lead (g/cm ³)
<i>DensityRest</i>	=	the density of the rest of the paint (other than lead) (g/cm ³)

The density of lead is 11.3 g/cm³, and the density of the rest of the paint is assumed to be equal to 1 g/cm³ consistent with the solid portion of modern paint (assumed to be lead-free), as calculated from Material Safety Data Sheets (MSDS) sheets.

The number of layers of paint on the wall at the time of the Dust Study job was estimated by assuming that painting had been done every seven years since the time the building was constructed. This value of seven years was selected based on information about typical renovation frequencies in child care centers (CCC data). For each of these previous painting jobs on the building, it was assumed that the surface was prepared for painting and then a layer of paint was applied. There is no way of knowing what method was used to remove paint and prepare the surface in these prior painting jobs. Thus, the representative value of 15% removal for surface preparation (Section D.1.3) was used in estimating the fraction of paint removed during each previous painting job. The Dust Study jobs were performed in 2006. Thus, the number of layers of paint in 2006 for each Dust Study building construction date were estimated and are shown in Table H-1.

In some cases, the age of the renovated building was unknown. The Dust Study residences were built between 1900 and 1925, and a table provided within the Dust Study report indicates that nearby properties were built between 1900 and 1920. For this analysis, a representative building year of 1920 was selected as a year within that range.

For the actual paint removal jobs performed during the Dust Study, Battelle provided information about the degree of paint removal. Some jobs were surface preparation activities (removed only a fraction of the total paint on the wall), while others removed all the paint on the wall. The fraction removed tended

to depend on the method used to perform the job, as shown in Table H-2. Thus, the amount of paint removed during each Dust Study job was estimated by multiplying the number of layers of paint estimated to be on the building in 2006 by the estimated fraction of paint removed during the particular job (100% for removal jobs and 15% for surface preparation jobs).

Table H-1. Layers of Paint By Vintage and Building Type

Building Construction Date	Estimated Layers of Paint On Buildings in 2006 at the Start of the Dust Study
1900	6.2
1910	5.3
1918	5.0
1920	5.0
1925	4.7
1967	3.3

Table H-2. Fraction of paint on the wall that is removed in the Dust Study experiments.

Job Type	Fraction of Paint Assumed to Be Removed During Dust Study Jobs
Power Sanding	Paint Removal; 100%
Needle Gun	Paint Removal; 100%
Torching	Paint Removal; 100%
High Heat Gun	Paint Removal; 100%
Low Heat Gun	Paint Removal; 100%
Dry Scrape	Surface Preparation; 15%
Trim Replacement	Surface Preparation; 15%
Door Replacement	Surface Preparation; 15%

These values were then used to estimate the total amount of paint removed from the wall in the Dust Study job per square foot of wall:

$$WallPaintRemoved = WallPaintCov \times PaintDens \times UnitConv \times LayersOfPaint \times FracRemoved$$

where:

<i>WallPaintRemoved</i>	=	the total paint per square foot of wall removed during the Dust Study job (mg/ft ² wall)
<i>WallPaintCov</i>	=	the amount of paint which covers a single square foot of wall (gallons/ft ²)
<i>UnitConv</i>	=	a conversion factor to convert from gallons to cm ³ and from mg to g
<i>PaintDens</i>	=	the density of the paint (g paint/cm ³ paint)
<i>LayersOfPaint</i>	=	the number of layers of paint
<i>FracRemoved</i>	=	the fraction of the total layers of paint that were removed during the Dust Study job

H.5. Percentage of Paint Emitted By Activity

Finally, the fraction of paint on the wall emitted per activity is estimated by dividing the amount emitted during the activity (Appendix H.3) by the total amount on the wall (Appendix H.4).

$$FracEmitted = \frac{MassDust_{total}}{WallPaint}$$

where:

<i>FracEmitted</i>	=	fraction of paint removed from wall that is emitted as aerosol
<i>MassDust_{total}</i>	=	total paint dust mass on the plastic (mg/ft ² disturbed)
<i>WallPaint</i>	=	the total paint per square foot of wall (mg/ft ² wall)

Then, the fractions for the different experiments were combined with the fractions from any available interior experiments, and the geometric mean across the different experiments was used to represent the overall activity emission fraction. The resulting emission fractions are shown in Table D-2.

For comparison purposes, Lee and Domanski (1999) examined the release of lead and abrasives during sandblasting operations to remove lead paint from bridges. They estimated that 9 percent of the lead on the bridge could be released as aerosol due to sandblasting. The emission fractions in this Approach tend to be on the order of this estimate. Power sanding, torching, and needle gun activities have a higher emission fraction, and these activities are expected to have a high potential for emission. The Lee and Domanski (1999) study suggests the emission fractions estimated here are reasonable.

Table H-3. Fraction of paint on the wall which is emitted as aerosolized particulate.

Renovation Activity	Fraction of Paint Removed (<i>FracRem</i>)	Fraction of Paint Aerosolized (<i>AerosolFrac</i>)¹	Fraction of Paint Emitted as Bulk Particulate (<i>PartDebFrac</i>)²
Power Sanding	0.15	0.248	0.051
Needle Gun	0.15	0.244	0.055
Torching	0.15	0.180	0.056
High Heat Gun	0.15	0.081	0.056
Low Heat Gun	0.15	0.077	0.059
Dry Scrape	0.15	0.070	0.060
Window/Door Replacement	0.15	0.069	0.060
Trim Replacement	0.15	0.070	0.060
Demolition	1.0	0.009	0.060

The general approach above was applied to the experiments in the Dust Study to compute the emission fractions. However, individual deviations from the generic layout and sampling protocol in Figure H-1 required additional assumptions in some experiments. The remainder of the Appendix details the assumptions, input data, regression results, and emission fraction calculations for each experiment. The figures in each Appendix represent the maps provided by Battelle, but all crosshatching (which represents regions where linear tapering is used to adjust loadings) were added during the estimation of the emission rates.

H.6. Power Sanding

H.6.1. Experiment 2

The geometry of Experiment 2 (see Figure H-3) was similar to the generic geometry in Figure H-2. . Because the measurement in Sample 1 was very high even though it was far to the left of the job area, loadings were not tapered linearly to zero at the edge of the plastic in this experiment. Instead, it was assumed that the dust generated during the power sanding experiments was emitted with momentum and could therefore travel laterally to further distances. Thus, the loadings were assumed to be constant across the entire width of the plastic (35 ft) and not just the width of the job (10 ft).

The measured lead loadings and associated distances are shown in Table H-4. No adjustments were made to the loadings since no linear tapering was assumed in this experiment. The loadings were divided by the size of the job (100 ft²) and the fraction of lead in the paint (0.117) to estimate the dust loadings per ft² disturbed in Table H-4. Sample 1 was excluded from the regression because it was within 3 ft of the job. Then, the natural logs of all loadings were used with the distances to estimate the regression parameters in

Table H-5. Regression Statistics in Experiment 2

. Here, *intercept* is the intercept of the linear regression in log space, and Load at 0 ft is the assumed loading at 0 ft calculated as $\exp(\textit{intercept})$.

The integral was performed over the regression equation out to a distance of 17 ft, which was the extent of the non-rule plastic. Masses were estimated both within the job area and outside the job area as shown in Table H-6. The estimated paint density using the lead fraction was 2.21 g/cm³. Because the renovated building was built in 1918, it was assumed to have 5.0 layers of paint at the time of the job. Power sanding was a paint removal activity, so all 5.0 layers were assumed to be removed. These values were used to estimate the total amount of paint on the wall, giving a final emission fraction of 0.108.

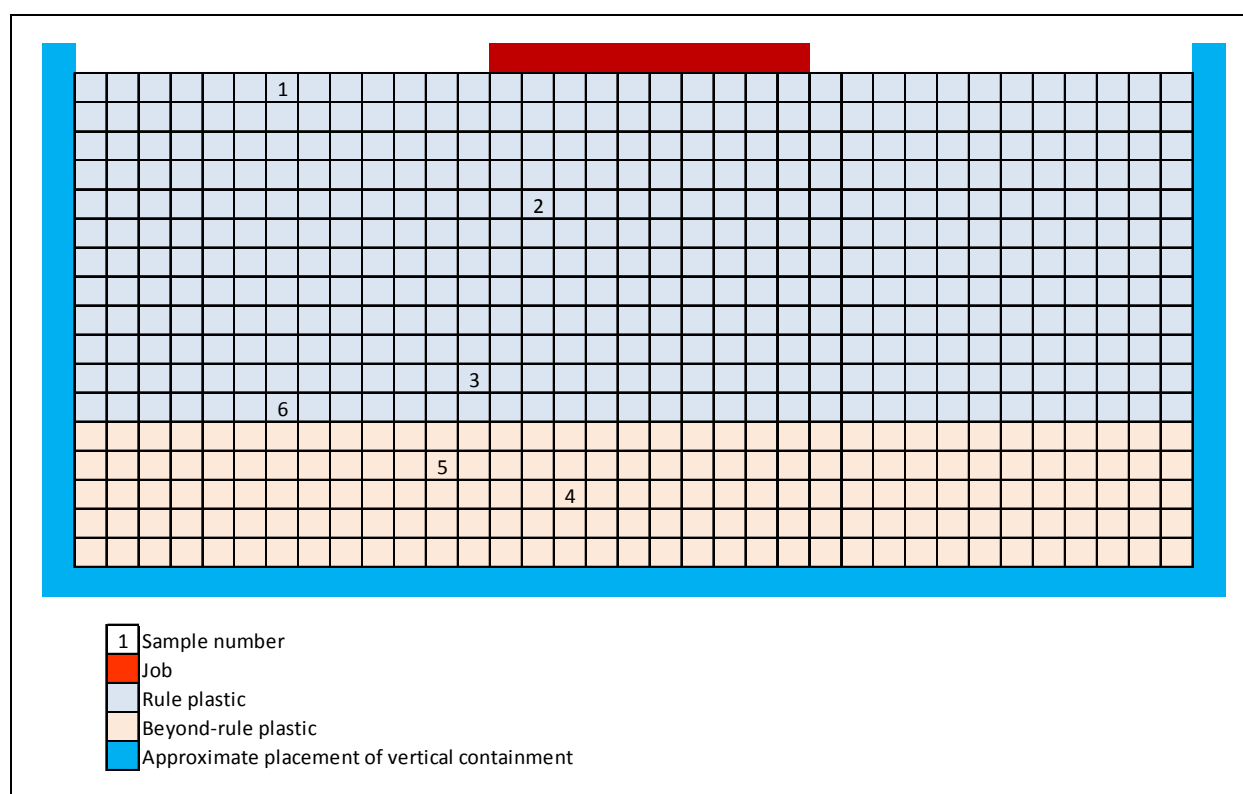


Figure H-3. Layout of Power Sanding Experiment 2

Table H-4. Dust Loading Measurements and Adjustments in Experiment 2

ID	Dist. From Wall (ft)	Adj. Dist. (ft)	Lead Loading (Dust Study) ¹	Lead Loading (adjusted)	Dust Load per ft ² Disturbed ²	Adjustment Parameters
1	1	NA	4,666,776	NA	398.87	None

Appendices to the Approach for Estimating Exposures and Incremental Health Effects from Lead due to Renovation, Repair, and Painting Activities in Public and Commercial Buildings

2	5	NA	328,358	NA	28.06	None
3	11	NA	102,291	NA	8.74	None
4	15	NA	56,460	NA	4.83	None
5	14	NA	82,678	NA	7.07	None
6	12	NA	63,192	NA	5.40	None

¹ Measurements that include bulk material are denoted in italics

² Measurements included in regression denoted in bold type

Table H-5. Regression Statistics in Experiment 2

Statistic	Value
Shape	-0.17
Intercept	4.09
R ²	0.90
Load at 0 ft (mg/ft ² plastic/ft ² disturbed)	59.71

Table H-6. Estimated Total Dust Emitted, Total Paint on Wall, and Emission Fraction in Experiment 2

Estimated Masses and Emission Fractions	Value
Mass of Dust Within Job Area (mg/ft ² disturbed)	3,306
Mass of Dust Not Within Job Area (mg/ft ² disturbed)	8,266
Total Mass of Dust on Plastic (mg/ft ² disturbed)	11,572
Total Paint on Surface (mg/ft ² disturbed)	107,206
Fraction Emitted	0.108

H.6.2. Experiment 3

The geometry for Experiment 3 is shown in Figure H-4. Similar to Experiment 2, the loadings in Experiment 3 were not tapered linearly to zero at the edge of the plastic in this experiment. Again, it was assumed that the dust generated during the power sanding experiments was emitted with momentum and could therefore travel laterally to further distances. Thus, the loadings were assumed to be constant across the entire width of the plastic (36 ft) and not just the width of the job (12 ft).

The measured lead loadings and associated distances are shown in

Table H-7. Dust Loading Measurements and Adjustments in Experiment 3

. No adjustments were made to the loadings since no linear tapering was assumed in this experiment. The loadings were divided by the size of the job (100 ft²) and the fraction of lead in the paint (0.131) to estimate the dust loadings per ft² disturbed in

Table H-7. Dust Loading Measurements and Adjustments in Experiment 3

. Sample 1 was excluded from the regression because it was within 3 ft of the job. Then, the natural logs of all loadings were used with the distances to estimate the regression parameters in Table H-8. Here, *intercept* is the intercept of the linear regression in log space, and Load at 0 ft is the assumed loading at 0 ft calculated as $\exp(\textit{intercept})$.

The integral was performed over the regression equation out to a distance of 17 ft, which was the extent of the non-rule plastic. Masses were estimated both within the job area and outside the job area as shown in Table H-9. The estimated paint density using the lead fraction was 2.35 g/cm^3 . Because the renovated building was built in 1918, it was assumed to have 5.0 layers of paint at the time of the job. Power sanding was a paint removal activity, so all 5.0 layers were assumed to be removed. These values were used to estimate the total amount of paint on the wall, giving a final emission fraction of 0.387.

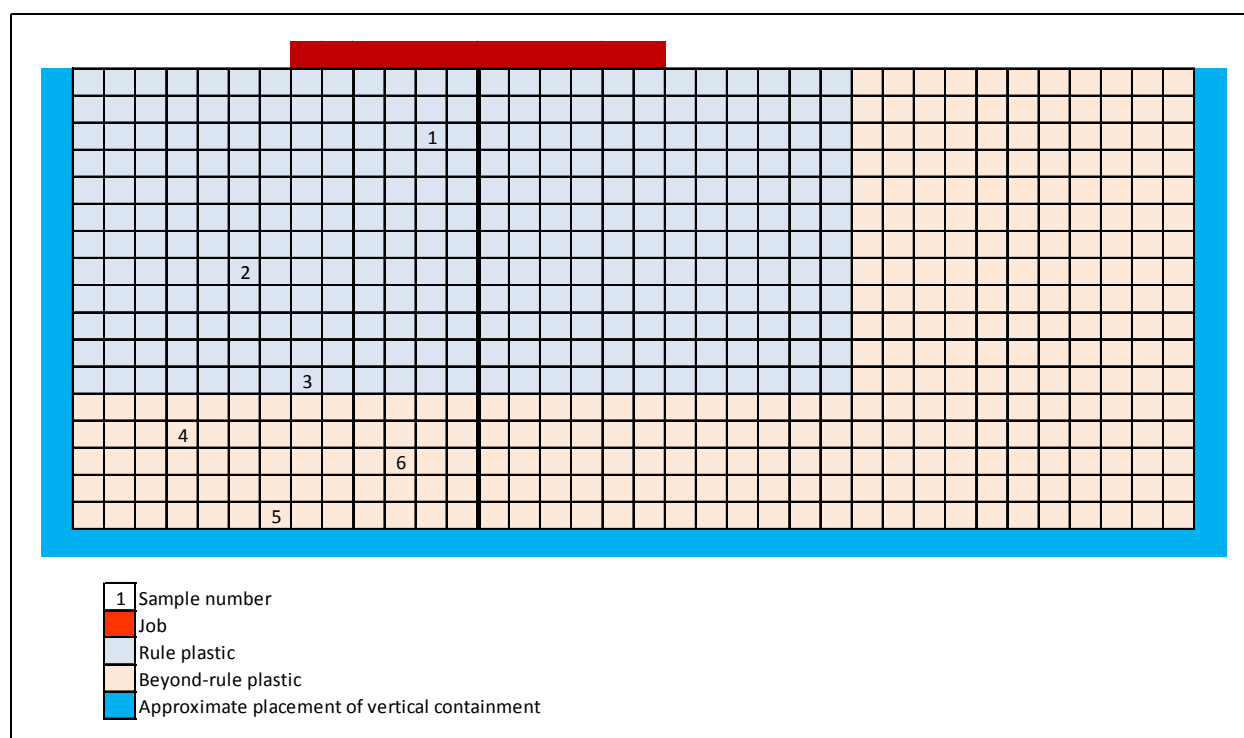


Figure H-4. Layout of Power Sanding Experiment 3

Table H-7. Dust Loading Measurements and Adjustments in Experiment 3

ID	Dist. From Wall (ft)	Adj. Dist. (ft)	Lead Loading (Dust Study) ¹	Lead Loading (adjusted)	Dust Load per ft ² Disturbed ²	Adjustment Parameters
1	3	NA	<i>8,289,211</i>	NA	632.76	None
2	8	NA	225,843	NA	17.24	None
3	12	NA	124,748	NA	9.52	None
4	14	NA	17,309	NA	1.32	None
5	17	NA	9,486	NA	0.72	None
6	15	NA	16,255	NA	1.24	None

¹ Measurements that include bulk material are denoted in italics

² Measurements included in regression denoted in bold type

Table H-8. Regression Statistics in Experiment 3

Statistic	Value
Shape	-0.39
Intercept	6.17
R ²	0.89
Load at 0 ft (mg/ft ² plastic/ft ² disturbed)	476.65

Table H-9. Estimated Total Dust Emitted, Total Paint on Wall, and Emission Fraction in Experiment 3

Estimated Masses and Emission Fractions	Value
Mass of Dust Within Job Area (mg/ft ² disturbed)	14,748
Mass of Dust Not Within Job Area (mg/ft ² disturbed)	29,496
Total Mass of Dust on Plastic (mg/ft ² disturbed)	44,244
Total Paint on Surface (mg/ft ² disturbed)	114,229
Fraction Emitted	0.387

H.7. Torching

The torching experiments were conducted on the ceilings of two different porches at residences. Scaffolding was used in both cases, and the scaffolding had gaps in it (to allow material to fall to the plastic during the experiment) and was dismantled prior to sample collection (to allow material on the scaffolding to fall onto the plastic). Because of these two details in the experimental setup, the torching

loadings were noted to be very high at large distances from the porch, and many of the samples were bulk samples, making the regression calculations difficult.

Thus, the torching experiments were treated differently to account for the scaffolding presence and the high bulk loadings. The high heat gun experiment (Experiment 66, see Appendix H.9) was also conducted on a ceiling (the awning over a door at a school). Three of the measurements were bulk loadings. Thus, the regression results calculated when excluding the bulk results from Experiment 66 were used to estimate the loadings at 0, 1, and 2 ft from the awning. Then, these predicted loadings (assumed to account for the non-bulk mass) were divided by the total bulk and non-bulk measurement at each distance to estimate the fraction that was bulk. The results are shown in Table H-10. In general, the ratio was fairly consistent at the three distances with an average value of 0.50.

Because the high heat gun paint removal technique is considered to be the most similar to the torching paint removal technique, this fraction was applied to the torching bulk measurements to estimate the non-bulk portion. This conversion is reflected in the “Lead Loading (adjusted)” columns in Table H-11 and Table H-14. Then, all the measurements were included in the regressions to estimate the emission fractions as described for each experiment below.

Table H-10. Torching Adjustment For Bulk Estimated from High Heat Gun Experiment

Dist. From Job (ft)	Bulk Dust Measurement Per ft ² Disturbed (mg/ft ² /ft ²)	Regression Prediction (mg/ft ² /ft ²)	Ratio
0	151.38	79.52	0.53
1	90.13	39.28	0.44
2	35.84	19.40	0.54
Average			0.50

H.7.1. Experiment 37

As discussed above, Experiment 37 removed paint on a porch ceiling at a residence (see Figure H-5). All bulk measurements were adjusted by a factor of 0.50 as discussed above to approximate the non-bulk portion. Then, the loadings were divided by the size of the job (98 ft²) and the fraction of lead in the paint (0.0518) to estimate the dust loadings per ft² disturbed in Table H-11. Because of the presence of the scaffolding that extended further than the porch area, the loadings were assumed to be constant all the way to the edge of the rule plastic, where very high bulk loadings were measured in the experiment. Thus, the adjusted distance was estimated to be 0 ft for all measurements under the porch or on the

rule plastic and the distance from the edge of the rule plastic to the measurement for the others. Then, the natural logs of loadings from all samples were used to estimate the regression parameters in Table H-12. Here, *intercept* is the intercept of the linear regression in log space, and Load at 0 ft is the assumed loading at 0 ft calculated as $\exp(\textit{intercept})$.

The masses were estimated in two different regions as shown in

Table H-13. Estimated Total Dust Emitted, Total Paint on Wall, and Emission Fraction in Experiment 37

. Under the job and on the rule plastic, the mass was estimated as the regression prediction at 0 ft (Load at 0 ft) multiplied by the area of the porch and rule plastic. Next, the mass on the beyond-rule plastic is estimated by integrating the regression equation over the length of the plastic (4 ft) and multiplying by the width (20 ft). The estimated paint density using the lead fraction was 1.28 g/cm³. Although the vintage of the renovated building was unknown, nearby buildings were believed to have been built at the same time and were built in 1920. Therefore, the building was assumed to have been built in 1920 and to have 5.0 layers of paint at the time of the job. Torching was a paint removal activity, so all 5.0 layers were assumed to be removed. These values were used to estimate the total amount of paint on the wall, giving a final emission fraction of 0.073.

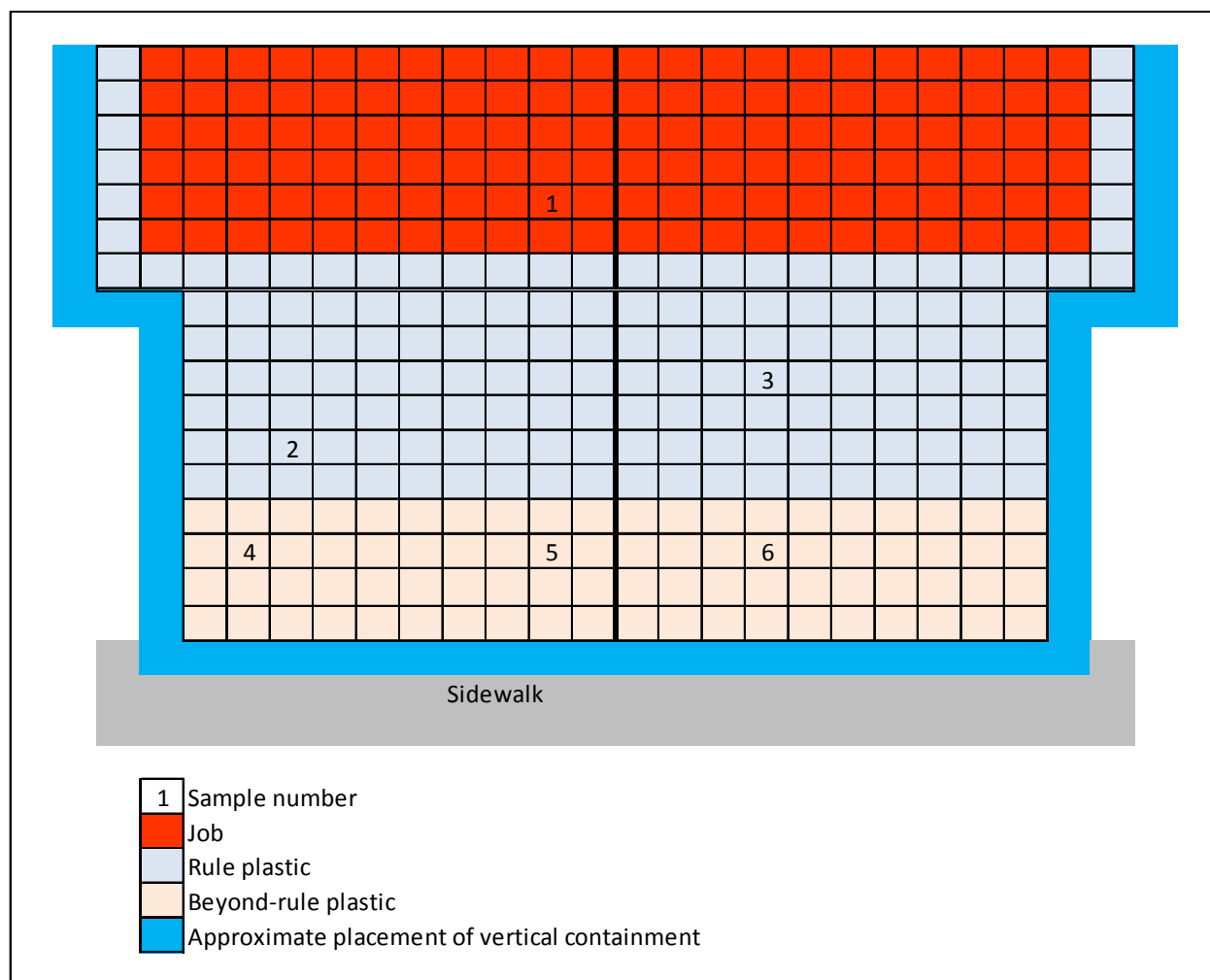


Figure H-5. Layout of Torching Experiment 37

Table H-11. Dust Loading Measurements and Adjustments in Experiment 37

ID	Dist. From Wall (ft)	Adj. Dist. (ft)	Lead Loading (Dust Study) ¹	Lead Loading (adjusted)	Dust Load per ft ² Disturbed ²	Adjustment Parameters
1	4.5	0	<i>1,134,829</i>	567,414	214.44	Distance adjusted to be from edge of rule plastic; Loading adjusted by factor of 0.5 to convert to non-bulk
2	12	0	919	NA	0.35	Distance adjusted to be from edge of rule plastic
3	10	0	<i>349,644</i>	174,822	66.07	Distance adjusted to be from edge of rule plastic; Loading adjusted by factor of 0.5 to convert to non-bulk
4	15	2	144	NA	0.05	Distance adjusted to be from edge of rule plastic
5	15	2	190	NA	0.07	Distance adjusted to be from edge of rule plastic
6	15	2	145	NA	0.05	Distance adjusted to be from edge of rule plastic

¹ Measurements that include bulk material are denoted in italics

² Measurements included in regression denoted in bold type

Table H-12. Regression Statistics in Experiment 37

Statistic	Value
Shape	-2.83
Intercept	2.83
R ²	0.67
Load at 0 ft (mg/ft ² plastic/ft ² disturbed)	17.01

Table H-13. Estimated Total Dust Emitted, Total Paint on Wall, and Emission Fraction in Experiment 37

Estimated Masses and Emission Fractions	Value
Mass of Dust Within Job Area (mg/ft ² disturbed)	4,422
Mass of Dust Not Within Job Area (mg/ft ² disturbed)	120
Total Mass of Dust on Plastic (mg/ft ² disturbed)	4,543
Total Paint on Surface (mg/ft ² disturbed)	62,054
Fraction Emitted	0.073

H.7.2. Experiment 38

As discussed above, Experiment 38 removed paint on a porch ceiling at a residence (see Figure H-6). All bulk measurements were adjusted by a factor of 0.50 as discussed above to approximate the non-bulk portion. Measurements made outside the job width were adjusted using a linear taper distance of 2 ft. This assumes the mass was the same on both sides but the loadings were somewhat higher on the left portion. Then, the loadings were divided by the size of the job (80 ft²) and the fraction of lead in the paint (0.114) to estimate the dust loadings per ft² disturbed in Table H-14. Because of the presence of the scaffolding that extended further than the porch area, the loadings were assumed to be constant all the way to the edge of the rule plastic, where very high bulk loadings were measured in the experiment. Thus, the adjusted distance was estimated to be 0 ft for all measurements under the porch or on the rule plastic and the distance from the edge of the rule plastic to the measurement for the others. Then, the natural logs of loadings from all samples were used to estimate the regression parameters in Table H-15. Here, *intercept* is the intercept of the linear regression in log space, and Load at 0 ft is the assumed loading at 0 ft calculated as $\exp(\textit{intercept})$.

The masses were estimated in two different regions as shown in

Table H-16. Estimated Total Dust Emitted, Total Paint on Wall, and Emission Fraction in Experiment 38

. The mass in the job area includes both the mass under the job and on the rule plastic within the job area and the mass on the beyond-rule plastic within the job area. The mass under the job and on the rule plastic was estimated as the regression prediction at 0 ft (Load at 0 ft) multiplied by the area of the porch (11 ft by 5 ft) and rule plastic (11 ft by 5 ft). Next, the mass on the beyond-rule plastic within the job area was estimated by integrating the regression equation over the length of the plastic (4 ft) and multiplying by the width (11 ft). Finally, the masses outside the job width were tapered linearly assuming a taper distance of 2 ft to reflect the distance on the left portion of the job. This assumes the mass was the same on both sides but the loadings were somewhat higher on the left portion. The estimated paint density using the lead fraction was 2.18 g/cm^3 . Because the renovated building was built in 1900, it was assumed to have 6.2 layers of paint at the time of the job. Torching was a paint removal activity, so all 6.2 layers were assumed to be removed. These values were used to estimate the total amount of paint on the wall, giving a final emission fraction of 0.287.

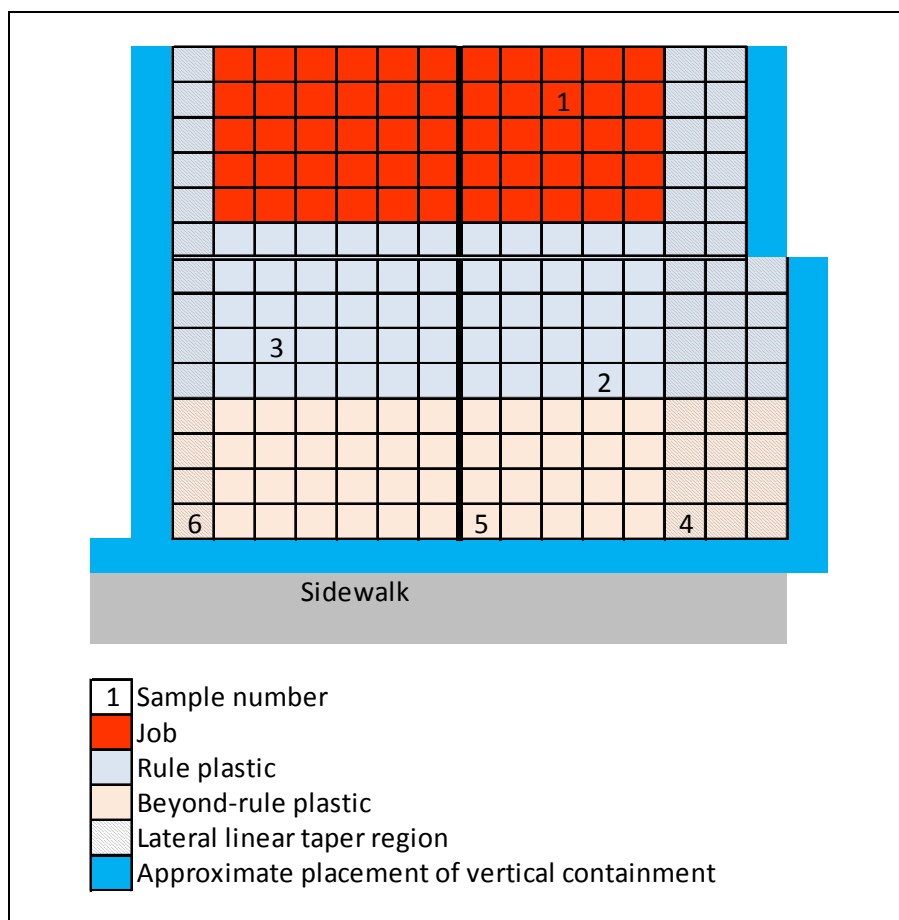


Figure H-6. Layout of Torching Experiment 38

Table H-14. Dust Loading Measurements and Adjustments in Experiment 38

ID	Dist. From Wall (ft)	Adj. Dist. (ft)	Lead Loading (Dust Study) ¹	Lead Loading (adjusted)	Dust Load per ft ² Disturbed ²	Adjustment Parameters
1	2	0	<i>29,401,680</i>	14,700,840	1611.93	Distance adjusted to be from edge of rule plastic; Loading adjusted by factor of 0.5 to convert to non-bulk
2	10.5	0	<i>1,560,303</i>	780,152	85.54	Distance adjusted to be from edge of rule plastic; Loading adjusted by factor of 0.5 to convert to non-bulk
3	9	0	<i>1,819,556</i>	909,778	99.76	Distance adjusted to be from edge of rule plastic; Loading adjusted by factor of 0.5 to convert to non-bulk
4	16.5	4	632	1264	0.14	Distance adjusted to be from edge of rule plastic; Loading adjusted to estimate loading within job area
5	16.5	4	1,766	NA	0.19	Distance adjusted to be from edge of rule plastic
6	16.5	4	1,051	2,102	0.23	Distance adjusted to be from edge of rule plastic; Loading adjusted to estimate loading within job area

¹ Measurements that include bulk material are denoted in italics

² Measurements included in regression denoted in bold type

Table H-15. Regression Statistics in Experiment 38

Statistic	Value
Shape	-1.79
Intercept	5.48
R ²	0.93
Load at 0 ft (mg/ft ² plastic/ft ² disturbed)	239.60

Table H-16. Estimated Total Dust Emitted, Total Paint on Wall, and Emission Fraction in Experiment 38

Estimated Masses and Emission Fractions	Value
Mass of Dust Within Job Area (mg/ft ² disturbed)	26,356
Mass of Dust Not Within Job Area (mg/ft ² disturbed)	6,527
Total Mass of Dust on Plastic (mg/ft ² disturbed)	32,884
Total Paint on Surface (mg/ft ² disturbed)	114,542
Fraction Emitted	0.287

H.8. Needle Gun

H.8.1. Experiment 65

Experiment 65 removed paint from a raised railing in a school courtyard (see Figure H-7). Thus, assumptions had to be made to account for this geometry. Plastic extended all around the job. It was assumed that the total masses emitted both in front of and behind the railing were equal. On the outer edge to the left of the job, the loadings were tapered to zero using a distance to the edge of the plastic of 8 ft. Sample 2 was adjusted to estimate the associated loading within the job area, and the adjusted loadings are shown in

Table H-17. Dust Loading Measurements and Adjustments in Experiment 65

The loadings were divided by the size of the job (30 ft²) and the fraction of lead in the paint (0.053) to estimate the dust loadings per ft² disturbed in

Table H-17. Dust Loading Measurements and Adjustments in Experiment 65

. Samples 1, 2 and 3 were excluded from the regression since they were within 3 ft of the job. Then, the natural logs of all loadings were used with the adjusted distances to estimate the regression parameters in Table H-18. Here, *intercept* is the intercept of the linear regression in log space, and Load at 0 ft is the assumed loading at 0 ft calculated as $\exp(\textit{intercept})$.

The integral was performed over the regression equation out to a distance of 12 ft (the length in front of the job) with a job width of 23 ft and then multiplied by two to account for the plastic behind the job. The estimated paint density using the lead fraction was 1.55 g/cm^3 . Because the renovated building was built in 1967, it was assumed to have 3.3 layers of paint at the time of the job. Needle gun was a paint removal activity, so all 3.3 layers were assumed to be removed. These values were used to estimate the total amount of paint on the wall in Table H-19, giving a final emission fraction of 0.244.

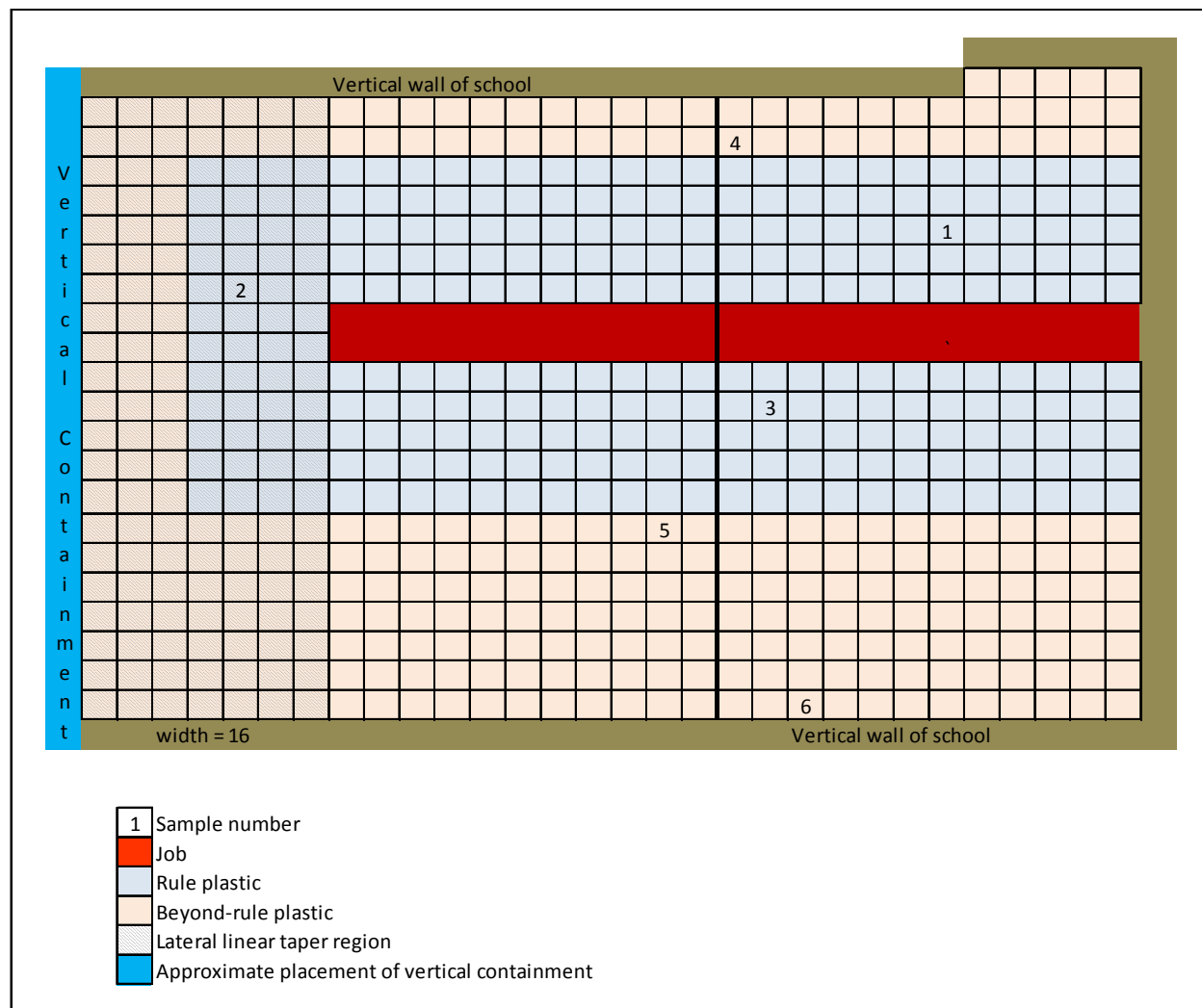


Figure H-7. Layout of Needle Gun Experiment 65

Table H-17. Dust Loading Measurements and Adjustments in Experiment 65

ID	Dist. From Wall (ft)	Adj. Dist. (ft)	Lead Loading (Dust Study) ¹	Lead Loading (adjusted)	Dust Load per ft ² Disturbed ²	Adjustment Parameters
1	3	NA	<i>381,586</i>	NA	239.99	None
2	3	NA	21,158	NA	13.31	None
3	2	NA	<i>888,167</i>	NA	558.60	None
4	6	NA	20,344	NA	12.79	None
5	6	NA	8,431	NA	5.30	None
6	12	NA	1,327	NA	0.83	None

¹ Measurements that include bulk material are denoted in italics

² Measurements included in regression denoted in bold type

Table H-18. Regression Statistics in Experiment 65

Statistic	Value
Shape	-0.38
Intercept	4.40
R ²	0.90
Load at 0 ft (mg/ft ² plastic/ft ² disturbed)	81.29

Table H-19. Estimated Total Dust Emitted, Total Paint on Wall, and Emission Fraction in Experiment 65

Estimated Masses and Emission Fractions	Value
Mass of Dust Within Job Area (mg/ft ² disturbed)	9,699
Mass of Dust Not Within Job Area (mg/ft ² disturbed)	1,687
Total Mass of Dust on Plastic (mg/ft ² disturbed)	11,386
Total Paint on Surface (mg/ft ² disturbed)	46,717
Fraction Emitted	0.244

H.9. High Heat Gun

H.9.1. Experiment 66

Experiment 66 removed paint on an awning above a door in a school courtyard (Figure H-8). Thus, assumptions had to be made to account for this geometry. Plastic extended to the left of the job. There

was a raised railing to the left of the job, but because the job was done on an awning at a height of 7 to 15 ft, it was assumed that the dust could travel over the railing and spread to the vertical school wall. In addition, it was assumed that the dust could spread the full length to the containment plastic in front of the job. The total masses emitted both in front of and just to the left of the awning were assumed to decrease exponentially with distance from the awning edge. In the remaining portion of plastic, it was assumed that loadings tapered both from the upper area and right area, tapering to zero over a length of 19 ft (from the upper portion to the containment plastic) and over a length of 15 ft (from the right portion over to the vertical wall of the school).

The loadings were divided by the size of the job (30 ft²) and the fraction of lead in the paint (0.183) to estimate the dust loadings per ft² disturbed in Table H-20. Sample 6 was adjusted to approximate the value of the loading within the width of the job. Samples 1, 2 and 3 were excluded from the regression since they were within 3 ft of the job. Then, the natural logs of loadings from Samples 4, 5, and 6 were used to estimate the regression parameters in Table H-21. Here, *intercept* is the intercept of the linear regression in log space, and Load at 0 ft is the assumed loading at 0 ft calculated as $\exp(\text{intercept})$.

The masses were estimated in three different regions. Under the job, the mass was estimated as the regression prediction at 0 ft (Load at 0 ft) multiplied by the area of the awning (5 ft by 9 ft). Next, the masses within the two job areas (lower and to the left of the job) were estimated by integrating the regression out to 15 ft and multiplying by a width of 5 ft (left portion) and integrating the regression out to 19 ft and multiplying by a width of 9 ft (lower portion). Finally, the mass in the remaining taper region was estimated by tapering the left and lower portions of the within-job loadings to zero over the remaining area. The estimated paint density using the lead fraction was 2.89 g/cm³. Because the renovated building was built in 1967, it was assumed to have 3.3 layers of paint at the time of the job. High heat gun was a paint removal activity, so all 3.3 layers were assumed to be removed. These values were used to estimate the total amount of paint on the wall, giving a final emission fraction of 0.081.

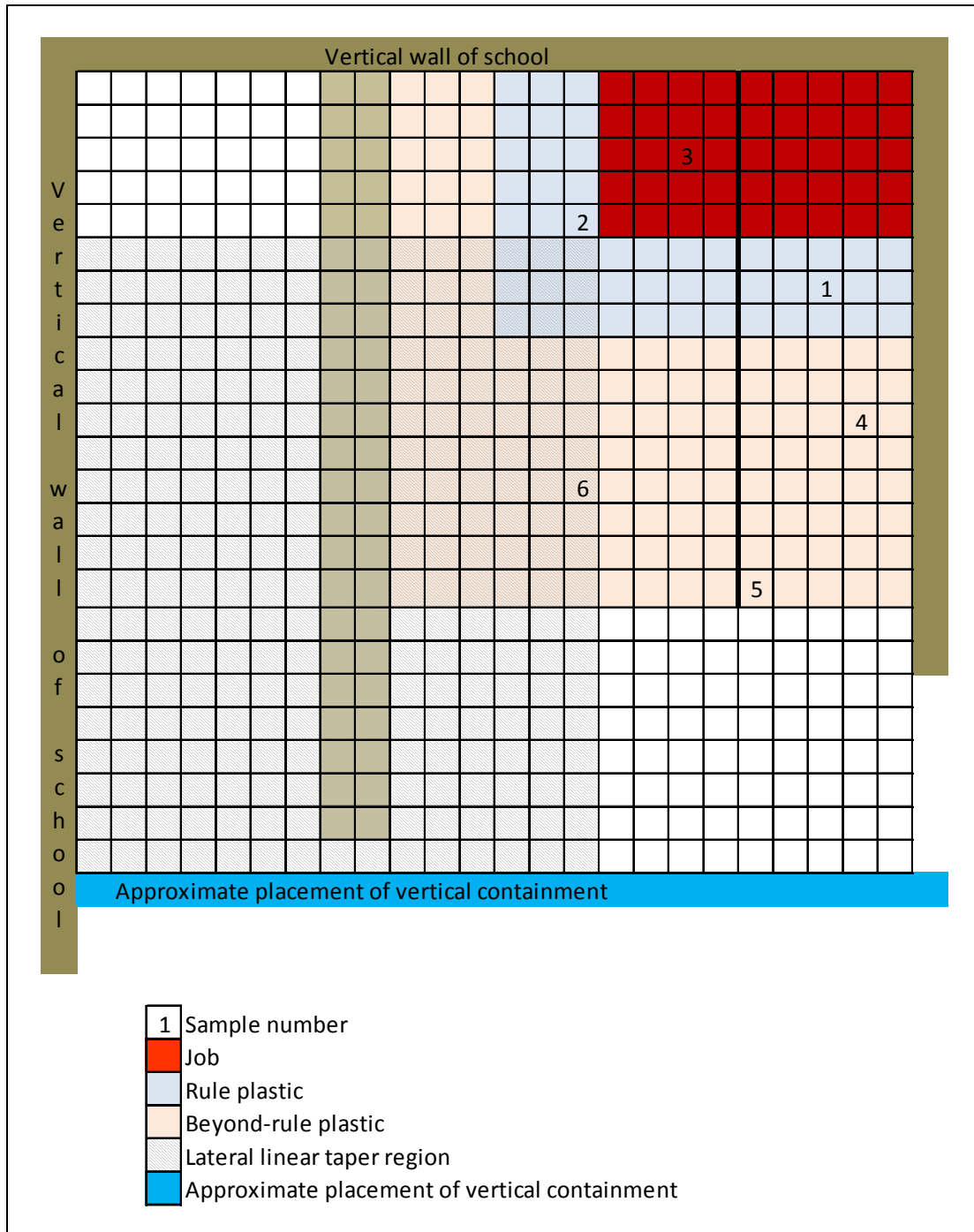


Figure H-8. Layout of High Heat Gun Experiment 66

Table H-20. Dust Loading Measurements and Adjustments in Experiment 66

ID	Dist. From Wall (ft)	Adj. Dist. (ft)	Lead Loading (Dust Study) ¹	Lead Loading (adjusted)	Dust Load per ft ² Disturbed ²	Adjustment Parameters
1	7	2	<i>196,760</i>	NA	35.84	Distance adjusted to be from edge of awning
2	5	1	<i>494,822</i>	NA	90.13	Distance adjusted to be from edge of awning
3	3	0	<i>831,062</i>	NA	151.38	Distance adjusted to be from edge of awning
4	11	6	14,124	NA	2.57	Distance adjusted to be from edge of awning
5	16	11	318	NA	0.06	Distance adjusted to be from edge of awning
6	13	8	349	407	0.07	Distance adjusted to be from edge of awning; Loading adjusted to estimate loading within job area

¹ Measurements that include bulk material are denoted in italics

² Measurements included in regression denoted in bold type

Table H-21. Regression Statistics in Experiment 66

Statistic	Value
Shape	-0.71
Intercept	4.38
R ²	0.70
Load at 0 ft (mg/ft ² plastic/ft ² disturbed)	79.52

Table H-22. Estimated Total Dust Emitted, Total Paint on Wall, and Emission Fraction in Experiment 66

Estimated Masses and Emission Fractions	Value
Mass of Dust Under Job Area (mg/ft ² disturbed)	3,578
Mass of Dust Within Job Area (mg/ft ² disturbed)	1,578
Mass of Dust Not Within Job Area (mg/ft ² disturbed)	1,917
Total Mass of Dust on Plastic (mg/ft ² disturbed)	7,073
Total Paint on Surface (mg/ft ² disturbed)	87,288
Fraction Emitted	0.081

H.10. Low Heat Gun

H.10.1. Experiment 64

Experiment 64 removed paint from a door at the bottom of a stairwell in a school courtyard (see Figure H-9). Thus, assumptions had to be made to account for this geometry. The space at the bottom of the stairs was confined and loadings measured there (even at distances greater than 3 ft from the door) were very high and included bulk material (Samples 2 and 4). Bulk samples 1, 2 and 4 were excluded from the regression. Sample 3 was not excluded because the presence of the corner was assumed to mediate the transfer of bulk material from the door to that location. Finally, it was assumed that because the job was performed at the bottom of a flight of stairs, the dust would not travel further than the edge of the plastic.

The loadings were divided by the size of the job (75 ft²) and the fraction of lead in the paint (0.315) to estimate the dust loadings per ft² disturbed in

Table H-23. Dust Loading Measurements and Adjustments in Experiment 64

. Samples 3, 5, and 6 were adjusted to estimate the associated loading within the job area, and the adjusted loadings are shown in

Table H-23. Dust Loading Measurements and Adjustments in Experiment 64

. Then, the natural logs of loadings from Samples 3, 5, and 6 were used to estimate the regression parameters in Table H-24. Here, *intercept* is the intercept of the linear regression in log space, and Load at 0 ft is the assumed loading at 0 ft calculated as $\exp(\textit{intercept})$.

The mass within the job area was estimated by integrating the regression equation over a length of 8 ft and multiplying by the job width of 5 ft. The mass outside the job area was estimated by calculating the integrated mass between 1 ft and 8 ft (to account for the presence of the corner) and tapered linearly assuming a taper distance of 6 ft. The estimated paint density using the lead fraction was 4.26 g/cm^3 . Because the renovated building was built in 1967, it was assumed to have 3.3 layers of paint at the time of the job. Low heat gun was a paint removal activity, so all 3.3 layers were assumed to be removed. These values were used to estimate the total amount of paint on the wall, giving a final emission fraction of 0.077.

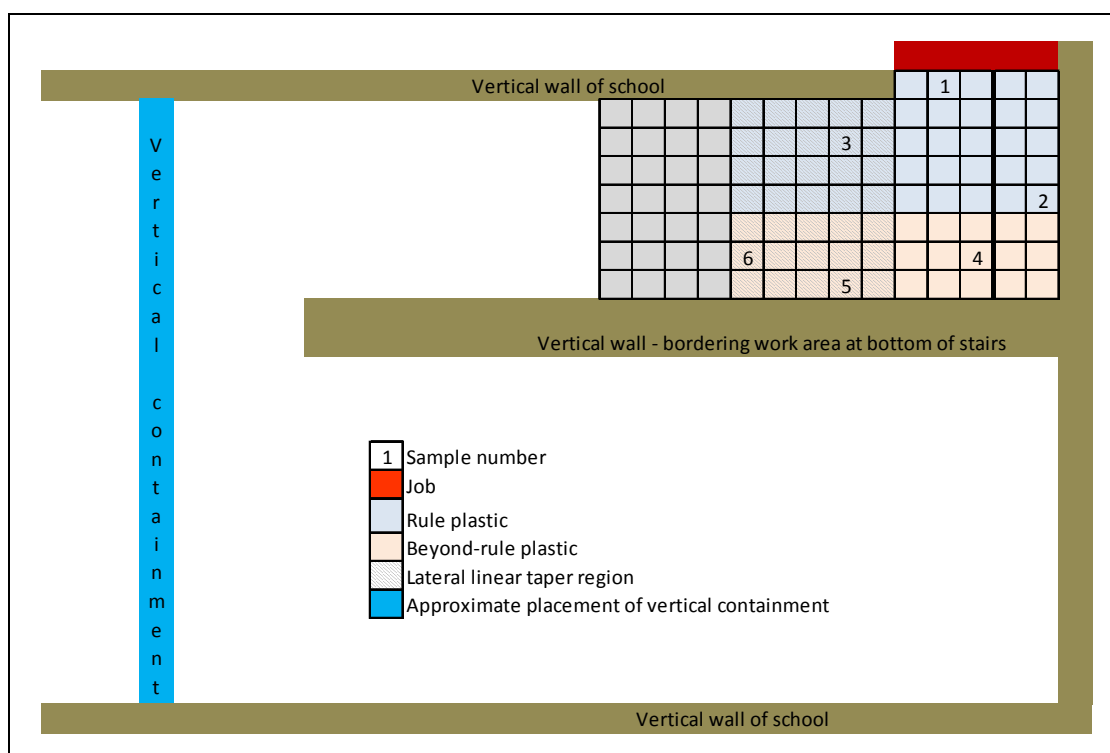


Figure H-9. Layout of Low Heat Gun Experiment 64

Table H-23. Dust Loading Measurements and Adjustments in Experiment 64

ID	Dist. From Wall (ft)	Adj. Dist. (ft)	Lead Loading (Dust Study) ¹	Lead Loading (adjusted)	Dust Load per ft ² Disturbed ²	Adjustment Parameters
1	1	NA	<i>130,674,045</i>	NA	5,531.18	None
2	5	NA	<i>1,133,090</i>	NA	47.96	None
3	3	NA	<i>2,538,052</i>	NA	107.43	None
4	7	NA	<i>2,692,069</i>	NA	113.95	None
5	8	NA	<i>26,587</i>	NA	1.13	None
6	7	NA	<i>16,235</i>	NA	0.69	None

¹ Measurements that include bulk material are denoted in italics

² Measurements included in regression denoted in bold type

Table H-24. Regression Statistics in Experiment 64

Statistic	Value
Shape	-0.83
Intercept	7.16
R ²	0.99
Load at 0 ft (mg/ft ² plastic/ft ² disturbed)	1290.60

Table H-25. Estimated Total Dust Emitted, Total Paint on Wall, and Emission Fraction in Experiment 64

Estimated Masses and Emission Fractions	Value
Mass of Dust Within Job Area (mg/ft ² disturbed)	7,800
Mass of Dust Not Within Job Area (mg/ft ² disturbed)	2,045
Total Mass of Dust on Plastic (mg/ft ² disturbed)	9,845
Total Paint on Surface (mg/ft ² disturbed)	128,483
Fraction Emitted	0.077

H.11. Dry Scrape

H.11.1. Experiment 1

The geometry of Experiment 1 (see Figure H-10) was similar to the generic geometry in Figure H-1. The beyond-rule plastic spread far to the left of the job. However, it was assumed that in the dry scrape experiment, the dust would tend to be largely bulk pieces and would not spread far in the lateral direction. Thus, the right width (3 ft) was used to taper the loadings to zero.

The measured lead loadings and associated distances are shown in Table H-26. No adjustments were necessary to approximate loadings within the job area, since all measurements were taken within the job width. The loadings were divided by the size of the job (90 ft²) and the fraction of lead in the paint (0.135) to estimate the dust loadings per ft² disturbed in Table H-26. Sample 1 was excluded from the regression because it was within 3 ft of the job. Then, the natural logs of all loadings were used with the distances to estimate the regression parameters in Table H-27. Here, *intercept* is the intercept of the linear regression in log space, and Load at 0 ft is the assumed loading at 0 ft calculated as $\exp(\textit{intercept})$.

The integral was performed over the regression equation out to a distance of 17 ft, which was the extent of the non-rule plastic. Masses were estimated both within the job area (8 ft wide) and outside the job area as shown in Table H-28. The estimated paint density using the lead fraction was 2.40 g/cm³. Because the renovated building was built in 1918, it was assumed to have 5.0 layers of paint at the time of the job. Dry scrape was a surface preparation activity, so 15% of the paint layers were assumed to be removed. These values were used to estimate the total amount of paint on the wall, giving a final emission fraction of 0.015.

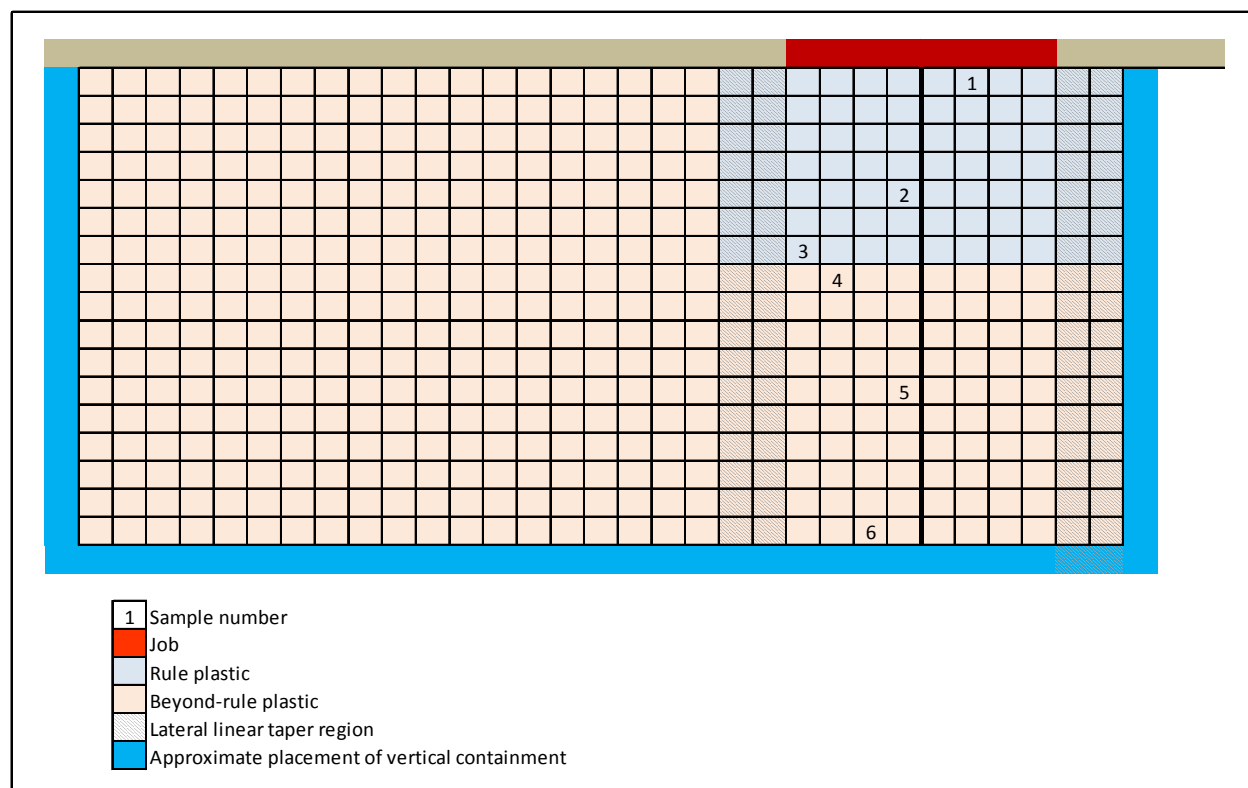


Figure H-10. Layout of Dry Scrape Experiment 1

Table H-26. Dust Loading Measurements and Adjustments in Experiment 1

ID	Dist. From Wall (ft)	Adj. Dist. (ft)	Lead Loading (Dust Study) ¹	Lead Loading (adjusted)	Dust Load per ft ² Disturbed ²	Adjustment Parameters
1	1	NA	12,516,130	NA	1,030.13	None
2	5	NA	48,865	NA	4.02	None
3	7	NA	8,227	NA	0.68	None
4	8	NA	4,018	NA	0.33	None
5	12	NA	916	NA	0.08	None
6	17	NA	893	NA	0.07	None

¹ Measurements that include bulk material are denoted in italics

² Measurements included in regression denoted in bold type

Table H-27. Regression Statistics in Experiment 1

Statistic	Value
Shape	-0.31
Intercept	1.97
R ²	0.78
Load at 0 ft (mg/ft ² plastic/ft ² disturbed)	7.17

Table H-28. Estimated Total Dust Emitted, Total Paint on Wall, and Emission Fraction in Experiment 1

Estimated Masses and Emission Fractions	Value
Mass of Dust Within Job Area (mg/ft ² disturbed)	185
Mass of Dust Not Within Job Area (mg/ft ² disturbed)	69
Total Mass of Dust on Plastic (mg/ft ² disturbed)	254
Total Paint on Surface (mg/ft ² disturbed)	17,435
Fraction Emitted	0.015

H.11.2. Experiment 21

The geometry of Experiment 21 (see Figure H-11) was similar to the generic geometry in Figure H-1. The job was not centered with respect to the plastic. The larger width on the left (6 ft) was used to taper the within-job loadings to zero at the edge of the plastic. This reflects the assumption that the total amount

of dust will be the same on both sides, but the loadings to the right will be somewhat higher since the dust spreads over a smaller distance. This is reflected in the diagram with darker crosshatching on that side.

The measured lead loadings and associated distances are shown in

Table H-29. Dust Loading Measurements and Adjustments in Experiment 21

. No adjustments were necessary to approximate loadings within the job area, since all measurements were taken within the job width. The loadings were divided by the size of the job (150 ft²) and the fraction of lead in the paint (0.013) to estimate the dust loadings per ft² disturbed in

Table H-29. Dust Loading Measurements and Adjustments in Experiment 21

. Sample 1 was excluded from the regression because it was within 3 ft of the job. Then, the natural logs of all loadings were used with the distances to estimate the regression parameters in Table H-30. Here, *intercept* is the intercept of the linear regression in log space, and Load at 0 ft is the assumed loading at 0 ft calculated as $\exp(\textit{intercept})$.

The integral was performed over the regression equation out to a distance of 18 ft, which was the extent of the non-rule plastic. Masses were estimated both within the job area (16 ft wide) and outside the job area as shown in Table H-31. The estimated paint density using the lead fraction was 1.13 g/cm³. Because the renovated building was built in 1920, it was assumed to have 5.0 layers of paint at the time of the job. Dry scrape was a surface preparation activity, so 15% of the paint layers were assumed to be removed. These values were used to estimate the total amount of paint on the wall, giving a final emission fraction of 0.041.

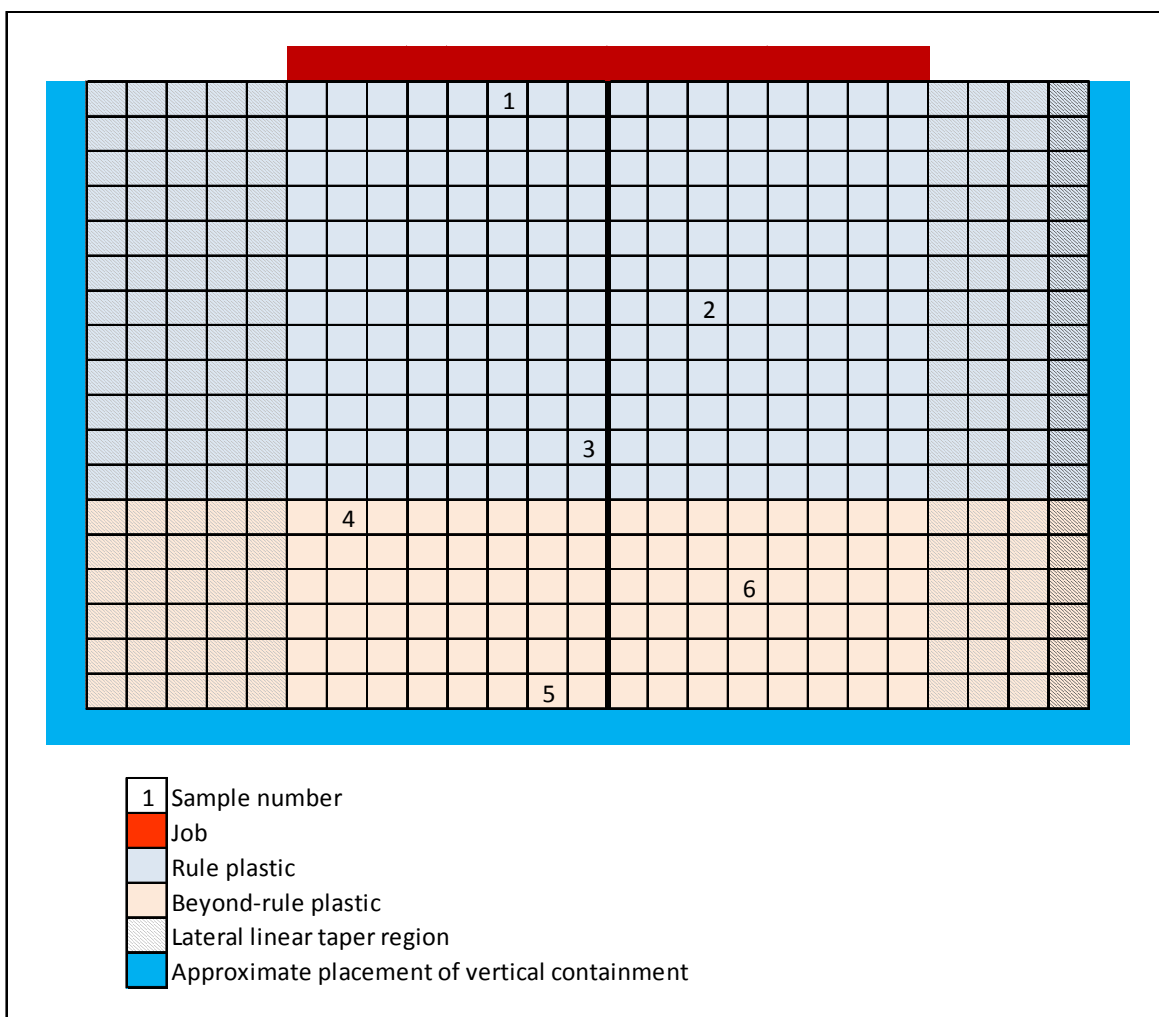


Figure H-11. Layout of Dry Scrape Experiment 21

Table H-29. Dust Loading Measurements and Adjustments in Experiment 21

ID	Dist. From Wall (ft)	Adj. Dist. (ft)	Lead Loading (Dust Study) ¹	Lead Loading (adjusted)	Dust Load per ft ² Disturbed ²	Adjustment Parameters
1	1	NA	<i>1,463,974</i>	NA	750.76	None
2	7	NA	2,266	NA	1.16	None
3	11	NA	401	NA	0.21	None
4	13	NA	263	NA	0.13	None
5	18	NA	165	NA	0.08	None
6	15	NA	552	NA	0.28	None

¹ Measurements that include bulk material are denoted in italics

² Measurements included in regression denoted in bold type

Table H-30. Regression Statistics in Experiment 21

Statistic	Value
Shape	-0.20
Intercept	1.18
R ²	0.72
Load at 0 ft (mg/ft ² plastic/ft ² disturbed)	3.25

Table H-31. Estimated Total Dust Emitted, Total Paint on Wall, and Emission Fraction in Experiment 21

Estimated Masses and Emission Fractions	Value
Mass of Dust Within Job Area (mg/ft ² disturbed)	248
Mass of Dust Not Within Job Area (mg/ft ² disturbed)	93
Total Mass of Dust on Plastic (mg/ft ² disturbed)	342
Total Paint on Surface (mg/ft ² disturbed)	8,255
Fraction Emitted	0.041

H.12. Experiment 75

The geometry of Experiment 75 (see Figure H-12) was similar to the generic geometry in Figure H-1. The job was not centered with respect to the plastic. The larger width on the left (6 ft) was used to taper the within-job loadings to zero at the edge of the plastic. This reflects the assumption that the total amount of dust will be the same on both sides, but the loadings to the right will be somewhat higher since the

dust spreads over a smaller distance. This is reflected in the diagram with darker crosshatching on that side.

The measured lead loadings and associated distances are shown in Table H-32. No adjustments were necessary to approximate loadings within the job area, since all measurements were taken within the job width. The loadings were divided by the size of the job (100 ft²) and the fraction of lead in the paint (0.013) to estimate the dust loadings per ft² disturbed in Table H-32. Sample 1 was excluded from the regression because it was within 3 ft of the job. Then, the natural logs of all loadings were used with the distances to estimate the regression parameters in Table H-33. Here, *intercept* is the intercept of the linear regression in log space, and Load at 0 ft is the assumed loading at 0 ft calculated as $\exp(\textit{intercept})$.

The integral was performed over the regression equation out to a distance of 16 ft, which was the extent of the non-rule plastic. Masses were estimated both within the job area (16 ft wide) and outside the job area as shown in Table H-34. The estimated paint density using the lead fraction was 1.13 g/cm³. Because the renovated building was built in 1920, it was assumed to have 5.0 layers of paint at the time of the job. Dry scrape was a surface preparation activity, so 15% of the paint layers were assumed to be removed. These values were used to estimate the total amount of paint on the wall, giving a final emission fraction of 0.188.

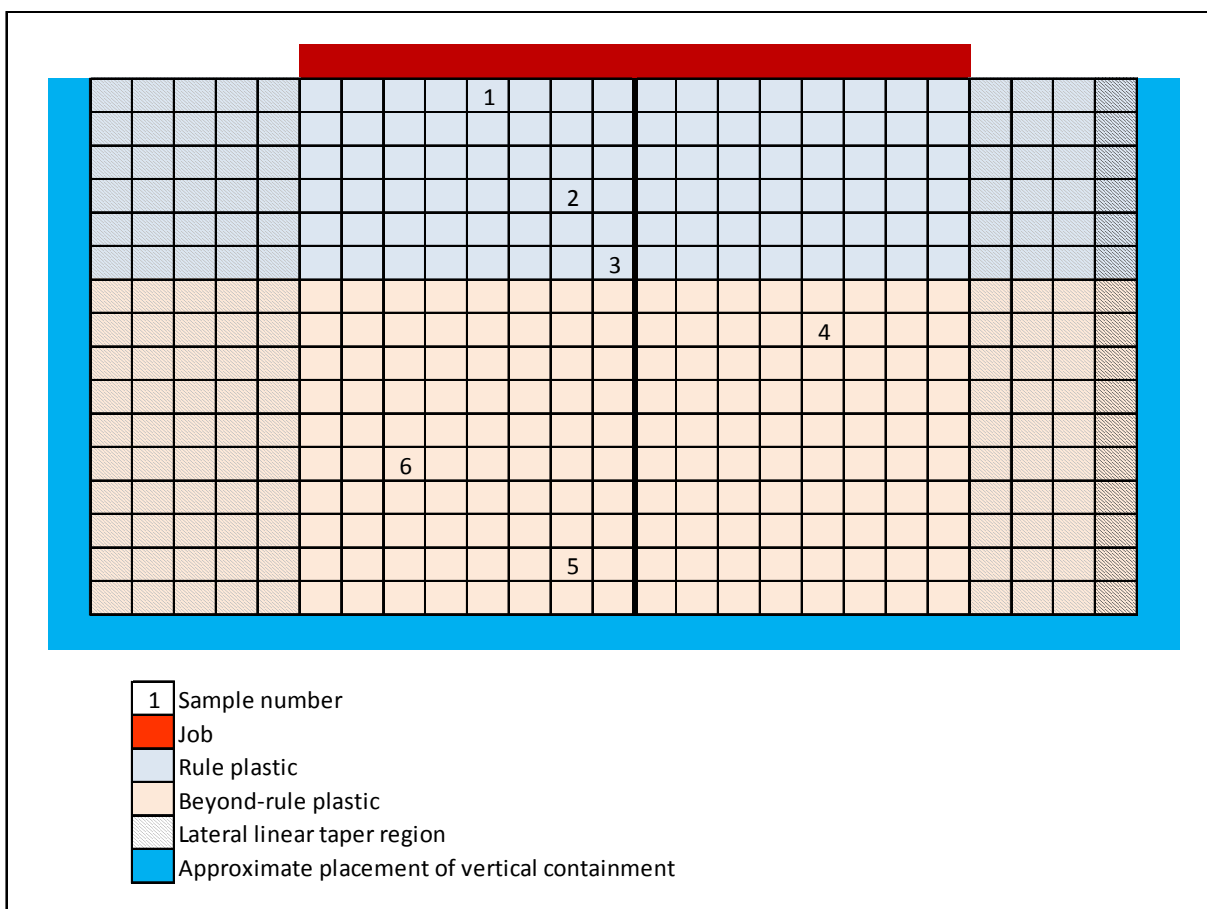


Figure H-12. Layout of Dry Scrape Experiment 75

Table H-32. Dust Loading Measurements and Adjustments in Experiment 75

ID	Dist. From Wall (ft)	Adj. Dist. (ft)	Lead Loading (Dust Study) ¹	Lead Loading (adjusted)	Dust Load per ft ² Disturbed ²	Adjustment Parameters
1	1	NA	<i>1,961,779</i>	NA	1509.06	None
2	4	NA	13,794	NA	10.61	None
3	7	NA	1,774	NA	1.36	None
4	8	NA	1,159	NA	0.89	None
5	15	NA	183	NA	0.14	None
6	12	NA	469	NA	0.36	None

¹ Measurements that include bulk material are denoted in italics

² Measurements included in regression denoted in bold type

Table H-33. Regression Statistics in Experiment 75

Statistic	Value
Shape	-0.36
Intercept	3.24
R ²	0.93
Load at 0 ft (mg/ft ² plastic/ft ² disturbed)	25.61

Table H-34. Estimated Total Dust Emitted, Total Paint on Wall, and Emission Fraction in Experiment 75

Estimated Masses and Emission Fractions	Value
Mass of Dust Within Job Area (mg/ft ² disturbed)	1,130
Mass of Dust Not Within Job Area (mg/ft ² disturbed)	424
Total Mass of Dust on Plastic (mg/ft ² disturbed)	1,553
Total Paint on Surface (mg/ft ² disturbed)	8,255
Fraction Emitted	0.188

H.12.1. Experiment 40

The geometry of Experiment 40 (see Figure H-13) was similar to the generic geometry in Figure H-1. The job extended over the entire width of the plastic, so no linear tapering or loading adjustments were necessary.

The loadings were divided by the size of the job (250 ft²) and the fraction of lead in the paint (0.157) to estimate the dust loadings per ft² disturbed in Table H-35. Sample 1 was excluded from the regression because it was within 3 ft of the job. Then, the natural logs of all loadings were used with the distances to estimate the regression parameters in Table H-36. Here, *intercept* is the intercept of the linear regression in log space, and Load at 0 ft is the assumed loading at 0 ft calculated as $\exp(\textit{intercept})$.

The integral was performed over the regression equation out to a distance of 12 ft, which was the extent of the non-rule plastic. Masses were estimated within the job area (20 ft wide). The estimated paint density using the lead fraction was 2.62 g/cm³. Because the renovated building was built in 1920, it was assumed to have 5.0 layers of paint at the time of the job. Dry scrape was a surface preparation activity, so 15% of the paint layers were assumed to be removed. These values were used to estimate the total amount of paint on the wall, giving a final emission fraction of 0.038.

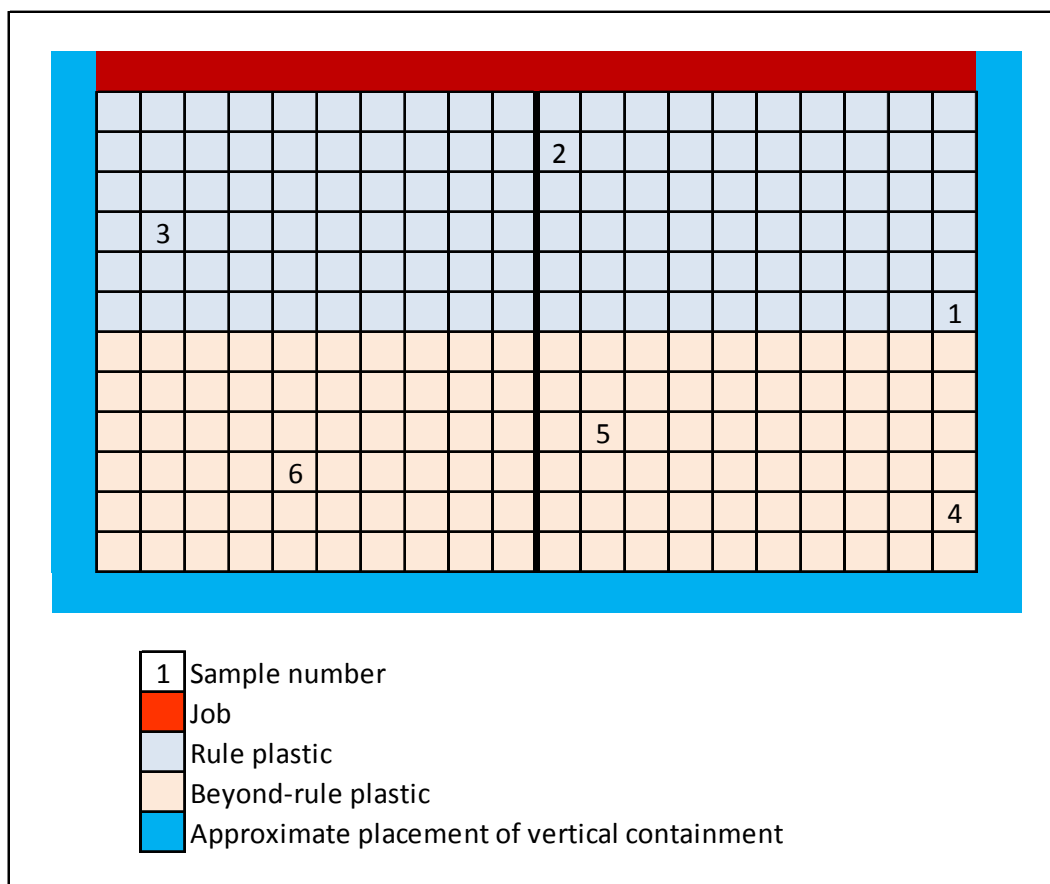


Figure H-13. Layout of Dry Scrape Experiment 40

Table H-35. Dust Loading Measurements and Adjustments in Experiment 40

ID	Dist. From Wall (ft)	Adj. Dist. (ft)	Lead Loading (Dust Study) ¹	Lead Loading (adjusted)	Dust Load per ft ² Disturbed ²	Adjustment Parameters
1	6	NA	13,796	NA	0.35	None
2	2	NA	11,480,352	NA	292.49	None
3	4	NA	268,359	NA	6.84	None
4	11	NA	7,303	NA	0.19	None
5	9	NA	11,701	NA	0.30	None
6	10	NA	15,959	NA	0.41	None

¹ Measurements that include bulk material are denoted in italics

² Measurements included in regression denoted in bold type

Table H-36. Regression Statistics in Experiment 40

Statistic	Value
Shape	-0.41
Intercept	2.70
R ²	0.70
Load at 0 ft (mg/ft ² plastic/ft ² disturbed)	14.92

Table H-37. Estimated Total Dust Emitted, Total Paint on Wall, and Emission Fraction in Experiment 40

Estimated Masses and Emission Fractions	Value
Mass of Dust Within Job Area (mg/ft ² disturbed)	721
Mass of Dust Not Within Job Area (mg/ft ² disturbed)	0
Total Mass of Dust on Plastic (mg/ft ² disturbed)	721
Total Paint on Surface (mg/ft ² disturbed)	19,091
Fraction Emitted	0.038

H.13. Trim Replacement

H.13.1. Experiment 4

Experiment 4 removed trim from the side of a home and was performed on two separate sides of the building (see Figure H-14). Thus, assumptions had to be made to account for this geometry. It was assumed that the loadings were constant on both walls within the job area. On the outer edges of the job on both walls, the loadings were tapered to zero using a distance to the edge of the plastic of 5 ft. Between the two sections of job wall, the loadings were assumed to taper linearly from both directions using a width of 7 ft in both directions. In actuality, the distance was 8 ft for the upper portion of the job. Thus, this assumption reflects that the total mass contribution will be the same from both directions even though the mass from the upper portion can spread over a wider distance. Samples 1, 2, and 6 were adjusted to estimate the associated loading within the job area, and the adjusted loadings are shown in Table H-38. Sample 1 was also adjusted so that the distance reflected the distance to the corner of the wall (3 ft).

The loadings were divided by the size of the job (40 ft²) and the fraction of lead in the paint (0.153) to estimate the dust loadings per ft² disturbed in Table H-38. Samples 2 and 3 were excluded from the regression since they were within 2 ft of the job. Sample 1 was included in the regression. It is within 3 ft

of the job but was not a bulk measurement. Then, the natural logs of all loadings were used with the adjusted distances to estimate the regression parameters in Table H-39. Here, *intercept* is the intercept of the linear regression in log space, and Load at 0 ft is the assumed loading at 0 ft calculated as $\exp(\textit{intercept})$. In this case, the regression coefficient is low, indicating there is additional uncertainty in this emission estimate.

The integral was performed over the regression equation out to a distance of 7 ft, which was the extent of the non-rule plastic in the lower portion of the job. The same distance was used for the upper portion, reflecting the assumption that the total mass contribution will be the same from both directions even though the mass from the upper portion can spread over a wider distance. Masses were estimated both within the job area and outside the job area (the two edge taper regions and the middle “double taper” region) as shown in Table H-40. The estimated paint density using the lead fraction was 2.58 g/cm³. Because the renovated building was built in 1920, it was assumed to have 5.0 layers of paint at the time of the job. Trim replacement was a surface preparation activity, so 15% of the paint layers were assumed to be removed. These values were used to estimate the total amount of paint on the wall, giving a final emission fraction of 0.070.

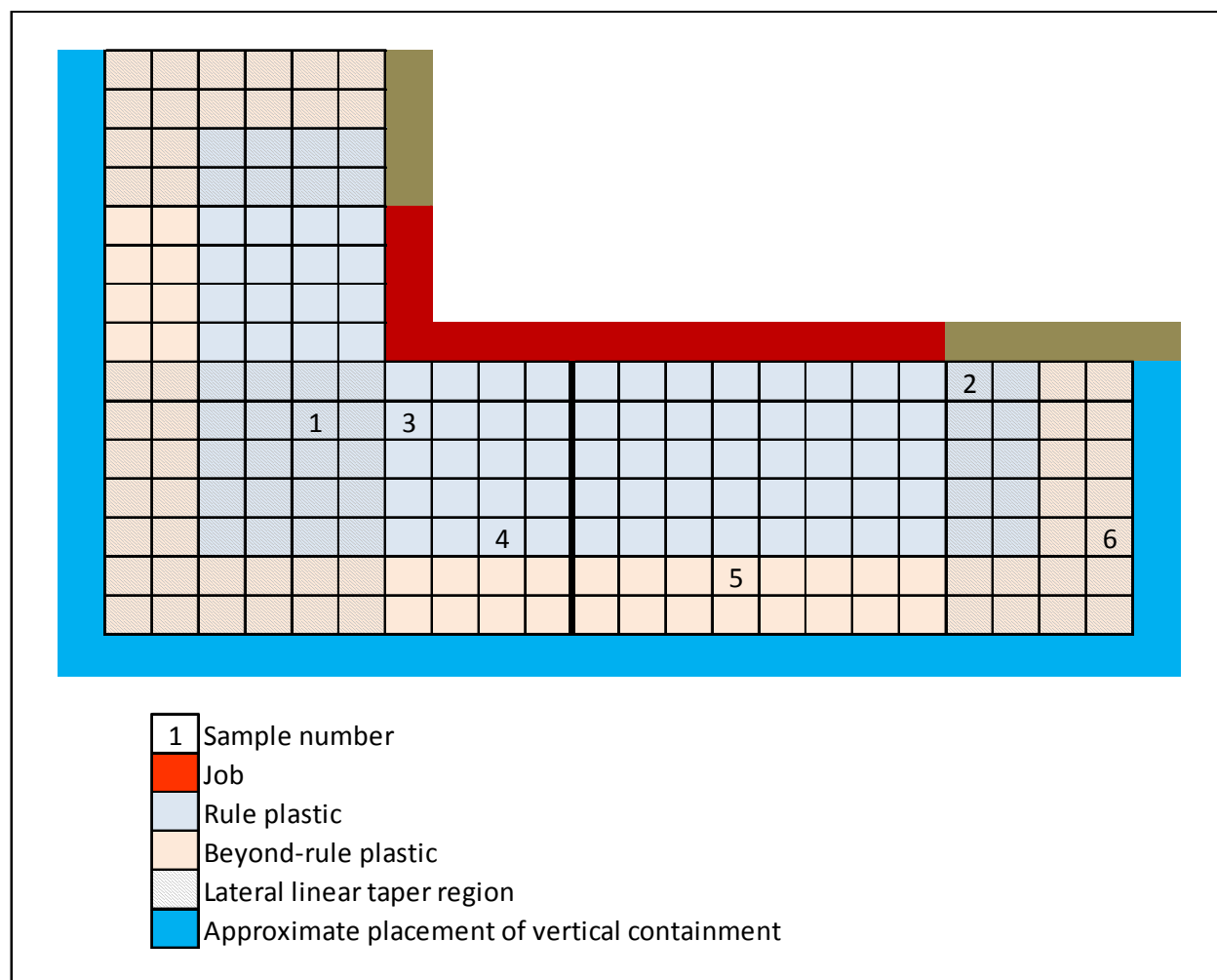


Figure H-14. Layout of Trim Replacement Experiment 4

Table H-38. Dust Loading Measurements and Adjustments in Experiment 4

ID	Dist. From Wall (ft)	Adj. Dist. (ft)	Lead Loading (Dust Study) ¹	Lead Loading (adjusted)	Dust Load per ft ² Disturbed ²	Adjustment Parameters
1	2	3	3,951	NA	0.65	Distance adjusted to be linear distance from job; Loading adjusted to estimate loading within job area
2	1	NA	<i>1,652,382</i>	2,065,478	337.50	Loading adjusted to estimate loading within job area
3	2	NA	110,776	NA	18.10	None
4	5	NA	59,027	NA	9.64	None
5	6	NA	26,040	NA	4.25	None
6	5	NA	52,742	263,710	43.09	Loading adjusted to estimate loading within job area

¹ Measurements that include bulk material are denoted in italics

² Measurements included in regression denoted in bold type

Table H-39. Regression Statistics in Experiment 4

Statistic	Value
Shape	0.86
Intercept	-2.32
R ²	0.38
Load at 0 ft (mg/ft ² plastic/ft ² disturbed)	0.10

Table H-40. Estimated Total Dust Emitted, Total Paint on Wall, and Emission Fraction in Experiment 4

Estimated Masses and Emission Fractions	Value
Mass of Dust Within Job Area (mg/ft ² disturbed)	747
Mass of Dust Not Within Job Area (mg/ft ² disturbed)	560
Total Mass of Dust on Plastic (mg/ft ² disturbed)	1,307
Total Paint on Surface (mg/ft ² disturbed)	18,790
Fraction Emitted	0.070

H.13.2. Experiment 36

Experiment 36 removed trim from the edge of a porch. The geometry is shown in Figure H-15. Three of the samples were collected within 3 ft of the job and were excluded from the regression (see Table H-41). However, the remaining three samples were all collected at the same distance from the edge of the porch (7 ft). Thus, in the absence of data at multiple distances, no regression can be performed. This experiment was excluded from the emission rate calculation.

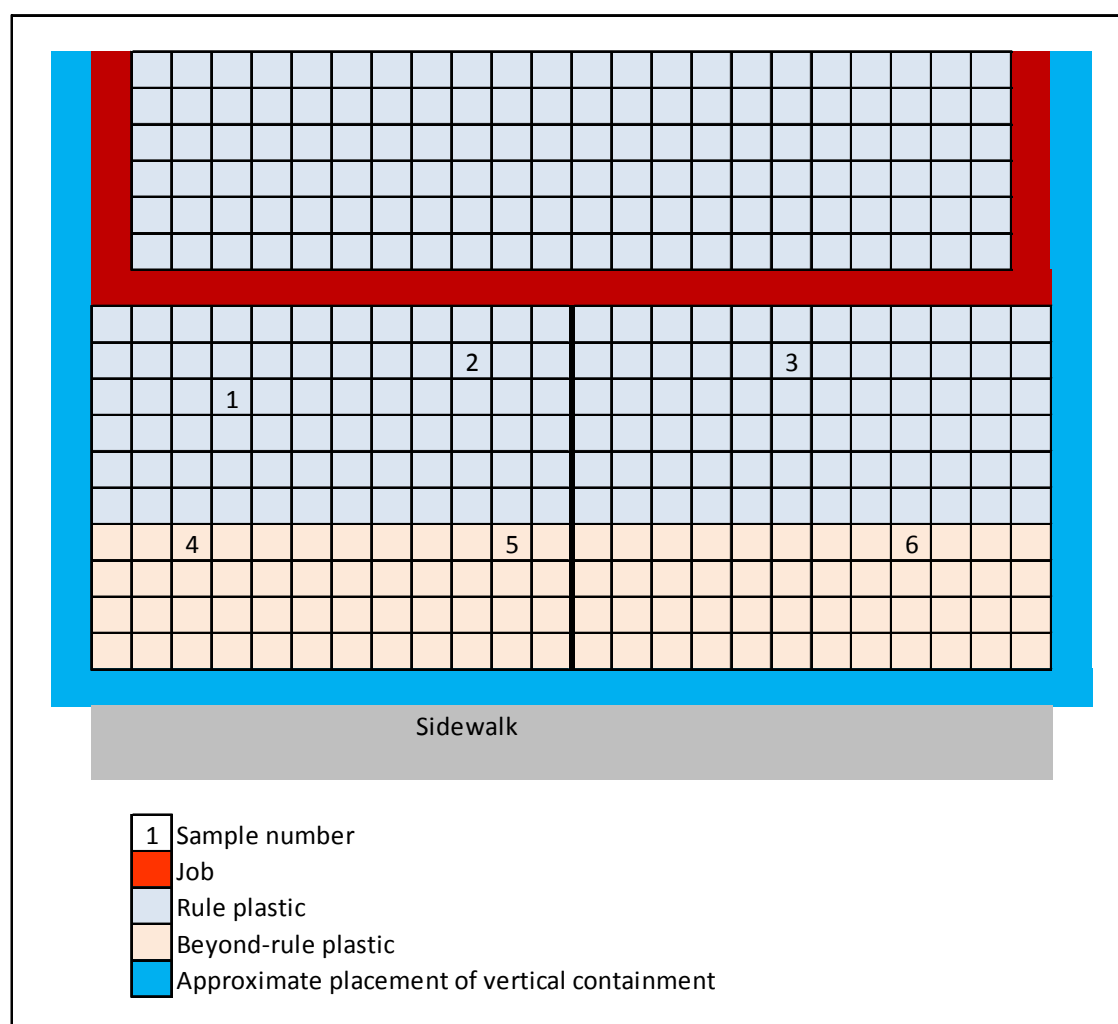


Figure H-15. Layout of Trim Replacement Experiment 36

Table H-41. Dust Loading Measurements and Adjustments in Experiment 36

ID	Dist. From Wall (ft)	Adj. Dist. (ft)	Lead Loading (Dust Study) ¹	Lead Loading (adjusted)	Dust Load per ft ² Disturbed ²	Adjustment Parameters
1	3	NA	154,825	NA	15.36	None
2	2	NA	<i>2,991,198</i>	NA	296.75	None
3	2	NA	<i>1,794,377</i>	NA	178.01	None
4	7	NA	18,536	NA	1.84	None
5	7	NA	128,549	NA	12.75	None
6	7	NA	209,520	NA	20.79	None

¹ Measurements that include bulk material are denoted in italics

² Measurements included in regression denoted in bold type

H.14. Door Replacement

H.14.1. Experiment 34

Experiment 34 replaced a door at a home. The geometry is shown in Figure H-16. Three of the samples were collected within 3 ft of the job and were excluded from the regression (see Table H-42). However, the remaining three samples were all collected at the same distance from the edge of the porch (6 ft). Thus, in the absence of data at multiple distances, no regression can be performed. This experiment was excluded from the emission rate calculation.

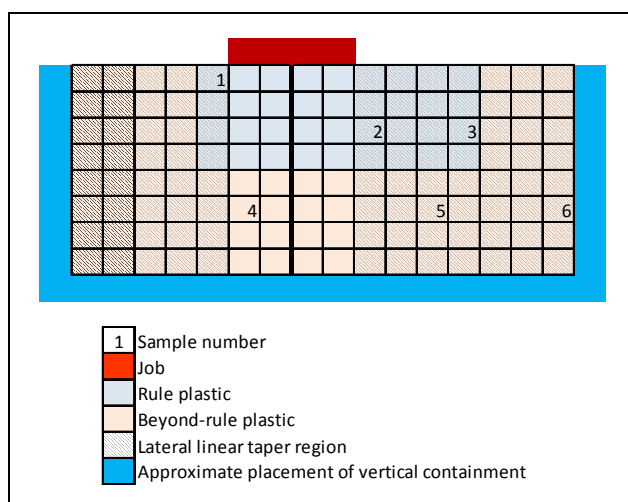


Figure H-16. Layout of Door Replacement Experiment 34

Table H-42. Dust Loading Measurements and Adjustments in Experiment 34

ID	Dist. From Wall (ft)	Adj. Dist. (ft)	Lead Loading (Dust Study) ¹	Lead Loading (adjusted)	Dust Load per ft ² Disturbed ²	Adjustment Parameters
1	1	NA	<i>217,108</i>	248,123	94.52	Loading adjusted to estimate loading within job area
2	3	NA	76,118	86,992	33.14	Loading adjusted to estimate loading within job area
3	3	NA	13,886	27,772	10.58	Loading adjusted to estimate loading within job area
4	6	NA	30,489	NA	11.61	None
5	6	NA	81,048	129,677	49.40	Loading adjusted to estimate loading within job area
6	6	NA	1,086	8,688	3.31	Loading adjusted to estimate loading within job area

¹ Measurements that include bulk material are denoted in italics

² Measurements included in regression denoted in bold type

H.14.2. Experiment 35

The geometry of Experiment 35 (Figure H-17) was similar to the generic geometry in Figure H-1. The job was not centered with respect to the plastic. The larger width on the left (8 ft) was used to taper the within-job loadings to zero at the edge of the plastic. This reflects the assumption that the total amount of dust will be the same on both sides, but the loadings to the right will be somewhat higher since the dust spreads over a smaller distance. This is reflected in the diagram with darker crosshatching on that side.

The measured lead loadings and associated distances are shown in

Table H-43. Dust Loading Measurements and Adjustments in Experiment 35

. Samples 1, 4, and 6 were adjusted to approximate the loadings at those distances within the job width. These adjusted loadings are shown in

Table H-43. Dust Loading Measurements and Adjustments in Experiment 35

. The loadings were divided by the size of the job (25 ft²) and the fraction of lead in the paint (0.112) to estimate the dust loadings per ft² disturbed in

Table H-43. Dust Loading Measurements and Adjustments in Experiment 35

. Samples 1 and 3 were excluded from the regression because they were within 2 ft of the job. Sample 2 was within 3 ft of the job, but it was not a bulk measurement so it was retained in the regression. Then, the natural logs of all loadings were used with the distances to estimate the regression parameters in Table H-44. Here, *intercept* is the intercept of the linear regression in log space, and Load at 0 ft is the assumed loading at 0 ft calculated as $\exp(\textit{intercept})$. In this case, the regression coefficient is low, indicating there is additional uncertainty in this emission estimate.

The integral was performed over the regression equation out to a distance of 8 ft, which was the extent of the non-rule plastic. Masses were estimated both within the job area (4 ft wide) and outside the job area as shown in Table H-45. The estimated paint density using the lead fraction was 2.16 g/cm^3 . Because the renovated building was built in 1925, it was assumed to have 4.7 layers of paint at the time of the job. Door replacement was a surface preparation activity, so 15% of the paint layers were assumed to be removed. These values were used to estimate the total amount of paint on the wall, giving a final emission fraction of 0.069.

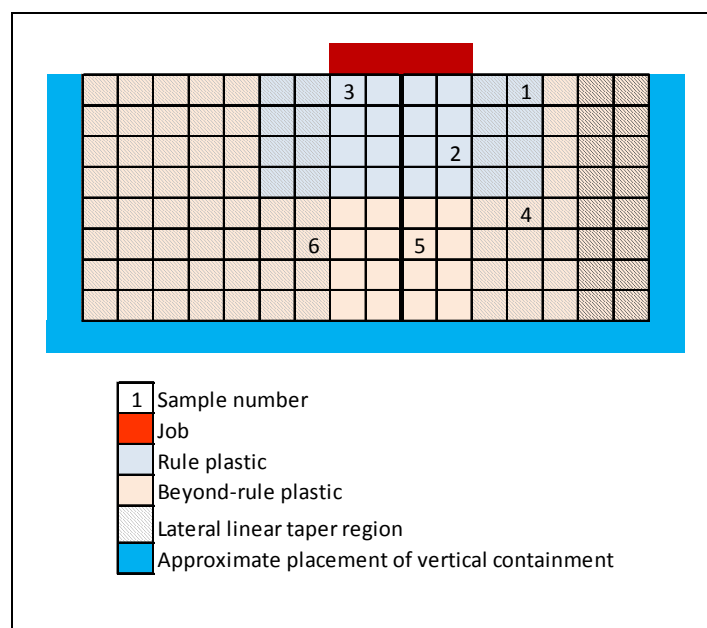


Figure H-17. Layout of Door Replacement Experiment 35

Table H-43. Dust Loading Measurements and Adjustments in Experiment 35

ID	Dist. From Wall (ft)	Adj. Dist. (ft)	Lead Loading (Dust Study) ¹	Lead Loading (adjusted)	Dust Load per ft ²	Adjustment Parameters
1	1	NA	28,904	43,356	15.48	Loading adjusted to estimate loading within job area
2	3	NA	42,285	NA	15.10	None
3	1	NA	145,898	NA	52.11	None
4	5	NA	3,648	5,472	1.95	Loading adjusted to estimate loading within job area
5	5.5	NA	29,256	NA	10.45	None
6	5.5	NA	16,914	19,330	6.90	Loading adjusted to estimate loading within job area

¹ Measurements that include bulk material are denoted in italics

² Measurements included in regression denoted in bold type

Table H-44. Regression Statistics in Experiment 35

Statistic	Value
Shape	-0.32
Intercept	3.45
R ²	0.19
Load at 0 ft (mg/ft ² plastic/ft ² disturbed)	31.57

Table H-45. Estimated Total Dust Emitted, Total Paint on Wall, and Emission Fraction in Experiment 35

Estimated Masses and Emission Fractions	Value
Mass of Dust Within Job Area (mg/ft ² disturbed)	361
Mass of Dust Not Within Job Area (mg/ft ² disturbed)	722
Total Mass of Dust on Plastic (mg/ft ² disturbed)	1,083
Total Paint on Surface (mg/ft ² disturbed)	15,705
Fraction Emitted	0.069

H.15. References for Appendix H

- Beck C; Geyh A; Srinivasa A; Breyse P; Eggleston P; Buckley T (2003). The impact of a building implosion on airborne particulate matter in an Urban community. *Journal of the Air and Waste Management Association* 54(10): 1256-1264.
- Capouch S., personal communication, 2012. Personal Communication by email between Heidi Hubbard of ICF International and Scott Capouch, Construction Project Manager with 10 years of experience, of US NIEHS. Title of email: Painting frequency. February 15, 2012.
- Farfel M; Orlova A; Lees P; Rohde C; Ashley P; Chisolm J (2003). A study of urban housing demolitions as sources of lead in ambient dust: demolition practices and exterior dust fall. *Environmental Health Perspectives* 111(11):1228-1234.
- Farfel MR; Orlova AO; Lees PS; Rohde C; Ashley PJ; Chisolm Jr. J (2005). A study of urban housing demolition as a source of lead in ambient dust on sidewalks, streets, and alleys. *Environ Res* 99(2): 204-213.
- Lee M. and Domansky J. (1999). Development of pollutant release estimates due to abrasive blasting for lead paint removal from New York City department of transportation steel bridges, Pittsburgh, PA, *Air and Waste Management Association*.
- Mucha A; Stites N; Evens A; MacRoy P (2009). Lead dustfall from demolition of scattered site family housing: Developing a sampling methodology. *Environmental Research* 109(1):143-148.
- Stefani D; Wardman D; Lambert T (2005). The implosion of the Calgary General Hospital: Ambient air quality issues. *Journal of the Air and Waste Management Association* 55: 52-59.
- US EPA. (2007a). Draft final report on characterization of dust lead levels after renovation, repair, and painting activities. Prepared for EPA's Office of Pollution Prevention and Toxics (OPPT). Available online at: <http://www.epa.gov/lead/pubs/duststudy01-23-07.pdf>
- Weather Underground. (2011). History for Baltimore, MD. Available online at: <http://www.weatherunderground.com>

Appendix I. Interior Fraction Emitted

I.1. Loading Data Conversions

Because each experiment was performed using different total wall disturbance sizes, the fraction of paint emitted was calculated on a per square foot of disturbed wall basis. Thus, as in the exterior analysis, each Dust Study post-work lead loading was divided by the area disturbed in the experiment to get the loading in units of lead mass per square foot of floor and per square foot of wall disturbed:

$$LeadLoad_{per\ wall\ unit} = \frac{LeadLoad}{AreaDist}$$

where:

$LeadLoad_{per\ wall\ unit}$	=	the total lead loading on the floor per unit of wall area disturbed ($\mu\text{g}/\text{ft}^2/\text{ft}^2$)
$LeadLoad$	=	the total lead loading on the floor ($\mu\text{g}/\text{ft}^2$)
$AreaDist$	=	the total wall area disturbed during renovation (ft^2)

In addition, because each experiment was performed on buildings with different compositions of lead within the paint, the fraction emitted was calculated based on the total amount of paint dust emitted rather than the total amount of lead emitted. This conversion assumes that each experiment within an activity should produce nearly uniform amounts of paint dust per square foot disturbed, even though the amount of lead will vary according to the lead content in the paint. To make this conversion, each lead loading was divided by the percentage of lead in the paint specified in the Dust Study to approximate loadings in units of mass of paint particles per square foot of floor and per square foot of wall disturbed (see equation below).

$$PaintDustLoad_{per\ wall\ unit} = \frac{LeadLoad_{per\ wall\ unit}}{frac} \times \frac{1}{1000\ \mu\text{g} / \text{mg}}$$

where:

$LeadLoad_{per\ wall\ unit}$	=	the total lead loading on the floor per unit of wall area disturbed ($\text{mg}/\text{ft}^2/\text{ft}^2$)
$PaintDustLoad_{per\ wall\ unit}$	=	the total paint dust loading on the floor per unit of wall area disturbed ($\text{mg}/\text{ft}^2/\text{ft}^2$)
$frac$	=	the fraction of paint which is lead by weight (unitless)

Note that this conversion assumes that all the emitted particles are paint particles and does not account for the fact that the total emitted dust might include wall substrate particles as well. Thus, the estimated paint dust emission rate will not represent the total dust emitted during the activity but is intended to account for all the lead emitted, assuming that there is lead in the paint but not within the substrate or other disturbed portions of the building.

Next, the along-wall distribution of dust was estimated. Following inspection of the general trends in the Dust Study experiments, it was assumed that the loadings were relatively constant over the width of the job and then tapered linearly to zero at the edge of the room in the along-wall direction (see Figure I-1). (US EPA 2007a) Thus, if measurements were made at locations wider than the job width (for example, Sample X in Figure I-1), these measurements were adjusted using a linear relationship to approximate the loading within the job area (for example, Sample X_{adj} in Figure I-1).

To make this linear conversion, the following equation was used:

$$PaintDustLoadAdj_{per\ wall\ unit} = \frac{DistPlast}{DistPlast - DistMeasure} PaintDustLoad_{per\ wall\ unit}$$

where:

- $PaintDustLoadAdj_{per\ wall\ unit}$ = the total paint dust loading on the floor per unit of wall area disturbed adjusted to the level within the job area (mg/ft²/ft²)
- $PaintDustLoad_{per\ wall\ unit}$ = the total paint dust loading on the floor per unit of wall area disturbed (mg/ft²/ft²)
- $DistPlast$ = the distance between the edge of the job and the edge of the room (ft)
- $DistMeasure$ = the distance between the edge of the job and the measurement (ft)

All of these distances were calculated from the information in the Dust Study job maps provided by Battelle. Because the dust is measured over discrete areas 1 ft wide, the measurements are assumed to apply to the center of the measurement area. Thus, the loadings were assumed to taper to zero over a distance 1 ft wider than shown in the diagrams. This assumption causes the loadings to fall to zero in the just at the edge of the room. The alternative assumption (loadings going to zero at the center of the box just inside the wall) was not used, since non-zero measurements were available at those locations in the Dust Study.

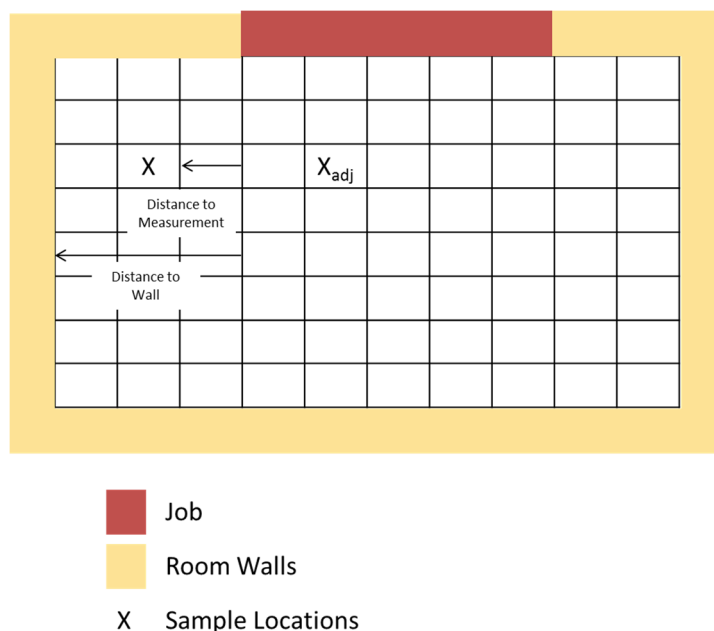


Figure I-1. Schematic of Interior Dust Study Experiments

I.2. Regression of Dust Study Data by Renovation Activity

To estimate the distribution of dust in the out-from-wall direction within the job area, a regression analysis was performed on the *PaintDustLoadAdj_{per wall unit}* values (or the *PaintDustLoad_{per wall unit}* values if no adjustment was necessary because the measurement was made within the job area) at each corresponding distance from the wall with Microsoft Excel® using the following equation for exponential decay:

$$PaintDustR_{egress} = Load_0 \times e^{Shape \times Dist}$$

where:

<i>PaintDustRegress</i>	=	paint dust loading (mg/ft ² /ft ² disturbed)
<i>Load₀</i>	=	loading just below the job at 0 ft (mg/ft ² /ft ² disturbed)
<i>Shape</i>	=	shape of exponential regression (/ft)
<i>Dist</i>	=	distance from renovation activity (ft)

I.3. Total Amount of Dust Emitted

Once these regression equations were determined, the total amount of dust on the floor was estimated by integrating the regression equation over the length of the room to get the total mass (out-from-wall direction) and multiplying by the width of room (along-wall direction):

$$MassDust = \frac{Load_0}{Shape} \times (e^{Shape \times LenRoom} - 1) \times RoomWidth$$

where:

$MassDust_{inside}$	=	paint dust mass on the floor inside the job area (mg/ft ² disturbed)
$Load_0$	=	loading just below the job at 0 ft (mg/ft ² disturbed)
$Shape$	=	shape of exponential regression (ft ⁻¹)
$LenRoom$	=	length of room in the out-from-wall direction (ft)
$RoomWidth$	=	the width of the room in the along-wall direction (ft)

For some experiments, the exact location of the job could not be determined based on experiment maps provided; these included small cutout jobs on the wall and ceiling and door planing jobs where the door was placed at an undisclosed location in the middle of the room on sawhorses. For these experiments, the regression could not be performed because the distance from the job wall for each sample was unknown. In these cases, the loadings per ft² disturbed were averaged and multiplied by the area of the room to estimate the total amount of mass. As a check of the regression method, this “averaging” method and the regression method predictions of total dust were compared, and in general the predictions were within 25% of each other (average = 12%).

I.4. Amount of Paint on the Wall

To estimate the total amount of paint on the wall for each renovation experiment, first the paint density and number of layers of paint were estimated. The average paint density for each activity was estimated for the Dust Study jobs using the fraction of lead in paint according to the equation:

$$PaintDens = frac \times DensityPb + (1 - frac) \times DensityRest$$

where:

$PaintDens$	=	the density of the paint (g paint/cm ³ paint)
$frac$	=	the fraction of paint which is lead by weight (unitless)
$DensityPb$	=	the density of lead (g/cm ³)

DensityRest = the density of the rest of the paint (other than lead) (g/cm³)

The density of lead is 11.3 g/cm³, and the density of the rest of the paint is assumed to be equal to 1 g/cm³ consistent with the solid portion of modern paint (assumed to be lead-free), as calculated from Material Safety Data Sheets (MSDS) sheets.

The number of layers of paint on the wall at the time of the Dust Study job was estimated by assuming that painting had been done every seven years since the time the building was constructed. This value of seven years was selected based on information about typical renovation frequencies in child care centers (CCC data). For each of these previous painting jobs on the building, it was assumed that the surface was prepared for painting and then a layer of paint was applied. There is no way of knowing what method was used to remove paint and prepare the surface in these prior painting jobs. Thus, the representative value of 15% removal for surface preparation (Section D.1.3) was used in estimating the fraction of paint removed during each previous painting job. The Dust Study jobs were performed in 2006. Thus, the number of layers of paint in 2006 for each Dust Study building construction date were estimated and are shown in Table H-1. (EPA 2007a)

In some cases, the age of the renovated building was unknown. The Dust Study residences were built between 1900 and 1925, and a table provided within the Dust Study report indicates that nearby properties were built between 1900 and 1920. For this analysis, a representative building year of 1920 was selected as a year within that range.

For the actual paint removal jobs performed during the Dust Study, Battelle provided information about the degree of paint removal. Some jobs were surface preparation activities (removed only a fraction of the total paint on the wall), while others removed all the paint on the wall. Thus, the amount of paint removed during each Dust Study job was estimated by multiplying the number of layers of paint estimated to be on the building in 2006 by the estimated fraction of paint removed during the particular job (100% for removal jobs and 15% for surface preparation jobs).

These values were then used to estimate the total amount of paint removed from the wall in the Dust Study job per square foot of wall:

$$WallPaintRemoved = WallPaintCov \times PaintDens \times UnitConv \times LayersOfPaint \times FracRemove$$

where:

WallPaintRemoved = the total paint per square foot of wall removed during the

<i>WallPaintCov</i>	=	Dust Study job (mg/ft ² wall) the amount of paint which covers a single square foot of wall (gallons/ft ²)
<i>UnitConv</i>	=	a conversion factor to convert from gallons to cm ³ and from mg to g
<i>PaintDens</i>	=	the density of the paint (g paint/cm ³ paint)
<i>LayersOfPaint</i>	=	the number of layers of paint
<i>FracRemoved</i>	=	the fraction of the total layers of paint that were removed during the Dust Study job

I.5. Percentage of Paint Emitted By Activity

Finally, the fraction of paint on the wall emitted per activity is estimated by dividing the amount emitted during the activity (Appendix I.3) by the total amount on the wall (Appendix I.4).

$$FracEmitted = \frac{MassDust}{WallPaint}$$

where:

<i>FracEmitted</i>	=	fraction of paint removed from wall that is emitted as aerosol
<i>MassDust</i>	=	total paint dust mass on the floor (mg/ft ² disturbed)
<i>WallPaint</i>	=	the total paint per square foot of wall (mg/ft ² wall)

Then, the fractions for the different experiments were combined with the fractions from any available exterior experiments, and the geometric mean across the different experiments was used to represent the overall activity emission fraction. The resulting emission fractions are shown in

Appendices to the Approach for Estimating Exposures and Incremental Health Effects from Lead due to Renovation, Repair, and Painting Activities in Public and Commercial Buildings

Table I-1.

Table I-1. Interior Analysis Fraction of Paint Emitted.

Activity type	Fraction of Paint That Remains as Lead Dust
Window, Saw	0.2137
Door Planing	0.1118
Heat Gun Plaster	0.0572
Dry Scrape	0.0380
Window, No Saw	0.0155
Heat Gun Wood	0.0119
Door Planing, with HEPA	0.0112
Cutouts	0.0056
Kitchen Gut (Cabinet/Shelf Removal in the Approach)	0.0030

The general approach above was applied to the experiments in the Dust Study to compute the emission fractions. The remainder of the Appendix details the assumptions, input data, regression results, and emission fraction calculations for each experiment. The figures in each Appendix represent the experiment maps provided by Battelle.

I.6. Window Replacement

I.6.1. Experiment 41

The geometry of Experiment 41 is shown in Figure I-2, and the measured lead loadings and associated distances are shown in

Table I-2. Post-Work Loading Measurements and Adjustments in Experiment 41

. Samples 2 and 4 were adjusted using the taper assumption since they were outside the lateral extent of the job. The loadings were divided by the size of the job (10 ft²) and the fraction of lead in the paint (0.009) to estimate the dust loadings per ft² disturbed in

Table I-2. Post-Work Loading Measurements and Adjustments in Experiment 41

. Then, the natural logs of all loadings were used with the distances to estimate the regression parameters in Table I-3. Here, *intercept* is the intercept of the linear regression in log space, and Load at 0 ft is the assumed loading at 0 ft calculated as $\exp(\textit{intercept})$.

The integral was performed over the regression equation out to a distance of 15 ft, (the length of the room), and the total mass of dust on the floor was estimated as shown in Table I-4. The estimated paint density using the lead fraction was 1.09 g/cm³. Although the vintage of the renovated building was unknown, nearby buildings were believed to have been built at the same time and were built in 1920. Therefore, the building was assumed to have been built in 1920 and to have 5.0 layers of paint at the time of the job. The experiment notes indicated that all paint was removed during the renovation, so all 5.0 layers were assumed to be removed. These values were used to estimate the total amount of paint on the wall, giving a final emission fraction of 0.538.

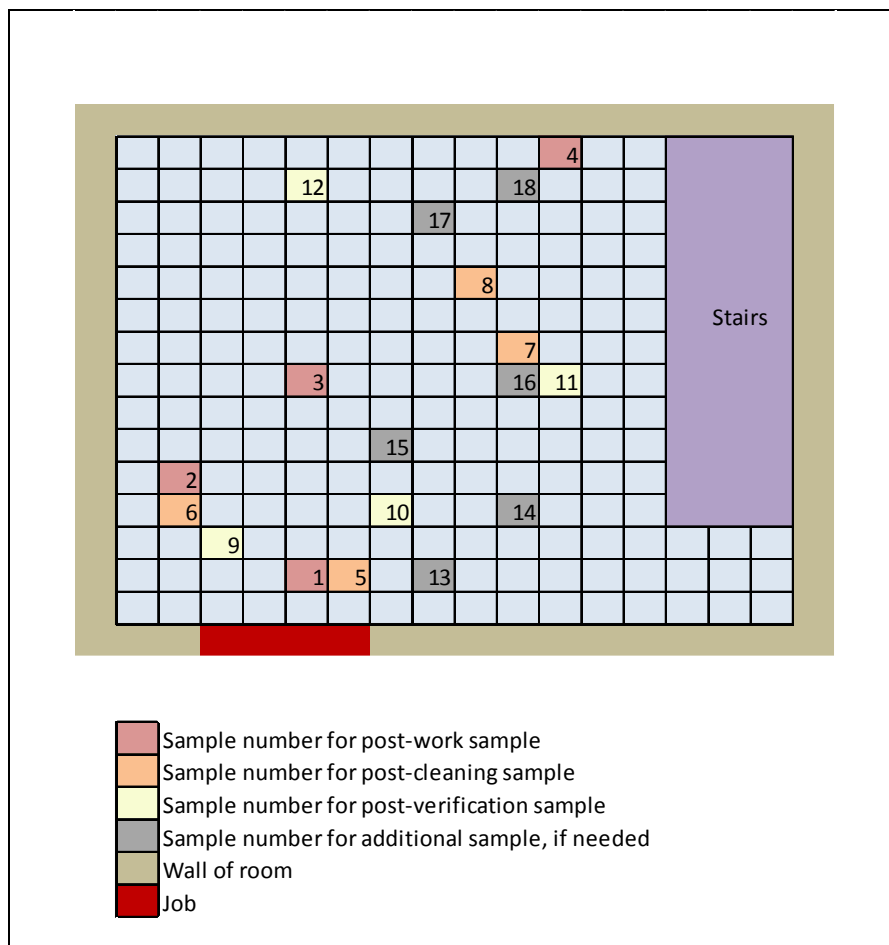


Figure I-2. Layout of Window Replacement Experiment 41

Table I-2. Post-Work Loading Measurements and Adjustments in Experiment 41

ID	Dist. From Wall (ft)	Lead Loading in $\mu\text{g}/\text{ft}^2$ (Dust Study)	Lead Loading in $\mu\text{g}/\text{ft}^2$ (adjusted)	Dust Load per ft^2 Disturbed (mg/ft^2 floor/ ft^2 wall)
1	2	61,134	61,134	679.27
2	5	1,852	2,777	30.86
3	8	9,948	9,948	110.53
4	15	1,387	3,698	41.09

Table I-3. Regression Statistics in Experiment 41

Statistic	Value
Shape	-0.15
Intercept	5.74
R ²	0.37
Load at 0 ft (mg/ft^2 floor/ ft^2 disturbed)	310.9

Table I-4. Estimated Total Dust Emitted, Total Paint on Wall, and Emission Fraction in Experiment 41

Estimated Masses and Emission Fractions	Value
Total Mass of Dust on Floor (mg/ft^2 disturbed)	29,254
Total Paint Removed From Surface (mg/ft^2 disturbed)	54,343
Fraction Emitted	0.538

I.6.2. Experiment 42

The geometry of Experiment 42 is shown in Figure I-3, and the measured lead loadings and associated distances are shown in Table I-5. Samples 1 and 4 were adjusted using the taper assumption since they were outside the lateral extent of the job. The loadings were divided by the size of the job (10 ft^2) and the fraction of lead in the paint (0.019) to estimate the dust loadings per ft^2 disturbed in Table I-5. Then, the natural logs of all loadings were used with the distances to estimate the regression parameters in Table I-6. Here, *intercept* is the intercept of the linear regression in log space, and Load at 0 ft is the assumed loading at 0 ft calculated as $\exp(\text{intercept})$.

The integral was performed over the regression equation out to a distance of 15 ft, (the length of the room), and the total mass of dust on the floor was estimated as shown in Table I-7. The estimated paint density using the lead fraction was 1.2 g/cm^3 . Although the vintage of the renovated building was unknown, nearby buildings were believed to have been built at the same time and were built in 1920. Therefore, the building was assumed to have been built in 1920 and to have 5.0 layers of paint at the time of the job. The experiment notes indicated that all paint was removed during the renovation, so all 5.0 layers were assumed to be removed. These values were used to estimate the total amount of paint on the wall, giving a final emission fraction of 0.326.

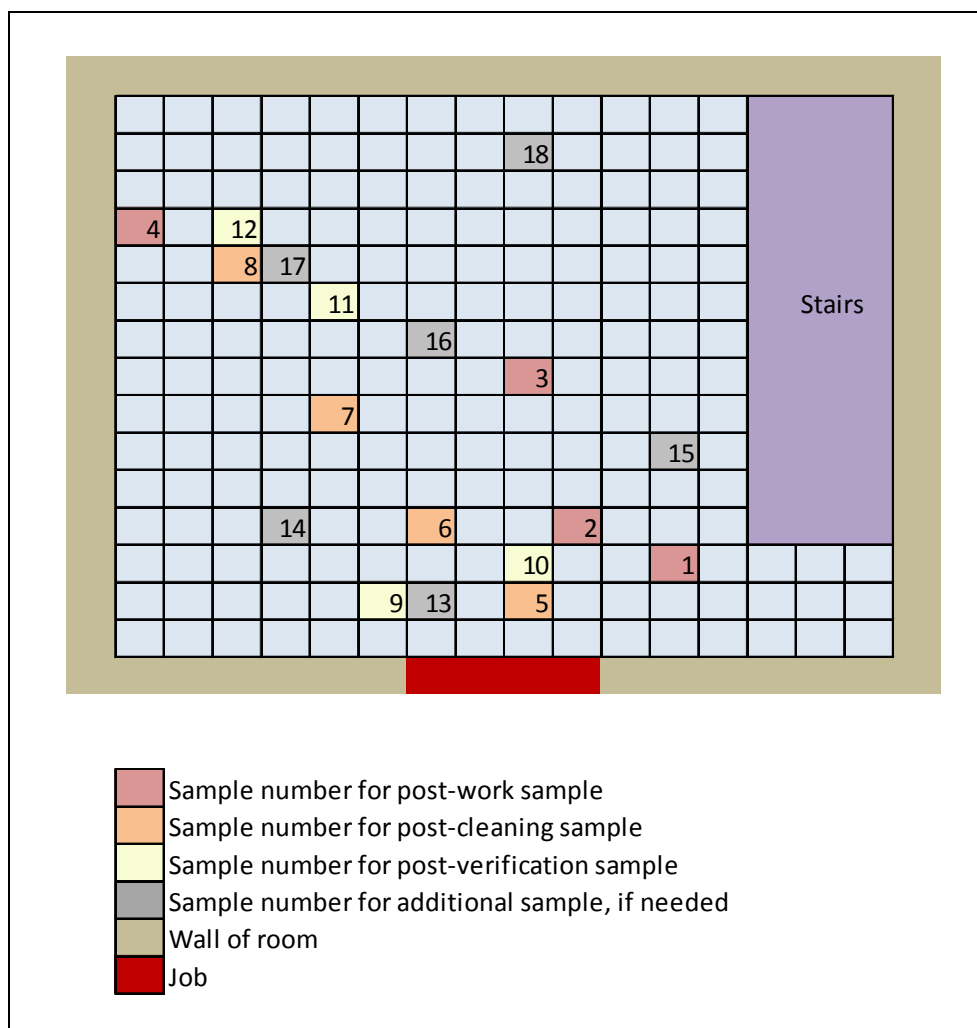


Figure I-3. Layout of Window Replacement Experiment 42

Table I-5. Post-Work Loading Measurements and Adjustments in Experiment 42

ID	Dist. From Wall (ft)	Lead Loading in $\mu\text{g}/\text{ft}^2$ (Dust Study)	Lead Loading in $\mu\text{g}/\text{ft}^2$ (adjusted)	Dust Load per ft^2 Disturbed (mg/ft^2 floor/ ft^2 wall)
1	3	18,575	26,004	136.87
2	4	19,100	19,100	100.53
3	8	10,251	10,251	53.95
4	12	252	1,767	9.30

Table I-6. Regression Statistics in Experiment 42

Statistic	Value
Shape	-0.28
Intercept	5.86
R ²	0.95
Load at 0 ft (mg/ft ² floor/ft ² disturbed)	349.50

Table I-7. Estimated Total Dust Emitted, Total Paint on Wall, and Emission Fraction in Experiment 42

Estimated Masses and Emission Fractions	Value
Total Mass of Dust on Floor (mg/ft ² disturbed)	19,387
Total Paint Removed From Surface (mg/ft ² disturbed)	59,485
Fraction Emitted	0.326

I.6.3. Experiment 43

The geometry of Experiment 43 is shown in Figure I-4, and the measured lead loadings and associated distances are shown in Table I-8. Samples 1, 3, and 4 were adjusted using the taper assumption since they were outside the lateral extent of the job. The loadings were divided by the size of the job (10 ft²) and the fraction of lead in the paint (0.019) to estimate the dust loadings per ft² disturbed in Table I-8. Then, the natural logs of all loadings were used with the distances to estimate the regression parameters in Table I-9. Here, *intercept* is the intercept of the linear regression in log space, and Load at 0 ft is the assumed loading at 0 ft calculated as $\exp(\textit{intercept})$.

The integral was performed over the regression equation out to a distance of 15 ft, (the length of the room), and the total mass of dust on the floor was estimated as shown in Table I-10. The estimated paint density using the lead fraction was 1.2 g/cm³. Although the vintage of the renovated building was unknown, nearby buildings were believed to have been built at the same time and were built in 1920. Therefore, the building was assumed to have been built in 1920 and to have 5.0 layers of paint at the time of the job. The experiment notes indicated that all paint was removed during the renovation, so all 5.0 layers were assumed to be removed. These values were used to estimate the total amount of paint on the wall, giving a final emission fraction of 0.172.

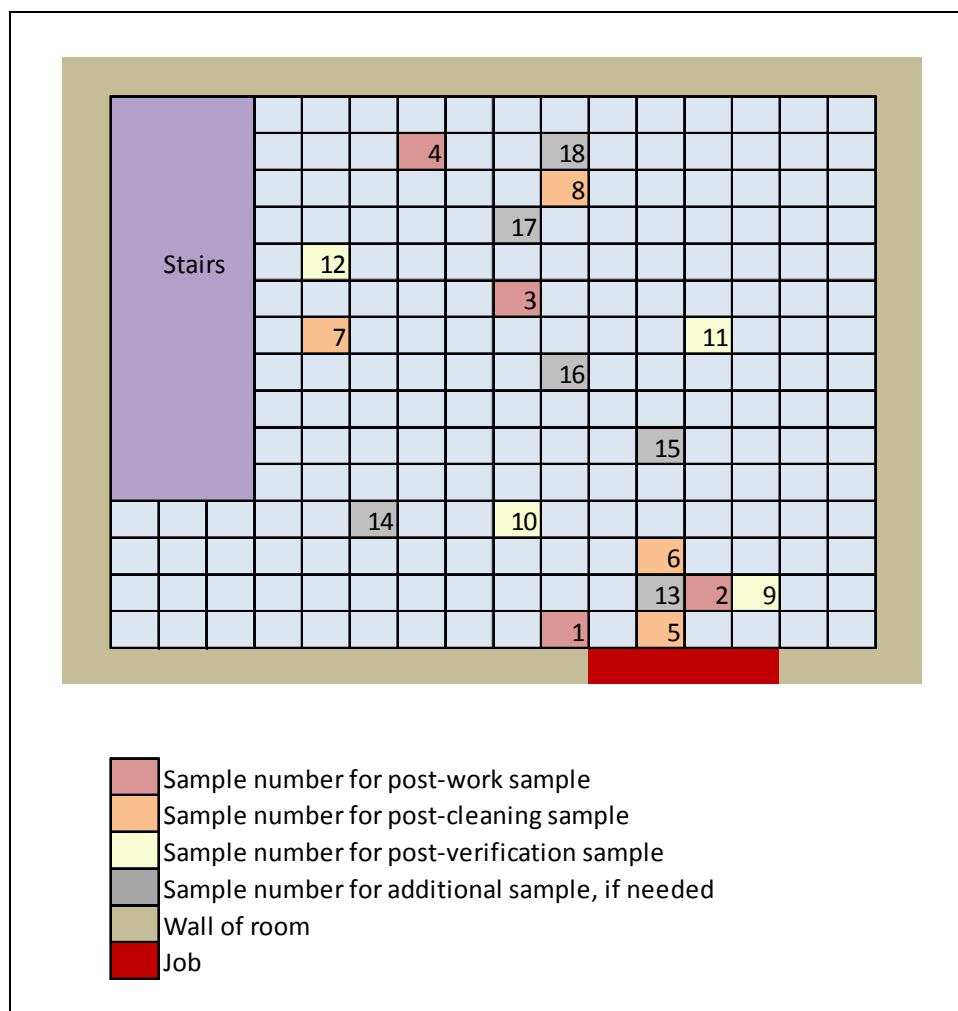


Figure I-4. Layout of Window Replacement Experiment 43

Table I-8. Post-Work Loading Measurements and Adjustments in Experiment 43

ID	Dist. From Wall (ft)	Lead Loading in $\mu\text{g}/\text{ft}^2$ (Dust Study)	Lead Loading in $\mu\text{g}/\text{ft}^2$ (adjusted)	Dust Load per ft^2 Disturbed (mg/ft^2 floor/ ft^2 wall)
1	1	26,831	29,514	155.34
2	2	18,223	18,223	95.91
3	10	1,180	1,573	8.28
4	14	571	1,141	6.01

Table I-9. Regression Statistics in Experiment 43

Statistic	Value
Shape	-0.26
Intercept	5.13
R ²	0.96
Load at 0 ft (mg/ft ² floor/ft ² disturbed)	169.15

Table I-10. Estimated Total Dust Emitted, Total Paint on Wall, and Emission Fraction in Experiment 43

Estimated Masses and Emission Fractions	Value
Total Mass of Dust on Floor (mg/ft ² disturbed)	10,215
Total Paint Removed From Surface (mg/ft ² disturbed)	59,485
Fraction Emitted	0.172

I.6.4. Experiment 44

The geometry of Experiment 44 is shown in Figure I-5, and the measured lead loadings and associated distances are shown in Table I-11. Samples 3 and 4 were adjusted using the taper assumption since they were outside the lateral extent of the job. The loadings were divided by the size of the job (10 ft²) and the fraction of lead in the paint (0.041) to estimate the dust loadings per ft² disturbed in Table I-11. Then, the natural logs of all loadings were used with the distances to estimate the regression parameters in Table I-12. Here, *intercept* is the intercept of the linear regression in log space, and Load at 0 ft is the assumed loading at 0 ft calculated as $\exp(\textit{intercept})$.

The integral was performed over the regression equation out to a distance of 15 ft, (the length of the room), and the total mass of dust on the floor was estimated as shown in Table I-13. The estimated paint density using the lead fraction was 1.42 g/cm³. Although the vintage of the renovated building was unknown, nearby buildings were believed to have been built at the same time and were built in 1920. Therefore, the building was assumed to have been built in 1920 and to have 5.0 layers of paint at the time of the job. The experiment notes indicated that all paint was removed during the renovation, so all 5.0 layers were assumed to be removed. These values were used to estimate the total amount of paint on the wall, giving a final emission fraction of 0.069.

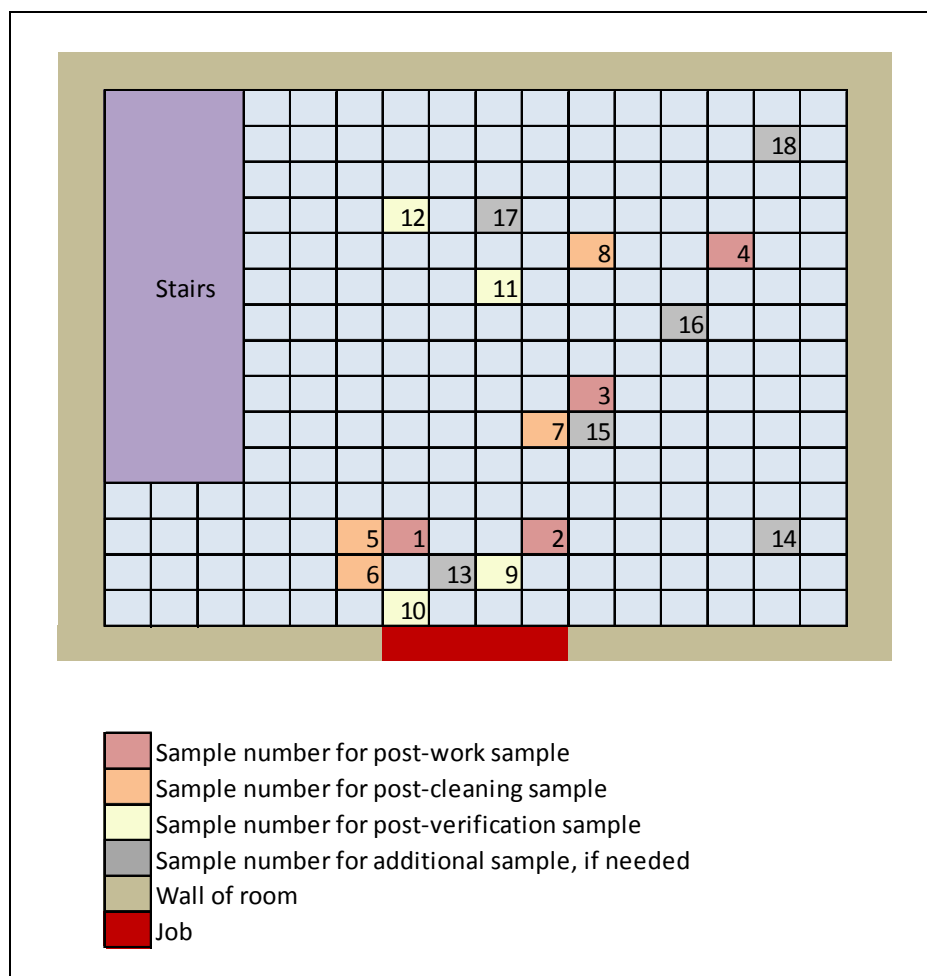


Figure I-5. Layout of Window Replacement Experiment 44

Table I-11. Post-Work Loading Measurements and Adjustments in Experiment 44

ID	Dist. From Wall (ft)	Lead Loading in $\mu\text{g}/\text{ft}^2$ (Dust Study)	Lead Loading in $\mu\text{g}/\text{ft}^2$ (adjusted)	Dust Load per ft^2 Disturbed (mg/ft^2 floor/ ft^2 wall)
1	3	28,492	28,492	69.49
2	3	12,960	12,960	31.61
3	7	1,786	2,084	5.08
4	11	1,084	2,528	6.17

Table I-12. Regression Statistics in Experiment 44

Statistic	Value
Shape	-0.28
Intercept	4.47
R ²	0.72
Load at 0 ft (mg/ft ² floor/ft ² disturbed)	87.42

Table I-13. Estimated Total Dust Emitted, Total Paint on Wall, and Emission Fraction in Experiment 44

Estimated Masses and Emission Fractions	Value
Total Mass of Dust on Floor (mg/ft ² disturbed)	4,905
Total Paint Removed From Surface (mg/ft ² disturbed)	70,797
Fraction Emitted	0.069

I.6.5. Experiment 9

The geometry of Experiment 9 is shown in Figure I-6, and the measured lead loadings and associated distances are shown in Table I-14. Samples 1, 2, and 3 were adjusted using the taper assumption since they were outside the lateral extent of the job. The loadings were divided by the size of the job (9 ft²) and the fraction of lead in the paint (0.073) to estimate the dust loadings per ft² disturbed in Table I-14. Then, the natural logs of all loadings were used with the distances to estimate the regression parameters in Table I-15. Here, *intercept* is the intercept of the linear regression in log space, and Load at 0 ft is the assumed loading at 0 ft calculated as $\exp(\textit{intercept})$.

The integral was performed over the regression equation out to a distance of 14 ft, (the length of the room), and the total mass of dust on the floor was estimated as shown in Table I-16. The estimated paint density using the lead fraction was 1.75 g/cm³. Although the vintage of the renovated building was unknown, nearby buildings were believed to have been built at the same time and were built in 1920. Therefore, the building was assumed to have been built in 1920 and to have 5.0 layers of paint at the time of the job. The experiment notes indicated that all paint was removed during the renovation, so all 5.0 layers were assumed to be removed. These values were used to estimate the total amount of paint on the wall, giving a final emission fraction of 0.013.

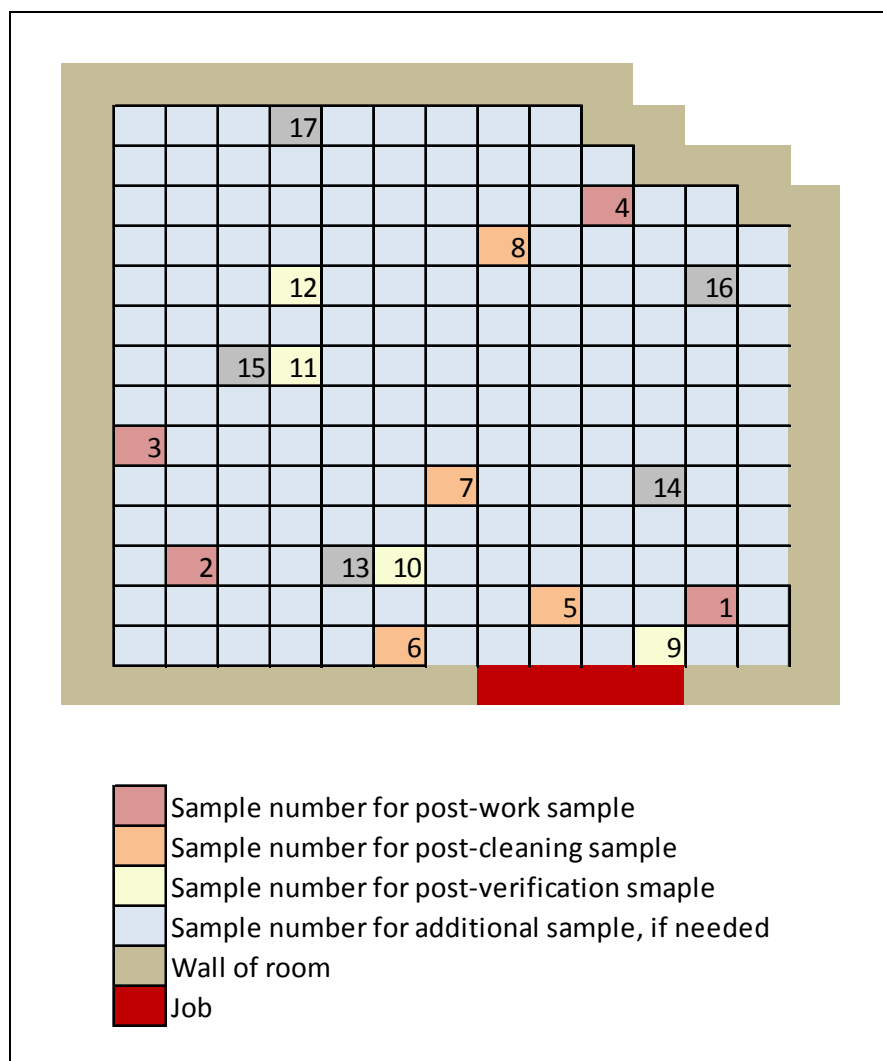


Figure I-6. Layout of Window Replacement Experiment 9

Table I-14. Post-Work Loading Measurements and Adjustments in Experiment 9

ID	Dist. From Wall (ft)	Lead Loading in $\mu\text{g}/\text{ft}^2$ (Dust Study)	Lead Loading in $\mu\text{g}/\text{ft}^2$ (adjusted)	Dust Load per ft^2 Disturbed (mg/ft^2 floor/ ft^2 wall)
1	2	11,634	17,450	26.56
2	3	403	1,610	2.45
3	6	1,344	10,754	16.37
4	12	561	561	0.85

Table I-15. Regression Statistics in Experiment 9

Statistic	Value
Shape	-0.25
Intercept	3.13
R ²	0.48
Load at 0 ft (mg/ft ² floor/ft ² disturbed)	22.82

Table I-16. Estimated Total Dust Emitted, Total Paint on Wall, and Emission Fraction in Experiment 9

Estimated Masses and Emission Fractions	Value
Total Mass of Dust on Floor (mg/ft ² disturbed)	1,160
Total Paint Removed From Surface (mg/ft ² disturbed)	87,250
Fraction Emitted	0.013

I.6.6. Experiment 10

The geometry of Experiment 10 is shown in Figure I-7, and the measured lead loadings and associated distances are shown in Table I-17. Samples 2 and 4 were adjusted using the taper assumption since they were outside the lateral extent of the job. The loadings were divided by the size of the job (9 ft²) and the fraction of lead in the paint (0.033) to estimate the dust loadings per ft² disturbed in Table I-17. Then, the natural logs of all loadings were used with the distances to estimate the regression parameters in Table I-18. Here, *intercept* is the intercept of the linear regression in log space, and Load at 0 ft is the assumed loading at 0 ft calculated as $\exp(\textit{intercept})$.

The integral was performed over the regression equation out to a distance of 14 ft, (the length of the room), and the total mass of dust on the floor was estimated as shown in Table I-19. The estimated paint density using the lead fraction was 1.34 g/cm³. Although the vintage of the renovated building was unknown, nearby buildings were believed to have been built at the same time and were built in 1920. Therefore, the building was assumed to have been built in 1920 and to have 5.0 layers of paint at the time of the job. The experiment notes indicated that all paint was removed during the renovation, so all 5.0 layers were assumed to be removed. These values were used to estimate the total amount of paint on the wall, giving a final emission fraction of 0.134.

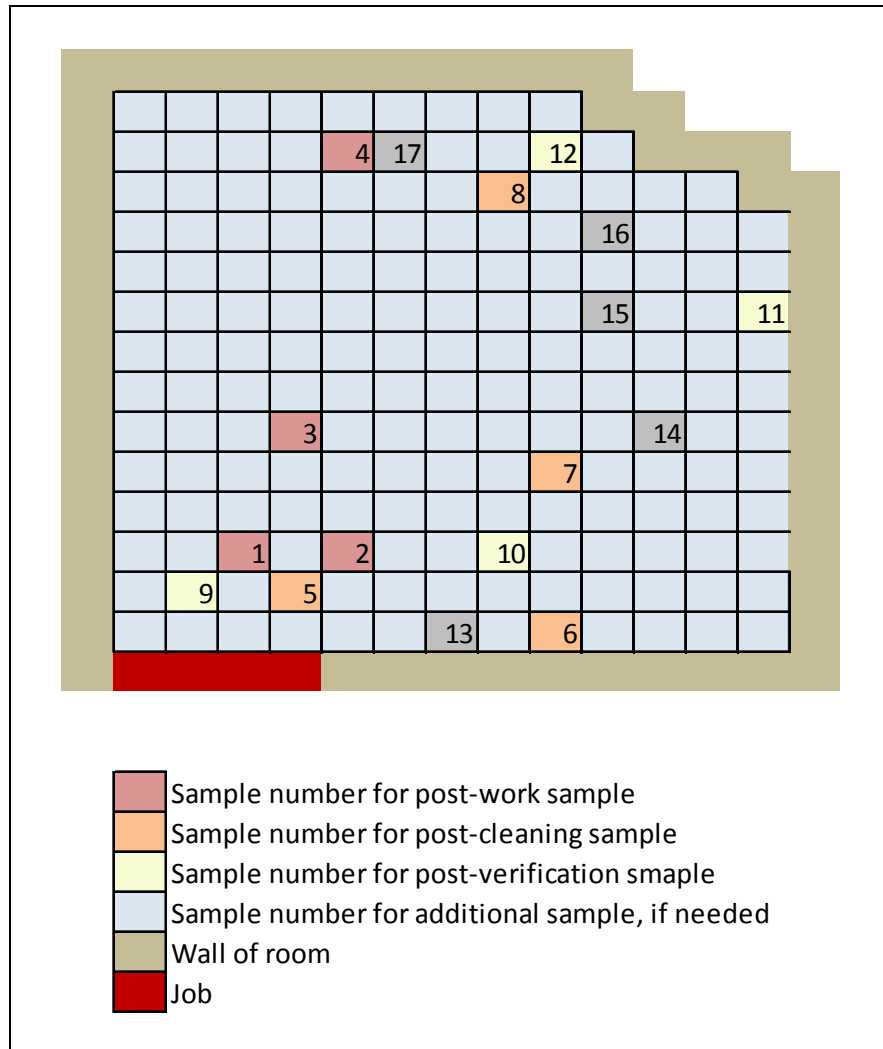


Figure I-7. Layout of Window Replacement Experiment 10

Table I-17. Post-Work Loading Measurements and Adjustments in Experiment 10

ID	Dist. From Wall (ft)	Lead Loading in $\mu\text{g}/\text{ft}^2$ (Dust Study)	Lead Loading in $\mu\text{g}/\text{ft}^2$ (adjusted)	Dust Load per ft^2 Disturbed (mg/ft^2 floor/ ft^2 wall)
1	3	15,817	15,817	53.25
2	3	14,746	16,384	55.17
3	6	15,031	15,031	50.61
4	13	113	132	0.44

Table I-18. Regression Statistics in Experiment 10

Statistic	Value
Shape	-0.49
Intercept	5.81
R ²	0.92
Load at 0 ft (mg/ft ² floor/ft ² disturbed)	333.70

Table I-19. Estimated Total Dust Emitted, Total Paint on Wall, and Emission Fraction in Experiment 10

Estimated Masses and Emission Fractions	Value
Total Mass of Dust on Floor (mg/ft ² disturbed)	8,920
Total Paint Removed From Surface (mg/ft ² disturbed)	66,683
Fraction Emitted	0.134

I.6.7. Experiment 11

The geometry of Experiment 11 is shown in Figure I-8, and the measured lead loadings and associated distances are shown in Table I-20. No adjustments were made to the loading since all samples were within the width of the job. The loadings were divided by the size of the job (18 ft²) and the fraction of lead in the paint (0.101) to estimate the dust loadings per ft² disturbed in Table I-20. Then, the natural logs of all loadings were used with the distances to estimate the regression parameters in Table I-21. Here, *intercept* is the intercept of the linear regression in log space, and Load at 0 ft is the assumed loading at 0 ft calculated as $\exp(\textit{intercept})$.

The integral was performed over the regression equation out to a distance of 14 ft, (the length of the room), and the total mass of dust on the floor was estimated as shown in Table I-22. The estimated paint density using the lead fraction was 2.04 g/cm³. Although the vintage of the renovated building was unknown, nearby buildings were believed to have been built at the same time and were built in 1920. Therefore, the building was assumed to have been built in 1920 and to have 5.0 layers of paint at the time of the job. The experiment notes indicated that all paint was removed during the renovation, so all 5.0 layers were assumed to be removed. These values were used to estimate the total amount of paint on the wall, giving a final emission fraction of 0.006.

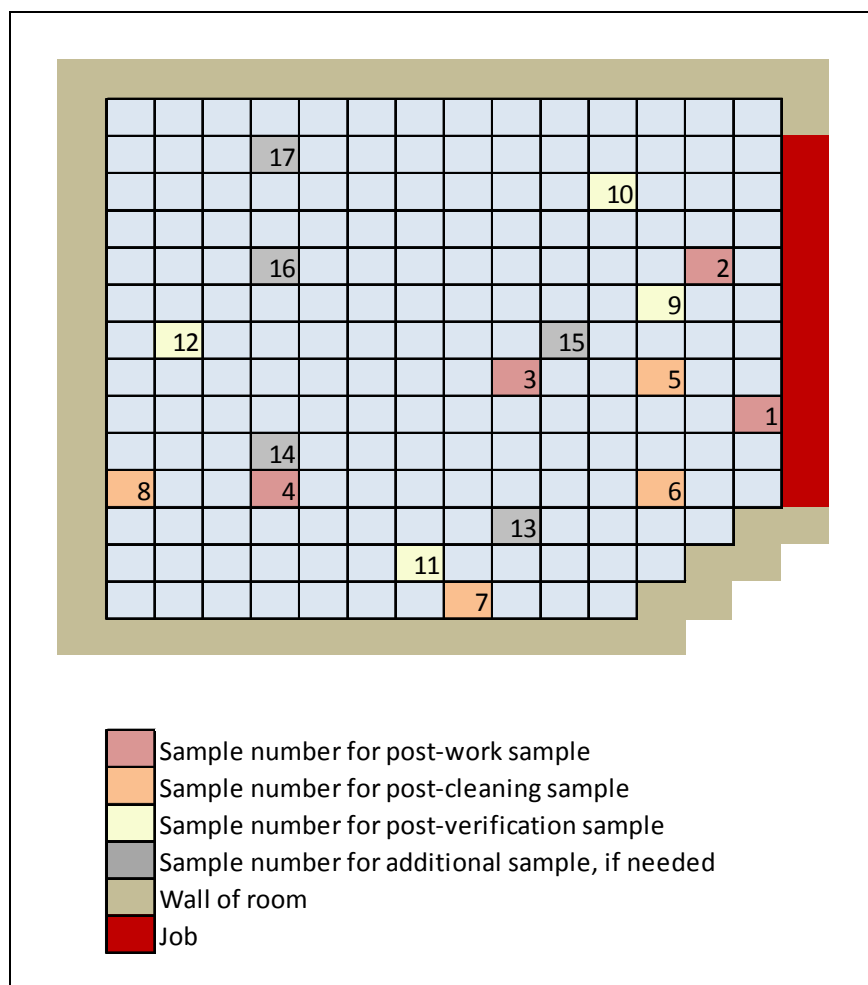


Figure I-8. Layout of Window Replacement Experiment 11

Table I-20. Post-Work Loading Measurements and Adjustments in Experiment 11

ID	Dist. From Wall (ft)	Lead Loading in $\mu\text{g}/\text{ft}^2$ (Dust Study)	Dust Load per ft^2 Disturbed (mg/ft^2 floor/ ft^2 wall)
1	1	11,211	6.17
2	2	16,203	8.91
3	6	3,783	2.08
4	11	2,204	1.21

Table I-21. Regression Statistics in Experiment 11

Statistic	Value
Shape	-0.19
Intercept	2.20
R ²	0.89
Load at 0 ft (mg/ft ² floor/ft ² disturbed)	9.0

Table I-22. Estimated Total Dust Emitted, Total Paint on Wall, and Emission Fraction in Experiment 11

Estimated Masses and Emission Fractions	Value
Total Mass of Dust on Floor (mg/ft ² disturbed)	609.42
Total Paint Removed From Surface (mg/ft ² disturbed)	101,646
Fraction Emitted	0.006

I.6.8. Experiment 12

The geometry of Experiment 12 is shown in Figure I-9, and the measured lead loadings and associated distances are shown in Table I-23. No adjustments were made to the loading since all samples were within the width of the job. The loadings were divided by the size of the job (11 ft²) and the fraction of lead in the paint (0.072) to estimate the dust loadings per ft² disturbed in Table I-23. Then, the natural logs of all loadings were used with the distances to estimate the regression parameters in Table I-24. Here, *intercept* is the intercept of the linear regression in log space, and Load at 0 ft is the assumed loading at 0 ft calculated as $\exp(\textit{intercept})$.

The integral was performed over the regression equation out to a distance of 12 ft, (the length of the room), and the total mass of dust on the floor was estimated as shown in Table I-25. The estimated paint density using the lead fraction was 1.74 g/cm³. Although the vintage of the renovated building was unknown, nearby buildings were believed to have been built at the same time and were built in 1920. Therefore, the building was assumed to have been built in 1920 and to have 5.0 layers of paint at the time of the job. The experiment notes indicated that all paint was removed during the renovation, so all 5.0 layers were assumed to be removed. These values were used to estimate the total amount of paint on the wall, giving a final emission fraction of 0.005.

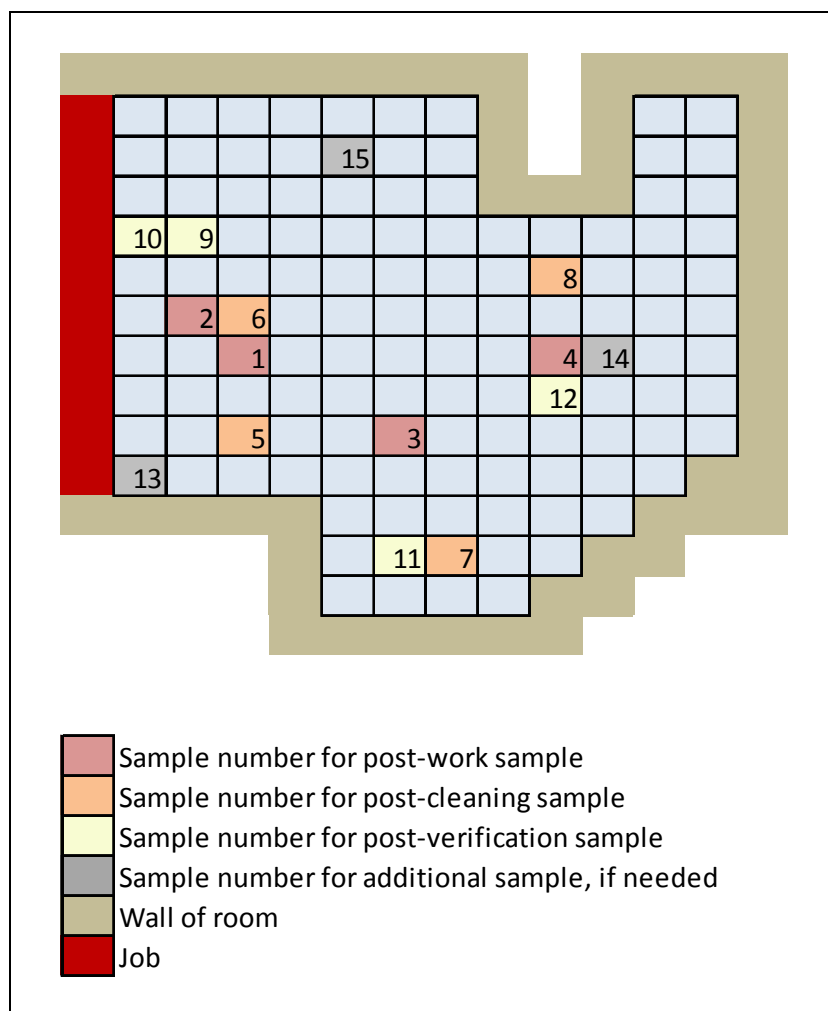


Figure I-9. Layout of Window Replacement Experiment 12

Table I-23. Post-Work Loading Measurements and Adjustments in Experiment 12

ID	Dist. From Wall (ft)	Lead Loading in $\mu\text{g}/\text{ft}^2$ (Dust Study)	Dust Load per ft^2 Disturbed (mg/ft^2 floor/ ft^2 wall)
1	3	9,757	12.32
2	2	1,559	1.97
3	6	2,748	3.47
4	9	585	0.74

Table I-24. Regression Statistics in Experiment 12

Statistic	Value
Shape	-0.23
Intercept	2.20
R ²	0.40
Load at 0 ft (mg/ft ² floor/ft ² disturbed)	9.05

Table I-25. Estimated Total Dust Emitted, Total Paint on Wall, and Emission Fraction in Experiment 12

Estimated Masses and Emission Fractions	Value
Total Mass of Dust on Floor (mg/ft ² disturbed)	472.30
Total Paint Removed From Surface (mg/ft ² disturbed)	86,736
Fraction Emitted	0.005

I.7. Cut Outs

I.7.1. Experiment 22

The geometry of Experiment 22 is shown in Figure I-10, but the exact location of the cutouts is unknown. Thus, no regression could be performed and the emission fraction is based on the average loadings. The loadings were divided by the size of the job (13 ft²) and the fraction of lead in the paint (0.036) to estimate the dust loadings per ft² disturbed in Table I-26. Then, the loadings were averaged and multiplied by the area of the room (190 ft²) to get the total mass of dust on the floor, as shown in Table I-27. The estimated paint density using the lead fraction was 1.37 g/cm³. Although the vintage of the renovated building was unknown, nearby buildings were believed to have been built at the same time and were built in 1920. Therefore, the building was assumed to have been built in 1920 and to have 5.0 layers of paint at the time of the job. The experiment notes indicated that all paint was removed during the renovation, so all 5.0 layers were assumed to be removed. These values were used to estimate the total amount of paint on the wall, giving a final emission fraction of 0.011.

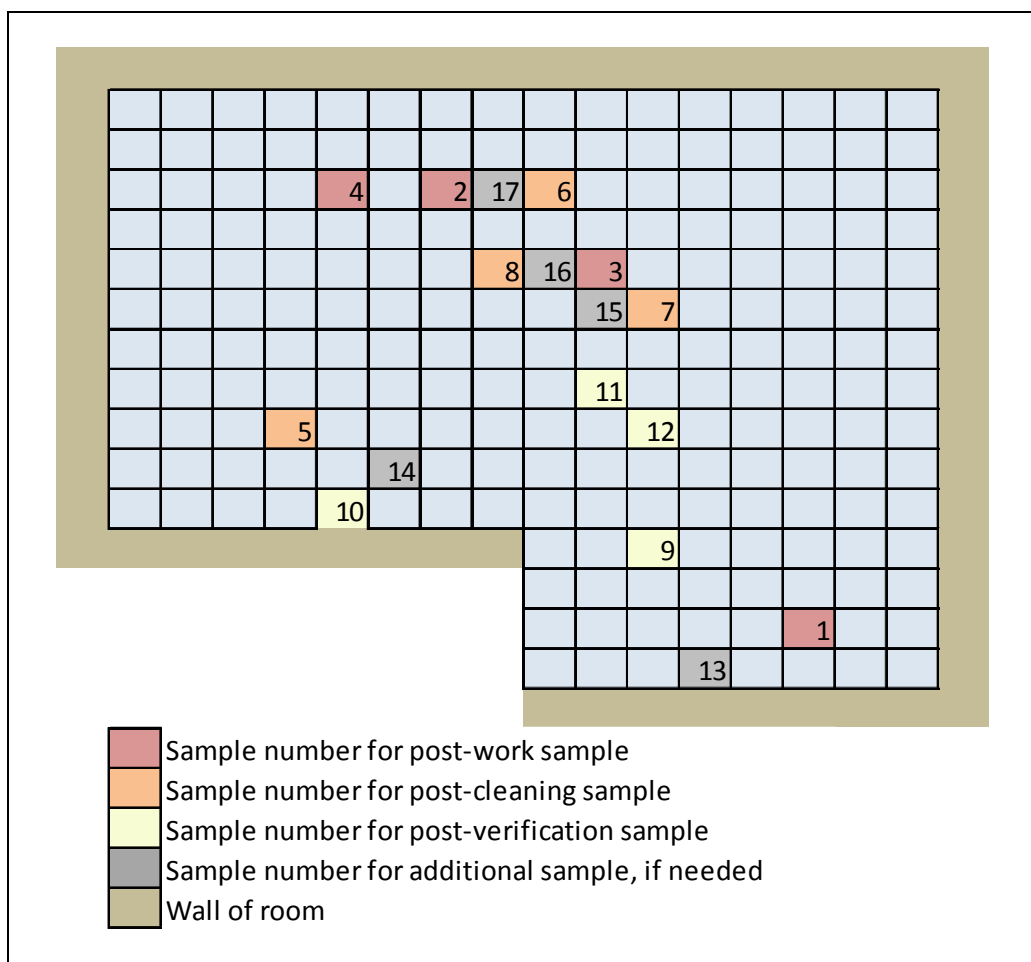


Figure I-10. Layout of Cut Outs Experiment 22

Table I-26. Post-Work Loading Measurements and Adjustments in Experiment 22

ID	Lead Loading in $\mu\text{g}/\text{ft}^2$ (Dust Study)	Dust Load per ft^2 Disturbed (mg/ft^2 floor/ ft^2 wall)
1	84	0.18
2	1,642	3.51
3	1,454	3.11
4	3,935	8.41

Table I-27. Estimated Total Dust Emitted, Total Paint on Wall, and Emission Fraction in Experiment 22

Estimated Masses and Emission Fractions	Value
Total Mass of Dust on Floor (mg/ft ² disturbed)	722
Total Paint Removed From Surface (mg/ft ² disturbed)	68,226
Fraction Emitted	0.011

I.7.2. Experiment 23

The geometry of Experiment 23 is shown in Figure I-11, but the exact location of the cutouts is unknown. Thus, no regression could be performed and the emission fraction is based on the average loadings. The loadings were divided by the size of the job (14 ft²) and the fraction of lead in the paint (0.036) to estimate the dust loadings per ft² disturbed in Table I-28. Then, the loadings were averaged and multiplied by the area of the room (190 ft²) to get the total mass of dust on the floor, as shown in Table I-29. The estimated paint density using the lead fraction was 1.37 g/cm³. Although the vintage of the renovated building was unknown, nearby buildings were believed to have been built at the same time and were built in 1920. Therefore, the building was assumed to have been built in 1920 and to have 5.0 layers of paint at the time of the job. The experiment notes indicated that all paint was removed during the renovation, so all 5.0 layers were assumed to be removed. These values were used to estimate the total amount of paint on the wall, giving a final emission fraction of 0.015.

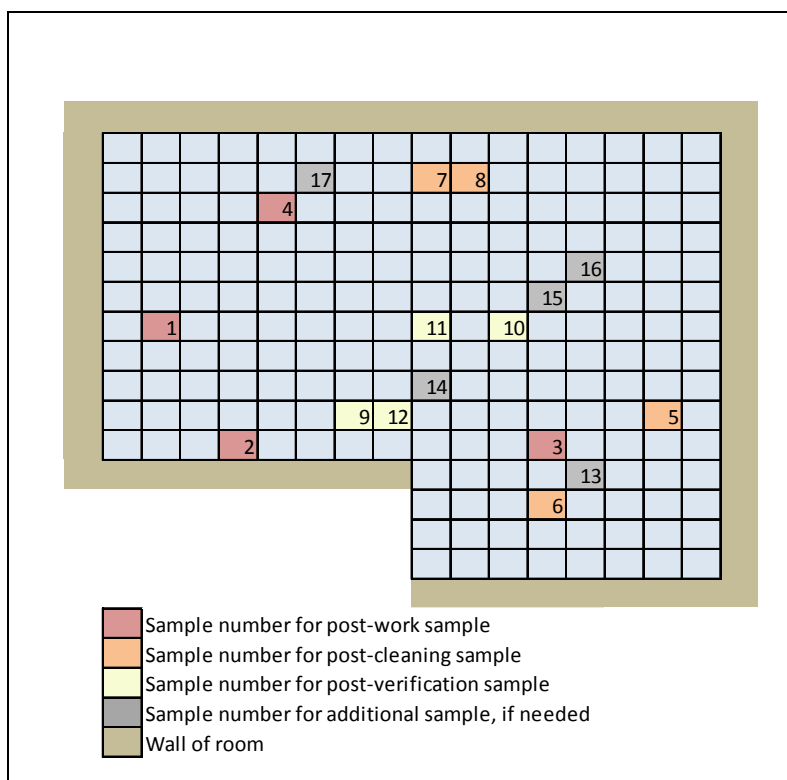


Figure I-11. Layout of Cut Outs Experiment 23

Table I-28. Post-Work Loading Measurements and Adjustments in Experiment 23

ID	Lead Loading in $\mu\text{g}/\text{ft}^2$ (Dust Study)	Dust Load per ft^2 Disturbed (mg/ft^2 floor/ ft^2 wall)
1	4,174	8.28
2	3,469	6.88
3	313	0.62
4	3,146	6.24

Table I-29. Estimated Total Dust Emitted, Total Paint on Wall, and Emission Fraction in Experiment 23

Estimated Masses and Emission Fractions	Value
Total Mass of Dust on Floor (mg/ft ² disturbed)	1046
Total Paint Removed From Surface (mg/ft ² disturbed)	68,226
Fraction Emitted	0.015

I.7.3. Experiment 24

The geometry of Experiment 24 is shown in Figure I-12, but the exact location of the cutouts is unknown. Thus, no regression could be performed and the emission fraction is based on the average loadings. The loadings were divided by the size of the job (40 ft²) and the fraction of lead in the paint (0.05) to estimate the dust loadings per ft² disturbed in Table I-30. Then, the loadings were averaged and multiplied by the area of the room (190 ft²) to get the total mass of dust on the floor, as shown in Table I-31. The estimated paint density using the lead fraction was 1.52 g/cm³. Although the vintage of the renovated building was unknown, nearby buildings were believed to have been built at the same time and were built in 1920. Therefore, the building was assumed to have been built in 1920 and to have 5.0 layers of paint at the time of the job. The experiment notes indicated that all paint was removed during the renovation, so all 5.0 layers were assumed to be removed. These values were used to estimate the total amount of paint on the wall, giving a final emission fraction of 0.0002.

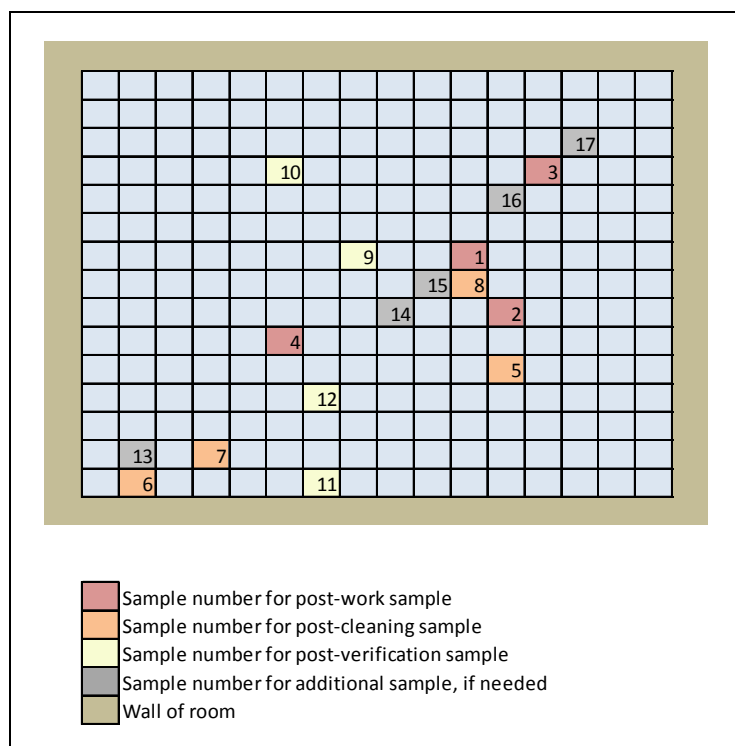


Figure I-12. Layout of Cut Outs Experiment 24

Table I-30. Post-Work Loading Measurements and Adjustments in Experiment 24

ID	Lead Loading in $\mu\text{g}/\text{ft}^2$ (Dust Study)	Dust Load per ft^2 Disturbed (mg/ft^2 floor/ ft^2 wall)
1	92	0.05
2	473	0.24
3	48	0.02
4	103	0.05

Table I-31. Estimated Total Dust Emitted, Total Paint on Wall, and Emission Fraction in Experiment 24

Estimated Masses and Emission Fractions	Value
Total Mass of Dust on Floor (mg/ft ² disturbed)	17
Total Paint Removed From Surface (mg/ft ² disturbed)	75,424
Fraction Emitted	0.0002

I.7.4. Experiment 25

The geometry of Experiment 25 is shown in Figure I-13, but the exact location of the cutouts is unknown. Thus, no regression could be performed and the emission fraction is based on the average loadings. The loadings were divided by the size of the job (14 ft²) and the fraction of lead in the paint (0.036) to estimate the dust loadings per ft² disturbed in Table I-32. Then, the loadings were averaged and multiplied by the area of the room (190 ft²) to get the total mass of dust on the floor, as shown in Table I-33. The estimated paint density using the lead fraction was 1.37 g/cm³. Although the vintage of the renovated building was unknown, nearby buildings were believed to have been built at the same time and were built in 1920. Therefore, the building was assumed to have been built in 1920 and to have 5.0 layers of paint at the time of the job. The experiment notes indicated that all paint was removed during the renovation, so all 5.0 layers were assumed to be removed. These values were used to estimate the total amount of paint on the wall, giving a final emission fraction of 0.0113.

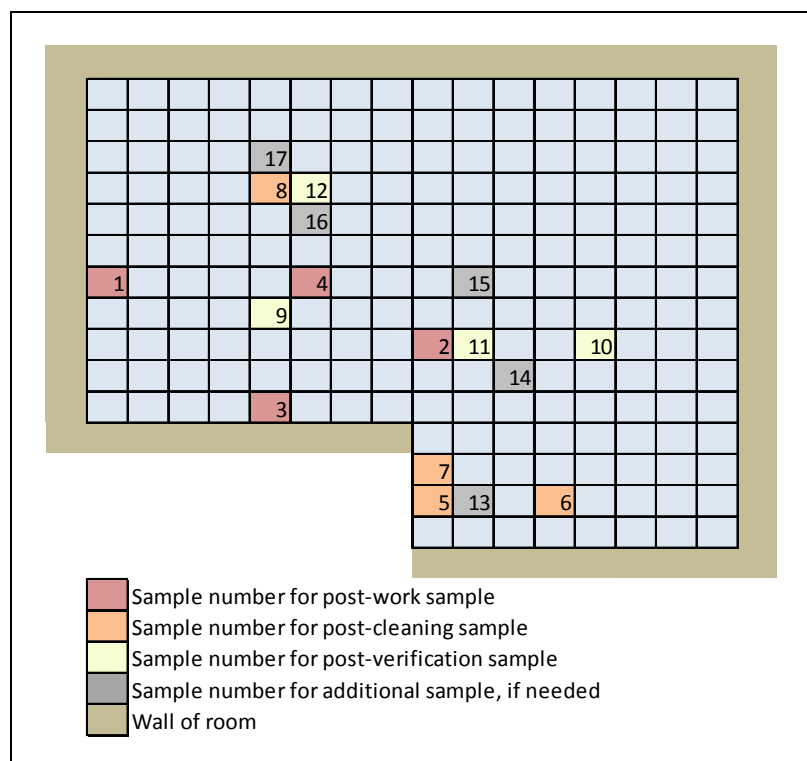


Figure I-13. Layout of Cut Outs Experiment 25

Table I-32. Post-Work Loading Measurements and Adjustments in Experiment 25

ID	Lead Loading in $\mu\text{g}/\text{ft}^2$ (Dust Study)	Dust Load per ft^2 Disturbed (mg/ft^2 floor/ ft^2 wall)
1	127	0.25
2	2,667	5.29
3	887	1.76
4	4,524	8.98

Table I-33. Estimated Total Dust Emitted, Total Paint on Wall, and Emission Fraction in Experiment 25

Estimated Masses and Emission Fractions	Value
Total Mass of Dust on Floor (mg/ft ² disturbed)	733
Total Paint Removed From Surface (mg/ft ² disturbed)	68,226
Fraction Emitted	0.011

I.7.5. Experiment 45

The geometry of Experiment 45 is shown in Figure I-14, and the measured lead loadings and associated distances are shown in Table I-34. Sample 2 was adjusted using the taper assumption since it was outside the lateral extent of the job. The loadings were divided by the size of the job (6 ft²) and the fraction of lead in the paint (0.018) to estimate the dust loadings per ft² disturbed in Table I-34. Then, the natural logs of all loadings were used with the distances to estimate the regression parameters in Table I-35. Here, *intercept* is the intercept of the linear regression in log space, and Load at 0 ft is the assumed loading at 0 ft calculated as $\exp(\text{intercept})$.

The integral was performed over the regression equation out to a distance of 12 ft, (the length of the room), and the total mass of dust on the floor was estimated as shown in Table I-36. However, the R² was very low, so the average method was used instead of the integral method. The estimated paint density using the lead fraction was 1.19 g/cm³. The building was built in 1910, thus, it was assumed to have 5.3 layers of paint at the time of the job. The experiment notes indicated that all paint was removed during the renovation, so all 5.3 layers were assumed to be removed. These values were used to estimate the total amount of paint on the wall, giving a final emission fraction of 0.0264.

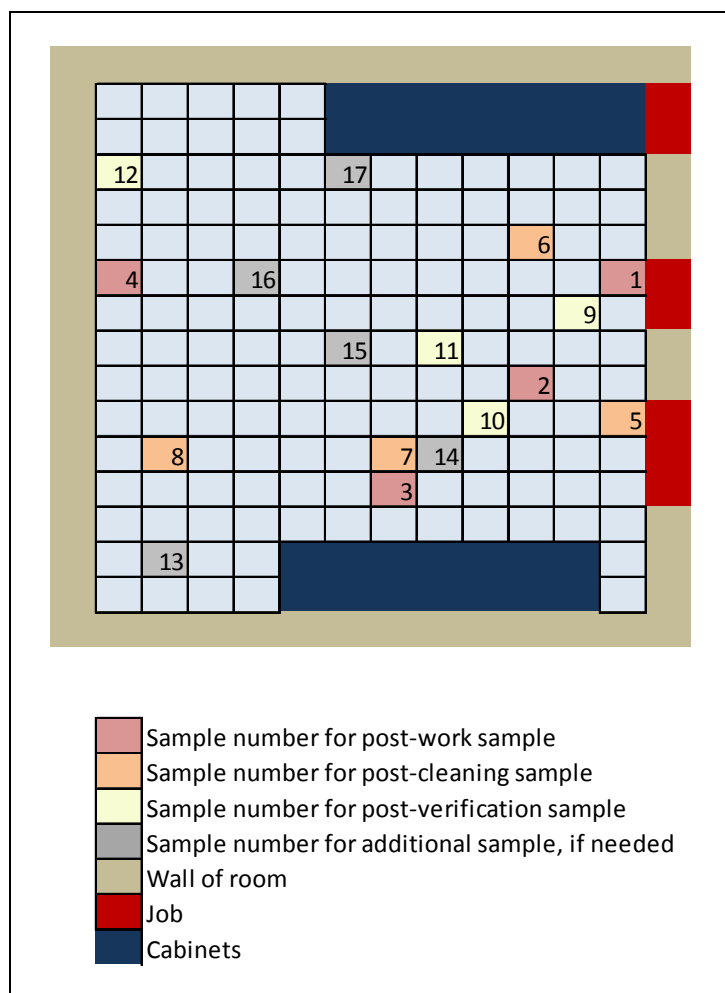


Figure I-14. Layout of Cut Outs Experiment 45

Table I-34. Post-Work Loading Measurements and Adjustments in Experiment 45

ID	Dist. From Wall (ft)	Lead Loading in $\mu\text{g}/\text{ft}^2$ (Dust Study)	Lead Loading in $\mu\text{g}/\text{ft}^2$ (adjusted)	Dust Load per ft^2 Disturbed (mg/ft^2 floor/ ft^2 wall)
1	1	2,101	2,101	19.45
2	3	110	137	1.27
3	6	909	909	8.41
4	12	621	621	5.75

Table I-35. Regression Statistics in Experiment 45

Statistic	Value
Shape	-0.02
Intercept	1.89
R ²	0.01
Load at 0 ft (mg/ft ² floor/ft ² disturbed)	6.64

Table I-36. Estimated Total Dust Emitted, Total Paint on Wall, and Emission Fraction in Experiment 45

Estimated Masses and Emission Fractions	Value
Total Mass of Dust on Floor (mg/ft ² disturbed)	1,558
Total Paint Removed From Surface (mg/ft ² disturbed)	58,971
Fraction Emitted	0.011

I.7.6. Experiment 46

The geometry of Experiment 46 is shown in Figure I-15, and the measured lead loadings and associated distances are shown in Table I-37. Sample 2 was adjusted using the taper assumption since it was outside the lateral extent of the job. The loadings were divided by the size of the job (7 ft²) and the fraction of lead in the paint (0.018) to estimate the dust loadings per ft² disturbed in Table I-37. Then, the natural logs of all loadings were used with the distances to estimate the regression parameters in Table I-38. Here, *intercept* is the intercept of the linear regression in log space, and Load at 0 ft is the assumed loading at 0 ft calculated as $\exp(\textit{intercept})$.

The integral was performed over the regression equation out to a distance of 12 ft, (the length of the room), and the total mass of dust on the floor was estimated as shown in Table I-39. The estimated paint density using the lead fraction was 1.19 g/cm³. The building was built in 1910, thus, it was assumed to have 5.3 layers of paint at the time of the job. The experiment notes indicated that all paint was removed during the renovation, so all 5.3 layers were assumed to be removed. These values were used to estimate the total amount of paint on the wall, giving a final emission fraction of 0.013.

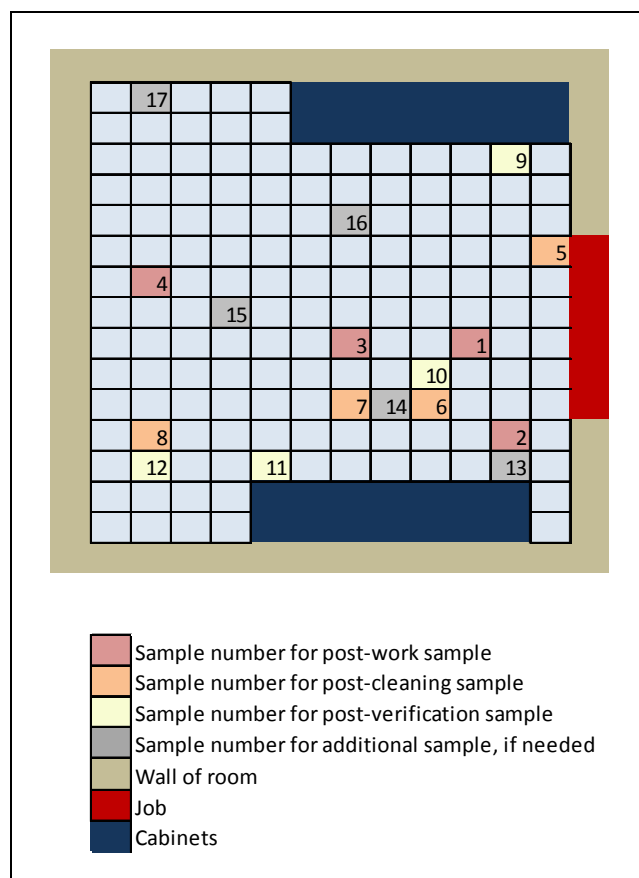


Figure I-15. Layout of Cut Outs Experiment 46

Table I-37. Post-Work Loading Measurements and Adjustments in Experiment 46

ID	Dist. From Wall (ft)	Lead Loading in $\mu\text{g}/\text{ft}^2$ (Dust Study)	Lead Loading in $\mu\text{g}/\text{ft}^2$ (adjusted)	Dust Load per ft^2 Disturbed (mg/ft^2 floor/ ft^2 wall)
1	3	1,586	1,586	12.59
2	2	529	794	6.30
3	6	216	216	1.71
4	11	90	90	0.71

Table I-38. Regression Statistics in Experiment 46

Statistic	Value
Shape	-0.29
Intercept	2.76
R ²	0.85
Load at 0 ft (mg/ft ² floor/ft ² disturbed)	15.75

Table I-39. Estimated Total Dust Emitted, Total Paint on Wall, and Emission Fraction in Experiment 46

Estimated Masses and Emission Fractions	Value
Total Mass of Dust on Floor (mg/ft ² disturbed)	781.02
Total Paint Removed From Surface (mg/ft ² disturbed)	58,971
Fraction Emitted	0.013

I.7.7. Experiment 71

The geometry of Experiment 71 is shown in Figure I-16, but the exact location of the cutouts is unknown. Thus, no regression could be performed and the emission fraction is based on the average loadings. The loadings were divided by the size of the job (6 ft²) and the fraction of lead in the paint (0.008) to estimate the dust loadings per ft² disturbed in Table I-40. Then, the loadings were averaged and multiplied by the area of the room (115 ft²) to get the total mass of dust on the floor, as shown in Table I-41. The estimated paint density using the lead fraction was 1.08 g/cm³. The building was built in 1900, thus it was assumed to have 6.2 layers of paint at the time of the job. The experiment notes indicated that all paint was removed during the renovation, so all 6.2 layers were assumed to be removed. These values were used to estimate the total amount of paint on the wall, giving a final emission fraction of 0.001.

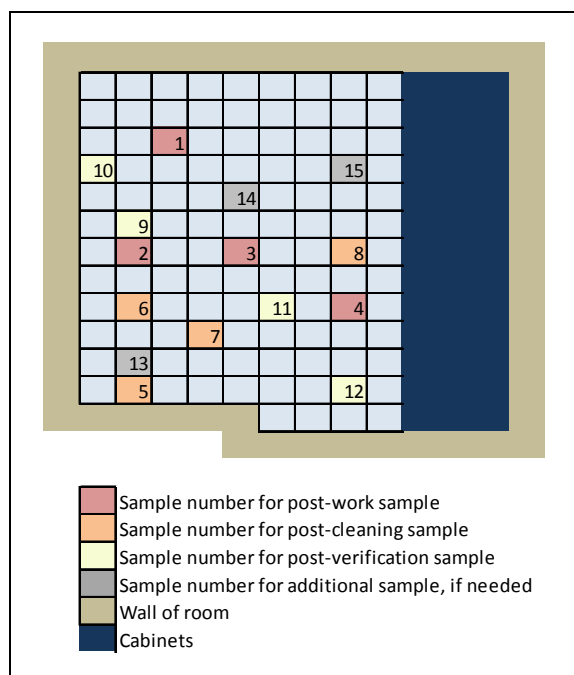


Figure I-16. Layout of Cut Outs Experiment 71

Table I-40. Post-Work Loading Measurements and Adjustments in Experiment 71

ID	Lead Loading in $\mu\text{g}/\text{ft}^2$ (Dust Study)	Dust Load per ft^2 Disturbed (mg/ft^2 floor/ ft^2 wall)
1	59	1.23
2	16	0.34
3	7	0.15
4	16	0.34

Table I-41. Estimated Total Dust Emitted, Total Paint on Wall, and Emission Fraction in Experiment 71

Estimated Masses and Emission Fractions	Value
Total Mass of Dust on Floor (mg/ft^2 disturbed)	59
Total Paint Removed From Surface (mg/ft^2 disturbed)	63,279
Fraction Emitted	0.001

I.7.8. Experiment 72

The geometry of Experiment 72 is shown in Figure I-17, but the exact location of the cutouts is unknown. Thus, no regression could be performed and the emission fraction is based on the average loadings. The loadings were divided by the size of the job (7 ft²) and the fraction of lead in the paint (0.01) to estimate the dust loadings per ft² disturbed in Table I-42. Then, the loadings were averaged and multiplied by the area of the room (115 ft²) to get the total mass of dust on the floor, as shown in Table I-43. The estimated paint density using the lead fraction was 1.10 g/cm³. The building was built in 1900, thus, it was assumed to have 6.2 layers of paint at the time of the job. The experiment notes indicated that all paint was removed during the renovation, so all 6.2 layers were assumed to be removed. These values were used to estimate the total amount of paint on the wall, giving a final emission fraction of 0.0208.

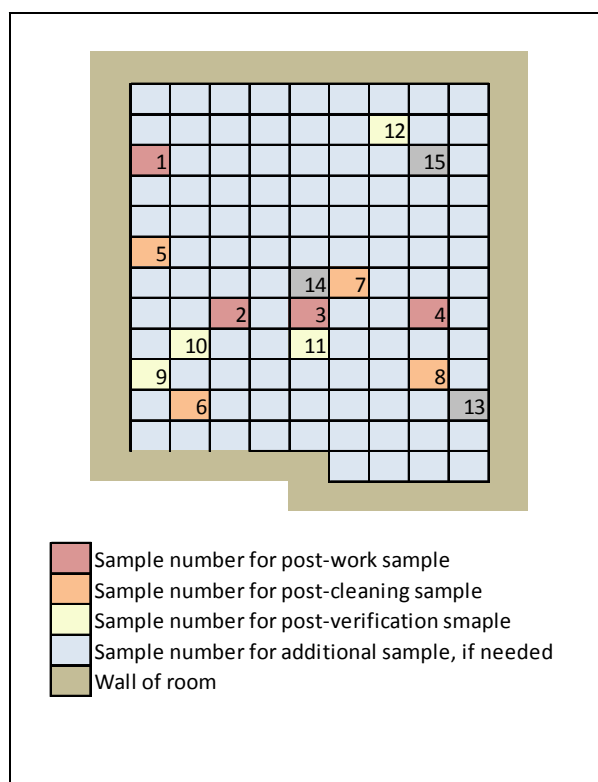


Figure I-17. Layout of Cut Outs Experiment 72

Table I-42. Post-Work Loading Measurements and Adjustments in Experiment 72

ID	Lead Loading in $\mu\text{g}/\text{ft}^2$ (Dust Study)	Dust Load per ft^2 Disturbed (mg/ft^2 floor/ ft^2 wall)
1	2,995	42.78
2	55	0.79
3	40	0.58
4	174	2.48

Table I-43. Estimated Total Dust Emitted, Total Paint on Wall, and Emission Fraction in Experiment 72

Estimated Masses and Emission Fractions	Value
Total Mass of Dust on Floor (mg/ft^2 disturbed)	1341
Total Paint Removed From Surface (mg/ft^2 disturbed)	64,488
Fraction Emitted	0.021

I.7.9. Experiment 52

The geometry of Experiment 52 is shown in Figure I-18, but the exact location of the cutouts is unknown. Thus, no regression could be performed and the emission fraction is based on the average loadings. The loadings were divided by the size of the job (6 ft^2) and the fraction of lead in the paint (0.095) to estimate the dust loadings per ft^2 disturbed in Table I-44. Then, the loadings were averaged and multiplied by the area of the room (120 ft^2) to get the total mass of dust on the floor, as shown in Table I-45. The estimated paint density using the lead fraction was $1.98 \text{ g}/\text{cm}^3$. The school was built in 1967, thus, it was assumed to have 3.3 layers of paint at the time of the job. The experiment notes indicated that all paint was removed during the renovation, so all 3.3 layers were assumed to be removed. These values were used to estimate the total amount of paint on the wall, giving a final emission fraction of 0.003.

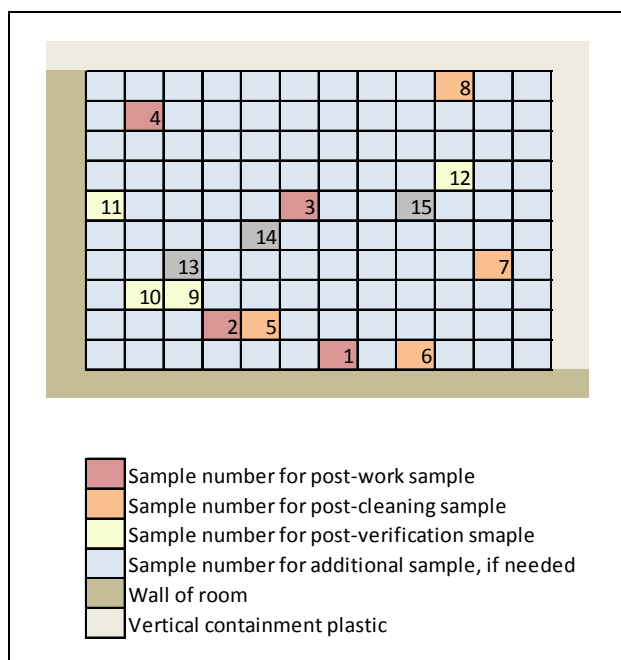


Figure I-18. Layout of Cut Outs Experiment 52

Table I-44. Post-Work Loading Measurements and Adjustments in Experiment 52

ID	Lead Loading in $\mu\text{g}/\text{ft}^2$ (Dust Study)	Dust Load per ft^2 Disturbed (mg/ft^2 floor/ ft^2 wall)
1	1,101	1.93
2	1,154	2.02
3	453	0.79
4	220	0.39

Table I-45. Estimated Total Dust Emitted, Total Paint on Wall, and Emission Fraction in Experiment 52

Estimated Masses and Emission Fractions	Value
Total Mass of Dust on Floor (mg/ft^2 disturbed)	154
Total Paint Removed From Surface (mg/ft^2 disturbed)	61,859
Fraction Emitted	0.003

I.7.10. Experiment 53

The geometry of Experiment 53 is shown in Figure I-19, but the exact location of the cutouts is unknown. Thus, no regression could be performed and the emission fraction is based on the average loadings. The loadings were divided by the size of the job (6 ft²) and the fraction of lead in the paint (0.074) to estimate the dust loadings per ft² disturbed in Table I-46. Then, the loadings were averaged and multiplied by the area of the room (120 ft²) to get the total mass of dust on the floor, as shown in Table I-47. The estimated paint density using the lead fraction was 1.77 g/cm³. The school was built in 1967, thus, it was assumed to have 3.3 layers of paint at the time of the job. The experiment notes indicated that all paint was removed during the renovation, so all 3.3 layers were assumed to be removed. These values were used to estimate the total amount of paint on the wall, giving a final emission fraction of 0.005.

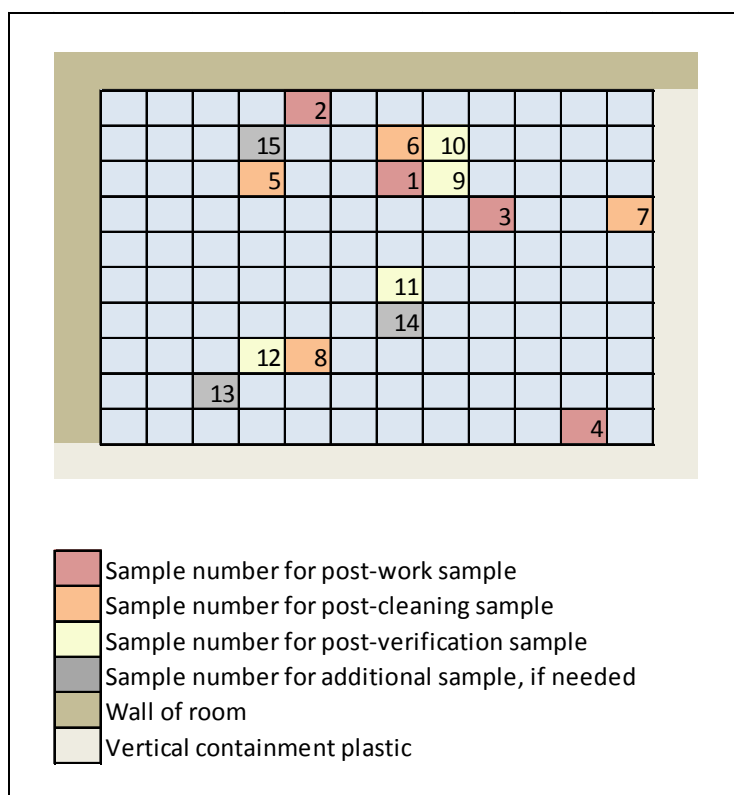


Figure I-19. Layout of Cut Outs Experiment 53

Table I-46. Post-Work Loading Measurements and Adjustments in Experiment 53

ID	Lead Loading in $\mu\text{g}/\text{ft}^2$ (Dust Study)	Dust Load per ft^2 Disturbed (mg/ft^2 floor/ ft^2 wall)
1	880	1.98
2	3,005	6.77
3	234	0.53
4	128	0.29

Table I-47. Estimated Total Dust Emitted, Total Paint on Wall, and Emission Fraction in Experiment 53

Estimated Masses and Emission Fractions	Value
Total Mass of Dust on Floor (mg/ft^2 disturbed)	287
Total Paint Removed From Surface (mg/ft^2 disturbed)	55,082
Fraction Emitted	0.005

I.7.11. Experiment 54

The geometry of Experiment 54 is shown in Figure I-20, but the exact location of the cutouts is unknown. Thus, no regression could be performed and the emission fraction is based on the average loadings. The loadings were divided by the size of the job (6 ft^2) and the fraction of lead in the paint (0.074) to estimate the dust loadings per ft^2 disturbed in Table I-48. Then, the loadings were averaged and multiplied by the area of the room (120 ft^2) to get the total mass of dust on the floor, as shown in Table I-49. The estimated paint density using the lead fraction was $1.77 \text{ g}/\text{cm}^3$. The school was built in 1967, thus, it was assumed to have 3.3 layers of paint at the time of the job. The experiment notes indicated that all paint was removed during the renovation, so all 3.3 layers were assumed to be removed. These values were used to estimate the total amount of paint on the wall, giving a final emission fraction of 0.006.

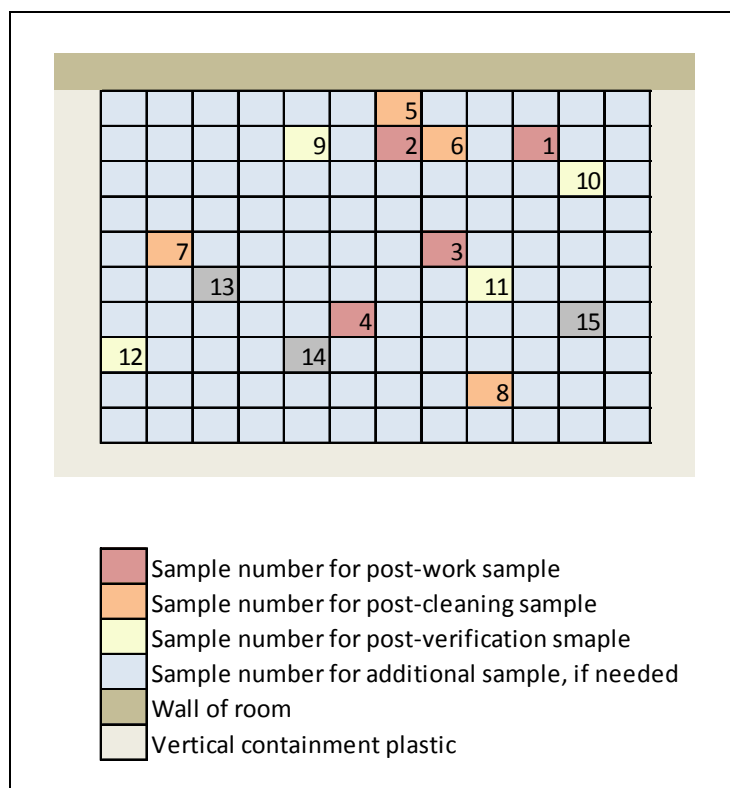


Figure I-20. Layout of Cut Outs Experiment 54

Table I-48. Post-Work Loading Measurements and Adjustments in Experiment 54

ID	Lead Loading in $\mu\text{g}/\text{ft}^2$ (Dust Study)	Dust Load per ft^2 Disturbed (mg/ft^2 floor/ ft^2 wall)
1	1,991	4.48
2	1,381	3.11
3	712	1.60
4	841	1.90

Table I-49. Estimated Total Dust Emitted, Total Paint on Wall, and Emission Fraction in Experiment 54

Estimated Masses and Emission Fractions	Value
Total Mass of Dust on Floor (mg/ft ² disturbed)	333
Total Paint Removed From Surface (mg/ft ² disturbed)	55,082
Fraction Emitted	0.006

I.7.12. Experiment 55

The geometry of Experiment 55 is shown in Figure I-21, but the exact location of the cutouts is unknown. Thus, no regression could be performed and the emission fraction is based on the average loadings. The loadings were divided by the size of the job (6 ft²) and the fraction of lead in the paint (0.074) to estimate the dust loadings per ft² disturbed in Table I-50. Then, the loadings were averaged and multiplied by the area of the room (120 ft²) to get the total mass of dust on the floor, as shown in Table I-51. The estimated paint density using the lead fraction was 1.77 g/cm³. The school was built in 1967, thus, it was assumed to have 3.3 layers of paint at the time of the job. The experiment notes indicated that all paint was removed during the renovation, so all 3.3 layers were assumed to be removed. These values were used to estimate the total amount of paint on the wall, giving a final emission fraction of 0.005.

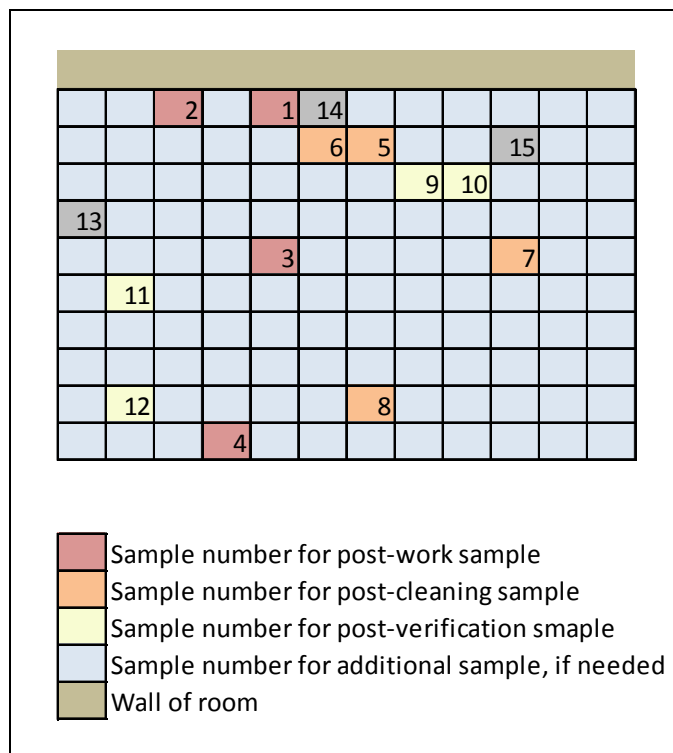


Figure I-21. Layout of Cut Outs Experiment 55

Table I-50. Post-Work Loading Measurements and Adjustments in Experiment 55

ID	Lead Loading in $\mu\text{g}/\text{ft}^2$ (Dust Study)	Dust Load per ft^2 Disturbed (mg/ft^2 floor/ ft^2 wall)
1	1,793	4.04
2	1,655	3.73
3	271	0.61
4	124	0.28

Table I-51. Estimated Total Dust Emitted, Total Paint on Wall, and Emission Fraction in Experiment 55

Estimated Masses and Emission Fractions	Value
Total Mass of Dust on Floor (mg/ft ² disturbed)	260
Total Paint Removed From Surface (mg/ft ² disturbed)	55,082
Fraction Emitted	0.005

I.8. Door Plane

I.8.1. Experiment 77

The geometry of Experiment 77 is shown in Figure I-22, but the exact location of the door is unknown. Thus, no regression could be performed and the emission fraction is based on the average loadings. The loadings were divided by the size of the job (26 ft²) and the fraction of lead in the paint (0.017) to estimate the dust loadings per ft² disturbed in Table I-52. Then, the loadings were averaged and multiplied by the area of the room (180 ft²) to get the total mass of dust on the floor, as shown in Table I-53. The estimated paint density using the lead fraction was 1.18 g/cm³. The building was built in 1910, thus, it was assumed to have 5.3 layers of paint at the time of the job. The experiment notes indicated that all paint was removed during the renovation, so all 5.3 layers were assumed to be removed. These values were used to estimate the total amount of paint on the wall, giving a final emission fraction of 0.216.

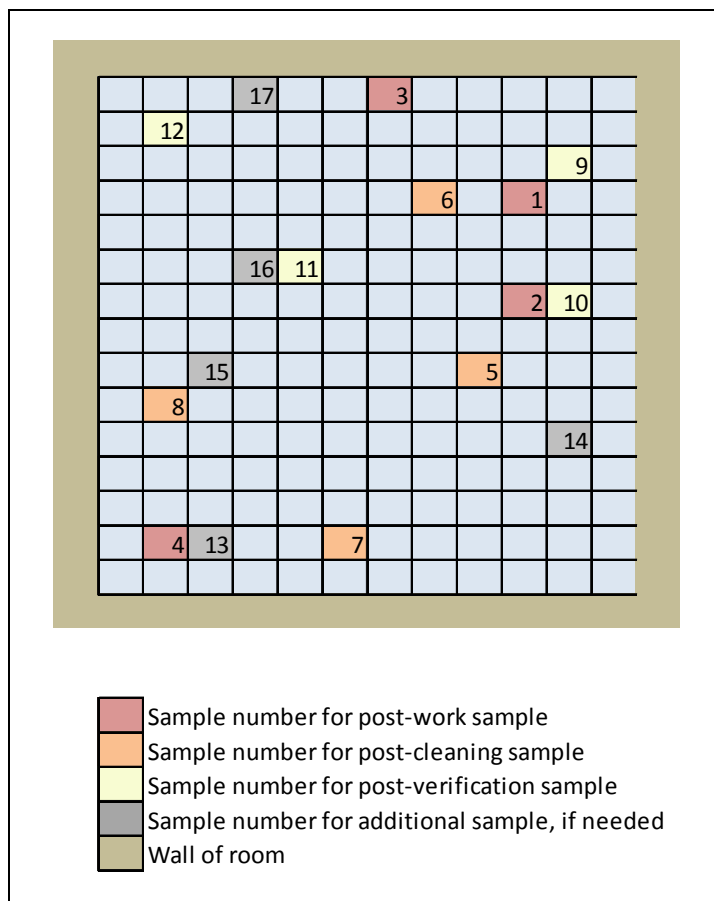


Figure I-22. Layout of Door Plane Experiment 77

Table I-52. Post-Work Loading Measurements and Adjustments in Experiment 77

ID	Lead Loading in $\mu\text{g}/\text{ft}^2$ (Dust Study)	Dust Load per ft^2 Disturbed (mg/ft^2 floor/ ft^2 wall)
1	31,648	71.60
2	36,137	81.76
3	34,162	231.87
4	21,771	73.88

Table I-53. Estimated Total Dust Emitted, Total Paint on Wall, and Emission Fraction in Experiment 77

Estimated Masses and Emission Fractions	Value
Total Mass of Dust on Floor (mg/ft ² disturbed)	12,596
Total Paint Removed From Surface (mg/ft ² disturbed)	58,457
Fraction Emitted	0.216

I.8.2. Experiment 78

The geometry of Experiment 78 is shown in Figure I-23, but the exact location of the door during the experiment is unknown. Thus, no regression could be performed and the emission fraction is based on the average loadings. The loadings were divided by the size of the job (25 ft²) and the fraction of lead in the paint (0.02) to estimate the dust loadings per ft² disturbed in Table I-54. Then, the loadings were averaged and multiplied by the area of the room (180 ft²) to get the total mass of dust on the floor, as shown in Table I-55. The estimated paint density using the lead fraction was 1.21 g/cm³. The building was built in 1910, thus, it was assumed to have 5.3 layers of paint at the time of the job. The experiment notes indicated that all paint was removed during the renovation, so all 5.3 layers were assumed to be removed. These values were used to estimate the total amount of paint on the wall, giving a final emission fraction of 0.161.

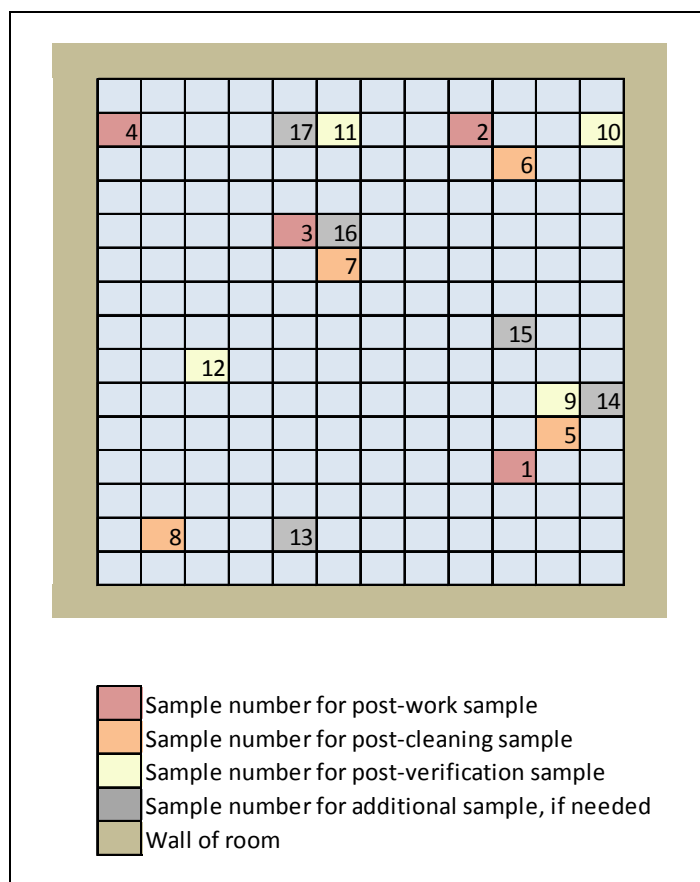


Figure I-23. Layout of Door Plane Experiment 78

Table I-54. Post-Work Loading Measurements and Adjustments in Experiment 78

ID	Lead Loading in $\mu\text{g}/\text{ft}^2$ (Dust Study)	Dust Load per ft^2 Disturbed (mg/ft^2 floor/ ft^2 wall)
1	36,423	72.85
2	38,237	114.71
3	27,352	54.70
4	4,999	15.00

Table I-55. Estimated Total Dust Emitted, Total Paint on Wall, and Emission Fraction in Experiment 78

Estimated Masses and Emission Fractions	Value
Total Mass of Dust on Floor (mg/ft ² disturbed)	9,631
Total Paint Removed From Surface (mg/ft ² disturbed)	59,999
Fraction Emitted	0.161

I.8.3. Experiment 79

The geometry of Experiment 79 is shown in Figure I-24, but the exact location of the door during the experiment is unknown. Thus, no regression could be performed and the emission fraction is based on the average loadings. Sample 2 was adjusted using the taper assumption since it was outside the lateral extent of the job. The loadings were divided by the size of the job (32 ft²) and the fraction of lead in the paint (0.021) to estimate the dust loadings per ft² disturbed in Table I-56. Then, the loadings were averaged and multiplied by the area of the room (140 ft²) to get the total mass of dust on the floor, as shown in Table I-57. The estimated paint density using the lead fraction was 1.22 g/cm³. Although the vintage of the renovated building was unknown, nearby buildings were believed to have been built at the same time and were built in 1920. Therefore, the building was assumed to have been built in 1920 and to have 5.0 layers of paint at the time of the job. The experiment notes indicated that all paint was removed during the renovation, so all 5.0 layers were assumed to be removed. These values were used to estimate the total amount of paint on the wall, giving a final emission fraction of 0.120.

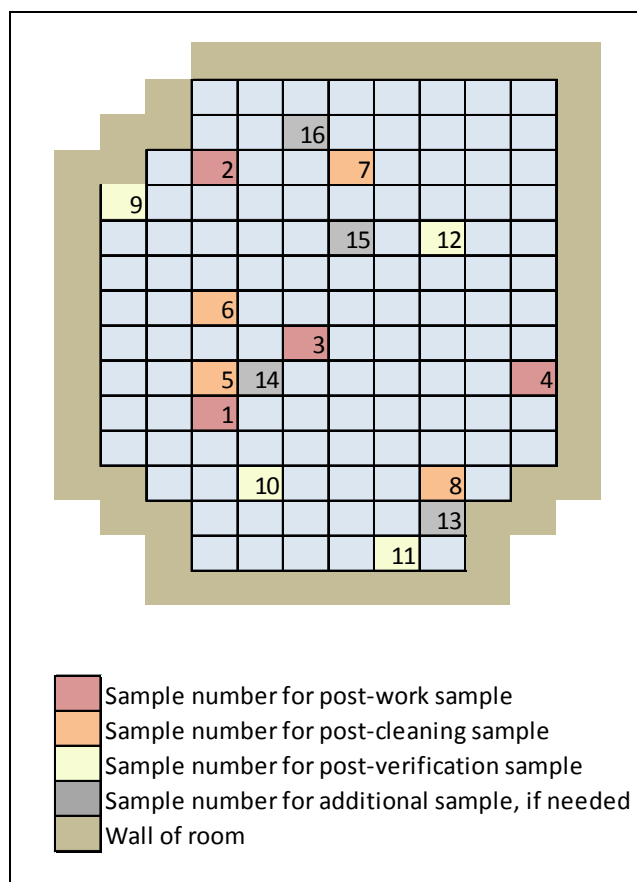


Figure I-24. Layout of Door Plane Experiment 79

Table I-56. Post-Work Loading Measurements and Adjustments in Experiment 79

ID	Lead Loading in $\mu\text{g}/\text{ft}^2$ (Dust Study)	Dust Load per ft^2 Disturbed (mg/ft^2 floor/ ft^2 wall)
1	72,601	108.04
2	31,651	70.65
3	22,105	32.89
4	13,484	20.07

Table I-57. Estimated Total Dust Emitted, Total Paint on Wall, and Emission Fraction in Experiment 79

Estimated Masses and Emission Fractions	Value
Total Mass of Dust on Floor (mg/ft ² disturbed)	7,283
Total Paint Removed From Surface (mg/ft ² disturbed)	60,513
Fraction Emitted	0.120

I.8.4. Experiment 80

The geometry of Experiment 80 is shown in Figure I-25, but the exact location of the door during the experiment is unknown. Thus, no regression could be performed and the emission fraction is based on the average loadings. No adjustments were made to the loading since all samples were within the width of the job. The loadings were divided by the size of the job (40 ft²) and the fraction of lead in the paint (0.059) to estimate the dust loadings per ft² disturbed in Table I-58. Then, the loadings were averaged and multiplied by the area of the room (180 ft²) to get the total mass of dust on the floor, as shown in Table I-59. The estimated paint density using the lead fraction was 1.61 g/cm³. Although the vintage of the renovated building was unknown, nearby buildings were believed to have been built at the same time and were built in 1920. Therefore, the building was assumed to have been built in 1920 and to have 5.0 layers of paint at the time of the job. The experiment notes indicated that all paint was removed during the renovation, so all 5.0 layers were assumed to be removed. These values were used to estimate the total amount of paint on the wall, giving a final emission fraction of 0.095.

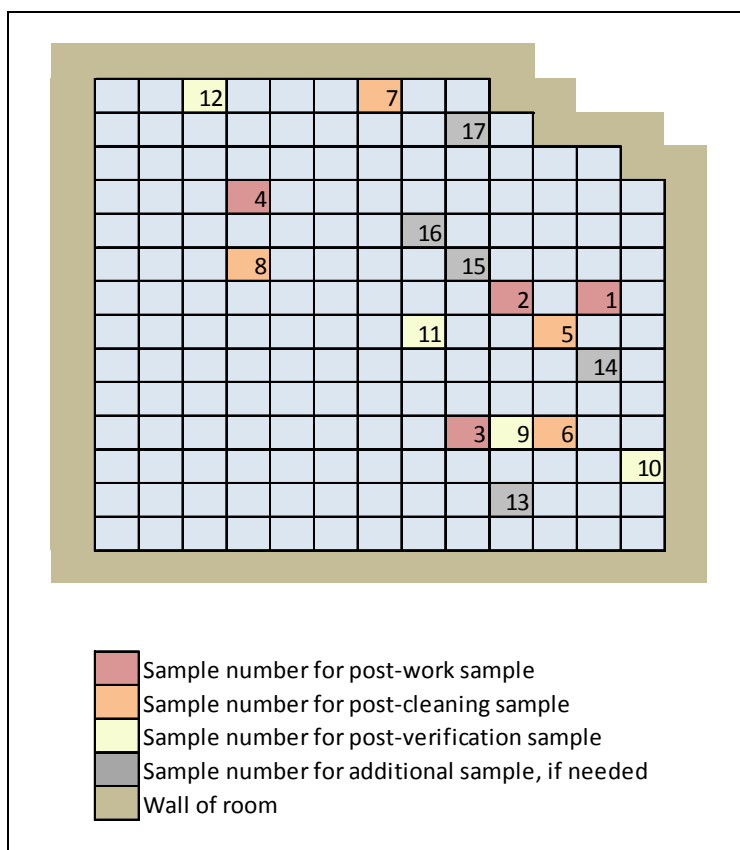


Figure I-25. Layout of Door Plane Experiment 80

Table I-58. Post-Work Loading Measurements and Adjustments in Experiment 80

ID	Lead Loading in $\mu\text{g}/\text{ft}^2$ (Dust Study)	Dust Load per ft^2 Disturbed (mg/ft^2 floor/ ft^2 wall)
1	49,254	20.87
2	166,383	70.50
3	140,057	59.35
4	41,628	17.64

Table I-59. Estimated Total Dust Emitted, Total Paint on Wall, and Emission Fraction in Experiment 80

Estimated Masses and Emission Fractions	Value
Total Mass of Dust on Floor (mg/ft ² disturbed)	7,576
Total Paint Removed From Surface (mg/ft ² disturbed)	80,051
Fraction Emitted	0.095

I.8.5. Experiment 47

The geometry of Experiment 47 is shown in Figure I-26, but the exact location of the door during the experiment is unknown. Thus, no regression could be performed and the emission fraction is based on the average loadings. Sample 2 was adjusted using the taper assumption since it was outside the lateral extent of the job. The loadings were divided by the size of the job (40 ft²) and the fraction of lead in the paint (0.039) to estimate the dust loadings per ft² disturbed in Table I-60. Then, the loadings were averaged and multiplied by the area of the room (180 ft²) to get the total mass of dust on the floor, as shown in Table I-61. The estimated paint density using the lead fraction was 1.40 g/cm³. The building was built in 1910, thus, it was assumed to have 5.3 layers of paint at the time of the job. The experiment notes indicated that all paint was removed during the renovation, so all 5.3 layers were assumed to be removed. These values were used to estimate the total amount of paint on the wall, giving a final emission fraction of 0.109.

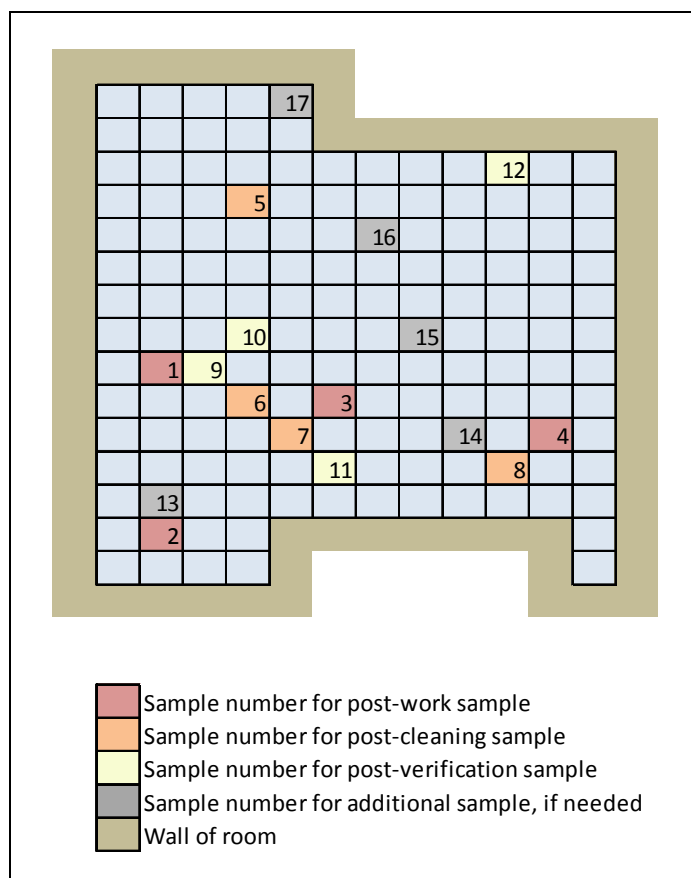


Figure I-26. Layout of Door Plane Experiment 47

Table I-60. Post-Work Loading Measurements and Adjustments in Experiment 47

ID	Lead Loading in $\mu\text{g}/\text{ft}^2$ (Dust Study)	Dust Load per ft^2 Disturbed (mg/ft^2 floor/ ft^2 wall)
1	209,798	134.49
2	30,305	38.85
3	11,958	7.67
4	11,267	7.22

Table I-61. Estimated Total Dust Emitted, Total Paint on Wall, and Emission Fraction in Experiment 47

Estimated Masses and Emission Fractions	Value
Total Mass of Dust on Floor (mg/ft ² disturbed)	7,596
Total Paint Removed From Surface (mg/ft ² disturbed)	69,768
Fraction Emitted	0.109

I.8.6. Experiment 48

The geometry of Experiment 48 is shown in Figure I-27, but the exact location of the door during the experiment is unknown. Thus, no regression could be performed and the emission fraction is based on the average loadings. The loadings were divided by the size of the job (40 ft²) and the fraction of lead in the paint (0.078) to estimate the dust loadings per ft² disturbed in Table I-62. Then, the loadings were averaged and multiplied by the area of the room (180 ft²) to get the total mass of dust on the floor, as shown in Table I-63. The estimated paint density using the lead fraction was 1.81 g/cm³. The building was built in 1910, thus, it was assumed to have 5.3 layers of paint at the time of the job. The experiment notes indicated that all paint was removed during the renovation, so all 5.3 layers were assumed to be removed. These values were used to estimate the total amount of paint on the wall, giving a final emission fraction of 0.039.

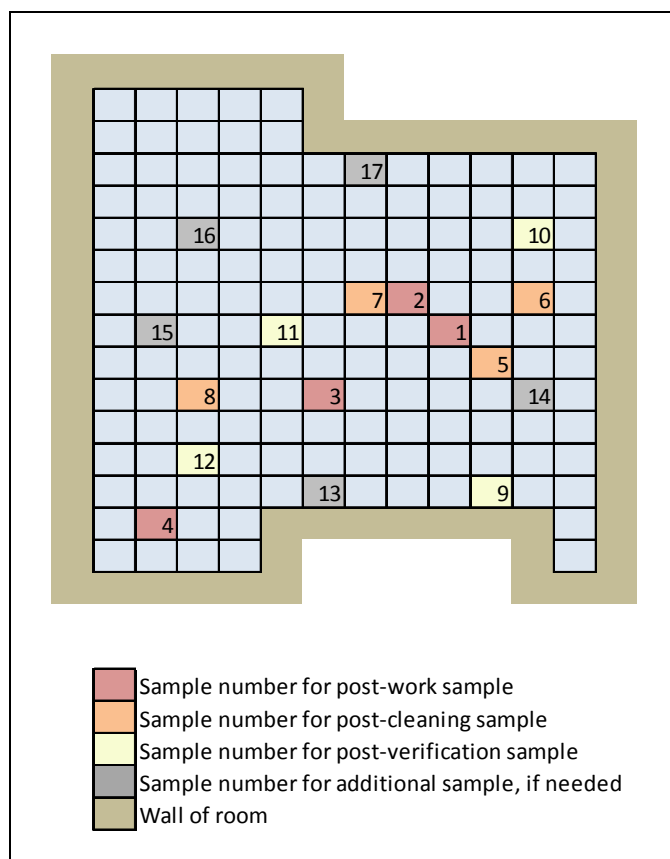


Figure I-27. Layout of Door Plane Experiment 48

Table I-62. Post-Work Loading Measurements and Adjustments in Experiment 48

ID	Lead Loading in $\mu\text{g}/\text{ft}^2$ (Dust Study)	Dust Load per ft^2 Disturbed (mg/ft^2 floor/ ft^2 wall)
1	81,228	26.03
2	57,536	18.44
3	68,305	21.89
4	38,101	30.53

Table I-63. Estimated Total Dust Emitted, Total Paint on Wall, and Emission Fraction in Experiment 48

Estimated Masses and Emission Fractions	Value
Total Mass of Dust on Floor (mg/ft ² disturbed)	3,536
Total Paint Removed From Surface (mg/ft ² disturbed)	89,821
Fraction Emitted	0.039

I.8.7. Experiment 73

The geometry of Experiment 73 is shown in Figure I-28, but the exact location of the door during the experiment is unknown. Thus, no regression could be performed and the emission fraction is based on the average loadings. The loadings were divided by the size of the job (31 ft²) and the fraction of lead in the paint (0.012) to estimate the dust loadings per ft² disturbed in Table I-64. Then, the loadings were averaged and multiplied by the area of the room (115 ft²) to get the total mass of dust on the floor, as shown in Table I-65. The estimated paint density using the lead fraction was 1.12 g/cm³. The building was built in 1900, thus, it was assumed to have 6.2 layers of paint at the time of the job. The experiment notes indicated that all paint was removed during the renovation, so all 6.2 layers were assumed to be removed. These values were used to estimate the total amount of paint on the wall, giving a final emission fraction of 0.107.

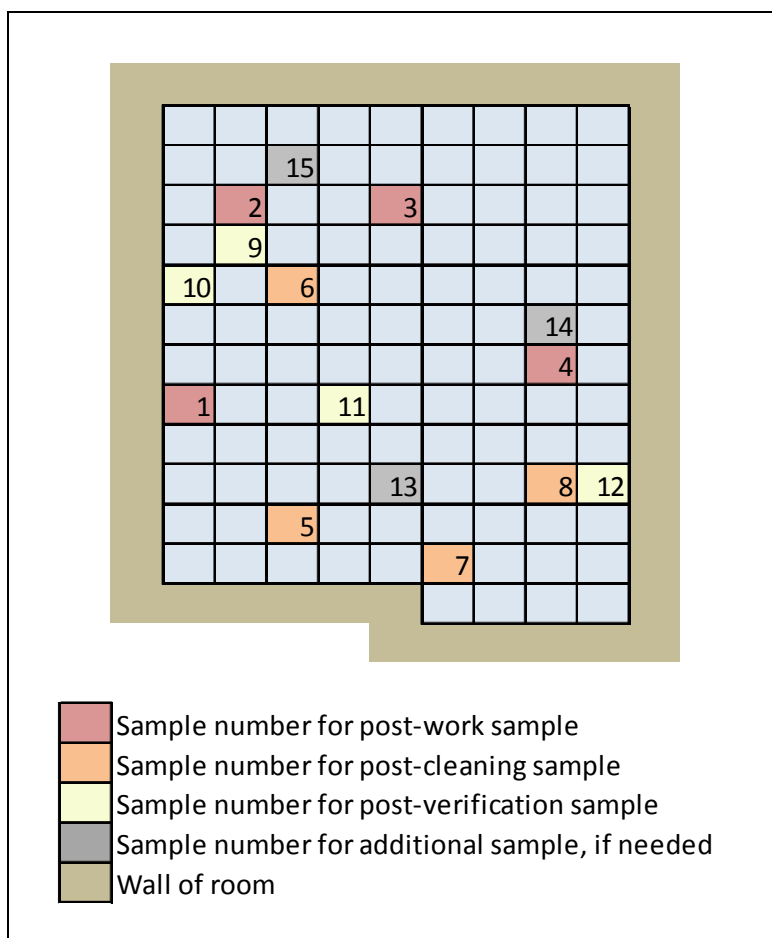


Figure I-28. Layout of Door Plane Experiment 73

Table I-64. Post-Work Loading Measurements and Adjustments in Experiment 73

ID	Lead Loading in $\mu\text{g}/\text{ft}^2$ (Dust Study)	Dust Load per ft^2 Disturbed (mg/ft^2 floor/ ft^2 wall)
1	16,511	44.38
2	29,248	78.62
3	17,936	48.21
4	27,380	73.60

Table I-65. Estimated Total Dust Emitted, Total Paint on Wall, and Emission Fraction in Experiment 73

Estimated Masses and Emission Fractions	Value
Total Mass of Dust on Floor (mg/ft ² disturbed)	7,039
Total Paint Removed From Surface (mg/ft ² disturbed)	65,697
Fraction Emitted	0.117

I.8.8. Experiment 74

The geometry of Experiment 74 is shown in Figure I-29, but the exact location of the door during the experiment is unknown. Thus, no regression could be performed and the emission fraction is based on the average loadings. The loadings were divided by the size of the job (26 ft²) and the fraction of lead in the paint (0.032) to estimate the dust loadings per ft² disturbed in Table I-66. Then, the loadings were averaged and multiplied by the area of the room (115 ft²) to get the total mass of dust on the floor, as shown in Table I-67. The estimated paint density using the lead fraction was 1.33 g/cm³. The building was built in 1900, thus, it was assumed to have 6.2 layers of paint at the time of the job. The experiment notes indicated that all paint was removed during the renovation, so all 6.2 layers were assumed to be removed. These values were used to estimate the total amount of paint on the wall, giving a final emission fraction of 0.040.

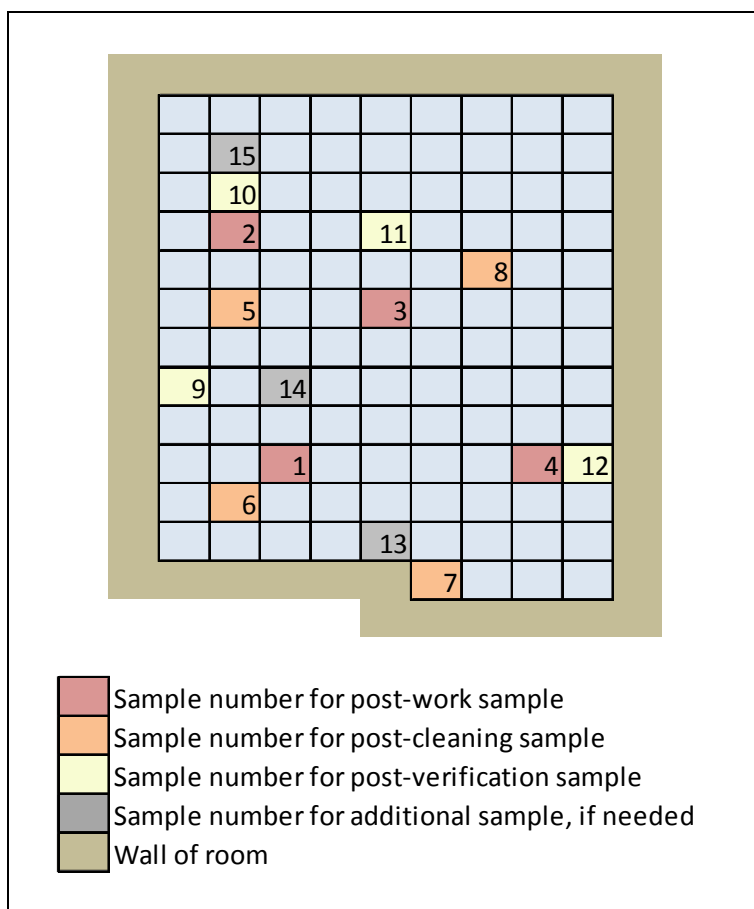


Figure I-29. Layout of Door Plane Experiment 74

Table I-66. Post-Work Loading Measurements and Adjustments in Experiment 74

ID	Lead Loading in $\mu\text{g}/\text{ft}^2$ (Dust Study)	Dust Load per ft^2 Disturbed (mg/ft^2 floor/ ft^2 wall)
1	17,982	21.61
2	26,293	31.60
3	13,378	16.08
4	33,363	40.10

Table I-67. Estimated Total Dust Emitted, Total Paint on Wall, and Emission Fraction in Experiment 74

Estimated Masses and Emission Fractions	Value
Total Mass of Dust on Floor (mg/ft ² disturbed)	3,145
Total Paint Removed From Surface (mg/ft ² disturbed)	77,785
Fraction Emitted	0.040

I.9. Dry Scrape

I.9.1. Experiment 5

The geometry of Experiment 5 is shown in Figure I-30, and the measured lead loadings and associated distances are shown in Table I-68. No adjustments were made to the loadings since all samples were within the width of the job. The loadings were divided by the size of the job (90 ft²) and the fraction of lead in the paint (0.016) to estimate the dust loadings per ft² disturbed in Table I-68. Then, the natural logs of all loadings were used with the distances to estimate the regression parameters in Table I-69. Here, *intercept* is the intercept of the linear regression in log space, and Load at 0 ft is the assumed loading at 0 ft calculated as $\exp(\textit{intercept})$.

The integral was performed over the regression equation out to a distance of 13 ft, (the length of the room), and the total mass of dust on the floor was estimated as shown in Table I-70. The estimated paint density using the lead fraction was 1.17 g/cm³. Although the vintage of the renovated building was unknown, nearby buildings were believed to have been built at the same time and were built in 1920. Therefore, the building was assumed to have been built in 1920 and to have 5.0 layers of paint at the time of the job. The experiment notes indicated that all paint was removed during the renovation, so all 5.0 layers were assumed to be removed. These values were used to estimate the total amount of paint on the wall, giving a final emission fraction of 0.003.

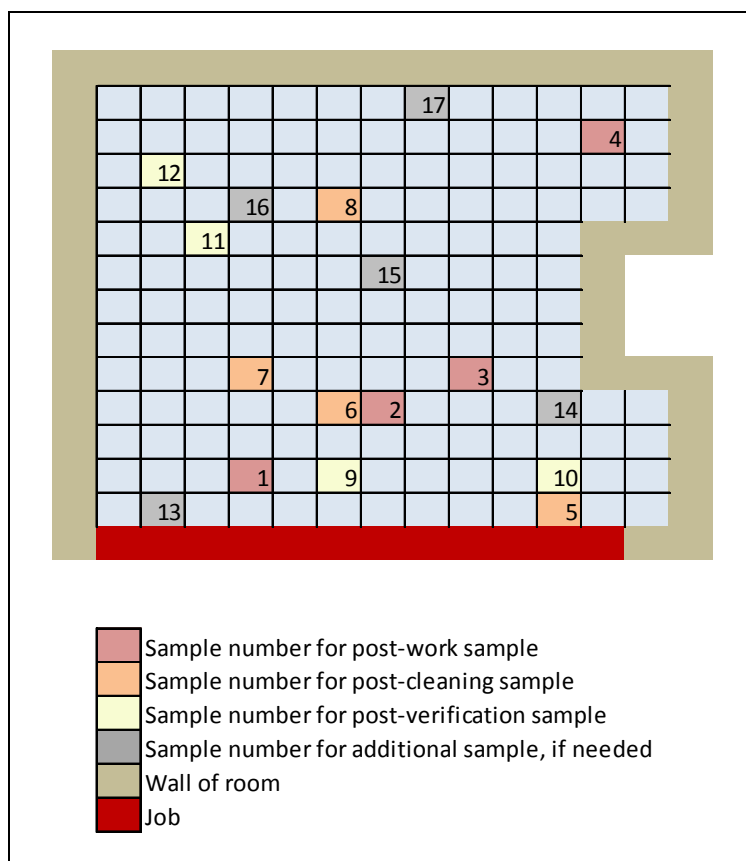


Figure I-30. Layout of Dry Scrap Experiment 5

Table I-68. Post-Work Loading Measurements and Adjustments in Experiment 5

ID	Dist. From Wall (ft)	Lead Loading in $\mu\text{g}/\text{ft}^2$ (Dust Study)	Dust Load per ft^2 Disturbed (mg/ft^2 floor/ ft^2 wall)
1	2	3,067	2.13
2	4	1,289	0.90
3	5	1,122	0.78
4	12	1,289	0.90

Table I-69. Regression Statistics in Experiment 5

Statistic	Value
Shape	-0.06
Intercept	0.39
R ²	0.27
Load at 0 ft (mg/ft ² floor/ft ² disturbed)	1.48

Table I-70. Estimated Total Dust Emitted, Total Paint on Wall, and Emission Fraction in Experiment 5

Estimated Masses and Emission Fractions	Value
Total Mass of Dust on Floor (mg/ft ² disturbed)	178
Total Paint Removed From Surface (mg/ft ² disturbed)	57,943
Fraction Emitted	0.003

I.9.2. Experiment 6

The geometry of Experiment 6 is shown in Figure I-31, and, the measured lead loadings and associated distances are shown in Table I-71. No adjustments were made to the loadings since all samples were within the width of the job. The loadings were divided by the size of the job (90 ft²) and the fraction of lead in the paint (0.027) to estimate the dust loadings per ft² disturbed in Table I-71. Then, the natural logs of all loadings were used with the distances to estimate the regression parameters in Table I-72. Here, *intercept* is the intercept of the linear regression in log space, and Load at 0 ft is the assumed loading at 0 ft calculated as $\exp(\textit{intercept})$.

The integral was performed over the regression equation out to a distance of 13 ft, (the length of the room), and the total mass of dust on the floor was estimated as shown in Table I-73. The estimated paint density using the lead fraction was 1.28 g/cm³. Although the vintage of the renovated building was unknown, nearby buildings were believed to have been built at the same time and were built in 1920. Therefore, the building was assumed to have been built in 1920 and to have 5.0 layers of paint at the time of the job. The experiment notes indicated that not all paint was removed during the renovation, so it was assumed that only 15% of the paint (or .8 layers) were removed. These values were used to estimate the total amount of paint on the wall, giving a final emission fraction of 0.032.

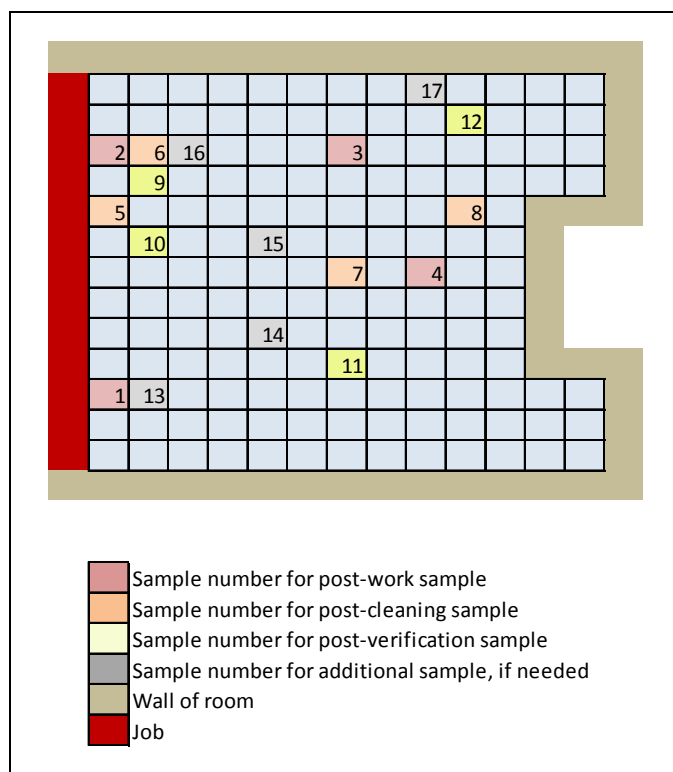


Figure I-31. Layout of Dry Scrap Experiment 6

Table I-71. Post-Work Loading Measurements and Adjustments in Experiment 6

ID	Dist. From Wall (ft)	Lead Loading in $\mu\text{g}/\text{ft}^2$ (Dust Study)	Dust Load per ft^2 Disturbed (mg/ft^2 floor/ ft^2 wall)
1	1	7,357	3.03
2	1	4,158	1.71
3	7	2,886	1.19
4	9	5,358	2.20

Table I-72. Regression Statistics in Experiment 6

Statistic	Value
Shape	-0.03
Intercept	0.81
R^2	0.13
Load at 0 ft (mg/ft^2 floor/ ft^2 disturbed)	2.24

Table I-73. Estimated Total Dust Emitted, Total Paint on Wall, and Emission Fraction in Experiment 6

Estimated Masses and Emission Fractions	Value
Total Mass of Dust on Floor (mg/ft ² disturbed)	305
Total Paint Removed From Surface (mg/ft ² disturbed)	9,540
Fraction Emitted	0.032

I.9.3. Experiment 7

The geometry of Experiment 7 is shown in Figure I-32, and the measured lead loadings and associated distances are shown in Table I-74. No adjustments were made to the loadings since all samples were within the width of the job. The loadings were divided by the size of the job (70 ft²) and the fraction of lead in the paint (0.017) to estimate the dust loadings per ft² disturbed in Table I-74. Then, the natural logs of all loadings were used with the distances to estimate the regression parameters in Table I-75. Here, *intercept* is the intercept of the linear regression in log space, and Load at 0 ft is the assumed loading at 0 ft calculated as $\exp(\textit{intercept})$.

The integral was performed over the regression equation out to a distance of 13 ft, (the length of the room), and the total mass of dust on the floor was estimated as shown in Table I-76. The estimated paint density using the lead fraction was 1.18 g/cm³. Although the vintage of the renovated building was unknown, nearby buildings were believed to have been built at the same time and were built in 1920. Therefore, the building was assumed to have been built in 1920 and to have 5.0 layers of paint at the time of the job. The experiment notes indicated that not all paint was removed during the renovation, so it was assumed that only 15% of the paint (or .8 layers) were removed. These values were used to estimate the total amount of paint on the wall, giving a final emission fraction of 0.062.

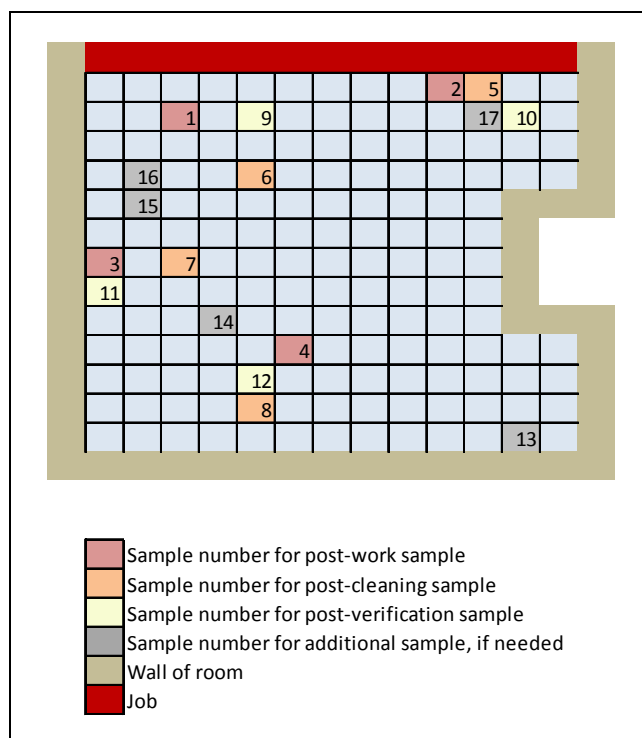


Figure I-32. Layout of Dry Scrap Experiment 7

Table I-74. Post-Work Loading Measurements and Adjustments in Experiment 7

ID	Dist. From Wall (ft)	Lead Loading in $\mu\text{g}/\text{ft}^2$ (Dust Study)	Dust Load per ft^2 Disturbed (mg/ft^2 floor/ ft^2 wall)
1	2	15,427	12.96
2	1	5,949	5.00
3	7	3,146	2.64
4	10	256	0.21

Table I-75. Regression Statistics in Experiment 7

Statistic	Value
Shape	-0.37
Intercept	2.74
R^2	0.79
Load at 0 ft (mg/ft^2 floor/ ft^2 disturbed)	15.50

Table I-76. Estimated Total Dust Emitted, Total Paint on Wall, and Emission Fraction in Experiment 7

Estimated Masses and Emission Fractions	Value
Total Mass of Dust on Floor (mg/ft ² disturbed)	543
Total Paint Removed From Surface (mg/ft ² disturbed)	8,768
Fraction Emitted	0.062

I.9.4. Experiment 8

The geometry of Experiment 8 is shown in Figure I-33, and the measured lead loadings and associated distances are shown in Table I-77. No adjustments were made to the loadings since all samples were within the width of the job. The loadings were divided by the size of the job (110 ft²) and the fraction of lead in the paint (0.017) to estimate the dust loadings per ft² disturbed in Table I-77. Then, the natural logs of all loadings were used with the distances to estimate the regression parameters in Table I-78. Here, *intercept* is the intercept of the linear regression in log space, and Load at 0 ft is the assumed loading at 0 ft calculated as $\exp(\text{intercept})$.

The integral was performed over the regression equation out to a distance of 13 ft, (the length of the room), and the total mass of dust on the floor was estimated as shown in Table I-79. The estimated paint density using the lead fraction was 1.18 g/cm³. Although the vintage of the renovated building was unknown, nearby buildings were believed to have been built at the same time and were built in 1920. Therefore, the building was assumed to have been built in 1920 and to have 5.0 layers of paint at the time of the job. The experiment notes indicated that not all paint was removed during the renovation, so it was assumed that only 15% of the paint (or .8 layers) were removed. These values were used to estimate the total amount of paint on the wall, giving a final emission fraction of 0.059.

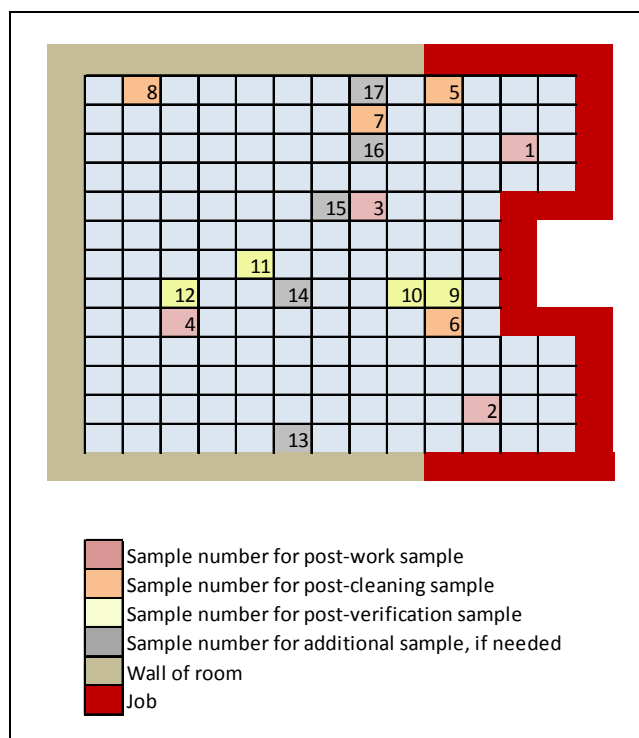


Figure I-33. Layout of Dry Scrap Experiment 8

Table I-77. Post-Work Loading Measurements and Adjustments in Experiment 8

ID	Dist. From Wall (ft)	Lead Loading in $\mu\text{g}/\text{ft}^2$ (Dust Study)	Dust Load per ft^2 Disturbed (mg/ft^2 floor/ ft^2 wall)
1	2	5,710	3.05
2	2	4,886	2.61
3	4	48,440	25.90
4	9	69	0.04

Table I-78. Regression Statistics in Experiment 8

Statistic	Value
Shape	-0.65
Intercept	3.25
R^2	0.60
Load at 0 ft (mg/ft^2 floor/ ft^2 disturbed)	25.86

Table I-79. Estimated Total Dust Emitted, Total Paint on Wall, and Emission Fraction in Experiment 8

Estimated Masses and Emission Fractions	Value
Total Mass of Dust on Floor (mg/ft ² disturbed)	521
Total Paint Removed From Surface (mg/ft ² disturbed)	8,768
Fraction Emitted	0.059

I.9.5. Experiment 26

The geometry of Experiment 26 is shown in Figure I-34, and the measured lead loadings and associated distances are shown in Table I-80. Sample 3 was adjusted using the taper assumption since it was outside the lateral extent of the job. The loadings were divided by the size of the job (60 ft²) and the fraction of lead in the paint (0.021) to estimate the dust loadings per ft² disturbed in Table I-80. Then, the natural logs of all loadings were used with the distances to estimate the regression parameters in Table I-81. Here, *intercept* is the intercept of the linear regression in log space, and Load at 0 ft is the assumed loading at 0 ft calculated as $\exp(\text{intercept})$.

The integral was performed over the regression equation out to a distance of 12 ft, (the length of the room), and the total mass of dust on the floor was estimated as shown in Table I-82. The estimated paint density using the lead fraction was 1.22 g/cm³. Although the vintage of the renovated building was unknown, nearby buildings were believed to have been built at the same time and were built in 1920. Therefore, the building was assumed to have been built in 1920 and to have 5.0 layers of paint at the time of the job. The experiment notes indicated that not all paint was removed during the renovation, so it was assumed that only 15% of the paint (or .8 layers) were removed. These values were used to estimate the total amount of paint on the wall, giving a final emission fraction of 0.048.

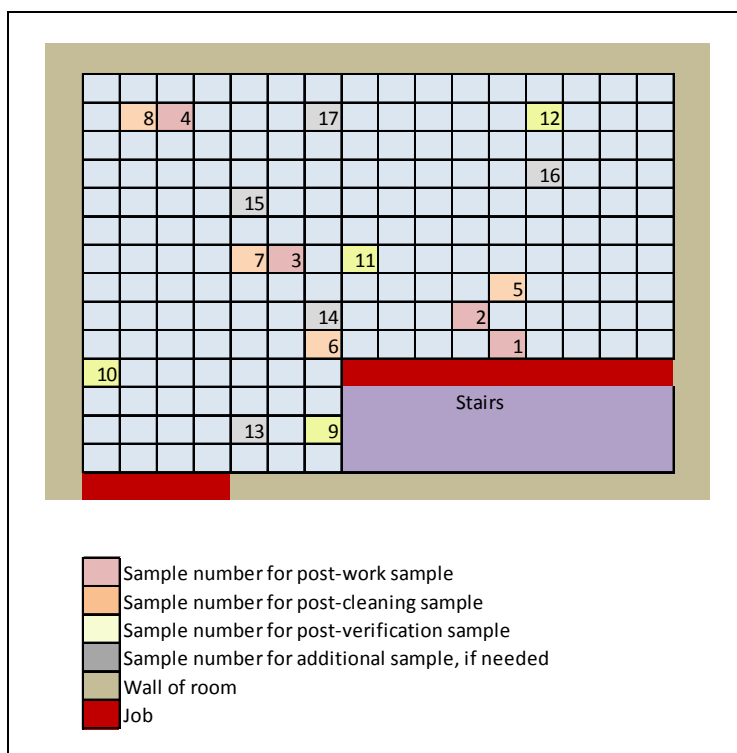


Figure I-34. Layout of Dry Scrap Experiment 26

Table I-80. Post-Work Loading Measurements and Adjustments in Experiment 26

ID	Dist. From Wall (ft)	Lead Loading in $\mu\text{g}/\text{ft}^2$ (Dust Study)	Lead Loading in $\mu\text{g}/\text{ft}^2$ (adjusted)	Dust Load per ft^2 Disturbed (mg/ft^2 floor/ ft^2 wall)
1	1	2,623	2,623	2.08
2	2	4,668	4,668	3.71
3	4	2,254	3,006	2.39
4	13	2,033	2,033	1.61

Table I-81. Regression Statistics in Experiment 26

Statistic	Value
Shape	-0.04
Intercept	1.06
R^2	0.47
Load at 0 ft (mg/ft^2 floor/ ft^2 disturbed)	2.90

Table I-82. Estimated Total Dust Emitted, Total Paint on Wall, and Emission Fraction in Experiment 26

Estimated Masses and Emission Fractions	Value
Total Mass of Dust on Floor (mg/ft ² disturbed)	434
Total Paint Removed From Surface (mg/ft ² disturbed)	9,077
Fraction Emitted	0.049

I.9.6. Experiment 27

The geometry of Experiment 27 is shown in Figure I-35, and the measured lead loadings and associated distances are shown in Table I-83. No adjustments were made to the loadings since all samples were within the width of the job. The loadings were divided by the size of the job (64 ft²) and the fraction of lead in the paint (0.025) to estimate the dust loadings per ft² disturbed in Table I-83. Then, the natural logs of all loadings were used with the distances to estimate the regression parameters in Table I-84. Here, *intercept* is the intercept of the linear regression in log space, and Load at 0 ft is the assumed loading at 0 ft calculated as $\exp(\textit{intercept})$.

The integral was performed over the regression equation out to a distance of 16 ft, (the length of the room), and the total mass of dust on the floor was estimated as shown in Table I-85. The estimated paint density using the lead fraction was 1.26 g/cm³. Although the vintage of the renovated building was unknown, nearby buildings were believed to have been built at the same time and were built in 1920. Therefore, the building was assumed to have been built in 1920 and to have 5.0 layers of paint at the time of the job. The experiment notes indicated that not all paint was removed during the renovation, so it was assumed that only 15% of the paint (or .8 layers) were removed. These values were used to estimate the total amount of paint on the wall, giving a final emission fraction of 0.021.

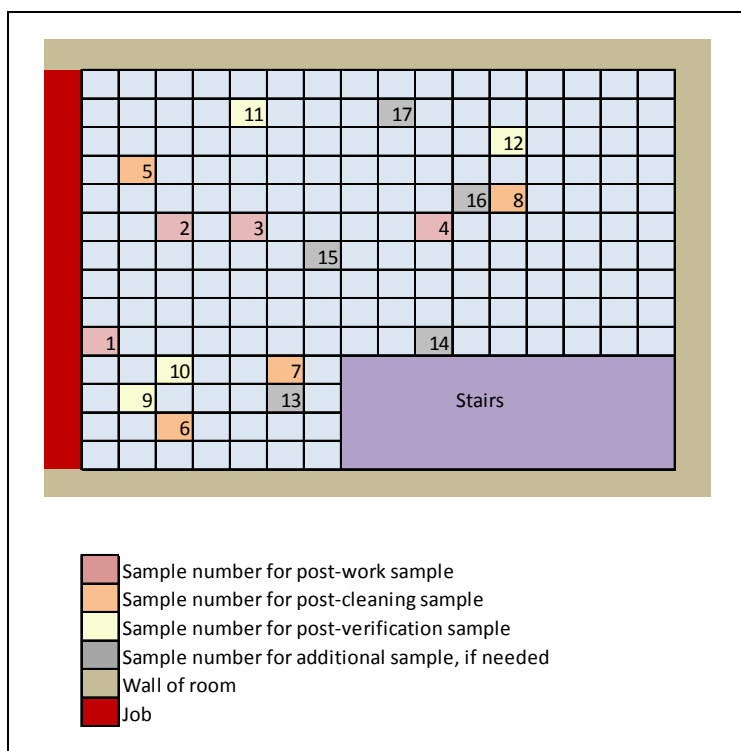


Figure I-35. Layout of Dry Scrap Experiment 27

Table I-83. Post-Work Loading Measurements and Adjustments in Experiment 27

ID	Dist. From Wall (ft)	Lead Loading in $\mu\text{g}/\text{ft}^2$ (Dust Study)	Dust Load per ft^2 Disturbed (mg/ft^2 floor/ ft^2 wall)
1	1	14,503	9.06
2	3	1,105	0.69
3	5	1,389	0.87
4	10	107	0.07

Table I-84. Regression Statistics in Experiment 27

Statistic	Value
Shape	-0.49
Intercept	2.07
R^2	0.88
Load at 0 ft (mg/ft^2 floor/ ft^2 disturbed)	7.90

Table I-85. Estimated Total Dust Emitted, Total Paint on Wall, and Emission Fraction in Experiment 27

Estimated Masses and Emission Fractions	Value
Total Mass of Dust on Floor (mg/ft ² disturbed)	194
Total Paint Removed From Surface (mg/ft ² disturbed)	9,385
Fraction Emitted	0.02

I.9.7. Experiment 28

The geometry of Experiment 28 is shown in Figure I-36, and the measured lead loadings and associated distances are shown in Table I-86. No adjustments were made to the loadings since all samples were within the width of the job. The loadings were divided by the size of the job (65 ft²) and the fraction of lead in the paint (0.025) to estimate the dust loadings per ft² disturbed in Table I-86. Then, the natural logs of all loadings were used with the distances to estimate the regression parameters in Table I-87. Here, *intercept* is the intercept of the linear regression in log space, and Load at 0 ft is the assumed loading at 0 ft calculated as $\exp(\text{intercept})$.

The integral was performed over the regression equation out to a distance of 12 ft, (the length of the room), and the total mass of dust on the floor was estimated as shown in Table I-88. The estimated paint density using the lead fraction was 1.26 g/cm³. Although the vintage of the renovated building was unknown, nearby buildings were believed to have been built at the same time and were built in 1920. Therefore, the building was assumed to have been built in 1920 and to have 5.0 layers of paint at the time of the job. The experiment notes indicated that not all paint was removed during the renovation, so it was assumed that only 15% of the paint (or .8 layers) were removed. These values were used to estimate the total amount of paint on the wall, giving a final emission fraction of 0.215.

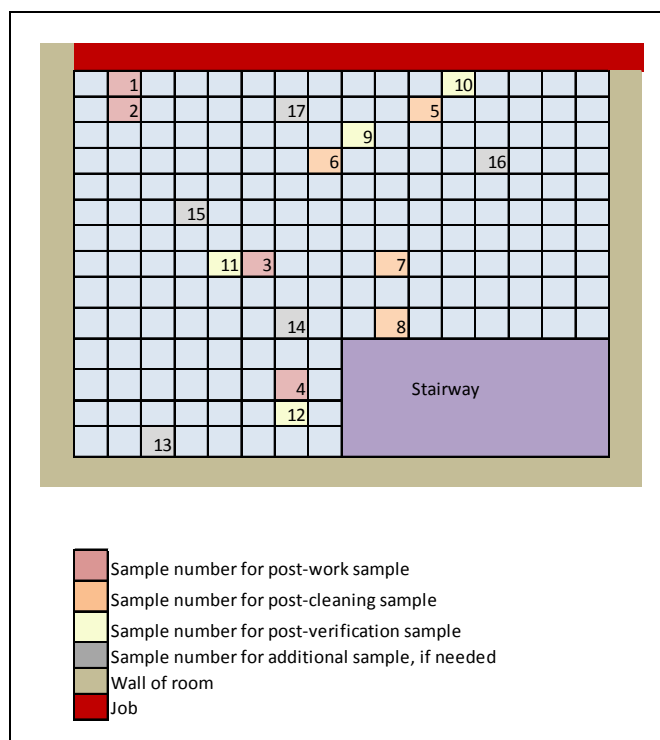


Figure I-36. Layout of Dry Scrap Experiment 28

Table I-86. Post-Work Loading Measurements and Adjustments in Experiment 28

ID	Dist. From Wall (ft)	Lead Loading in $\mu\text{g}/\text{ft}^2$ (Dust Study)	Dust Load per ft^2 Disturbed (mg/ft^2 floor/ ft^2 wall)
1	1	44,197	27.20
2	2	43,302	26.65
3	8	4,241	2.61
4	12	458	0.28

Table I-87. Regression Statistics in Experiment 28

Statistic	Value
Shape	-0.42
Intercept	3.97
R^2	0.98
Load at 0 ft (mg/ft^2 floor/ ft^2 disturbed)	53.16

Table I-88. Estimated Total Dust Emitted, Total Paint on Wall, and Emission Fraction in Experiment 28

Estimated Masses and Emission Fractions	Value
Total Mass of Dust on Floor (mg/ft ² disturbed)	2,021
Total Paint Removed From Surface (mg/ft ² disturbed)	9,385
Fraction Emitted	0.215

I.9.8. Experiment 29

The geometry of Experiment 29 is shown in Figure I-37, and the measured lead loadings and associated distances are shown in Table I-89. Sample 4 was adjusted using the taper assumption since it was outside the lateral extent of the job. The loadings were divided by the size of the job (72 ft²) and the fraction of lead in the paint (0.026) to estimate the dust loadings per ft² disturbed in Table I-89. Then, the natural logs of all loadings were used with the distances to estimate the regression parameters in Table I-90. Here, *intercept* is the intercept of the linear regression in log space, and Load at 0 ft is the assumed loading at 0 ft calculated as $\exp(\text{intercept})$.

The integral was performed over the regression equation out to a distance of 16 ft, (the length of the room), and the total mass of dust on the floor was estimated as shown in Table I-91. The estimated paint density using the lead fraction was 1.27 g/cm³. Although the vintage of the renovated building was unknown, nearby buildings were believed to have been built at the same time and were built in 1920. Therefore, the building was assumed to have been built in 1920 and to have 5.0 layers of paint at the time of the job. The experiment notes indicated that not all paint was removed during the renovation, so it was assumed that only 15% of the paint (or .8 layers) were removed. These values were used to estimate the total amount of paint on the wall, giving a final emission fraction of 0.028.

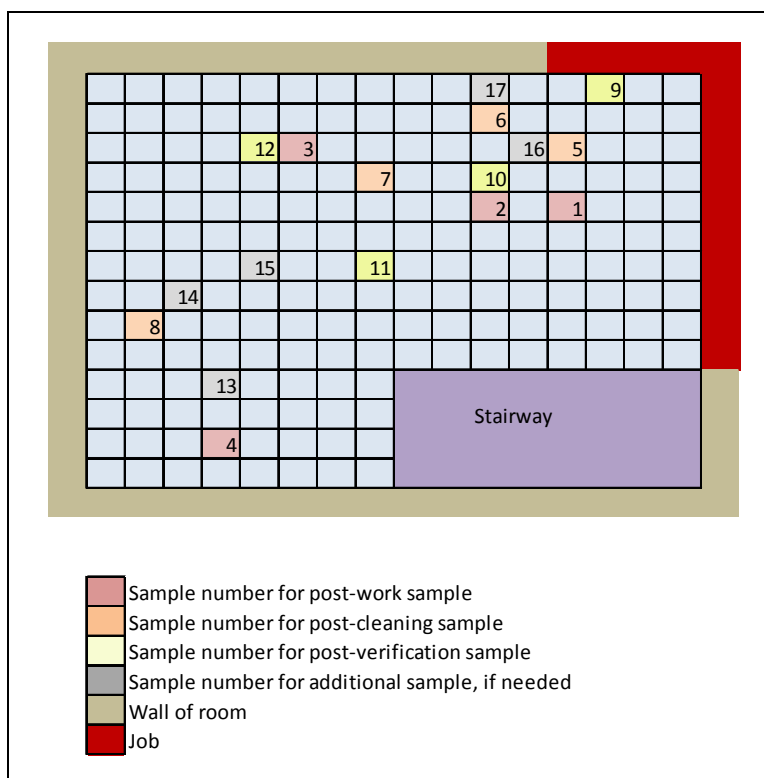


Figure I-37. Layout of Dry Scrap Experiment 29

Table I-89. Post-Work Loading Measurements and Adjustments in Experiment 29

ID	Dist. From Wall (ft)	Lead Loading in $\mu\text{g}/\text{ft}^2$ (Dust Study)	Lead Loading in $\mu\text{g}/\text{ft}^2$ (adjusted)	Dust Load per ft^2 Disturbed (mg/ft^2 floor/ ft^2 wall)
1	4	3,989	3,989	2.13
2	6	2,410	2,410	1.29
3	11	1,575	1,575	0.84
4	13	386	965	0.52

Table I-90. Regression Statistics in Experiment 29

Statistic	Value
Shape	-0.14
Intercept	1.24
R ²	0.95

Load at 0 ft (mg/ft ² floor/ft ² disturbed)	3.45
---	------

Table I-91. Estimated Total Dust Emitted, Total Paint on Wall, and Emission Fraction in Experiment 29

Estimated Masses and Emission Fractions	Value
Total Mass of Dust on Floor (mg/ft ² disturbed)	263
Total Paint Removed From Surface (mg/ft ² disturbed)	9,463
Fraction Emitted	0.028

I.10. Kitchen Gut

I.10.1. Experiment 49

The geometry of Experiment 5 is shown in Figure I-30, but the exact location of the removed kitchen components is unknown. Thus, no regression could be performed and the emission fraction is based on the average loadings. The loadings were divided by the size of the job (55 ft²) and the fraction of lead in the paint (0.017) to estimate the dust loadings per ft² disturbed in Table I-92. Then, the loadings were averaged and multiplied by the area of the room (80 ft²) to get the total mass of dust on the floor, as shown in Table I-93. The estimated paint density using the lead fraction was 1.18 g/cm³. Although the vintage of the renovated building was unknown, nearby buildings were believed to have been built at the same time and were built in 1920. Therefore, the building was assumed to have been built in 1920 and to have 5.0 layers of paint at the time of the job. The experiment notes indicated that all paint was removed during the renovation, so all 5.0 layers were assumed to be removed. These values were used to estimate the total amount of paint on the wall, giving a final emission fraction of 0.008.

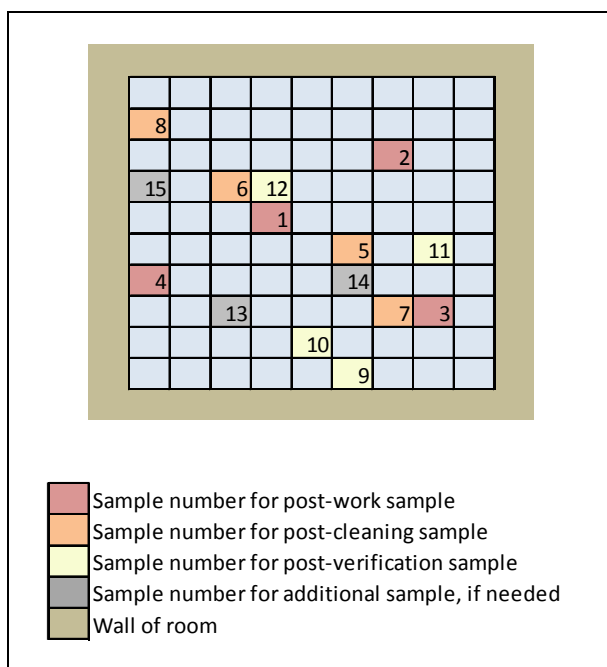


Figure I-38. Layout of Kitchen Gut Experiment 49

Table I-92. Post-Work Loading Measurements and Adjustments in Experiment 49

ID	Lead Loading in $\mu\text{g}/\text{ft}^2$ (Dust Study)	Dust Load per ft^2 Disturbed (mg/ft^2 floor/ ft^2 wall)
1	4,010	4.29
2	2,291	2.45
3	14,229	15.22
4	1,433	1.53

Table I-93. Estimated Total Dust Emitted, Total Paint on Wall, and Emission Fraction in Experiment 49

Estimated Masses and Emission Fractions	Value
Total Mass of Dust on Floor (mg/ft^2 disturbed)	470
Total Paint Removed From Surface (mg/ft^2 disturbed)	58,457
Fraction Emitted	0.008

I.10.2. Experiment 50

The geometry of Experiment 50 is shown in Figure I-39, but the exact location of the removed kitchen components is unknown. Thus, no regression could be performed and the emission fraction is based on the average loadings. The loadings were divided by the size of the job (40 ft²) and the fraction of lead in the paint (0.023) to estimate the dust loadings per ft² disturbed in Table I-94. Then, the loadings were averaged and multiplied by the area of the room (80 ft²) to get the total mass of dust on the floor, as shown in Table I-95. The estimated paint density using the lead fraction was 1.24 g/cm³. Although the vintage of the renovated building was unknown, nearby buildings were believed to have been built at the same time and were built in 1920. Therefore, the building was assumed to have been built in 1920 and to have 5.0 layers of paint at the time of the job. The experiment notes indicated that all paint was removed during the renovation, so all 5.0 layers were assumed to be removed. These values were used to estimate the total amount of paint on the wall, giving a final emission fraction of 0.006.

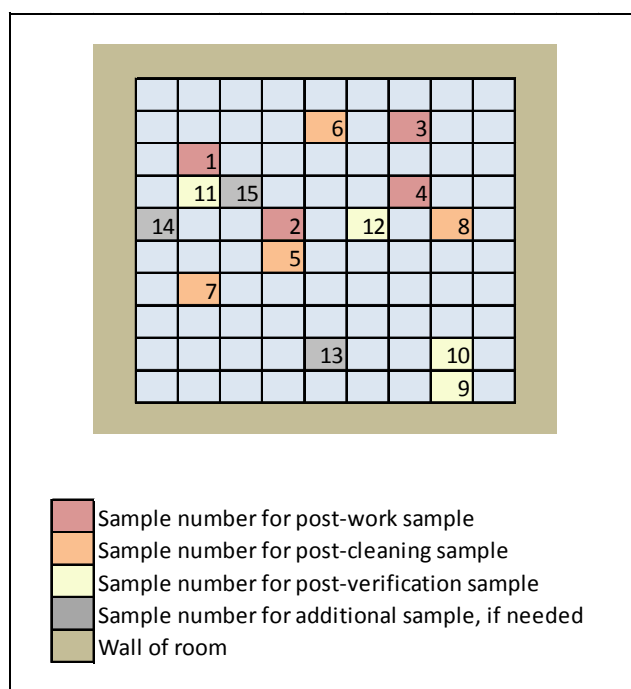


Figure I-39. Layout of Kitchen Gut Experiment 50

Table I-94. Post-Work Loading Measurements and Adjustments in Experiment 50

ID	Lead Loading in $\mu\text{g}/\text{ft}^2$ (Dust Study)	Dust Load per ft^2 Disturbed (mg/ft^2 floor/ ft^2 wall)
1	162	0.18
2	1,414	1.54
3	14,560	15.83
4	481	0.52

Table I-95. Estimated Total Dust Emitted, Total Paint on Wall, and Emission Fraction in Experiment 50

Estimated Masses and Emission Fractions	Value
Total Mass of Dust on Floor (mg/ft^2 disturbed)	361
Total Paint Removed From Surface (mg/ft^2 disturbed)	61,542
Fraction Emitted	0.006

I.10.3. Experiment 51

The geometry of Experiment 51 is shown in Figure I-40, but the exact location of the removed kitchen components is unknown. Thus, no regression could be performed and the emission fraction is based on the average loadings. The loadings were divided by the size of the job (66 ft^2) and the fraction of lead in the paint (0.035) to estimate the dust loadings per ft^2 disturbed in Table I-96. Then, the loadings were averaged and multiplied by the area of the room (80 ft^2) to get the total mass of dust on the floor, as shown in Table I-97. The estimated paint density using the lead fraction was $1.36 \text{ g}/\text{cm}^3$. Although the vintage of the renovated building was unknown, nearby buildings were believed to have been built at the same time and were built in 1920. Therefore, the building was assumed to have been built in 1920 and to have 5.0 layers of paint at the time of the job. The experiment notes indicated that all paint was removed during the renovation, so all 5.0 layers were assumed to be removed. These values were used to estimate the total amount of paint on the wall, giving a final emission fraction of 0.001.

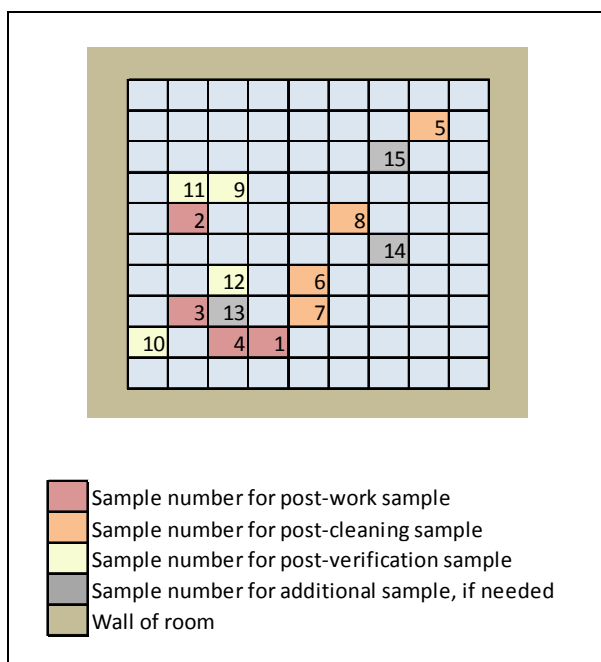


Figure I-40. Layout of Kitchen Gut Experiment 51

Table I-96. Post-Work Loading Measurements and Adjustments in Experiment 51

ID	Lead Loading in $\mu\text{g}/\text{ft}^2$ (Dust Study)	Dust Load per ft^2 Disturbed (mg/ft^2 floor/ ft^2 wall)
1	1,896	0.82
2	481	0.21
3	3,139	1.36
4	2,624	1.14

Table I-97. Estimated Total Dust Emitted, Total Paint on Wall, and Emission Fraction in Experiment 51

Estimated Masses and Emission Fractions	Value
Total Mass of Dust on Floor (mg/ft^2 disturbed)	70
Total Paint Removed From Surface (mg/ft^2 disturbed)	67,712
Fraction Emitted	0.001

I.10.4. Experiment 76

The geometry of Experiment 76 is shown in Figure I-41, but the exact location of the removed kitchen components is unknown. Thus, no regression could be performed and the emission fraction is based on the average loadings. The loadings were divided by the size of the job (60 ft²) and the fraction of lead in the paint (0.016) to estimate the dust loadings per ft² disturbed in Table I-98. Then, the loadings were averaged and multiplied by the area of the room (80 ft²) to get the total mass of dust on the floor, as shown in Table I-99. The estimated paint density using the lead fraction was 1.17 g/cm³. Although the vintage of the renovated building was unknown, nearby buildings were believed to have been built at the same time and were built in 1920. Therefore, the building was assumed to have been built in 1920 and to have 5.0 layers of paint at the time of the job. The experiment notes indicated that all paint was removed during the renovation, so all 5.0 layers were assumed to be removed. These values were used to estimate the total amount of paint on the wall, giving a final emission fraction of 0.018.

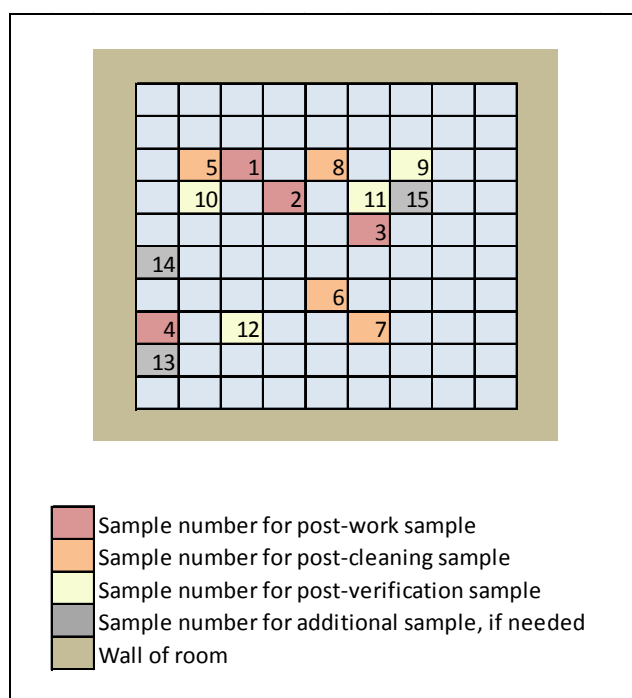


Figure I-41. Layout of Kitchen Gut Experiment 76

Table I-98. Post-Work Loading Measurements and Adjustments in Experiment 76

ID	Lead Loading in $\mu\text{g}/\text{ft}^2$ (Dust Study)	Dust Load per ft^2 Disturbed (mg/ft^2 floor/ ft^2 wall)
1	10.171	10.59
2	137	0.14
3	16,409	17.09
4	20,074	20.91

Table I-99. Estimated Total Dust Emitted, Total Paint on Wall, and Emission Fraction in Experiment 76

Estimated Masses and Emission Fractions	Value
Total Mass of Dust on Floor (mg/ft^2 disturbed)	975
Total Paint Removed From Surface (mg/ft^2 disturbed)	55,183
Fraction Emitted	0.02

I.10.5. Experiment 67

The geometry of Experiment 67 is shown in Figure I-42, and the measured lead loadings and associated distances are shown in Table I-100. Sample 2 was adjusted using the taper assumption since it was outside the lateral extent of the job. The loadings were divided by the size of the job (40 ft^2) and the fraction of lead in the paint (0.012) to estimate the dust loadings per ft^2 disturbed in Table I-100. Then, the natural logs of all loadings were used with the distances to estimate the regression parameters in

Table I-101. Regression Statistics in Experiment 67

. Here, *intercept* is the intercept of the linear regression in log space, and Load at 0 ft is the assumed loading at 0 ft calculated as $\exp(\textit{intercept})$.

The integral was performed over the regression equation out to a distance of 13 ft, (the adjusted approximate length of the room), and the total mass of dust on the floor was estimated as shown in Table I-102. The estimated paint density using the lead fraction was 1.12 g/cm³. Although the vintage of the renovated building was unknown, nearby buildings were believed to have been built at the same time and were built in 1920. Therefore, the building was assumed to have been built in 1920 and to have 5.0 layers of paint at the time of the job. The experiment notes indicated that all paint was removed during the renovation, so all 5.0 layers were assumed to be removed. These values were used to estimate the total amount of paint on the wall, giving a final emission fraction of 0.001.

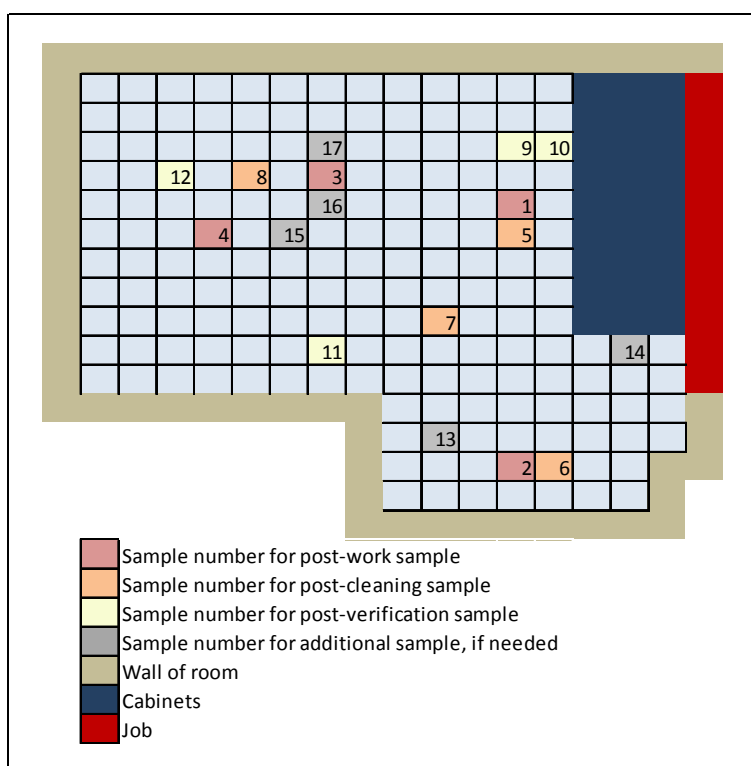


Figure I-42. Layout of Kitchen Gut Experiment 67

Table I-100. Post-Work Loading Measurements and Adjustments in Experiment 67

ID	Dist. From Wall (ft)	Lead Loading in $\mu\text{g}/\text{ft}^2$ (Dust Study)	Lead Loading in $\mu\text{g}/\text{ft}^2$ (adjusted)	Dust Load per ft^2 Disturbed (mg/ft^2 floor/ ft^2 wall)
1	2	474	474	0.99
2	2	162	405	0.84
3	7	10	7	0.01
4	10	10	7	0.01

Table I-101. Regression Statistics in Experiment 67

Statistic	Value
Shape	-0.57
Intercept	0.86
R ²	0.90
Load at 0 ft (mg/ft ² floor/ft ² disturbed)	2.36

Table I-102. Estimated Total Dust Emitted, Total Paint on Wall, and Emission Fraction in Experiment 67

Estimated Masses and Emission Fractions	Value
Total Mass of Dust on Floor (mg/ft ² disturbed)	62
Total Paint Removed From Surface (mg/ft ² disturbed)	55,886
Fraction Emitted	0.001

I.10.6. Experiment 68

The geometry of Experiment 68 is shown in Figure I-43, and the measured lead loadings and associated distances are shown in Table I-103. No adjustments were made to the loadings since all samples were within the width of the job. The loadings were divided by the size of the job (34 ft²) and the fraction of lead in the paint (0.025) to estimate the dust loadings per ft² disturbed in Table I-103. Then, the natural logs of all loadings were used with the distances to estimate the regression parameters in

Table I-104. Regression Statistics in Experiment 68

. Here, *intercept* is the intercept of the linear regression in log space, and Load at 0 ft is the assumed loading at 0 ft calculated as $\exp(\text{intercept})$.

The integral was performed over the regression equation out to a distance of 16 ft, (the length of the room), and the total mass of dust on the floor was estimated as shown in Table I-105. The estimated paint density using the lead fraction was 1.26 g/cm³. Although the vintage of the renovated building was unknown, nearby buildings were believed to have been built at the same time and were built in 1920. Therefore, the building was assumed to have been built in 1920 and to have 5.0 layers of paint at the time of the job. The experiment notes indicated that all paint was removed during the renovation, so all 5.0 layers were assumed to be removed. These values were used to estimate the total amount of paint on the wall, giving a final emission fraction of 0.003.

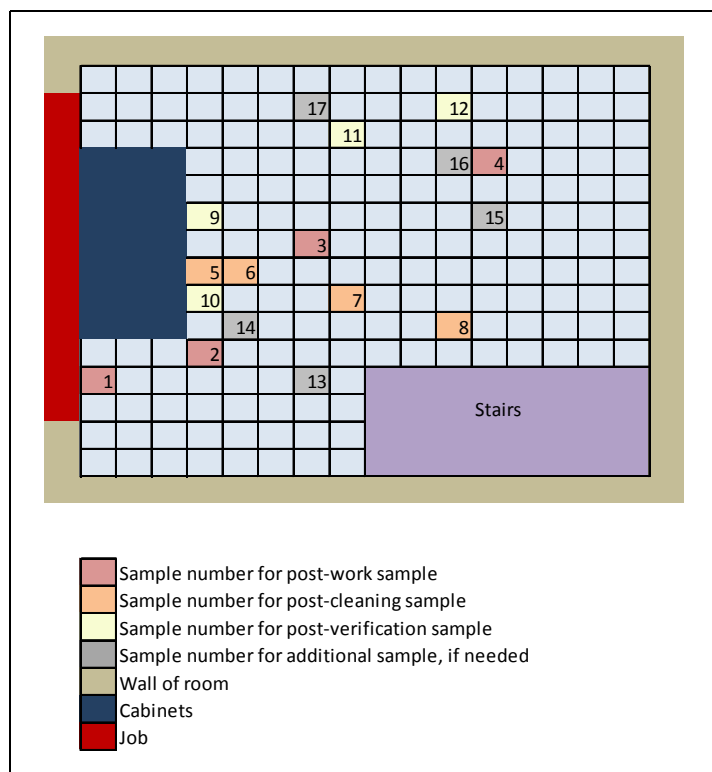


Figure I-43. Layout of Kitchen Gut Experiment 68

Table I-103. Post-Work Loading Measurements and Adjustments in Experiment 68

ID	Dist. From Wall (ft)	Lead Loading in $\mu\text{g}/\text{ft}^2$ (Dust Study)	Dust Load per ft^2 Disturbed (mg/ft^2 floor/ ft^2 wall)
1	1	3,133	3.69
2	1	7,386	8.69
3	4	222	0.26
4	9	12	0.01

Table I-104. Regression Statistics in Experiment 68

Statistic	Value
Shape	-0.75
Intercept	2.29
R ²	0.96
Load at 0 ft (mg/ft ² floor/ft ² disturbed)	9.86

Table I-105. Estimated Total Dust Emitted, Total Paint on Wall, and Emission Fraction in Experiment 68

Estimated Masses and Emission Fractions	Value
Total Mass of Dust on Floor (mg/ft ² disturbed)	197
Total Paint Removed From Surface (mg/ft ² disturbed)	62,570
Fraction Emitted	0.003

I.10.7. Experiment 69

The geometry of Experiment 69 is shown in Figure I-44, and the measured lead loadings and associated distances are shown in Table I-106. Sample 3 was adjusted using the taper assumption since it was outside the lateral extent of the job. The loadings were divided by the size of the job (69 ft²) and the fraction of lead in the paint (0.052) to estimate the dust loadings per ft² disturbed in Table I-106. Then, the natural logs of all loadings were used with the distances to estimate the regression parameters in Table I-107. Here, *intercept* is the intercept of the linear regression in log space, and Load at 0 ft is the assumed loading at 0 ft calculated as $\exp(\text{intercept})$. The R² of the regression was very low, so the average approach was used instead.

The total mass of dust on the floor was estimated as shown in Table I-108. The estimated paint density using the lead fraction was 1.54 g/cm³. The building was built in 1910, thus, it was assumed to have 5.3 layers of paint at the time of the job. The experiment notes indicated that all paint was removed during the renovation, so all 5.3 layers were assumed to be removed. These values were used to estimate the total amount of paint on the wall, giving a final emission fraction of 0.002.

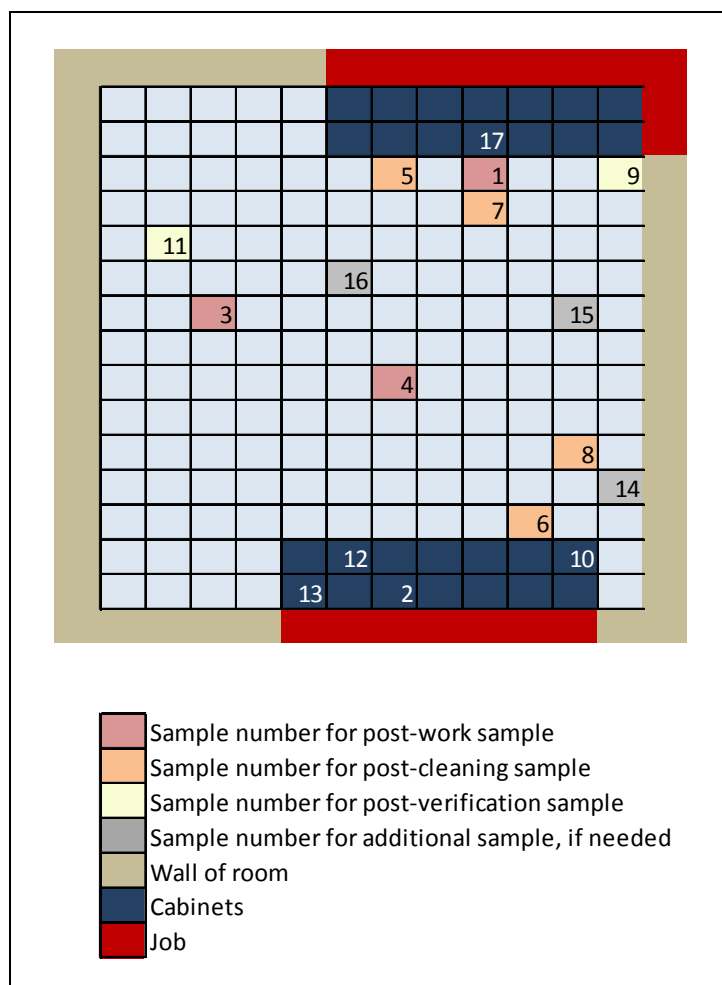


Figure I-44. Layout of Kitchen Gut Experiment 69

Table I-106. Post-Work Loading Measurements and Adjustments in Experiment 69

ID	Dist. From Wall (ft)	Lead Loading in $\mu\text{g}/\text{ft}^2$ (Dust Study)	Lead Loading in $\mu\text{g}/\text{ft}^2$ (adjusted)	Dust Load per ft^2 Disturbed (mg/ft^2 floor/ ft^2 wall)
1	3	3,265	3,265	0.91
2	15	911	911	0.25
3	7	196	391	0.11
4	9	5,238	5,238	1.46

Table I-107. Regression Statistics in Experiment 69

Statistic	Value
Shape	-0.07
Intercept	-0.27
R ²	0.08
Load at 0 ft (mg/ft ² floor/ft ² disturbed)	0.76

Table I-108. Estimated Total Dust Emitted, Total Paint on Wall, and Emission Fraction in Experiment 69

Estimated Masses and Emission Fractions	Value
Total Mass of Dust on Floor (mg/ft ² disturbed)	121
Total Paint Removed From Surface (mg/ft ² disturbed)	76,452
Fraction Emitted	0.002

I.10.8. Experiment 70

The geometry of Experiment 70 is shown in Figure I-45, and the measured lead loadings and associated distances are shown in Table I-109. No adjustments were made to the loadings since all samples were within the width of the job. The loadings were divided by the size of the job (61 ft²) and the fraction of lead in the paint (0.008) to estimate the dust loadings per ft² disturbed in Table I-109. Then, the natural logs of all loadings were used with the distances to estimate the regression parameters in

Table I-110. Regression Statistics in Experiment 70

. Here, *intercept* is the intercept of the linear regression in log space, and Load at 0 ft is the assumed loading at 0 ft calculated as $\exp(\textit{intercept})$. The R^2 of the regression was very low, so the average approach was used instead.

The total mass of dust on the floor was estimated as shown in Table I-111. The estimated paint density using the lead fraction was 1.08 g/cm^3 . The building was built in 1900, thus, it was assumed to have 5.0 layers of paint at the time of the job. The experiment notes indicated that all paint was removed during the renovation, so all 6.2 layers were assumed to be removed. These values were used to estimate the total amount of paint on the wall, giving a final emission fraction of 0.008.

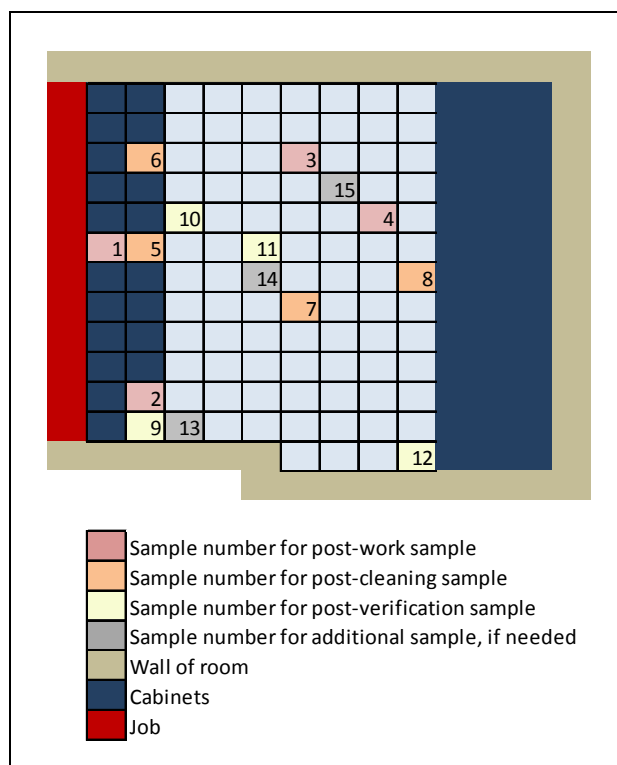


Figure I-45. Layout of Kitchen Gut Experiment 70

Table I-109. Post-Work Loading Measurements and Adjustments in Experiment 70

ID	Dist. From Wall (ft)	Lead Loading in $\mu\text{g}/\text{ft}^2$ (Dust Study)	Lead Loading in $\mu\text{g}/\text{ft}^2$ (adjusted)	Dust Load per ft^2 Disturbed (mg/ft^2 floor/ ft^2 wall)
1	1	2,940	2,940	6.02
2	2	1,704	1,704	3.49
3	6	18	18	0.04
4	8	3,513	3,513	7.20

Table I-110. Regression Statistics in Experiment 70

Statistic	Value
Shape	-0.21
Intercept	1.34
R ²	0.08
Load at 0 ft (mg/ft ² floor/ft ² disturbed)	3.83

Table I-111. Estimated Total Dust Emitted, Total Paint on Wall, and Emission Fraction in Experiment 70

Estimated Masses and Emission Fractions	Value
Total Mass of Dust on Floor (mg/ft ² disturbed)	482
Total Paint Removed From Surface (mg/ft ² disturbed)	63,279
Fraction Emitted	0.008

I.11. Heat Gun

I.11.1. Experiment 30

The geometry of Experiment 30 is shown in Figure I-46, but the exact location of the heat gun activity is unknown. Thus, no regression could be performed and the emission fraction is based on the average loadings. The loadings were divided by the size of the job (65 ft²) and the fraction of lead in the paint (0.1) to estimate the dust loadings per ft² disturbed in Table I-112. Then, the loadings were averaged and multiplied by the area of the room (150 ft²) to get the total mass of dust on the floor, as shown in Table I-113. The estimated paint density using the lead fraction was 2.03 g/cm³. The building was built in 1900, thus, it was assumed to have 6.2 layers of paint at the time of the job. The experiment notes indicated that all paint was removed during the renovation, so all 6.2 layers were assumed to be removed. These values were used to estimate the total amount of paint on the wall, giving a final emission fraction of 0.010.

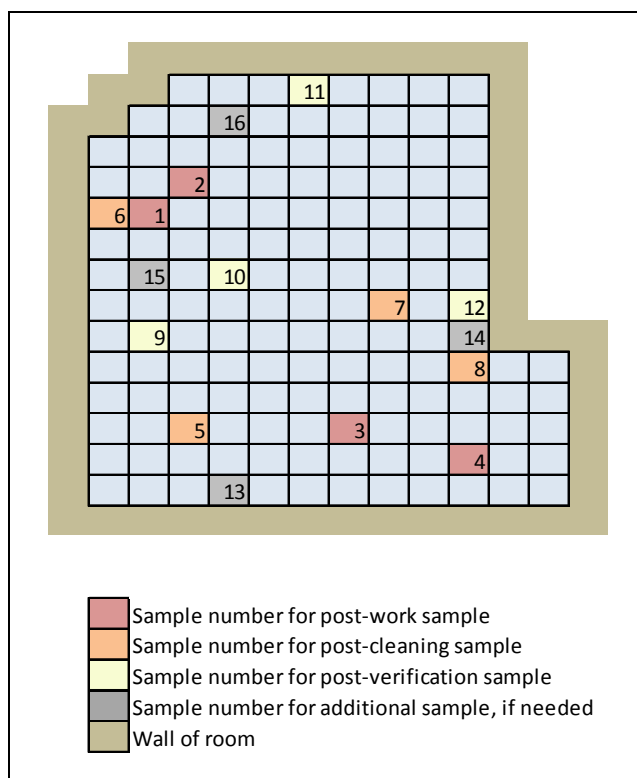


Figure I-46. Layout of Heat Gun Experiment 30

Table I-112. Post-Work Loading Measurements and Adjustments in Experiment 30

ID	Lead Loading in $\mu\text{g}/\text{ft}^2$ (Dust Study)	Dust Load per ft^2 Disturbed (mg/ft^2 floor/ ft^2 wall)
1	30,100	4.63
2	24,194	4.65
3	53,599	21.99
4	91,472	56.29

Table I-113. Estimated Total Dust Emitted, Total Paint on Wall, and Emission Fraction in Experiment 30

Estimated Masses and Emission Fractions	Value
Total Mass of Dust on Floor (mg/ft ² disturbed)	1,150
Total Paint Removed From Surface (mg/ft ² disturbed)	118,886
Fraction Emitted	0.010

I.11.2. Experiment 31

The geometry of Experiment 31 is shown in Figure I-47, but the exact location of the heat gun activity is unknown. Thus, no regression could be performed and the emission fraction is based on the average loadings. The loadings were divided by the size of the job (65 ft²) and the fraction of lead in the paint (0.051) to estimate the dust loadings per ft² disturbed in Table I-114. Then, the loadings were averaged and multiplied by the area of the room (150 ft²) to get the total mass of dust on the floor, as shown in Table I-115. The estimated paint density using the lead fraction was 1.53 g/cm³. The building was built in 1900, thus, it was assumed to have 6.2 layers of paint at the time of the job. The experiment notes indicated that all paint was removed during the renovation, so all 6.2 layers were assumed to be removed. These values were used to estimate the total amount of paint on the wall, giving a final emission fraction of 0.016.

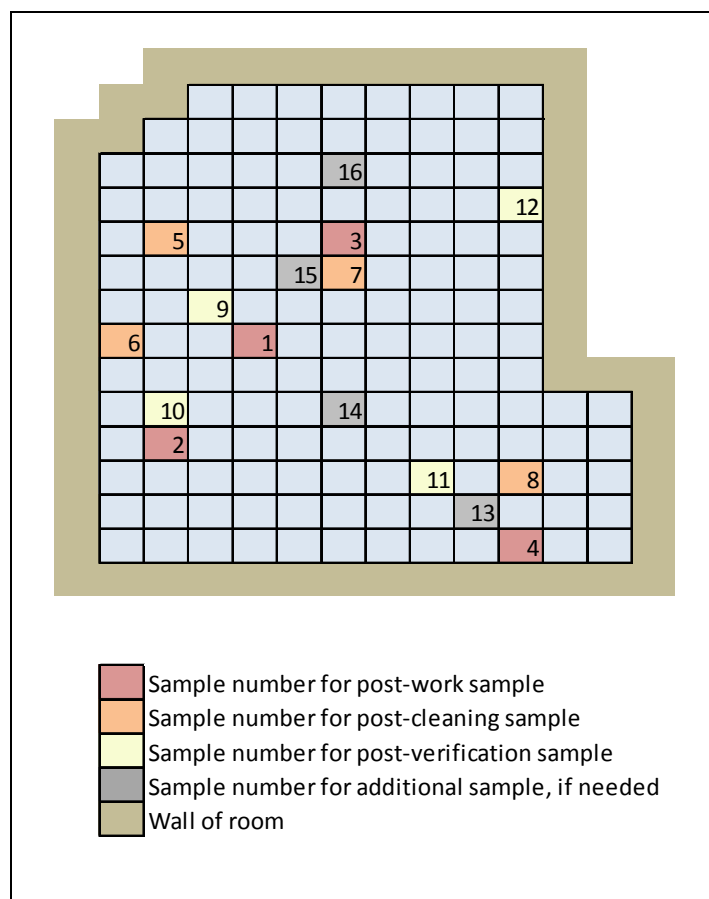


Figure I-47. Layout of Heat Gun Experiment 31

Table I-114. Post-Work Loading Measurements and Adjustments in Experiment 31

ID	Lead Loading in $\mu\text{g}/\text{ft}^2$ (Dust Study)	Dust Load per ft^2 Disturbed (mg/ft^2 floor/ ft^2 wall)
1	23,124	7.97
2	26,394	15.92
3	43,516	13.13
4	32,040	77.32

Table I-115. Estimated Total Dust Emitted, Total Paint on Wall, and Emission Fraction in Experiment 31

Estimated Masses and Emission Fractions	Value
Total Mass of Dust on Floor (mg/ft ² disturbed)	1,415
Total Paint Removed From Surface (mg/ft ² disturbed)	89,269
Fraction Emitted	0.0168

I.11.3. Experiment 32

The geometry of Experiment 32 is shown in Figure I-48, but the exact location of the heat gun activity is unknown. Thus, no regression could be performed and the emission fraction is based on the average loadings. The loadings were divided by the size of the job (69 ft²) and the fraction of lead in the paint (0.085) to estimate the dust loadings per ft² disturbed in Table I-116. Then, the loadings were averaged and multiplied by the area of the room (150 ft²) to get the total mass of dust on the floor, as shown in Table I-117. The estimated paint density using the lead fraction was 1.88 g/cm³. The building was built in 1900, thus, it was assumed to have 6.2 layers of paint at the time of the job. The experiment notes indicated that all paint was removed during the renovation, so all 6.2 layers were assumed to be removed. These values were used to estimate the total amount of paint on the wall, giving a final emission fraction of 0.021.

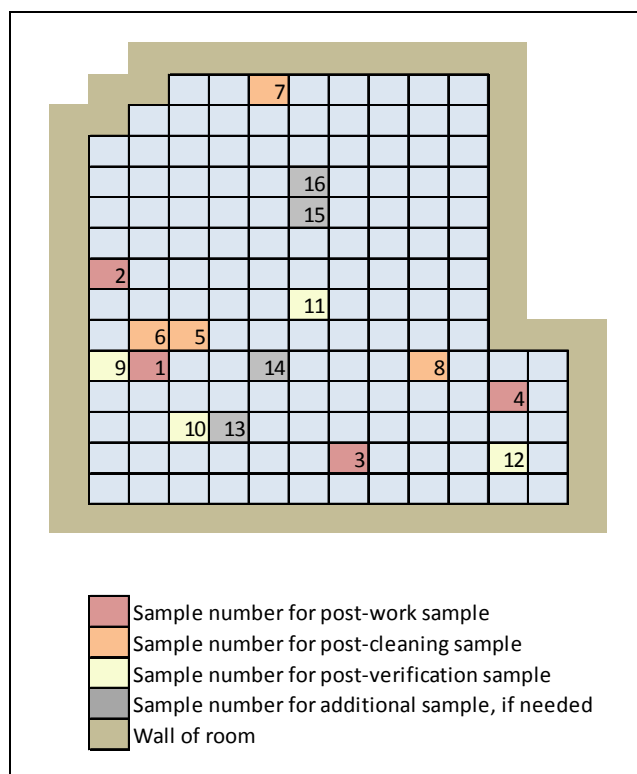


Figure I-48. Layout of Heat Gun Experiment 32

Table I-116. Post-Work Loading Measurements and Adjustments in Experiment 32

ID	Lead Loading in $\mu\text{g}/\text{ft}^2$ (Dust Study)	Dust Load per ft^2 Disturbed (mg/ft^2 floor/ ft^2 wall)
1	66,896	18.25
2	114,711	19.56
3	144,393	98.48
4	36,275	12.37

Table I-117. Estimated Total Dust Emitted, Total Paint on Wall, and Emission Fraction in Experiment 32

Estimated Masses and Emission Fractions	Value
Total Mass of Dust on Floor (mg/ft ² disturbed)	2,316
Total Paint Removed From Surface (mg/ft ² disturbed)	109,820
Fraction Emitted	0.02

I.11.4. Experiment 33

The geometry of Experiment 33 is shown in Figure I-49, but the exact location of the heat gun activity is unknown. Thus, no regression could be performed and the emission fraction is based on the average loadings. The loadings were divided by the size of the job (60 ft²) and the fraction of lead in the paint (0.035) to estimate the dust loadings per ft² disturbed in Table I-118. Then, the loadings were averaged and multiplied by the area of the room (150 ft²) to get the total mass of dust on the floor, as shown in Table I-119. The estimated paint density using the lead fraction was 1.36 g/cm³. The building was built in 1900, thus, it was assumed to have 6.2 layers of paint at the time of the job. The experiment notes indicated that all paint was removed during the renovation, so all 6.2 layers were assumed to be removed. These values were used to estimate the total amount of paint on the wall, giving a final emission fraction of 0.034.

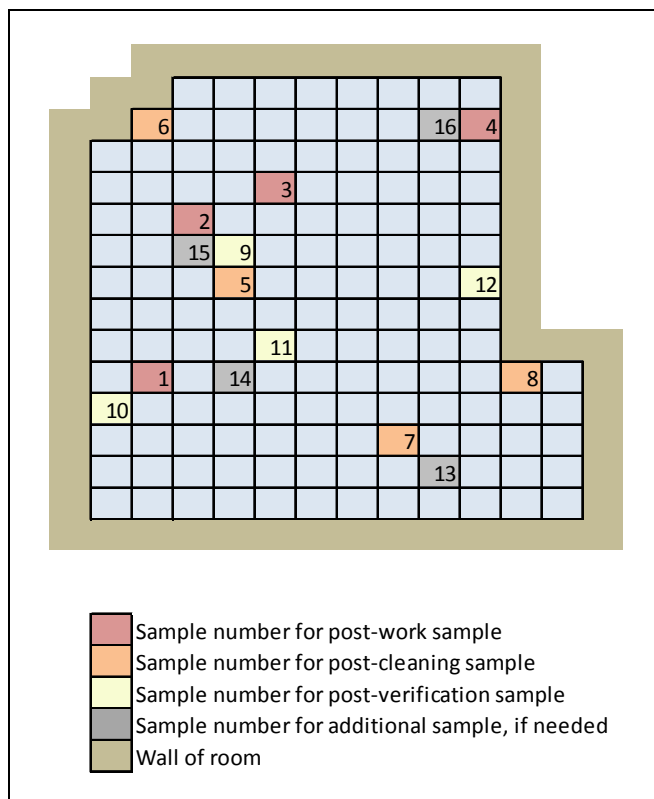


Figure I-49. Layout of Heat Gun Experiment 33

Table I-118. Post-Work Loading Measurements and Adjustments in Experiment 33

ID	Lead Loading in $\mu\text{g}/\text{ft}^2$ (Dust Study)	Dust Load per ft^2 Disturbed (mg/ft^2 floor/ ft^2 wall)
1	16,454	12.54
2	41,859	19.93
3	87,849	52.29
4	5,774	6.87

Table I-119. Estimated Total Dust Emitted, Total Paint on Wall, and Emission Fraction in Experiment 33

Estimated Masses and Emission Fractions	Value
Total Mass of Dust on Floor (mg/ft ² disturbed)	2,713
Total Paint Removed From Surface (mg/ft ² disturbed)	79,599
Fraction Emitted	0.034

I.11.5. Experiment 13

The geometry of Experiment 13 is shown in Figure I-51, and the measured lead loadings and associated distances are shown in Table I-120. No adjustments were made to the loadings since all samples were within the width of the job. The loadings were divided by the size of the job (53 ft²) and the fraction of lead in the paint (0.081) to estimate the dust loadings per ft² disturbed in Table I-120. Then, the natural logs of all loadings were used with the distances to estimate the regression parameters in Table I-121. Here, *intercept* is the intercept of the linear regression in log space, and Load at 0 ft is the assumed loading at 0 ft calculated as $\exp(\textit{intercept})$.

The integral was performed over the regression equation out to a distance of half the length and half the width for each of the four walls, since the job encompassed the whole room. The total mass of dust on the floor was estimated as shown in Table I-122. The estimated paint density using the lead fraction was 1.84 g/cm³. Although the vintage of the renovated building was unknown, nearby buildings were believed to have been built at the same time and were built in 1920. Therefore, the building was assumed to have been built in 1920 and to have 5.0 layers of paint at the time of the job. The experiment notes indicated that all paint was removed during the renovation, so all 5.0 layers were assumed to be removed. These values were used to estimate the total amount of paint on the wall, giving a final emission fraction of 0.014.

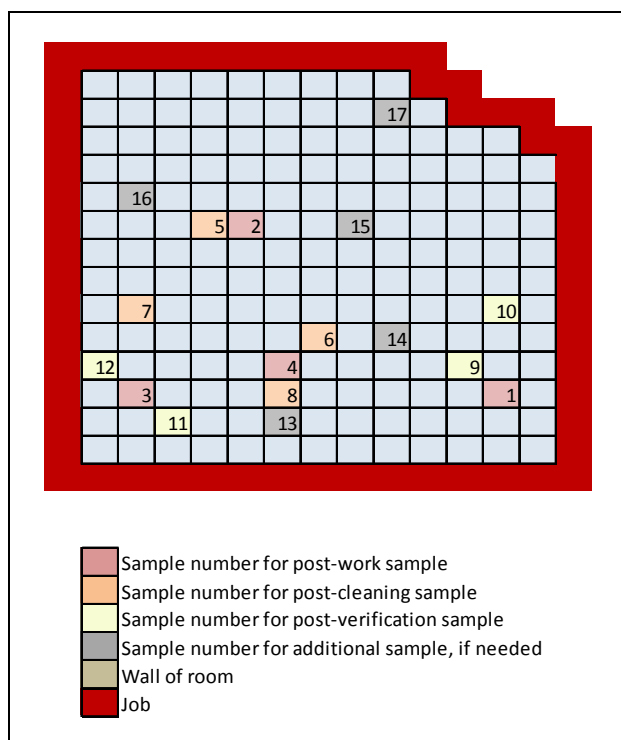


Figure I-50. Layout of Heat Gun Experiment 13

Table I-120. Post-Work Loading Measurements and Adjustments in Experiment 13

ID	Dist. From Wall (ft)	Lead Loading in $\mu\text{g}/\text{ft}^2$ (Dust Study)	Dust Load per ft^2 Disturbed (mg/ft^2 floor/ ft^2 wall)
1	2	40,378	9.41
2	2	27,630	6.44
3	5	25,391	5.91
4	6	24,874	5.79

Table I-121. Regression Statistics in Experiment 13

Statistic	Value
Shape	-0.08
Intercept	2.21
R^2	0.52
Load at 0 ft (mg/ft^2 floor/ ft^2 disturbed)	9.07

Table I-122. Estimated Total Dust Emitted, Total Paint on Wall, and Emission Fraction in Experiment 13

Estimated Masses and Emission Fractions	Value
Total Mass of Dust on Floor (mg/ft ² disturbed)	1,292
Total Paint Removed From Surface (mg/ft ² disturbed)	91,363
Fraction Emitted	0.001

I.11.6. Experiment 14

The geometry of Experiment 14 is shown in Figure I-52, and the measured lead loadings and associated distances are shown in Table I-123. No adjustments were made to the loadings since all samples were within the width of the job. The loadings were divided by the size of the job (75 ft²) and the fraction of lead in the paint (0.02) to estimate the dust loadings per ft² disturbed in Table I-123. Then, the natural logs of all loadings were used with the distances to estimate the regression parameters in Table I-124. Here, *intercept* is the intercept of the linear regression in log space, and Load at 0 ft is the assumed loading at 0 ft calculated as $\exp(\textit{intercept})$.

The integral was performed over the regression equation out to a distance of half the length and half the width for each of the four walls, since the job encompassed the whole room. The total mass of dust on the floor was estimated as shown in Table I-125. The estimated paint density using the lead fraction was 1.21 g/cm³. Although the vintage of the renovated building was unknown, nearby buildings were believed to have been built at the same time and were built in 1920. Therefore, the building was assumed to have been built in 1920 and to have 5.0 layers of paint at the time of the job. The experiment notes indicated that all paint was removed during the renovation, so all 5.0 layers were assumed to be removed. These values were used to estimate the total amount of paint on the wall, giving a final emission fraction of 0.007.

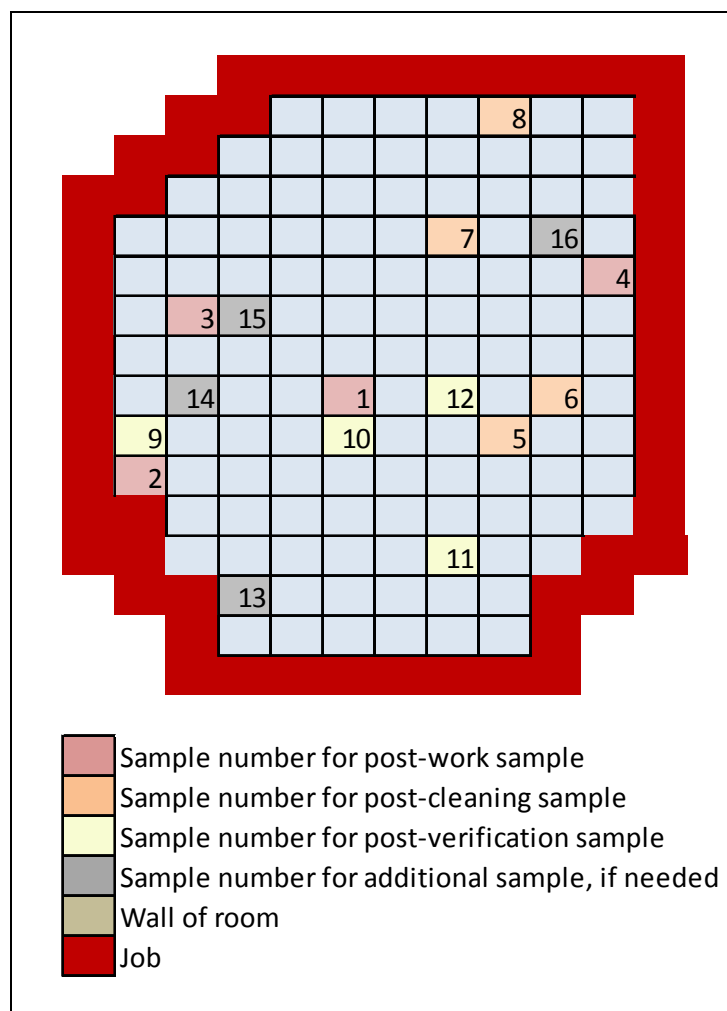


Figure I-51. Layout of Heat Gun Experiment 14

Table I-123. Post-Work Loading Measurements and Adjustments in Experiment 14

ID	Dist. From Wall (ft)	Lead Loading in $\mu\text{g}/\text{ft}^2$ (Dust Study)	Dust Load per ft^2 Disturbed (mg/ft^2 floor/ ft^2 wall)
1	5	427	0.28
2	1	5,204	3.47
3	2	6,223	4.15
4	1	9,359	6.24

Table I-124. Regression Statistics in Experiment 14

Statistic	Value
Shape	-0.71
Intercept	2.41
R ²	0.93
Load at 0 ft (mg/ft ² floor/ft ² disturbed)	11.16

Table I-125. Estimated Total Dust Emitted, Total Paint on Wall, and Emission Fraction in Experiment 14

Estimated Masses and Emission Fractions	Value
Total Mass of Dust on Floor (mg/ft ² disturbed)	426
Total Paint Removed From Surface (mg/ft ² disturbed)	59,999
Fraction Emitted	0.007

I.11.7. Experiment 15

The geometry of Experiment 15 is shown in Figure I-53, and the measured lead loadings and associated distances are shown in Table I-126. No adjustments were made to the loadings since all samples were within the width of the job. The loadings were divided by the size of the job (75 ft²) and the fraction of lead in the paint (0.102) to estimate the dust loadings per ft² disturbed in Table I-126. Then, the natural logs of all loadings were used with the distances to estimate the regression parameters in Table I-127. Here, *intercept* is the intercept of the linear regression in log space, and Load at 0 ft is the assumed loading at 0 ft calculated as $\exp(\textit{intercept})$.

The integral was performed over the regression equation out to a distance of 14 ft, (the length of the room), and the total mass of dust on the floor was estimated as shown in Table I-128. The estimated paint density using the lead fraction was 2.05 g/cm³. Although the vintage of the renovated building was unknown, nearby buildings were believed to have been built at the same time and were built in 1920. Therefore, the building was assumed to have been built in 1920 and to have 5.0 layers of paint at the time of the job. The experiment notes indicated that all paint was removed during the renovation, so all 5.0 layers were assumed to be removed. These values were used to estimate the total amount of paint on the wall, giving a final emission fraction of 0.007.

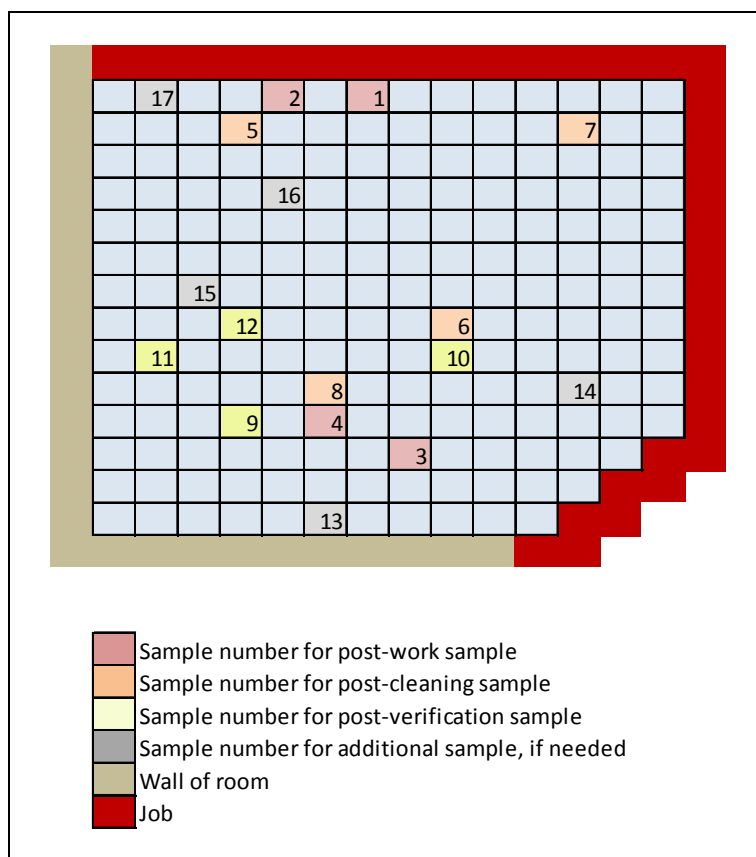


Figure I-52. Layout of Heat Gun Experiment 15

Table I-126. Post-Work Loading Measurements and Adjustments in Experiment 15

ID	Dist. From Wall (ft)	Lead Loading in $\mu\text{g}/\text{ft}^2$ (Dust Study)	Dust Load per ft^2 Disturbed (mg/ft^2 floor/ ft^2 wall)
1	1	101,104	13.22
2	1	34,976	4.57
3	4	180,281	23.57
4	6	6,096	0.80

Table I-127. Regression Statistics in Experiment 15

Statistic	Value
Shape	-0.32
Intercept	2.71
R ²	0.27
Load at 0 ft (mg/ft ² floor/ft ² disturbed)	15.07

Table I-128. Estimated Total Dust Emitted, Total Paint on Wall, and Emission Fraction in Experiment 15

Estimated Masses and Emission Fractions	Value
Total Mass of Dust on Floor (mg/ft ² disturbed)	679
Total Paint Removed From Surface (mg/ft ² disturbed)	102,160
Fraction Emitted	0.001

I.11.8. Experiment 16

The geometry of Experiment 16 is shown in Figure I-53, and the measured lead loadings and associated distances are shown in Table I-129. No adjustments were made to the loadings since all samples were within the width of the job. The loadings were divided by the size of the job (75 ft²) and the fraction of lead in the paint (0.04) to estimate the dust loadings per ft² disturbed in Table I-129. Then, the natural logs of all loadings were used with the distances to estimate the regression parameters in Table I-130. Here, *intercept* is the intercept of the linear regression in log space, and Load at 0 ft is the assumed loading at 0 ft calculated as $\exp(\textit{intercept})$.

The integral was performed over the regression equation out to a distance of 13 ft, (the length of the room), and the total mass of dust on the floor was estimated as shown in Table I-131. The estimated paint density using the lead fraction was 1.41 g/cm³. Although the vintage of the renovated building was unknown, nearby buildings were believed to have been built at the same time and were built in 1920. Therefore, the building was assumed to have been built in 1920 and to have 5.0 layers of paint at the time of the job. The experiment notes do not specify the amount of paint removed during the renovation, so all 5.0 layers were assumed to be removed. These values were used to estimate the total amount of paint on the wall, giving a final emission fraction of 0.005.

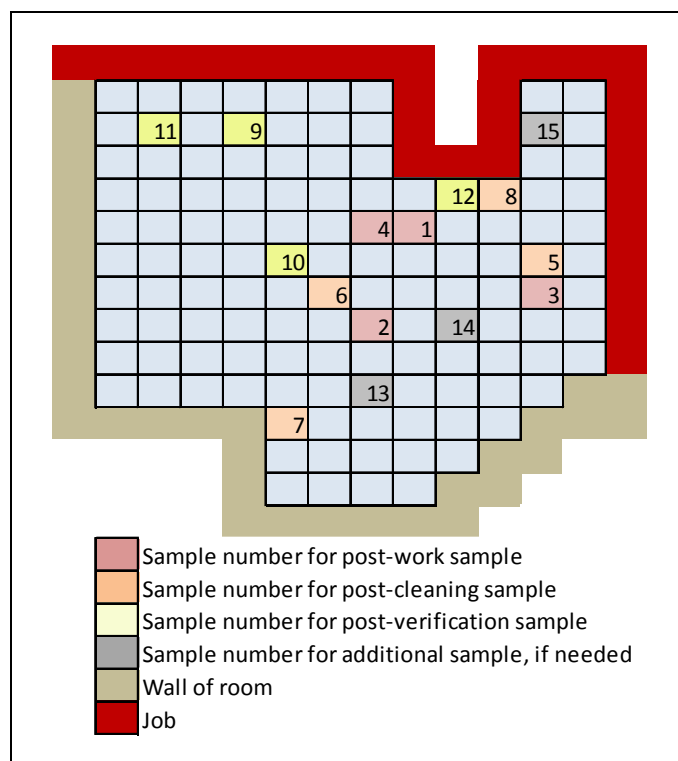


Figure I-53. Layout of Heat Gun Experiment 16

Table I-129. Post-Work Loading Measurements and Adjustments in Experiment 16

ID	Dist. From Wall (ft)	Lead Loading in $\mu\text{g}/\text{ft}^2$ (Dust Study)	Dust Load per ft^2 Disturbed (mg/ft^2 floor/ ft^2 wall)
1	2	3,802	1.27
2	4	5,505	1.83
3	2	4,393	1.46
4	2	5,905	1.97

Table I-130. Regression Statistics in Experiment 16

Statistic	Value
Shape	0.09
Intercept	0.26
R^2	0.19
Load at 0 ft (mg/ft^2 floor/ ft^2 disturbed)	1.29

Table I-131. Estimated Total Dust Emitted, Total Paint on Wall, and Emission Fraction in Experiment 16

Estimated Masses and Emission Fractions	Value
Total Mass of Dust on Floor (mg/ft ² disturbed)	376
Total Paint Removed From Surface (mg/ft ² disturbed)	70,282
Fraction Emitted	0.001

I.11.9. Experiment 60

The geometry of Experiment 60 is shown in Figure I-54, and the measured lead loadings and associated distances are shown in Table I-132. Samples 2 and 4 were adjusted using the taper assumption since they were outside the lateral extent of the job. The loadings were divided by the size of the job (75 ft²) and the fraction of lead in the paint (0.029) to estimate the dust loadings per ft² disturbed in Table I-132. Then, the natural logs of all loadings were used with the distances to estimate the regression parameters in Table I-133. Here, *intercept* is the intercept of the linear regression in log space, and Load at 0 ft is the assumed loading at 0 ft calculated as $\exp(\textit{intercept})$.

The integral was performed over the regression equation out to a distance of 10 ft, (the length of the room), and the total mass of dust on the floor was estimated as shown in Table I-134. The estimated paint density using the lead fraction was 1.30 g/cm³. The school was built in 1967, thus, it was assumed to have 3.3 layers of paint at the time of the job. The experiment notes indicated that not all paint was removed during the renovation, so it was assumed that only 15% of the paint (or 0.5 layers) were removed. These values were used to estimate the total amount of paint on the wall, giving a final emission fraction of 0.027.

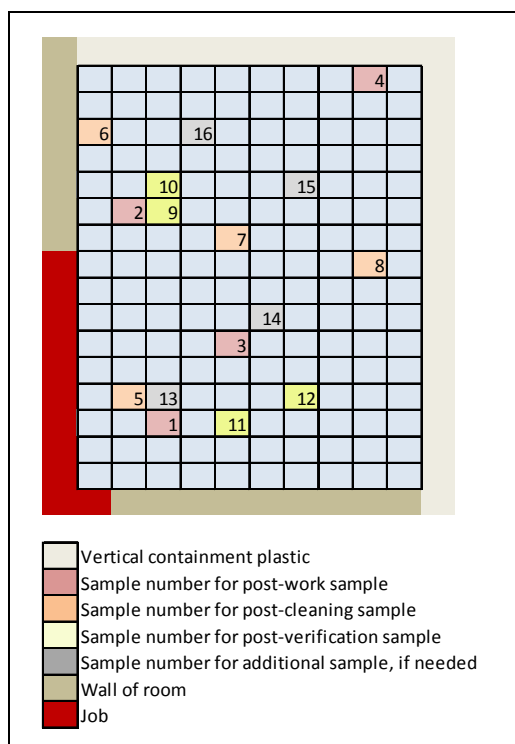


Figure I-54. Layout of Heat Gun Experiment 60

Table I-132. Post-Work Loading Measurements and Adjustments in Experiment 60

ID	Dist. From Wall (ft)	Lead Loading in $\mu\text{g}/\text{ft}^2$ (Dust Study)	Lead Loading in $\mu\text{g}/\text{ft}^2$ (adjusted)	Dust Load per ft^2 Disturbed (mg/ft^2 floor/ ft^2 wall)
1	3	3,014	3,014	1.39
2	2	2,611	3,481	1.60
3	5	1,443	1,443	0.66
4	9	193	1,546	0.71

Table I-133. Regression Statistics in Experiment 60

Statistic	Value
Shape	-0.12
Intercept	0.58
R^2	0.66
Load at 0 ft (mg/ft^2 floor/ ft^2 disturbed)	1.78

Table I-134. Estimated Total Dust Emitted, Total Paint on Wall, and Emission Fraction in Experiment 60

Estimated Masses and Emission Fractions	Value
Total Mass of Dust on Floor (mg/ft ² disturbed)	166
Total Paint Removed From Surface (mg/ft ² disturbed)	6,084
Fraction Emitted	0.027

I.11.10. Experiment 61

The geometry of Experiment 61 is shown in Figure I-55, and the measured lead loadings and associated distances are shown in Table I-135. Sample 3 was adjusted using the taper assumption since it was outside the lateral extent of the job. The loadings were divided by the size of the job (75 ft²) and the fraction of lead in the paint (0.022) to estimate the dust loadings per ft² disturbed in Table I-135. Then, the natural logs of all loadings were used with the distances to estimate the regression parameters in Table I-136. Here, *intercept* is the intercept of the linear regression in log space, and Load at 0 ft is the assumed loading at 0 ft calculated as $\exp(\textit{intercept})$.

The integral was performed over the regression equation out to a distance of 10 ft, (the length of the room), and the total mass of dust on the floor was estimated as shown in Table I-137. The estimated paint density using the lead fraction was 1.23 g/cm³. The school was built in 1967, thus, it was assumed to have 3.3 layers of paint at the time of the job. The experiment notes indicated that not all paint was removed during the renovation, so it was assumed that only 15% of the paint (or 0.5 layers) were removed. These values were used to estimate the total amount of paint on the wall, giving a final emission fraction of 0.017.

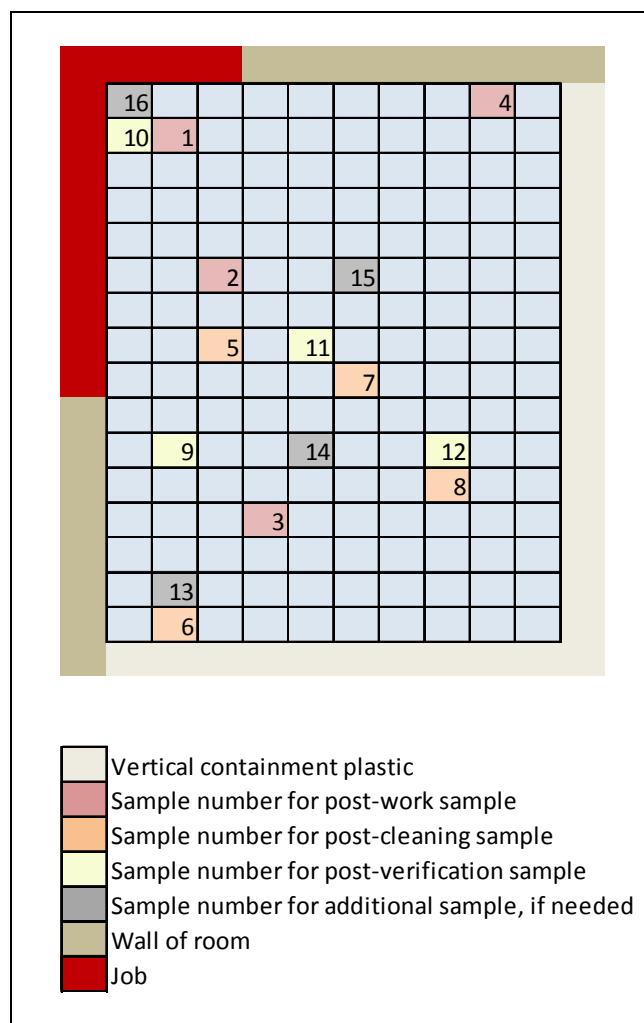


Figure I-55. Layout of Heat Gun Experiment 61

Table I-135. Post-Work Loading Measurements and Adjustments in Experiment 61

ID	Dist. From Wall (ft)	Lead Loading in $\mu\text{g}/\text{ft}^2$ (Dust Study)	Lead Loading in $\mu\text{g}/\text{ft}^2$ (adjusted)	Dust Load per ft^2 Disturbed (mg/ft^2 floor/ ft^2 wall)
1	2	3,624	3,624	2.20
2	3	1,351	1,351	0.82
3	4	95	191	0.12
4	9	51	51	0.03

Table I-136. Regression Statistics in Experiment 61

Statistic	Value
Shape	-0.56
Intercept	1.26
R ²	0.82
Load at 0 ft (mg/ft ² floor/ft ² disturbed)	3.53

Table I-137. Estimated Total Dust Emitted, Total Paint on Wall, and Emission Fraction in Experiment 61

Estimated Masses and Emission Fractions	Value
Total Mass of Dust on Floor (mg/ft ² disturbed)	100
Total Paint Removed From Surface (mg/ft ² disturbed)	5,745
Fraction Emitted	0.017

I.11.11. Experiment 62

The geometry of Experiment 62 is shown in Figure I-56, and the measured lead loadings and associated distances are shown in Table I-138. Samples 1 and 3 were adjusted using the taper assumption since they were outside the lateral extent of the job. The loadings were divided by the size of the job (73 ft²) and the fraction of lead in the paint (0.022) to estimate the dust loadings per ft² disturbed in Table I-138. Then, the natural logs of all loadings were used with the distances to estimate the regression parameters in Table I-139. Here, *intercept* is the intercept of the linear regression in log space, and Load at 0 ft is the assumed loading at 0 ft calculated as $\exp(\textit{intercept})$.

The integral was performed over the regression equation out to a distance of 10 ft, (the length of the room), and the total mass of dust on the floor was estimated as shown in Table I-140. The estimated paint density using the lead fraction was 1.23 g/cm³. The school was built in 1967, thus, it was assumed to have 3.3 layers of paint at the time of the job. The experiment notes indicated that not all paint was removed during the renovation, so it was assumed that only 15% of the paint (or 0.5 layers) were removed. These values were used to estimate the total amount of paint on the wall, giving a final emission fraction of 0.042.

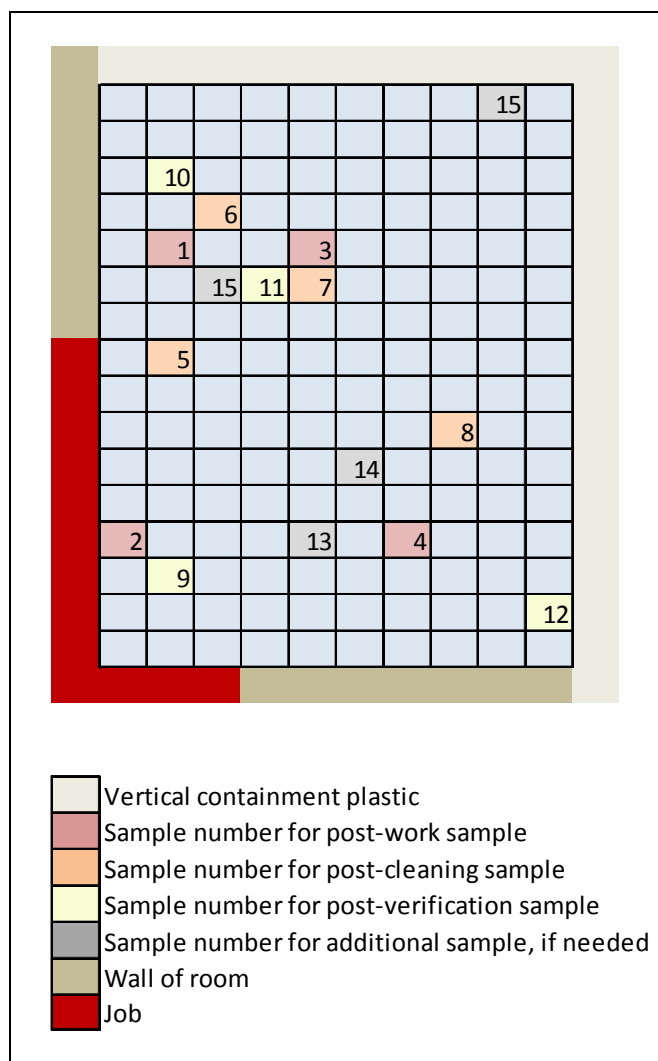


Figure I-56. Layout of Heat Gun Experiment 62

Table I-138. Post-Work Loading Measurements and Adjustments in Experiment 62

ID	Dist. From Wall (ft)	Lead Loading in $\mu\text{g}/\text{ft}^2$ (Dust Study)	Lead Loading in $\mu\text{g}/\text{ft}^2$ (adjusted)	Dust Load per ft^2 Disturbed (mg/ft^2 floor/ ft^2 wall)
1	2	5,001	8,001	4.98
2	1	3,676	3,676	2.29
3	5	478	764	0.48
4	7	1,974	1,974	1.23

Table I-139. Regression Statistics in Experiment 62

Statistic	Value
Shape	-0.24
Intercept	1.36
R ²	0.42
Load at 0 ft (mg/ft ² floor/ft ² disturbed)	3.88

Table I-140. Estimated Total Dust Emitted, Total Paint on Wall, and Emission Fraction in Experiment 62

Estimated Masses and Emission Fractions	Value
Total Mass of Dust on Floor (mg/ft ² disturbed)	239
Total Paint Removed From Surface (mg/ft ² disturbed)	5,745
Fraction Emitted	0.042

I.11.12. Experiment 63

The geometry of Experiment 63 is shown in Figure I-57, and the measured lead loadings and associated distances are shown in Table I-141. Sample 1 was adjusted using the taper assumption since it was outside the lateral extent of the job. The loadings were divided by the size of the job (75 ft²) and the fraction of lead in the paint (0.026) to estimate the dust loadings per ft² disturbed in Table I-141. Then, the natural logs of all loadings were used with the distances to estimate the regression parameters in Table I-142. Here, *intercept* is the intercept of the linear regression in log space, and Load at 0 ft is the assumed loading at 0 ft calculated as $\exp(\textit{intercept})$.

The integral was performed over the regression equation out to a distance of 10 ft, (the length of the room), and the total mass of dust on the floor was estimated as shown in Table I-143. The estimated paint density using the lead fraction was 1.27 g/cm³. The school was built in 1967, thus, it was assumed to have 3.3 layers of paint at the time of the job. The experiment notes indicated that not all paint was removed during the renovation, so it was assumed that only 15% of the paint (or 0.5 layers) were removed. These values were used to estimate the total amount of paint on the wall, giving a final emission fraction of 0.040.

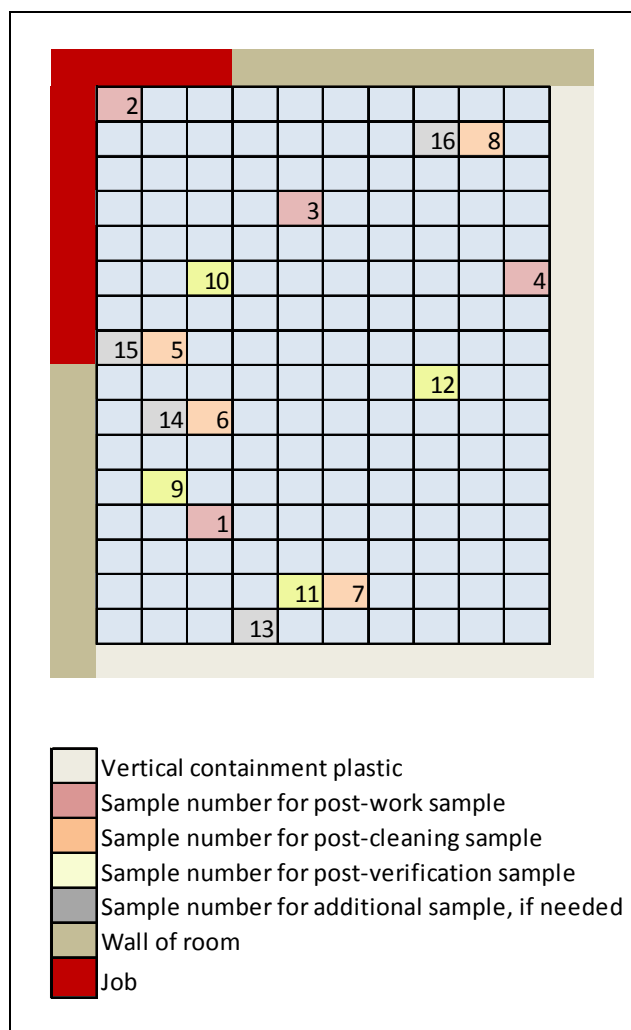


Figure I-57. Layout of Heat Gun Experiment 63

Table I-141. Post-Work Loading Measurements and Adjustments in Experiment 63

ID	Dist. From Wall (ft)	Lead Loading in $\mu\text{g}/\text{ft}^2$ (Dust Study)	Lead Loading in $\mu\text{g}/\text{ft}^2$ (adjusted)	Dust Load per ft^2 Disturbed (mg/ft^2 floor/ ft^2 wall)
1	3	1,914	4,305	2.21
2	1	10,384	10,384	5.33
3	5	471	471	0.24
4	10	65	65	0.03

Table I-142. Regression Statistics in Experiment 63

Statistic	Value
Shape	-0.58
Intercept	2.16
R ²	0.96
Load at 0 ft (mg/ft ² floor/ft ² disturbed)	8.64

Table I-143. Estimated Total Dust Emitted, Total Paint on Wall, and Emission Fraction in Experiment 63

Estimated Masses and Emission Fractions	Value
Total Mass of Dust on Floor (mg/ft ² disturbed)	238
Total Paint Removed From Surface (mg/ft ² disturbed)	5,939
Fraction Emitted	0.040

I.12. Low Heat

I.12.1. Experiment 56

The geometry of Experiment 56 is shown in Figure I-58, and the measured lead loadings and associated distances are shown in Table I-144. Samples 3 and 4 were adjusted using the taper assumption since they were outside the lateral extent of the job. The loadings were divided by the size of the job (50 ft²) and the fraction of lead in the paint (0.022) to estimate the dust loadings per ft² disturbed in Table I-144. Then, the natural logs of all loadings were used with the distances to estimate the regression parameters in Table I-145. Here, *intercept* is the intercept of the linear regression in log space, and Load at 0 ft is the assumed loading at 0 ft calculated as $\exp(\textit{intercept})$.

The integral was performed over the regression equation out to a distance of 12 ft, (the length of the room), and the total mass of dust on the floor was estimated as shown in Table I-146. The estimated paint density using the lead fraction was 1.23 g/cm³. The school was built in 1967, thus, it was assumed to have 3.3 layers of paint at the time of the job. The experiment notes indicated that not all paint was removed during the renovation, so it was assumed that only 15% of the paint (or 0.5 layers) were removed. These values were used to estimate the total amount of paint on the wall, giving a final emission fraction of 0.159.

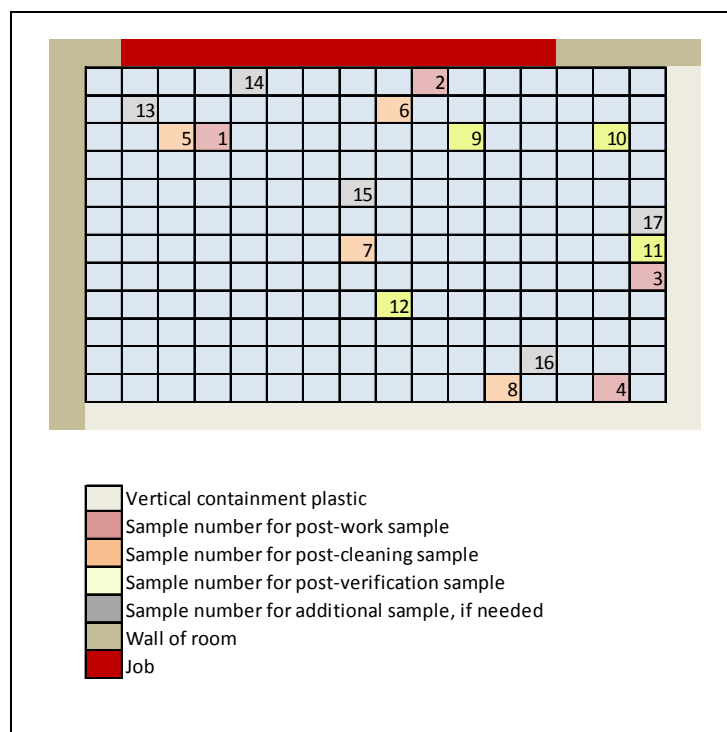


Figure I-58. Layout of Low Heat Experiment 56

Table I-144. Post-Work Loading Measurements and Adjustments in Experiment 56

ID	Dist. From Wall (ft)	Lead Loading in $\mu\text{g}/\text{ft}^2$ (Dust Study)	Lead Loading in $\mu\text{g}/\text{ft}^2$ (adjusted)	Dust Load per ft^2 Disturbed (mg/ft^2 floor/ ft^2 wall)
1	3	7,837	7,837	7.12
2	1	16,046	16,046	14.59
3	8	325	1,298	1.18
4	12	295	590	0.54

Table I-145. Regression Statistics in Experiment 56

Statistic	Value
Shape	-0.31
Intercept	2.89
R^2	0.98
Load at 0 ft (mg/ft^2 floor/ ft^2 disturbed)	17.94

Table I-146. Estimated Total Dust Emitted, Total Paint on Wall, and Emission Fraction in Experiment 56

Estimated Masses and Emission Fractions	Value
Total Mass of Dust on Floor (mg/ft ² disturbed)	912
Total Paint Removed From Surface (mg/ft ² disturbed)	5,745
Fraction Emitted	0.159

I.12.2. Experiment 57

The geometry of Experiment 57 is shown in Figure I-59, and the measured lead loadings and associated distances are shown in Table I-147. Samples 1 and 2 were adjusted using the taper assumption since they were outside the lateral extent of the job. The loadings were divided by the size of the job (50 ft²) and the fraction of lead in the paint (0.024) to estimate the dust loadings per ft² disturbed in Table I-147. Then, the natural logs of all loadings were used with the distances to estimate the regression parameters in Table I-148. Here, *intercept* is the intercept of the linear regression in log space, and Load at 0 ft is the assumed loading at 0 ft calculated as $\exp(\textit{intercept})$.

The integral was performed over the regression equation out to a distance of 12 ft, (the length of the room), and the total mass of dust on the floor was estimated as shown in Table I-149. The estimated paint density using the lead fraction was 1.25 g/cm³. The school was built in 1967, thus, it was assumed to have 3.3 layers of paint at the time of the job. The experiment notes indicated that not all paint was removed during the renovation, so it was assumed that only 15% of the paint (or 0.5 layers) were removed. These values were used to estimate the total amount of paint on the wall, giving a final emission fraction of 0.189.

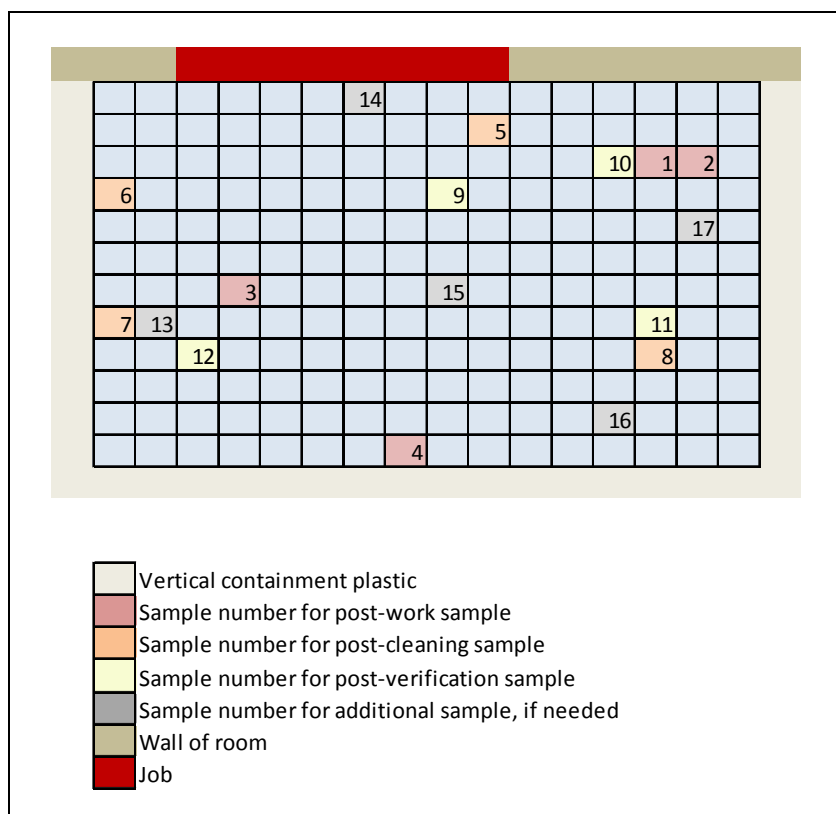


Figure I-59. Layout of Low Heat Experiment 57

Table I-147. Post-Work Loading Measurements and Adjustments in Experiment 57

ID	Dist. From Wall (ft)	Lead Loading in $\mu\text{g}/\text{ft}^2$ (Dust Study)	Lead Loading in $\mu\text{g}/\text{ft}^2$ (adjusted)	Dust Load per ft^2 Disturbed (mg/ft^2 floor/ ft^2 wall)
1	3	5,768	13,459	2.42
2	3	2,374	8,310	1.94
3	7	730	730	-0.50
4	12	120	120	-2.30

Table I-148. Regression Statistics in Experiment 57

Statistic	Value
Shape	-0.51
Intercept	3.56
R ²	0.97
Load at 0 ft (mg/ft ² floor/ft ² disturbed)	35.03

Table I-149. Estimated Total Dust Emitted, Total Paint on Wall, and Emission Fraction in Experiment 57

Estimated Masses and Emission Fractions	Value
Total Mass of Dust on Floor (mg/ft ² disturbed)	1,103
Total Paint Removed From Surface (mg/ft ² disturbed)	5,842
Fraction Emitted	0.189

I.12.3. Experiment 58

The geometry of Experiment 58 is shown in Figure I-60, and the measured lead loadings and associated distances are shown in Table I-150. Samples 3 and 4 were adjusted using the taper assumption since they were outside the lateral extent of the job. The loadings were divided by the size of the job (50 ft²) and the fraction of lead in the paint (0.028) to estimate the dust loadings per ft² disturbed in Table I-150. Then, the natural logs of all loadings were used with the distances to estimate the regression parameters in Table I-151. Here, *intercept* is the intercept of the linear regression in log space, and Load at 0 ft is the assumed loading at 0 ft calculated as $\exp(\textit{intercept})$.

The integral was performed over the regression equation out to a distance of 12 ft, (the length of the room), and the total mass of dust on the floor was estimated as shown in Table I-152. The estimated paint density using the lead fraction was 1.29 g/cm³. The school was built in 1967, thus, it was assumed to have 3.3 layers of paint at the time of the job. The experiment notes indicated that not all paint was removed during the renovation, so it was assumed that only 15% of the paint (or 0.5 layers) were removed. These values were used to estimate the total amount of paint on the wall, giving a final emission fraction of 0.020.

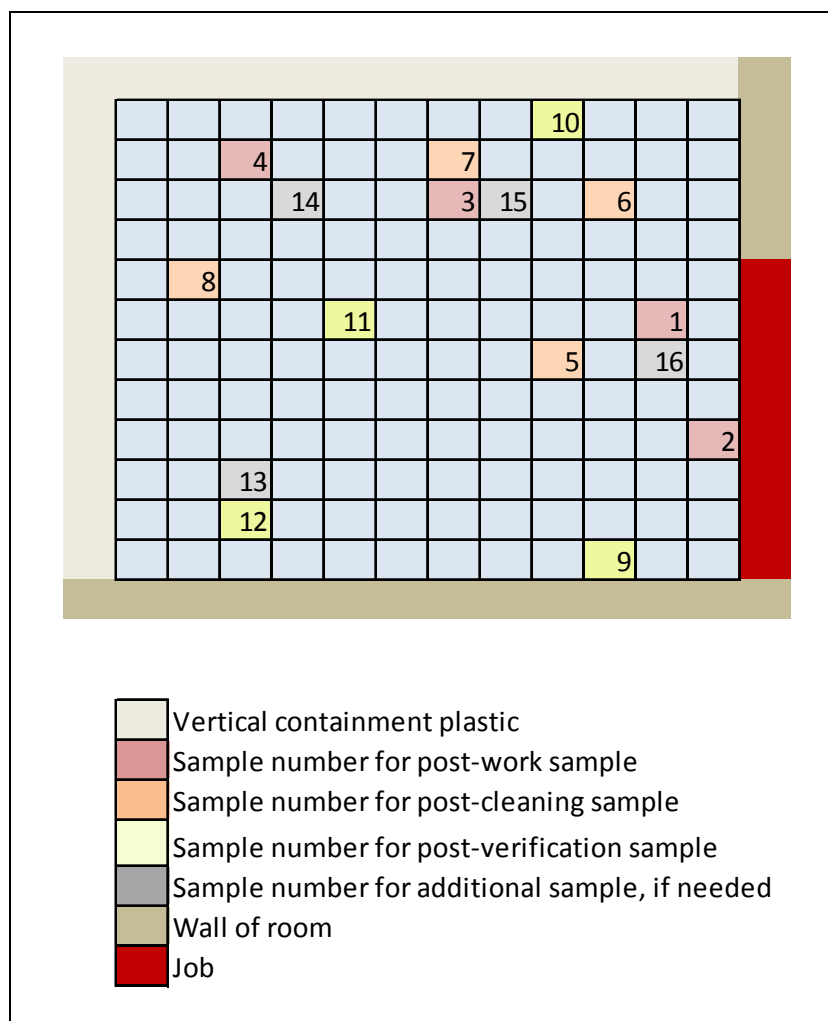


Figure I-60. Layout of Low Heat Experiment 58

Table I-150. Post-Work Loading Measurements and Adjustments in Experiment 58

ID	Dist. From Wall (ft)	Lead Loading in $\mu\text{g}/\text{ft}^2$ (Dust Study)	Lead Loading in $\mu\text{g}/\text{ft}^2$ (adjusted)	Dust Load per ft^2 Disturbed (mg/ft^2 floor/ ft^2 wall)
1	2	2,759	2,759	1.97
2	1	4,145	4,145	2.96
3	6	198	330	0.24
4	10	65	162	0.12

Table I-151. Regression Statistics in Experiment 58

Statistic	Value
Shape	-0.38
Intercept	1.32
R ²	0.95
Load at 0 ft (mg/ft ² floor/ft ² disturbed)	3.76

Table I-152. Estimated Total Dust Emitted, Total Paint on Wall, and Emission Fraction in Experiment 58

Estimated Masses and Emission Fractions	Value
Total Mass of Dust on Floor (mg/ft ² disturbed)	119
Total Paint Removed From Surface (mg/ft ² disturbed)	6,036
Fraction Emitted	0.020

I.12.4. Experiment 59

The geometry of Experiment 13 is shown in Figure I-61, and the measured lead loadings and associated distances are shown in Table I-153. No adjustments were made to the loadings since all samples were within the width of the job. The loadings were divided by the size of the job (50 ft²) and the fraction of lead in the paint (0.13) to estimate the dust loadings per ft² disturbed in Table I-153. Then, the natural logs of all loadings were used with the distances to estimate the regression parameters in Table I-154. Here, *intercept* is the intercept of the linear regression in log space, and Load at 0 ft is the assumed loading at 0 ft calculated as $\exp(\textit{intercept})$.

The integral was performed over the regression equation out to a distance of 10 ft, (the length of the room), and the total mass of dust on the floor was estimated as shown in Table I-155. The estimated paint density using the lead fraction was 2.34 g/cm³. The school was built in 1967, thus, it was assumed to have 3.3 layers of paint at the time of the job. The experiment notes indicated that not all paint was removed during the renovation, so it was assumed that only 15% of the paint (or 0.5 layers) were removed. These values were used to estimate the total amount of paint on the wall, giving a final emission fraction of 0.128.

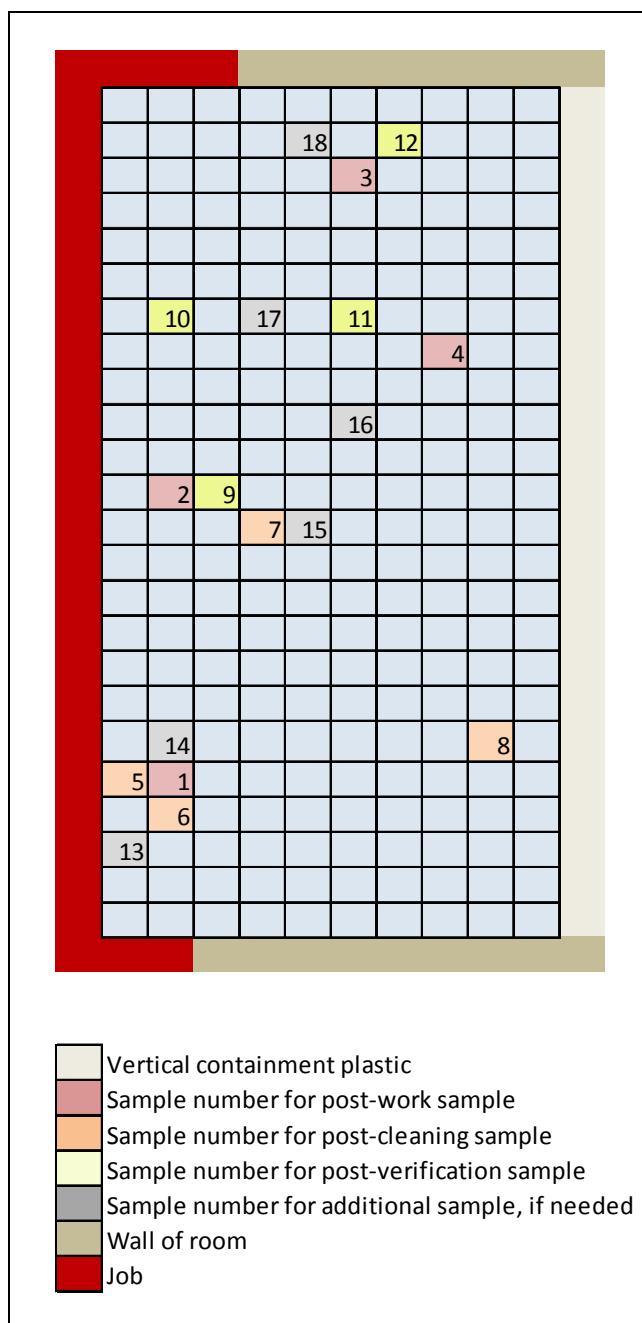


Figure I-61. Layout of Heat Experiment 59

Table I-153. Post-Work Loading Measurements and Adjustments in Experiment 59

ID	Dist. From Wall (ft)	Lead Loading in $\mu\text{g}/\text{ft}^2$ (Dust Study)	Dust Load per ft^2 Disturbed (mg/ft^2 floor/ ft^2 wall)
1	2	65,994	10.15
2	2	59,156	9.10
3	6	11,403	1.75
4	8	1,302	0.20

Table I-154. Regression Statistics in Experiment 59

Statistic	Value
Shape	-0.60
Intercept	3.55
R ²	0.95
Load at 0 ft (mg/ft^2 floor/ ft^2 disturbed)	34.93

Table I-155. Estimated Total Dust Emitted, Total Paint on Wall, and Emission Fraction in Experiment 59

Estimated Masses and Emission Fractions	Value
Total Mass of Dust on Floor (mg/ft^2 disturbed)	1,402
Total Paint Removed From Surface (mg/ft^2 disturbed)	10,973
Fraction Emitted	0.13

I.13. References for Appendix I

US EPA. (2007a). Draft final report on characterization of dust lead levels after renovation, repair, and painting activities. Prepared for EPA's Office of Pollution Prevention and Toxics (OPPT). Available online at: <http://www.epa.gov/lead/pubs/duststudy01-23-07.pdf>

Appendix J. Dust Model for Exterior Analysis

In order to estimate the time-dependent indoor dust loading arising from exterior renovation activities, a mechanistic model was developed to incorporate the relevant source and removal terms for lead in a typical indoor environment. The mechanistic model is designed to capture the physical transfer of mass from one medium to another under the assumption of mass balance. Previous studies have also built mass balance models of indoor dust. Allott et al. (1994) constructed a mass balance model to estimate the residence time of contaminated soil particles in the indoor environment based on observations in four homes in England contaminated by the Chernobyl incident. Thatcher and Layton (1995) constructed an indoor mass balance model of a home in California to estimate deposition rates, resuspension rates, and infiltration factors. Recognizing the key role of tracked-in soil on indoor dust loadings, Johnson (2008) built the DIRT model simulating the spatial pattern of tracked-in soil for a given total soil mass flux into the home. And Layton and Beamer (2009) built a model simulating tracked-in soil and penetration of outdoor air and the subsequent physical processes governing indoor dust loadings. The model here is a general set of equations that follows the same mass balance methods as in these papers.

The general form of the mass balance equation for a single compartment of interest is:

$$\frac{d[Mass]}{dt} = Flux\ of\ Mass\ In - Flux\ of\ Mass\ Out$$

where:

$d[Mass]/dt$	=	change over time of the mass
$Flux\ of\ Mass\ In$	=	flux of mass into the compartment
$Flux\ of\ Mass\ Out$	=	flux of mass out of the compartment

In the dust model, two “compartments” of interest are defined: the indoor air and the floor. Both of these compartments contain particulates associated with indoor dust, and by parameterizing the processes that govern the flux of mass to and from each compartment, the model can provide an inventory of dust in the air and on the floor through time.

The relevant sources and sinks of lead to the indoor dust for this Approach include:

- ambient air particles which penetrate the indoor environment and settle on the floor,
- outdoor soil particles which are tracked into the home, and

- the routine cleaning that remove lead from the floor.

Figure J-1 shows a schematic of the various lead and particulate mass flux terms used in the mechanistic model to account for all sources and sinks of lead.

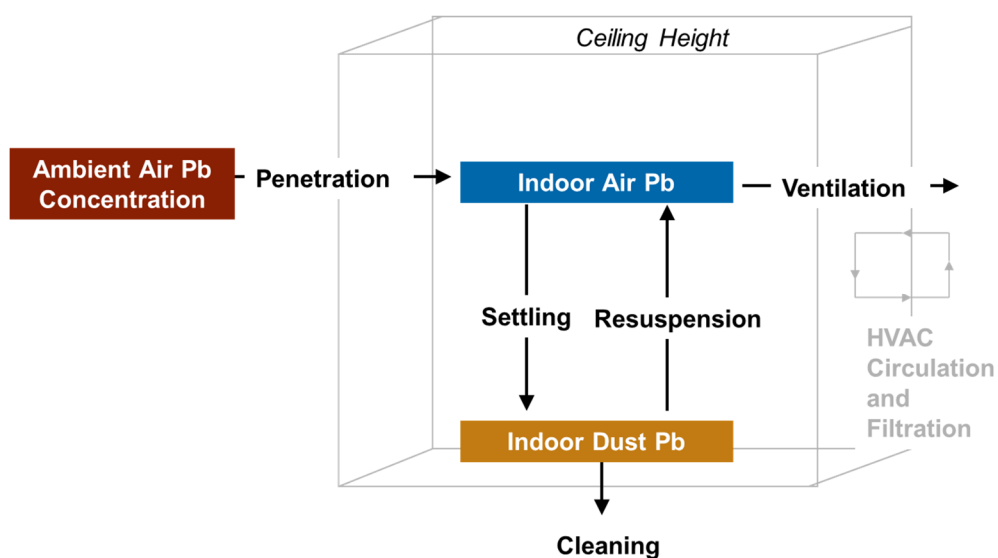


Figure J-1. Mechanistic Indoor Dust Model Schematic

For the indoor air compartment, the fluxes for mass include penetration of air and particles from outdoors, ventilation of indoor air back to the outdoor environment, deposition of mass out of the air, and resuspension of accumulated mass on the floor back into the air¹:

$$\frac{dINAIR_{Pb}}{dt} = Penetration Flux_{Pb} - Ventilation Flux_{Pb} - Deposition Flux_{Pb} + Resuspension Flux_{Pb}$$

¹ The presence of an HVAC system will tend to re-circulate indoor air, passing the air through a filter with each circulation. This system will tend to remove mass from the indoor environment (both in the air and on the floor) and act as a further sink. However, because the circulation rate and filtration efficiency of such systems has not been comprehensively described in the literature and because use of such systems changes across the seasons and different geographic regions, removal of mass during recirculation is not included in the mechanistic model.

where:

- $dINAIRPb/dt$ = change in time of the indoor air lead mass
- Penetration Flux* = penetration of lead-containing particles from outdoors
- Ventilation Flux* = ventilation of indoor air back to the outdoor environment
- Deposition Flux* = deposition of mass out of the air
- Resuspension Flux* = resuspension of mass back to the air

In general, each flux is parameterized as the mass of the "donor" compartment multiplied by the rate (expressed in reciprocal time) of the physical exchange process. In some cases, an efficiency factor is also included to account for the fractional efficiency of the removal process. For the Penetration Flux,

$$PenetrationFlux_{pb} = AER \times P \times PbAir \times V$$

where:

- Penetration Flux_{pb}* = penetration of air lead from outdoors ($\mu\text{g}/\text{h}$)
- AER* = air exchange rate (h^{-1})
- P* = penetration efficiency (unitless)
- PbAIR* = concentration of lead in ambient air ($\mu\text{g}/\text{m}^3$)
- V* = volume of the building (m^3)

Because the air exchange rate (*AER*) specifies the number of times the indoor air is replaced by outdoor air in a given hour, it represents both the rate of penetration in and ventilation out. The ventilation flux out of the building is thus given by:

$$VentilationFlux_{pb} = AER \times INAIR_{pb}$$

where:

- Ventilation Flux_{pb}* = ventilation of indoor lead in air back to the outdoor environment ($\mu\text{g}/\text{h}$)
- AER* = air exchange rate (h^{-1})
- INAIR_{Pb}* = indoor mass of lead in air (μg)

The deposition flux (Deposition Flux) is defined as the amount of mass in the air times a deposition rate:

$$DepositionFlux_{pb} = DepRate \times INAIR_{pb}$$

where:

<i>Deposition Flux_{pb}</i>	=	deposition of lead out of the air (µg/h)
<i>DepRate</i>	=	deposition rate (h ⁻¹)
<i>INAI_RP_b</i>	=	indoor mass of lead in air (µg)

So, using the penetration, ventilation, deposition fluxes, and indoor source terms, the equation for the change in time of the indoor air lead mass is:

$$\frac{dINAIR_{pb}}{dt} = AER \times P \times PbAIR \times V - AER \times INAIR_{pb} - DepRate \times INAIR_{pb}$$

where:

<i>dINAI_RP_b/dt</i>	=	change in time of the indoor air lead mass (µg/h)
<i>INAI_RP_b</i>	=	indoor mass of lead in air (µg)
<i>FLOORP_b</i>	=	mass of lead on the floor (µg)
<i>PbAIR</i>	=	concentration of lead in ambient air (µg/m ³)
<i>AER</i>	=	air exchange rate (hour ⁻¹)
<i>P</i>	=	penetration efficiency (unitless)
<i>V</i>	=	volume of the building (m ³)
<i>DepRate</i>	=	deposition rate (h ⁻¹)

For the indoor floor dust compartment (*FLOOR*), the fluxes include deposition of lead from the air onto the floor, resuspension of lead from the floor into the air, tracking of lead from outdoor soil, and removal of lead due to routine cleaning:

$$\frac{dFLOOR_{pb}}{dt} = Deposition Flux_{pb} + Tracking Flux_{pb} - Resuspension Flux_{pb} - Cleaning Flux_{pb}$$

where:

<i>dFLOOR/dt</i>	=	change in time of the indoor floor mass
<i>Deposition Flux</i>	=	deposition of mass out of the air onto the floor
<i>Tracking Flux</i>	=	tracking of soil inside from outdoors
<i>Resuspension Flux</i>	=	resuspension of mass back to the air
<i>Cleaning Flux</i>	=	removal of lead due to routine cleaning

The deposition flux (*Deposition Flux*) and resuspension flux (*Resuspension Flux*) retain the same form as in the *INAIR* equations.

The tracking flux (*Tracking Flux*) is parameterized specifically according to the limited data available about the process. Von Lindern (2003) measured the amount of particulate deposited on front mats in 276 houses in two locations near the Bunker Hill Superfund Site. The lead levels reported in the paper are expected to be high-end and are not expected to represent general population exposures. However, the assumption is made that the rate of accumulation of dust (as opposed to the lead in the dust) on doormats is not strongly affected by the location and can be used to represent a national population of homes. In addition, Thatcher and Layton (1995) measured the difference between particulate accumulation in tracked and untracked areas in the home as well as the amount on the front mat. From these two data sources, it is possible to estimate a distribution of mat particulate accumulation rates as well as the fraction of material that remains on the mat compared to being tracked into the home. For this reason, the tracking is parameterized as:

$$TrackingFlux_{Pb} = PbSoilConcen \times TrackingRate \times (1 - MatFrac)$$

where:

<i>TrackingFluxPb</i>	=	accumulation of tracked-in lead on the floor (µg/h)
<i>PbSoilConcen</i>	=	concentration of lead in the tracked-in soil (µg/g)
<i>TrackingRate</i>	=	rate at which particulate is deposited on front mats (g/h)
<i>MatFrac</i>	=	fraction of total tracked material which is deposited on the front mat (as opposed to the remainder of the building) (unitless)

The cleaning flux (*Cleaning Flux*) is parameterized assuming a cleaning efficiency (*CE*) and cleaning frequency (*CF*) and multiplying these by the mass on the floor (*FLOOR*):

$$CleaningFlux_{Pb} = CE \times CF \times FLOOR_{Pb}$$

where:

<i>Cleaning FluxPb</i>	=	removal of lead due to routine cleaning (µg/h)
<i>CE</i>	=	cleaning efficiency (unitless)
<i>CF</i>	=	cleaning frequency (cleanings/h)
<i>FLOORPb</i>	=	mass of lead on the floor (µg)

Combining the floor fluxes then gives:

$$\frac{dFLOOR_{Pb}}{dt} = DepRate \times INAIR_{Pb} - PbSoilConcen \times TrackingRate \times (1 - MatFrac) - CE \times CF \times FLOOR_{Pb}$$

where:

$dFLOOR_{Pb}/dt$	=	change in time of the indoor floor lead mass ($\mu\text{g}/\text{h}$)
$INAIR_{Pb}$	=	indoor mass of lead in air (μg)
$FLOOR_{Pb}$	=	mass of lead on the floor (μg)
$DepRate$	=	deposition rate (h^{-1})
$PbSoilConcen$	=	concentration of lead in the tracked-in soil ($\mu\text{g}/\text{g}$)
$TrackingRate$	=	rate at which particulate is deposited on front mats (g/h)
$MatFrac$	=	fraction of total tracked material which is deposited on the front mat (as opposed to the remainder of the building) (unitless)
CE	=	cleaning efficiency (unitless)
CF	=	cleaning frequency (cleanings/h)

The above equations can be converted to difference equations by assuming a discrete time step and the model can be integrated forward in time to describe the lead and particulate accumulation at any moment.

J.1. References for Appendix J

Allott et al 1994. A model of environmental behaviour of contaminated dust and its application to determining dust fluxes and residence times. *Atmospheric Environment*. (28) 4. 679-687.

Johnson D. (2008). A first generation dynamic ingress, redistribution, and transport model of soil track-in: DIRT. *Environ Geochemistry Health* 30: 589-596.

Layton D; Beamer P. (2009). Migration of contaminated soil and airborne particles to indoor dust. *Envir. Science and Technol.* 43: 8199-8205.

Thatcher T; Layton D. (1995). Deposition, resuspension, and penetration of particles within a residence. *Atmospheric Environment*. 29(13): 1487-1497.

von Lindern I; Spalinger S; Bero B; Petrosyan V; von Braun, M. (2003). The influence of soil remediation on lead in house dust. *Sci. Total Environ* 303(1-2): 59-78.

Appendices to the Approach for Estimating Exposures and Incremental Health Effects from Lead due to Renovation, Repair, and Painting Activities in Public and Commercial Buildings

Appendix K. Loading to Concentration Conversion

The indoor dust model provides an estimate of the lead loading in terms of mass of lead per square foot of floor. However, the selected biokinetic blood lead model, Leggett, cannot accept lead loadings as inputs. Instead, it requires lead concentrations, or the amount of lead per mass of ingested dust.

EPA previously analyzed the available evidence on the relationship between dust-lead loading statistics and dust-lead concentrations and developed an empirical approach that uses a regression relationship between dust-lead loading and dust-concentration measurements (US EPA, 2008c). A log-log model was fitted to data from HUD's National Survey of Lead-Based Paint in Housing ("HUD Survey Data"), which are provided in Appendix C-1 of EPA's risk assessment for TSCA Appendix 403 (US EPA, 1998).

EPA further considered the loading to concentration relationship when evaluating possible hazard standards for residences and public and commercial buildings in 2011. A mechanistic model and an empirical approach were presented and described in Appendix E of both documents. Based on SAB feedback, the empirical model was used.

Considering the previous use of and SAB preference for an empirical approach, EPA searched for additional data sources to supplement the HUD Survey Data. There were two goals of identifying additional data sources. The first was to determine if other data sources showed a similar relationship between lead dust loading and concentration, further validating use of this approach. The second was to increase the overall sample size and improve the overall fit of the regression.

Three data sources were pooled together to develop a more robust loading to concentration relationship. The HUD Survey data measured floor dust loadings based on vacuum samples and used an empirical equation to estimate the associated wipe loadings. It is anticipated that the wipe samples better capture the total lead present in the home; the vacuum samples are subject to vacuum collection efficiencies. Thus, the estimated wipe lead loadings were paired with the Blue Nozzle lead concentrations at each home to develop the loading-to-concentration statistical relationship. Blue Nozzle sampling is an older sampling technique, which assumes that the concentration is roughly uniform across all particles and the particles collected by the Blue Nozzle device are representative of the true average concentration. Summary statistics from HUD survey data are provided below in Table K-1. In general, the spread in the data is large and covers loadings up to 375 $\mu\text{g}/\text{ft}^2$ and concentrations up to 50,400 $\mu\text{g}/\text{g}$. (HUD et al 2002)

Table K-1. Statistics from the HUD survey data.

Statistic	Loading ($\mu\text{g}/\text{ft}^2$)	Concentration ($\mu\text{g}/\text{g}$)
Average	19.48	520
Min	0.51	0.09
Max	375.00	50,400
50th percentile	6.35	190

A study by Adgate et al in 1995 examined the relationship between dust loading, lead loading, and lead concentration in house dust in 216 homes in Jersey City, New Jersey. The total sample size was 444 data points. The data points from the scatterplot in Figure 7A were digitized using the GetData®; because some of the data points were located on top of each other, only 312 of the 444 data points were captured during the digitization. The R^2 in Adgate Figure 7A corresponding to the log/log relationship between lead loading and lead concentration was 0.65. Wipe samples were collected for lead loadings and were compared to dust concentrations collected by a vacuum cleaner from wall to wall carpet and area rugs greater than 48 square feet. The total amount of dust was adjusted for vacuum collection efficiency using an algorithm developed by Wang et al 1995. Summary statistics from the Adgate data are provided below in Table K-2. In general, the spread in the data is large and covers loadings up to 9,626.97 $\mu\text{g}/\text{ft}^2$ and concentrations up to 33,113.40 $\mu\text{g}/\text{g}$. (Adgate et al 1995)

Table K-2. Statistics from the Adgate data.

Statistic	Loading ($\mu\text{g}/\text{ft}^2$)	Concentration ($\mu\text{g}/\text{g}$)
Average	96.34	1,004.65
Min	0.38	18.64
Max	9,626.97	33,113.40
50th percentile	22.32	468.69

The Canadian House Dust Study (CHDS) collected dust samples from 1,025 homes across 13 cities and was designed to estimate nationally representative urban house dust metal concentrations and metal loadings. Trained technicians followed a vacuum sampling protocol to collect a composite sample of active dust from all dry living areas of each house. Participants were instructed not to clean for at least one week prior to sample collection. Fine ($<80 \mu\text{m}$) and coarse ($80\text{--}300 \mu\text{m}$) particle size fractions were collected and were combined to calculate loading values based on: measurements of the area sampled, dust mass, dust lead concentration, and time elapsed since cleaning (details in Rasmussen et al., 2013).

As area measurements were not available for three houses, the overall sample size for the loading calculation was 1,022. The distributions of metal loads obtained using the CHDS vacuum sampling protocol are consistent with population-based distributions obtained using wipe sampling methods from other studies. Summary statistics from the Canadian House are provided below in Table K-3. In general, the spread in the data is smaller and covers concentrations up to 7,800 ug/g (Rasmussen et al 2013).

**Table K-3. Statistics from the Canadian House
Dust Study**

Statistic	Loading ($\mu\text{g}/\text{ft}^2$)	Concentration ($\mu\text{g}/\text{g}$)
Average	2.88	210
Min	0.019	14.2
Max	89.4	7,800
50 th percentile	0.77	100

These three data sources were pooled together and an outlier analysis was conducted. Three outliers were detected and excluded from the pooled sample resulting in an overall sample size of 1,643. The summary statistics for the pooled data set are provided below in Table K-4.

Table K-4. Statistics for the Pooled Data Set

Statistic	Loading ($\mu\text{g}/\text{ft}^2$)	Concentration ($\mu\text{g}/\text{g}$)
Average	22.86	370.10
Min	0.019	2.01
Max	9,626.9	14,935.96
50 th percentile	2.02	137

From the raw data, each loading and concentration was transformed by taking the natural log, and the average of the natural log of the loadings across all data points was subtracted from each loading. The latter step re-centers the data and makes the estimated slope and intercept uncorrelated. A regression was performed on these data using the add-on Regression function in Excel® to calculate a predictive distribution as detailed in Qian (2010). The regression was used to calculate the degrees of freedom, slope, intercept, error variance, and estimated standard deviation of the slope and intercept using the following regression equation:

$$\ln(\text{Conc}) = \text{Intercept} + \text{Slope} * (\text{Adj } \ln(\text{Load})) + \text{ErrorVariance}$$

$$\text{where: Adj } \ln(\text{Load}) = \ln(\text{Load}) - \text{Average}(\ln(\text{Load}))$$

The regression modeling treated the lead data as a simple random sample and did not take the survey weights and survey design in the HUD data into account. Each individual measurement is assumed to give equal information about the relationship between loading and concentration. The results of the regression modeling are presented below in Table K-5.

Table K-5. Regression results for loading- concentration conversion.

Parameter	Value
Degrees of Freedom	1641
Intercept	5.145
Slope	0.421
Error variance	0.544
Estimated standard deviation (standard error) of intercept	0.018
Estimated standard deviation (standard error) of slope	0.009
R Square	0.55

The error variance term represents the true variability around the regression line, which captures the reality that a $\ln(\text{Load})$ can be associated with a range of $\ln(\text{Conc})$. Because the regression is calculated using 1643 concentration and loading data pairs, there is some uncertainty in the predicted intercept and slope, captured as the estimated standard deviation, or standard error, of the intercept and slope. However, both of these values were reduced when using the larger pooled data set when compared to using the HUD Survey data set alone. The standard error of the intercept was reduced from 0.04 to 0.018, the standard error of the slope was reduced from 0.05 to 0.009, and the R Square was improved from 0.465 to 0.55. The overall uncertainty and variability within the predicted $\ln(\text{Conc})$ is represented by the sum of the error variance (modeled as a chi-squared distribution) in the predicted intercept and the variance in the predicted slope (each represented by Normals). The Monte Carlo model samples from each distribution for each realization when converting from loading to concentration.

To bound the range of concentrations that the Monte Carlo model can predict from a known loading, 90 percent prediction intervals were calculated using a T-distribution with 1641 residual degrees of freedom (based on the full regression data set).

K.1. References for Appendix K

Adgate et al 1995. Lead in House Dust. Relationships between Exposure Metrics. Environmental Research (70) 134-147.

HUD (U.S. Department of Housing and Urban Development). (2002). National Survey of Lead and Allergens in Housing: Final Report, Revision 6. Office of Lead Hazard Control. October 31. Available at: <http://www.hud.gov/offices/lead/techstudies/survey.cfm#natsurvey>

Rasmussen et al (2013). Canadian House Dust Study: Population-based concentrations, loads and loading rates of arsenic, cadmium, chromium, copper, nickel, lead, and zinc inside urban homes. Science of the Total Environment 443 (2013) 520–529

Qian S. (2010). Environmental and ecological statistics with R. Chapman and Hall, Section 9.2

US EPA. (1998). Risk analysis to support standards for lead in paint, dust, and soil. Appendix G: Health effects associated with exposure to lead and internal lead doses in humans. (Report No. EPA 747-R-97-006). Washington, DC: US Environmental Protection Agency, Office of Pollution Prevention and Toxics. Available online at: <http://www.epa.gov/lead/pubs/toc.pdf>.

US EPA. (2008a). Economic analysis for the TSCA lead renovation, repair, and painting program Final Rule for Target Housing and Child-Occupied Facilities. Washington, DC: US Environmental Protection Agency, Office of Pollution Prevention and Toxics (OPPT).

US EPA. (2010a). Proposed approach for developing lead dust hazard standards for residences. SAB Consultation Draft. Washington, DC: US Environmental Protection Agency, Office of Pollution Prevention and Toxics (OPPT). Prepared for July 6-7, 2010 consultation

Appendix L. Estimates of Exposure Factors

L.1. Age Groups and Ages Within Each Group

For the analysis, a set of age groups were selected for which the different health effects would be estimated in aggregate. It was necessary to group together individuals of different ages in order to create a reasonable number of scenarios in the model. In order to ensure the age group was representative of the individual members, the groups were selected by examining the selected health effect papers to determine the population ages in the studies (Table L-1). In general, the age groups were selected to cover the populations in the different papers as best as possible. For low birth weight, additional consideration of the population distribution of maternal age at pregnancy in the United States was also considered. In addition, cohort distributions provided in the studies were considered to ensure that pertinent data were not excluded from the analysis.

Table L-1. Age Ranges in the Health Effect Study Subjects.

Health Effect and Study	Age Range of Study Subjects
IQ effects, Lanphear et al. 2005	0 to 10 years old
Low Birth Weight, Zhu et al. 2010	15 to 49 years old
Kidney effects, Navas-Acien et al. 2009	20 to 90 years old (NHANES population)
Cardiovascular disease mortality, Menke et al. 2006	20 to 90 years old (NHANES population)

Based on these considerations, the following age groups were selected to closely match the ages noted in the study population:

- Age 0-10: IQ effects
- Age 18-49: Low birth weight, kidney, and cardiovascular disease mortality effects
- Age 50-80: Kidney and cardiovascular disease mortality effects

The Monte Carlo model requires a cumulative probability distribution for each age group; that distribution is sampled during each iteration to determine the age of the person within the group for the blood lead and health effect calculations. The American Community Survey data from 2010-2012 (<http://www.census.gov/acs/www/>) were used to estimate these distributions. (ACS 2012) In each age group, the total population in that group was used to calculate the probability of occurrence of each age

in increments of years. Table L-2 and Table L-3 show the distributions for the children and adults, respectively.

Table L-2. Probability Distribution for Children.

Age	Population	Probability	Cumulative Probability
Age 0-10			
Under 1 year	3,728,928	0.08	0.08
1 Year	3,920,811	0.09	0.17
2 Years	4,070,061	0.09	0.26
3 Years	4,128,393	0.09	0.35
4 Years	4,177,518	0.09	0.45
5 Years	4,174,548	0.09	0.54
6 Years	4,062,915	0.09	0.63
7 Years	4,114,308	0.09	0.72
8 Years	4,016,352	0.09	0.81
9 Years	4,111,269	0.09	0.91
10 years	4,178,124	0.09	1.00

Table L-3. Probability Distributions for Adults

Age	Population	Probability	Cumulative Probability	Age	Population	Probability	Cumulative Probability
Age 18-49				Age 50-80			
18 years	4,597,878	0.03	0.03	50 years	4,826,172	0.05	0.05
19 years	4,374,663	0.03	0.07	51 years	4,464,354	0.05	0.10
20 years	4,782,129	0.04	0.10	52 years	4,463,964	0.05	0.15
21 years	4,694,160	0.03	0.14	53 years	4,377,144	0.05	0.20
22 years	4,375,500	0.03	0.17	54 years	4,385,244	0.05	0.25
23 years	4,171,068	0.03	0.20	55 years	4,360,065	0.05	0.29
24 years	4,029,537	0.03	0.23	56 years	4,115,214	0.04	0.34
25 years	4,379,898	0.03	0.26	57 years	4,024,680	0.04	0.38
26 years	4,178,904	0.03	0.29	58 years	3,875,571	0.04	0.42
27 years	4,217,025	0.03	0.32	59 years	3,729,201	0.04	0.46
28 years	4,204,608	0.03	0.35	60 years	3,872,127	0.04	0.51
29 years	4,147,719	0.03	0.38	61 years	3,541,116	0.04	0.55
30 years	4,462,401	0.03	0.42	62 years	3,519,627	0.04	0.58
31 years	4,111,062	0.03	0.45	63 years	3,495,222	0.04	0.62
32 years	4,117,977	0.03	0.48	64 years	3,272,820	0.04	0.66
33 years	3,916,908	0.03	0.51	65 years	3,017,097	0.03	0.69
34 years	3,896,793	0.03	0.53	66 years	2,613,507	0.03	0.72
35 years	4,093,446	0.03	0.56	67 years	2,604,534	0.03	0.75
36 years	3,826,857	0.03	0.59	68 years	2,503,611	0.03	0.77
37 years	3,887,709	0.03	0.62	69 years	2,354,469	0.03	0.80
38 years	4,013,214	0.03	0.65	70 years	2,246,490	0.02	0.82
39 years	4,039,923	0.03	0.68	71 years	1,995,159	0.02	0.85
40 years	4,633,614	0.03	0.72	72 years	1,925,682	0.02	0.87
41 years	4,197,336	0.03	0.75	73 years	1,838,373	0.02	0.89
42 years	4,178,478	0.03	0.78	74 years	1,696,614	0.02	0.91
43 years	4,072,578	0.03	0.81	75 years	1,667,943	0.02	0.92
44 years	4,109,589	0.03	0.84	76 years	1,548,294	0.02	0.94
45 years	4,323,045	0.03	0.87	77 years	1,453,188	0.02	0.96
46 years	4,333,803	0.03	0.90	78 years	1,368,168	0.01	0.97
47 years	4,454,691	0.03	0.93	79 years	1,317,393	0.01	0.99
48 years	4,510,179	0.03	0.97	80 years	1,317,870	0.01	1.00

For the low birth weight health effect, the effects are restricted to pregnant women and their newborns rather than the general population. The distribution for the general population between ages 18-50 is fairly uniform while the distribution for pregnancy peaks in the 20's and tapers significantly during the late 30's and 40's (**Error! Reference source not found.**, http://www.cdc.gov/nchs/data/nvsr/nvsr62/nvsr62_09.pdf).

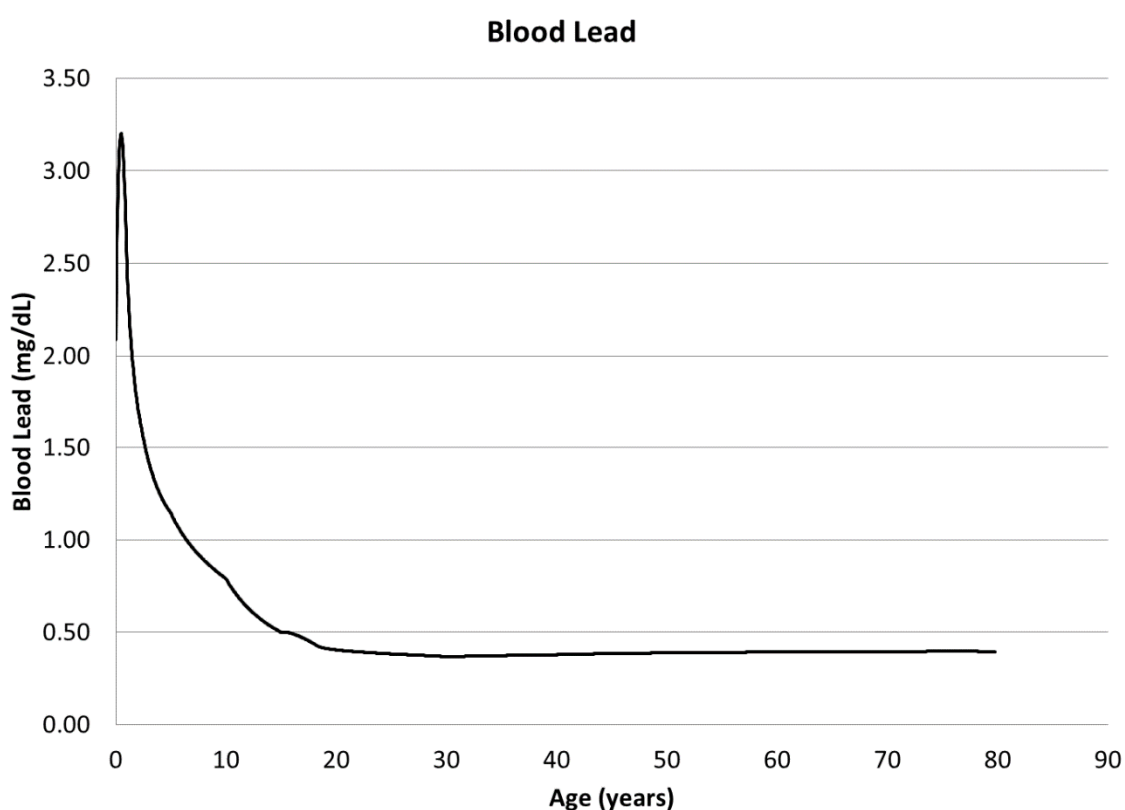


Figure L-1 Table L-4. Probability Distribution for Pregnancy by Age

Age	Probability	Cumulative Probability	Age	Probability	Cumulative Probability
18	0.0221	0.0221	34	0.0525	0.8475
19	0.0346	0.0567	35	0.0245	0.8719
20	0.0475	0.1042	36	0.0245	0.8964
21	0.0475	0.1516	37	0.0245	0.9209
22	0.0475	0.1991	38	0.0245	0.9453
23	0.0475	0.2466	39	0.0245	0.9698

24	0.0475	0.2941	40	0.0057	0.9754
25	0.0582	0.3523	41	0.0057	0.9811
26	0.0582	0.4105	42	0.0057	0.9868
27	0.0582	0.4687	43	0.0057	0.9925
28	0.0582	0.5269	44	0.0057	0.9981
29	0.0582	0.5851	45	0.0003	0.9985
30	0.0525	0.6376	46	0.0003	0.9988
31	0.0525	0.6900	47	0.0003	0.9991
32	0.0525	0.7425	48	0.0003	0.9994
33	0.0525	0.7950	49	0.0003	0.9997
34	0.0525	0.8475	50	0.0003	1.0000

However, the Leggett blood lead model does not predict significantly different blood lead values between age 20 and age 50. This is illustrated in Figure L-1 where the model was run with constant intakes at the current background level from birth to an age of 80. The model does not respond to intake significantly differently during the adult years. Owing to computational resource limitations, the low birth weight health effect distribution was simulated using the general population distribution (i.e., the same distribution used for the other adult health effects). However, because the blood leads do not vary significantly during this portion of adulthood, this assumption is not expected to dramatically affect the predicted distribution.

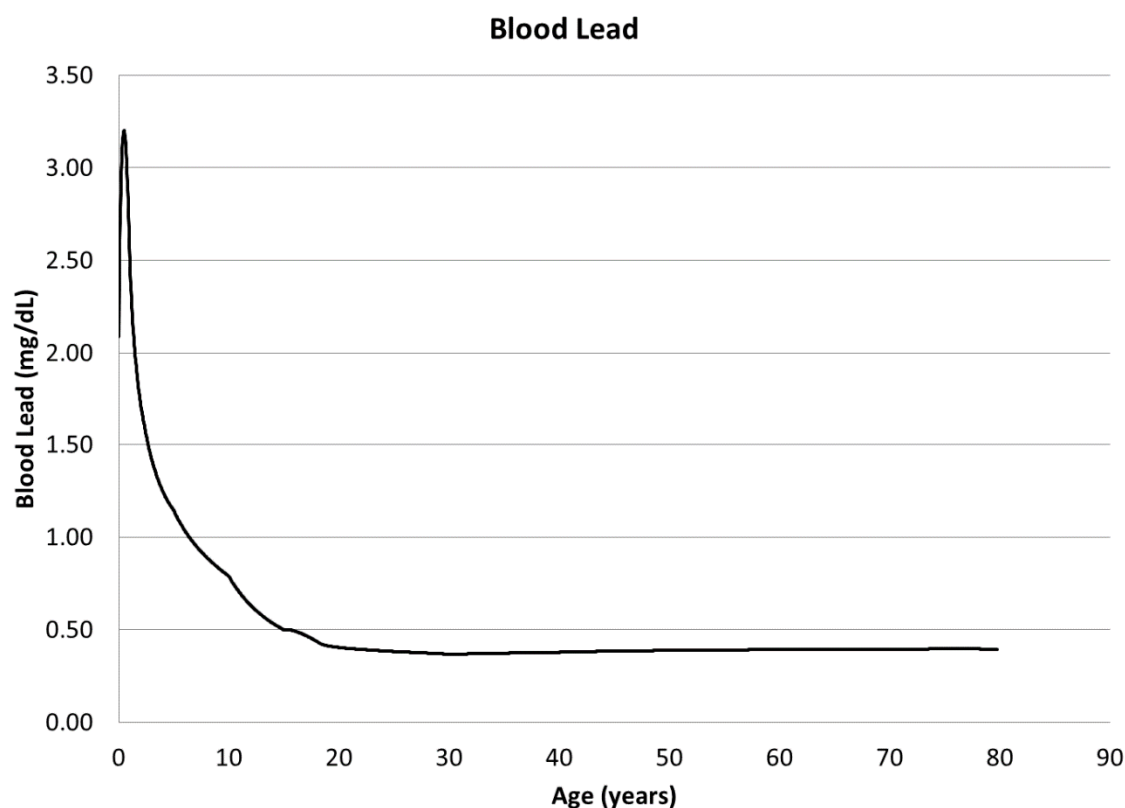


Figure L-1. Blood Lead Profile for an Individual with Constant Background Intake from Birth to Age 80 using Leggett model

L.2. Time Spent

The amount of time that children and adults spend in different types of Public and Commercial Buildings is highly variable and is a sensitive variable in estimating the exposure to lead from either an interior or exterior P&CB renovation activity. The Consolidated Human Activity Database (CHAD) contains the most robust human activity data available (CHAD). The CHAD database contains activity information from survey respondents who logged their whereabouts for one or multiple days. The database contains this information for individuals on different days and for people ranging from young children to adults.

The most up-to-date CHAD database was obtained on March 6, 2014. The database contains information from different surveys, and all data were used in the analysis. As a first step, an initial quality control step was performed. The number of unique entries in the database was determined to

be 1,901,301. The number of unique entries in the database after removing entries where field QCmiss > 60 (either activity or location is unknown for more than 1 hr/day) and field qcsleep is missing (no sleep time entered) was 1,633,914. The corresponding unique number of activity days captured in the database is 42,090.

Then, the location types in the CHAD database were mapped to the interior and exterior receptor building types. The mapping is shown in Table L-5 for interiors and

Table L-6 for exteriors. Other CHAD codes were not included in the analysis and generally covered individuals who were spending time traveling from one place to another or spending time outside. Then, percentiles were estimated for each age group and for each analysis category. The percentiles were rounded to the nearest 15-minute (quarter hour) increment; if a percentile was 0.0 hours per day, then it was rounded to 15 minutes to account for noise at the low percentiles. Finally, the data in hours per day were divided by 24 hours to give the average fraction of the day. Table L-7 and Table L-8 give the resulting hours per day and fractions for each percentile. In the Monte Carlo model, the percentiles were used as the cumulative distribution function and the fraction of the day values were sampled for each iteration and for each age group.

In estimating the percentiles, special consideration was given for “child occupied facilities” (COFs) which are defined as a “building, or a portion of a building, constructed prior to 1978, visited regularly by the same child, under 6 years of age, on at least two different days within any week, provided that each day’s visit lasts at least 3 hours, and the combined weekly visits last at least 6 hours, and the combined annual visits last at least 60 hours.” Daycare facilities and preschools are typically thought of as child-occupied facilities, but the definition above is not limited to only those types of buildings. Other types of public and commercial buildings qualify as child occupied facilities if all of the conditions in the definition are met. However, if any one of these conditions is not met, the building would not qualify as a child-occupied facility.

For children 5 and under, only the schools building category had a 50th percentile time spent of greater than 3 hours per days. Other building types exceeded 3 hours per day, but only at the upper percentiles. For children 5 and under, the upper and lower percentiles of the original distribution for the interior analysis categories were altered so that estimates tended toward the 50th percentile value and do not account for visits longer than 3 hours per day. This is the same as removing longer time spent values above the previously defined COF threshold.

Table L-5. Mapping from Interior Analysis Codes to CHAD Codes

Interior Building Type	CHAD Codes Mapped to Interior Building Type
1i: Office, Public assembly, Public safety, Religious Worship, Outpatient healthcare	32100 : Office building / bank / post office 33400 : At work : no specific location, moving among location
2i: Warehouse, Industrial, Agricultural, Supermarket	32200 : Industrial plant / factory / warehouse 32900 : Public building / library / museum / theater 32920 : Library / courtroom / museum / theater 33700 : At Church 32300 : Grocery store / convenience store
3i: Food sales, mall, strip mall, Services, Non-mall retail	32400 : Shopping mall / non-grocery store 32500 : Bar / night club / bowling alley 32510 : Bar / Night Club 32520 : Bowling alley 32600 : Repair shop 32610 : Auto repair shop /gas station 32620 : Other repair shop 32700 : Indoor gym / sports or health club 32910 : Auditorium, sport's arena / concert hall 33100 : Laundromat 33300 : Beauty parlor / barber shop / hair dresser's 33600 : At Restaurant 33900 : At Dry cleaners
4i : Education	33500 : At School
5i: Lodging, hospital	33200 : Hospital / health care facility / doctor's office 33800 : At Hotel /Motel

Table L-6. Mapping from Exterior Analysis Codes to CHAD Codes

Exterior Building Type	CHAD Codes Mapped to Exterior Building Type	
1e: Agricultural	36200 : Farm	
2e: Industrial	32200 : Industrial plant / factory / warehouse	
3e: Commercial/ Public/ Government	32100 : Office building / bank / post office 33400 : At work : no specific location, moving among locat 32900 : Public building / library / museum / theater 32920 : Library / courtroom / museum / theater 33700 : At Church 32300 : Grocery store / convenience store 32400 : Shopping mall / non-grocery store 32500 : Bar / night club / bowling alley 32510 : Bar / Night Club 32520 : Bowling alley 32600 : Repair shop	32610 : Auto repair shop /gas station 32620 : Other repair shop 32700 : Indoor gym / sports or health club 32910 : Auditorium, sport's arena / concert hall 33100 : Laundromat 33300 : Beauty parlor / barber shop / hair dresser's 33600 : At Restaurant 33900 : At Dry cleaners 33200 : Hospital / health care facility / doctor's office 33800 : At Hotel /Motel 34200 : Laboratory
4e: Schools	33500 : At School	
5e: Residences	30000 : Residence, General 30010 : Your Residence 30020 : Other's Residence 30100 : Residence, indoor 30120 : Your residence, indoor 30121 : Kitchen 30122 : Living room / family room 30123 : Dining room 30124 : Bathroom 30125 : Bedroom 30126 : Study / Office 30127 : Basement 30128 : Utility room / Laundry room 30129 : Other indoor 30130 : Other's residence, indoor 30131 : Other's Kitchen 30132 : Other's living room / family room 30133 : Other's Dining room 30134 : Other's Bathroom 30135 : Other's Bedroom 30136 : Other's Study / Office 30137 : Other's Basement	30138 : Other's utility room / laundry room 30139 : Other indoor 30200 : Residence, Outdoor 30210 : Your residence, Outdoor 30211 : Your residence - Pool, spa 30219 : Your residence - Other outdoor 30220 : Other's residence, outdoor 30221 : Other's residence - Pool, spa 30229 : Other's residence - Other outdoor 30300 : Garage 30310 : Indoor garage 30320 : Outdoor garage 30330 : Your garage 30331 : Your indoor garage 30332 : Your outdoor garage 30340 : Other's garage 30341 : Other's indoor garage 30342 : Other's outdoor garage 30400 : Other, residence 32810 : Childcare facility, house

Table L-7. Percentiles for Time Spent in Different Interior Building Types

Interior Analysis, Hours per Day																
PnCB Category	Under 5 years old, Percentiles								5-17 years old, Percentiles							
	5th	10th	25th	50th	75th	90th	95th	99th	5th	10th	25th	50th	75th	90th	95th	99th
1i	0.25	0.25	0.25	0.5	1.00	1.75	2.9	2.9	0.25	0.25	0.25	0.75	2.00	4.25	8.5	10
2i	0.25	0.25	0.5	1.25	2.5	2.9	2.9	2.9	0.25	0.25	1.00	2.00	3.00	4.5	5.5	8.25
3i	0.25	0.25	0.5	1.00	1.75	2.9	2.9	2.9	0.25	0.25	0.5	1.25	2.25	3.75	5.00	7.75
4i	0.25	1.00	2.75	2.9	2.9	2.9	2.9	2.9	1.00	3.00	5.00	6.5	7.25	8.00	9.0	10.25
5i	0.25	0.5	0.5	1.00	1.75	2.9	2.9	2.9	0.25	0.5	0.75	1.5	5.00	8.75	10.00	13.5
PnCB Category	18-49 years old, Percentiles								50 years old and above, Percentiles							
	5th	10th	25th	50th	75th	90th	95th	99th	5th	10th	25th	50th	75th	90th	95th	99th
1i	0.25	0.75	3.75	7.75	8.75	9.75	10.5	12.75	0.25	0.5	2.0	6.0	8.5	9.5	10.25	12
2i	0.25	0.25	0.5	1.25	3.25	8.25	9.25	11.75	0.25	0.25	0.5	1.25	2.5	4.5	7.25	10
3i	0.25	0.25	0.75	1.25	2.75	5.25	8	11.25	0.25	0.25	0.75	1.25	2.0	3.5	4.75	9.0
4i	0.25	0.25	0.75	3.0	6.75	8.25	9.25	11.75	0.25	0.25	1.0	2.25	6.75	8.5	9.0	10.75
5i	0.25	0.5	1.0	2.5	8.25	10.25	12.0	15.0	0.25	0.5	0.75	1.5	3.75	8.25	9.5	13.5
Interior Analysis, Fraction of Week																
PnCB Category	Under 5 years old, Percentiles								5-17 years old, Percentiles							
	5th	10th	25th	50th	75th	90th	95th	99th	5th	10th	25th	50th	75th	90th	95th	99th
1i	0.01	0.01	0.01	0.02	0.04	0.07	0.12	0.12	0.01	0.01	0.01	0.03	0.08	0.18	0.35	0.42
2i	0.01	0.01	0.02	0.05	0.10	0.12	0.12	0.12	0.01	0.01	0.04	0.08	0.13	0.19	0.23	0.34
3i	0.01	0.01	0.02	0.04	0.07	0.12	0.12	0.12	0.01	0.01	0.02	0.05	0.09	0.16	0.21	0.32
4i	0.01	0.04	0.11	0.12	0.12	0.12	0.12	0.12	0.08	0.13	0.21	0.27	0.30	0.33	0.38	0.43
5i	0.01	0.02	0.02	0.04	0.07	0.12	0.12	0.12	0.01	0.02	0.03	0.06	0.21	0.36	0.42	0.56
PnCB Category	18-49 years old, Percentiles								50 years old and above, Percentiles							
	5th	10th	25th	50th	75th	90th	95th	99th	5th	10th	25th	50th	75th	90th	95th	99th
1i	0.01	0.03	0.16	0.32	0.36	0.41	0.44	0.53	0.01	0.02	0.08	0.25	0.35	0.40	0.43	0.50
2i	0.01	0.01	0.02	0.05	0.14	0.34	0.39	0.49	0.01	0.01	0.02	0.05	0.10	0.19	0.30	0.42
3i	0.01	0.01	0.03	0.05	0.11	0.22	0.33	0.47	0.01	0.01	0.03	0.05	0.08	0.15	0.20	0.38
4i	0.01	0.01	0.03	0.13	0.28	0.34	0.39	0.49	0.01	0.01	0.04	0.09	0.28	0.35	0.38	0.45
5i	0.01	0.02	0.04	0.10	0.34	0.43	0.50	0.63	0.01	0.02	0.03	0.06	0.16	0.34	0.40	0.56

Table L-8. Percentiles for Time Spent in Different Exterior Building Types

Exterior Analysis, Hours per Day																
PnCB Category	Under 5 years old, Percentiles								5-17 years old, Percentiles							
	5th	10th	25th	50th	75th	90th	95th	99th	5th	10th	25th	50th	75th	90th	95th	99th
1e	0.10	0.20	0.60	1.20	2.00	2.40	2.90	2.90	0.50	0.50	1.00	1.75	3.25	4.25	4.50	7.50
2e	0.30	0.30	0.30	0.30	0.50	0.60	0.60	0.60	0.25	0.25	0.25	0.75	3.25	4.50	8.00	8.00
3e	0.30	0.40	0.80	1.40	2.50	3.80	4.70	7.90	0.25	0.25	1.00	2.00	3.25	5.25	6.50	10.25
4e	0.70	1.80	3.30	5.80	8.40	9.50	9.90	11.00	2.00	3.00	5.25	6.50	7.25	8.25	9.00	10.50
5e	13.90	15.60	19.00	21.50	23.40	24.00	24.00	24.00	12.50	13.75	15.75	19.00	22.00	23.75	24.00	24.00
PnCB Category	18-49 years old, Percentiles								50 years old and above, Percentiles							
	5th	10th	25th	50th	75th	90th	95th	99th	5th	10th	25th	50th	75th	90th	95th	99th
1e	0.25	0.25	1.00	3.00	8.75	11.75	13.00	16.00	0.25	0.50	0.75	2.50	4.75	8.25	8.75	15.50
2e	0.25	0.50	4.00	8.25	9.00	10.50	11.25	12.75	0.25	0.50	3.25	8.25	9.00	10.00	11.00	13.75
3e	0.25	0.75	1.75	4.50	8.75	10.25	11.25	14.50	0.50	0.75	1.50	3.25	7.50	9.50	10.50	13.25
4e	0.00	0.00	0.75	2.75	6.50	8.25	9.00	12.25	0.00	0.25	1.00	2.25	6.75	8.50	9.00	10.50
5e	9.75	11.25	13.25	16.25	20.75	23.00	24.00	24.00	11.00	12.50	14.75	19.50	22.50	24.00	24.00	24.00
Exterior Analysis, Fraction of Week																
PnCB Category	Under 5 years old, Percentiles								5-17 years old, Percentiles							
	5th	10th	25th	50th	75th	90th	95th	99th	5th	10th	25th	50th	75th	90th	95th	99th
1e	0.01	0.01	0.03	0.05	0.08	0.10	0.12	0.12	0.02	0.02	0.04	0.07	0.14	0.18	0.19	0.31
2e	0.01	0.01	0.01	0.01	0.02	0.03	0.03	0.03	0.01	0.01	0.01	0.03	0.14	0.19	0.33	0.33
3e	0.01	0.02	0.03	0.06	0.10	0.16	0.20	0.33	0.01	0.01	0.04	0.08	0.14	0.22	0.27	0.43
4e	0.03	0.08	0.14	0.24	0.35	0.40	0.41	0.46	0.08	0.13	0.22	0.27	0.30	0.34	0.38	0.44
5e	0.58	0.65	0.79	0.90	0.98	1.00	1.00	1.00	0.52	0.57	0.66	0.79	0.92	0.99	1.00	1.00
PnCB Category	18-49 years old, Percentiles								50 years old and above, Percentiles							
	5th	10th	25th	50th	75th	90th	95th	99th	5th	10th	25th	50th	75th	90th	95th	99th
1e	0.01	0.01	0.04	0.13	0.36	0.49	0.54	0.67	0.01	0.02	0.03	0.10	0.20	0.34	0.36	0.65
2e	0.01	0.02	0.17	0.34	0.38	0.44	0.47	0.53	0.01	0.02	0.14	0.34	0.38	0.42	0.46	0.57
3e	0.01	0.03	0.07	0.19	0.36	0.43	0.47	0.60	0.02	0.03	0.06	0.14	0.31	0.40	0.44	0.55
4e	0.01	0.01	0.03	0.11	0.27	0.34	0.38	0.51	0.01	0.01	0.04	0.09	0.28	0.35	0.38	0.44
5e	0.41	0.47	0.55	0.68	0.86	0.96	1.00	1.00	0.46	0.52	0.61	0.81	0.94	1.00	1.00	1.00

L.3. Length of Time Between Renovation and Blood Lead Measurement

In the Approach, all renovation activities are assumed to occur in 2014 so that incremental health effects could be aggregated and attributed to renovation activities in a given year. The Approach samples the population age distribution discussed in Section L.1 to determine the individual's age at the time of renovation. Based on that age, the individual's birth year (relative to 2014) is calculated, and they are assigned the correct background intake profile to match that birth year.

To be consistent with the methods in the health effect papers, blood lead and health effect status was determined at a specific point in time post-renovation. Similar to the NHANES survey (on which some of the health effect studies are based), it is assumed in the Approach assumes that the health effect risk is based on this single point estimate of blood lead.

People tend to enter different public and commercial buildings numerous times each week, and they will encounter numerous public and commercial building renovations over the period of their lives. In this Approach, it is not feasible to try to model every renovation; the possible combinations of buildings and ages during the renovation are nearly infinite and cannot be incorporated into the model. Instead, the Approach models the most recent renovation that occurred in a building with lead-containing paint.

Thus, the Approach assumes that a given person enters a given public and commercial building as part of their day-to-day activities. They may spend either a large or small amount of time in the building, and that will be accounted for separately in the "time spent" variable. That one given building will be renovated using different activities with varying frequency. To quantify the frequency, the Approach uses the 2011 RSMeans Facilities Maintenance & Repair Cost Data (Mossman and Plotner 2011). The RSMeans data book includes information on the frequency (in years) for a variety of systems, including interior finishes, exterior closures, plumbing, HVAC, electrical systems, and window and door replacements. We decided to consider a range of years for each event type because the number of years can vary widely based on material and size. For example, the frequency of painting concrete block walls (exteriors) is every 25 years; however, finished wood shingles (exteriors) are painted every 5 years.

Table L-9. Frequency of Renovations in Commercial and Public Buildings, by Event Type

presents the range of frequencies, by event type, for selected data from RSMeans. The total annual frequency of exposure from renovations in public and commercial buildings was calculated in two different ways. To calculate the numbers in the first total row we assumed that the probability of performing each renovation activity is independent of the probabilities of performing the other renovation activities. For example, we assume that the probability of replacing pipes is independent of the probability that walls are repainted. Thus, if the annual frequency of interior painting is 0.2 and the annual frequency of replacing pipes is 0.01, the probability of doing either of these jobs in a given year is the sum of the two annual frequencies, or 0.21. However, it may be more realistic to assume that the probabilities of performing different renovation activities are not independent. For example, if the wall must be disturbed to replace pipes it's a good time to repaint the room at the same time. The second total row in

Table L-9. Frequency of Renovations in Commercial and Public Buildings, by Event Type

accounts for this by taking the most frequent interior activity and assuming that the less frequent interior activities will be performed at the same time as the most frequent activity. For example, if interior painting is done every 4 years and HVAC systems are replaced every 20 years, we assume that the building owner will choose to coincide the HVAC replacement with one of the painting events, so the HVAC will be replaced at the same time as the interior painting (i.e., pipes are replaced at the same time as every 5th interior painting job).

As shown in

Table L-9. Frequency of Renovations in Commercial and Public Buildings, by Event Type

, the annual renovation frequency is estimated to be between 0.24 and 0.70. In other words, the average person will be exposed to renovations that may disturb lead-based paint between every 1.4 to 4.2 years.

However, the person in question is assumed to be present during the renovation and their blood lead is measured at some later date. As a proxy for when a person's blood is measured, it is assumed in the Approach that the person will have been in a building being renovated at least within the last 4.2 years. In reality, they enter numerous buildings that each may or may not have lead based paint and that may or may not have been recently renovated. However, the assumption that a renovation happened at least 4.2 years ago states that "the person enters at least one public and commercial building that contains lead-based paint, and that building was renovated sometime within the last 4.2 years'.

To implement this assumption in the Approach, the renovation is always assumed to occur in 2014. Then, the concurrent blood lead is recorded at nine different time periods after the renovation: 1 month, 5 months, 10 months, 15 months, 20 months, 25 months, 30 months, 40 months, and 50 months, where 50 months is approximately 4.2 years. This sampling pattern is shown in Figure L-2 in the top panel. Capturing all the different time periods allows analysis of the health effects over the range of assumed time periods since the renovation.

Table L-9. Frequency of Renovations in Commercial and Public Buildings, by Event Type

Event	Frequency (in Years)		Annual Frequency	
	Low	High	Low	High
Interior Painting	5	4	0.2	0.25
Exterior Painting	25	5	0.04	0.20
Replace plumbing pipes and fixtures	75	10	0.01	0.10
Replace HVAC Systems	75	20	0.01	0.05
Replace Electrical System and Fixtures	20	20	0.05	0.05
Window and Door Replacement Events	60	20	0.02	0.05
TOTAL (Assuming Renovation Types are Performed Separately)	3.0^a	1.4^b	0.33^a	0.70^b
TOTAL (Assuming Renovation Interior Activities are performed together and Exterior Activities are performed together. For example, HVAC and other interior activities are performed at the same time as interior repainting; window replacement and other exterior activities are performed at the same time as exterior repainting).	4.2^c	2.2^d	0.24^c	0.45^d
<p>a. The 0.33 total annual frequency is calculated by summing the annual frequencies of the individual events above (0.2+0.04+0.01+0.01+0.05+0.02=0.33). The annual frequency is converted to a frequency in years by taking its reciprocal (1/0.33=3).</p> <p>b. The 0.70 total annual frequency is calculated by summing the annual frequencies of the individual events above (0.25+0.2+0.1+0.05+0.05+0.05=0.7). The annual frequency is converted to a frequency in years by taking its reciprocal (1/0.7=1.4).</p> <p>c. The 0.24 total annual frequency is calculated by summing the most frequent interior activity frequency (0.2) and the most frequent exterior activity frequency (0.04) annual frequencies of the individual events above (0.2+0.04=0.24). The annual frequency is converted to a frequency in years by taking its reciprocal (1/0.24=4.2).</p> <p>d. The 0.45 total annual frequency is calculated by summing the most frequent interior activity frequency (0.25) and the most frequent exterior activity frequency (0.2) annual frequencies of the individual events above (0.25+0.2=0.45). The annual frequency is converted to a frequency in years by taking its reciprocal (1/0.45=2.2).</p>				

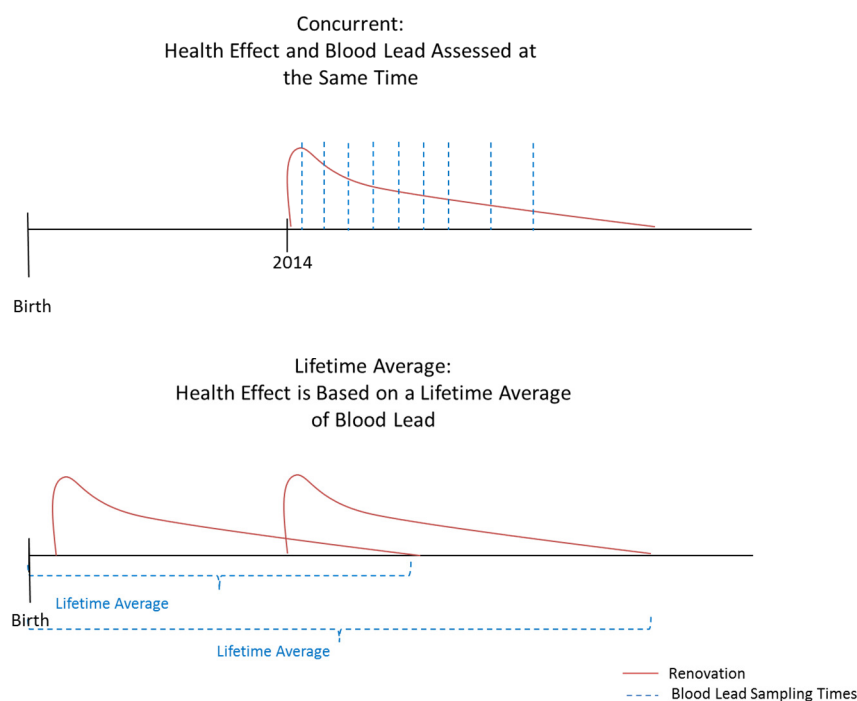


Figure L-2. Diagram of Concurrent and Lifetime Average Blood Lead Metrics in the Approach

As an additional blood lead metric, the lifetime average blood lead is also estimated for each iteration and age group. This lifetime average is defined as the average from birth until the post-renovation time when blood lead returns to the background value. This metric, rather than being a biologically-based metric, is an exposure-based one. Because the health effect studies and other literature do not provide information on a biologically relevant window of susceptibility for the health effects, the exposure-based lifetime average definition is used as a surrogate. This lifetime average is depicted in the lower panel of Figure L-2.

L.4. Exposure Factors for Lead Renovation Intake Estimates

The Leggett model requires intakes as inputs rather than media concentrations. To convert the renovation-related media concentrations to intakes for each age group, the following equations were used:

$$OralIntake = DustSoilIngestRate \times (1 - FracSoil) \times DustConcen$$

$$InhalIntake = VentilationRate \times AirConcen$$

where:

<i>OralIntake</i>	=	oral intake of renovation-related dust ($\mu\text{g}/\text{day}$)
<i>DustSoilIngestRate</i>	=	ingestion rate of dust and soil per day (g/day)
<i>FracSoil</i>	=	fraction of dust and soil intake that is soil
<i>DustConcen</i>	=	lead concentration in dust ($\mu\text{g}/\text{g}$)
<i>InhallIntake</i>	=	inhalation intake of renovation-related particulate ($\mu\text{g}/\text{day}$)
<i>VentilationRate</i>	=	inhalation rate of air (m^3/day)
<i>AirConcen</i>	=	lead concentration in air ($\mu\text{g}/\text{m}^3$)

Table L-10 shows the values used for the exposure factors in the Approach. It also shows the absorption fraction used in the Leggett model to determine how much of the oral intake enters the blood stream.

Table L-10. Exposure Factors Used in Approach

Parameter	Source	0-1	1-2	2-3	3-4	4-5	5-6	6-7	7-10	18-80
Soil and Dust Ingestion Rate (g/day)	Exposure Factors Handbook (US EPA, 2011)	0.06	0.1	0.1	0.1	0.1	0.1	0.1	0.1	0.05
Fraction of soil and dust ingestion that is soil	Exposure Factors Handbook (US EPA, 2011)	0.45								
Ventilation Rate (m^3/day)	Exposure Factors Handbook (US EPA, 2011)	5.4	8	9.5	10.9	10.9	10.9	12.4	14.4	13.3
Absorption Fraction in Leggett Model	Leggett (1993)	0.45	0.3	0.3	0.3	0.3	0.3	0.3	0.3	0.15

L.5. References for Appendix L:

American Community Survey ACS 2012. Estimates of US Population by Age. Available online at <http://www.census.gov/acs/www/>

Lanphear BP, Hornung R, Khoury J, et al. (2005). Low-level environmental lead exposure and children's intellectual function: an international pooled analysis. *Environ Health Perspect*, 113, 894–9.

Leggett RW. (1993). An age-specific kinetic model of lead metabolism in humans. *Environmental Health Perspectives* 101:598–616.

Menke et al (2006). Blood lead below 0.48 micromol/L (10 microg/dL) and mortality among US adults. *Circulation*. 114:1388–1394.

Mossman M; Plotner S; Babbitt C; Baker T; Balboni B, Eds. (2011). RSMMeans Facilities Construction Cost Data

Navas-Acien et al (2009). Blood Cadmium and Lead and Chronic Kidney Disease in US Adults: A Joint Analysis. *Am. J. Epidemiol.* (2009) 170 (9): 1156-1164.

US EPA, 2011. Exposure Factors Handbook. Available at <http://www.epa.gov/ncea/efh/pdfs/efh-complete.pdf>.

Zhu et al (2010). Maternal Low-Level Lead Exposure and Fetal Growth. *Environmental Health Perspectives*. Volume 118. Number 10.

Appendix M. Updates to the Leggett Model

The Leggett biokinetic model (Leggett, 1993) synthesized a wide variety of sometimes disparate sources of information related to the biokinetics of lead in humans. The Leggett model was informed by:

1. Lead tracer studies of injection, ingestion, and inhalation in healthy adult humans,
2. Measurements of lead in environmentally exposed men, women, and children at autopsy,
3. Lead mass-balance studies on adult humans,
4. Bioassay and autopsy measurements on occupationally exposed subjects,
5. Lead studies in laboratory animals at different life stages
6. Experimental, occupational, environmental, and medical data on the biokinetics of elements that serve as physiological analogues of lead, and
7. Basic physiological information on the human body.

As such, the Leggett model structure is a minimal system of body compartments and mass exchange terms needed to synthesize all these data sets. The modular form of the model allows investigators to modify specific parameter values to address special problems in lead toxicology or to incorporate new information related to lead biokinetics. The original Leggett model included:

- a. **Input file:** an ASCII input file containing information describing the lead exposure scenario and the age-dependent lead transfer rates for each compartment, and
- b. **Model code:** an executable FORTRAN program which reads the input file and performs the prescribed calculations, and writes the outputs to an ASCII file.

This approach was designed to provide maximum flexibility and versatility rather than user-friendliness.

The original Leggett model has, on several occasions, been translated onto other software platforms or into other programming languages. These adaptations include porting the FORTRAN code to a C++ version by Michael Korsch (personal communication), a MatLab version (LeggettPlus) by the OEHHA (2013), and Excel scripts to support an exposure module by ICF and SRC (personal communication). In each case, these adaptations were undertaken to provide a more user friendly interface or to support iterative analyses.

In addition, the original FORTRAN code has been changed to create four distinct versions of the model, and these versions have been distributed to researchers in academia and government (e.g. EPA) upon

request. It is important to note that these four FORTRAN versions did not alter the algorithms and equations of the model itself, but rather facilitate output of new variables:

- **Version 1:** ICRPv001.FOR added line#53 in the input file and added a module to the FORTRAN code for chelation (R. Leggett, 1996)
- **Version 2:** ICRPv002.FOR created output options to convert CRTCON and TRBCON (μg lead/g wet bone) to CORTCONBM and TRBCONBM (μg lead/g bone mineral) to better simulate XRF measurements of bone lead (J. Pounds, 1997)
- **Version 3:** ICRPv003.FOR converted output time from DAYS to YEARS (J. Pounds, 1997)
- **Version 4:** ICRPv004.FOR added output options for UPTAKEGI, UPTAKERI, UPTAKE and added additional output precision to YEARS (J. Pounds and R. Leggett, 1997).

With respect to bone (the storage site of lead in the body), the Leggett model includes a series of compartments that exchange lead mass with plasma. This compartmental structure includes more exchange compartments than other existing models, as shown in Figure M-1. The transfer rates help determine the relative storage of lead in the bone and the overall half-life of lead in the body. Thus, these parameter values are highly sensitive variables.

The Approach requires accurate simulation of both children and adult blood lead values at typical background exposure levels and over short-term renovation related changes. Thus, as part of the development of this Approach, Version 4 (ICRPv004.FOR) of the original Leggett Lead Model (Leggett, 1993) was updated to Version 5 (ICRPv005.FOR) by J. Pounds to resolve some limitations of the original model and to incorporate new input data available in the literature. The tasks undertaken included:

1. Scaling tissue lead concentrations for children and adolescents,
2. Evaluating and updating bone lead transfer rates, and
3. Evaluating and calibrating the model using human data sets for children and adults.

These updates were undertaken so that the model remains backward-compatible with existing input files. That is, when possible, only the parameter values in the model input file (*.DAT) were modified. If necessary, FORTRAN code was updated, or both the code and the default input file were edited to incorporate the changes. In instances for which reliable data were not available and thus required judgment, the minimal numerical changes from the original Leggett model were employed. The changes are discussed in detail below, and the FORTRAN code with an example input file (*.DAT) are provided as attachments.

The California Office of Environmental Health Hazard Assessment (OEHHA) also recently revisited the Leggett model (OEHHA, 2013), building the “Leggett Plus” model. Their changes were reviewed and considered during this effort. However, because their focus was on adult occupational exposure, additional changes were made to ensure model appropriateness for the hypothetical individuals (children and adults experiencing typical non-occupational background lead exposure with the addition of a short-term renovation-related increase in lead exposure) being considered in this present analysis.

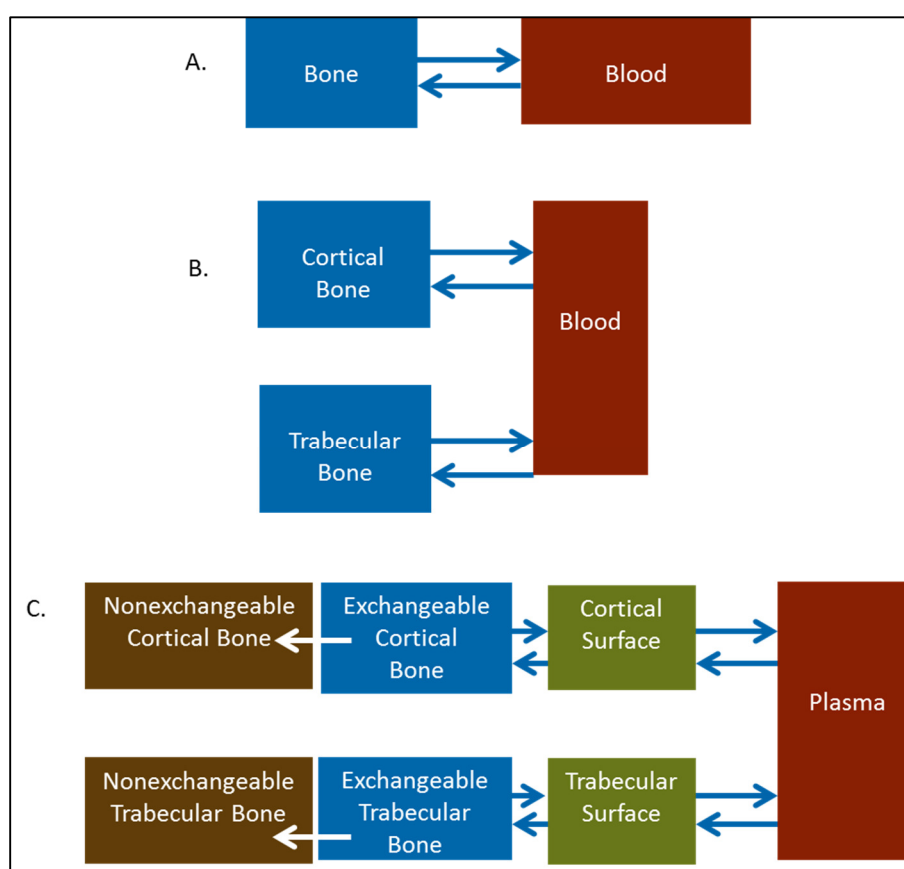


Figure M-1. The Skeletal and blood compartments of representative biokinetic models for lead metabolism in humans. a). Rabinowitz et al. 1983; b) Nie et al. 2005, c) Leggett, 1993.

M.1. Scaling Model Parameters for Children

The Leggett model is a mass-balance model, meaning it keeps track of the input, movement, and output of lead from the body. In order to estimate concentrations for each simulated body compartment (e.g., blood lead), the lead mass (μg) in each compartment is divided by the age-dependent volume (or weight) of the compartment. In the original Leggett model, some tissue volumes were limited to adult

values. Thus, although some tissue concentrations were calculated for all ages, some outputs were only valid for adults. For the new version of the Leggett model that is presented here, the kidney mass (KIDWT), total skeletal mass (TSKELWT), fraction of skeletal mass that is trabecular bone (FRTRAB), trabecular bone mass (TTRABWT), cortical bone mass (TCORTWT), red blood cell volume (RBCVOL), and plasma volume (PLSVOL) were updated to allow lead concentrations to change from birth to adulthood. The RBC saturation values were also revisited as discussed below. The revisions for scaling consisted of

1. Identifying age-dependent tissue volumes/weights at 14 different ages from birth to 75 years of age, and
2. Editing the FORTRAN code to read these values and interpolate to ages that are not explicitly defined consistent with the interpolation approach used by the Leggett model (1993).

M.1.1. Kidney mass, total skeletal mass, red blood cell volume, and plasma volume

Not all tissues are scaled for children in the Leggett versions 1-4. Thus, model outputs for lead concentration in these tissues are only valid for adults. The age-dependent compartmental volumes for kidney, total skeleton, red blood cell, and plasma were estimated using values in ICRP Publication 89 “Basic Anatomical and Physiological Data for Use in Radiological Protection Reference Values” (Valentin, 2002). The kidney and skeletal values were used directly while the red blood cell and plasma volumes were estimated from age-dependent hematocrit and total blood values. In each case, the age-dependent values for males were selected. This selection was done to provide consistency with parameter selection in original Leggett model (Leggett, 1993) which evolved from the ICRP model for radioisotopes of lead in the workplace. The implementation of gender-dependent computation and outputs is beyond the scope of the present effort. The implementation of gender-dependent computation and outputs is beyond the scope of the present effort. The most critical limitation of the updated Leggett model with respect to gender is during and menopause; that is, the current version of the Leggett model (like all previous versions) does not consider gender dependent changes in bone mass, bone mineral metabolism, and skeletal mass during adolescence and menopause. The Leggett-93 approach is justified by the poor availability of experimental studies on lead kinetics in females compared to males. The consequence of applying the Leggett models to simulate blood lead concentrations in females has not been evaluated. Such evaluation would require information describing gender-dependent lead intake and uptake in addition to age-dependent physiological data.

The updated compartmental volume values were hard-coded into the FORTRAN code at specific ages, and linear interpolation was performed between the age bins to determine intermediate values consistent with Leggett model handling of age-dependent parameters. The updated parameter values are shown in Table M-1.

M.1.2. Fraction of Skeleton that is Trabecular Bone

The age-dependent trabecular and cortical bone volumes were estimated using the total skeletal volumes and multiplying by an age-dependent fraction that accounts for the fraction of the skeleton that is trabecular bone. Infants are born with nearly all of their body consisting of trabecular bone while adult's trabecular bone is approximately 20% of skeletal mass (Brinckmann et al., 2002). An extensive literature search was undertaken, but reliable, age-dependent changes between these two extremes with age could not be located. In the absence of such information, it was assumed that the body is half trabecular and half cortical bone at age 5 (Brinckmann et al. 2002) and the other values were interpolated to get the full distribution with age. The values are shown in Table M-1.

Table M-1. Updated Age-Dependent Model Compartment Volumes

Age (yr)	Kidney Mass (g)	Skeletal Mass (g)	Fraction Skeleton that is Trabecular	Total Blood Volume (dL)	Hematocrit	Red Blood Cell Volume (dL)	Plasma Volume (dL)
0	25	370	0.95	2.7	0.575	1.55	1.15
0.27	36	642	0.90	3.1	0.37	1.15	1.95
1	70	1170	0.85	5	0.35	1.75	3.25
5	110	2430	0.50	14	0.38	5.32	8.68
10	180	4500	0.34	24	0.38	9.12	14.88
15	250	7950	0.23	45	0.4	18.00	27.00
18	310	10500	0.20	53	0.42	22.26	30.74
24	310	10500	0.20	53	0.45	23.85	29.15
30	310	10500	0.20	53	0.45	23.85	29.15
40	310	10500	0.20	53	0.45	23.85	29.15
45	310	10500	0.20	53	0.45	23.85	29.15
55	310	10500	0.20	53	0.45	23.85	29.15
65	310	10500	0.20	53	0.45	23.85	29.15
75	310	10500	0.20	53	0.45	23.85	29.15

M.1.3. RBC saturation

The nonlinear accumulation of lead by erythrocytes at high blood lead levels is widely accepted (USEPA, 2013). Moreover, non-linear binding saturation is conceptually logical as high affinity lead-binding sites on proteins and other molecules will become saturated at high lead levels. The original Leggett model set a threshold and a maximum saturation of 25 µg/dL whole blood and 350 µg/dL RBC respectively. The OEHHA implementation of the Leggett model (OEHHA, 2013) set the threshold to zero and the maximum limit of saturation to 270 µg /dL), since the mechanistic and empirical basis for a threshold is

not well defined. The difference between using threshold values of 0 versus 25 $\mu\text{g}/\text{dL}$ and using saturation values of 270 and 350 $\mu\text{g}/\text{dL}$ are shown in Figure M-2. Overall, blood lead levels using no threshold and a saturation value of 270 are lower than blood lead levels using the original Leggett (1993) parameters. The difference, as determined in test runs as part of the current effort, is a decrease by approximately 33% at both 20 $\mu\text{g}/\text{dL}$ and 30 $\mu\text{g}/\text{dL}$, with smaller differences at lower blood lead levels.

For this effort, the parameters in the input file (input line 17) were changed to reflect threshold and maximum saturation of 0 and 270, respectively, and the nonlinearity in the model was turned on. It should be recognized that the issue of threshold and saturation is not necessarily settled but awaits better experimental data and insight to establish these parameters.

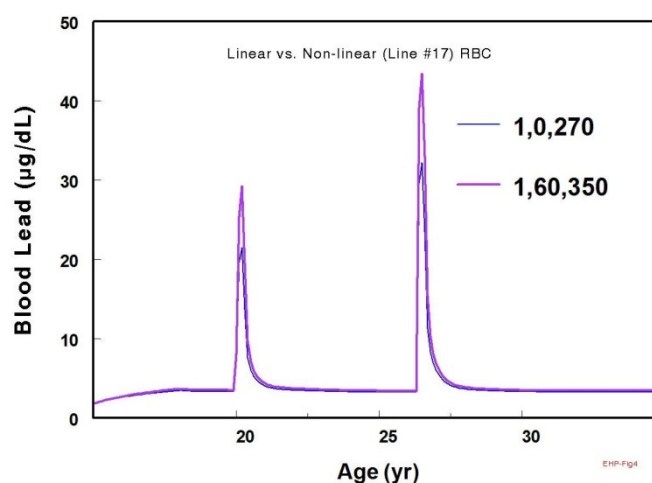


Figure M-2. The Effect of Different Nonlinear Threshold and Saturation Value Assumptions.

The “1” in the figure legend indicates that the nonlinearity in the model was turned on.

M.1.4. Additional Parameter Changes

Other parameters were changed during the course of model calibration to support age-dependent model outputs of lead concentrations and to improve simulation of blood lead in children. Both the deposition fraction from plasma to red blood cells and the transfer rate from red blood cells to plasma were adjusted to improve agreement between the modeled blood lead for children ages 1 to 7 years and the NHANES average blood leads for the same age range, as discussed in Section M.3.

The selection of the adult values used by Leggett (1993) were obtained from a limited radiotracer study conducted in adults only, and thus no age-dependent transfer rates were available. Leggett (1993) concluded that “approximately” 24% of plasma lead entered the RBC and this variable was not modified for age in Leggett-93. The transfer rates between plasma and red blood cells were empirically updated

to provide more accurate simulation of blood lead levels in children. The adult transfer rates were also adjusted slightly to provide better agreement with the occupational calibration data set. The updated values are shown in Table M-2. No contemporary studies were identified to support an objective definition of these parameters.

We also reviewed and updated the default maternal blood lead concentration to be more appropriate to contemporary blood lead data and to better simulate blood leads in children. The Leggett-93 model set the maternal blood lead at 10 µg lead/dL at time of birth (input file line #18). This variable in turn defines the starting blood and tissue lead concentrations at birth (input file line #19). This variable was updated following review of maternal blood leads from the 2011-2012 NHANES survey (CDC, 2012). The average blood lead was estimated across the female population age 18 to 50. An average value of 0.7 µg lead/dL was calculated and thus 0.7 µg lead/dL was used as the new default maternal blood lead in the Leggett input file.

Table M-2. Additional Parameters Updated in the Leggett Model

Age	Deposition Fraction to RBC	Transfer Rate from RBC***
0	0.562*	0.20
0.27	0.562*	0.20
1	0.562*	0.20
5	0.277	0.20
10	0.277**	0.21
15	0.139	0.22
18	0.139	0.22
24	0.139	0.22
30	0.139	0.22
40	0.139	0.22
45	0.139	0.22
55	0.139	0.22
65	0.139	0.22
75	0.139	0.22

* Changed from 0.462

** Changed from 0.139

*** All changed from 0.24

M.2. Bone Transfer Rates

There are two major kinds of structural bone, trabecular and cortical. Cortical bone is much more dense and stronger than trabecular bone and comprises about 80% of the adult skeletal mass. Trabecular bone is more vascular, more flexible, less dense, and has a higher surface/mass ratio. The vascularity and

surface to mass ratio facilitate more rapid deposition and exchange of Ca^{2+} or Pb^{2+} and other bone-seeking metals. Kinetic models for bone mineral metabolism, including lead, generally include compartments for both bone types with or without kinetic sub-compartments. The bone transfer rates for the Leggett (and other) models are derived from available data from human and animal studies with priority given to data derived from humans. This primary objective for reevaluation of the bone-lead transfer (in addition to scaling for children and adolescents) is to incorporate more information on the skeletal lead metabolism in the aged human. That is, the fractional skeletal transfer rates in the original Leggett model were not adjusted after age 25. This adjustment is important as age (with diet, gender, exercise, genetics, etc.) determines the rate of bone formation, resorption, bone turnover, and bone loss.

Difficulty in defining bone-lead transfer rates. There is excellent potential to apply new data, not available to Leggett in 1993, to inform revision of the Leggett model bone-lead transfer rates. These new data include (a) more elaborate non-invasive measures of lead in cortical and trabecular bone by XRF, (b) development of blood and urinary biomarkers of bone formation and resorption, and (c) more widely applied studies of Dual Energy X-ray absorptiometry (DEXA) measures of bone density and bone mass. Electronic searches using Medline, Quertle, and Google Scholar were conducted to identify useful papers.

It must be recognized that biokinetic compartments and transfer integrate many chemical and biological processes. For example, the transfer of lead from trabecular bone to plasma (RTRAB) is the sum of the chemical loss by displacement of lead from hydroxyapatite, bone matrix proteins, or bone cells by Ca^{2+} or H^+ . Pb^{2+} may also be lost from bone as the mineralized and proteinaceous bone matrix is degraded by osteoclasts.

The last two decades have seen the identification, development, and clinical application of numerous biomarkers for anabolic and catabolic skeletal biology. The use of these biomarkers is limited as, for example, a marker of bone resorption, does not distinguish between turnover of trabecular and cortical bone. Moreover, bone resorption or turnover as defined by a biomarker may not be equivalent to loss of Pb as Pb^{2+} may be simply redistributed to another site in bone.

Finally, it is not appropriate to directly compare, or utilize, bone-lead transfer rates from other biokinetic or PBPK models of lead as the number of transfer rates varies considerably. Twelve fractional transfer rates and six compartments comprise the skeletal component of the Leggett model. In contrast, the Rabinowitz model includes a single compartment and two transfer rates for skeletal lead (Rabinowitz et al. 1976). Other kinetic models lie between these two extremes (see Figure M-1).

Values and data sources for trabecular and cortical bone-lead transfer rates were evaluated. Bone formation and turnover rates from different sources were reviewed including:

- Age-dependent bone formation and turnover rates as defined by tracer studies of Ca, Pb, Sr, or other bone-volume-seeking elements.
- Age-dependent bone formation and turnover rates as defined by blood and urinary biomarkers were also reviewed.
- Age-dependent bone-lead transfer rates described in the scientific literature since 1993 including values in PBPK models or other compartmental models.

The use of blood or urinary concentrations of Osteocalcin, bone-specific alkaline phosphatase, procollagen I extension peptides, acid phosphatase, telopeptides of type I collagen, pyridinoline and deoxypyridinoline crosslinks are used as biomarkers of bone formation, resorption, and turnover. Unfortunately, the medical studies reviewed were focused on individuals at risk for skeletal disease(s) and did not encompass age-dependent studies of a general population suitable to inform modification of bone-lead transfer parameters. This literature however, has promise to inform age-dependent bone-lead transfer parameters and should be re-evaluated in the future.

Several biokinetic and PBPK lead models published since the Leggett 1993 publication included bone-lead transfer rates. The values of a single representative parameter, transfer from trabecular bone to plasma, are illustrated in Figure M-3. For this effort, the values used in the Coon et al. (2006) implementation of the Leggett model, originally from Rowland (1964), were selected. These values include bone lead transfer rates for trabecular and cortical bone to age 70 yr, including changes in bone mineral metabolism associated with senectitude, as shown in Table M-3.

The published bone-lead parameters from more recent publications were not used to update the Leggett model in the current effort because (a) they did not include age-dependent parameters (e.g. Nie et al. 2005; OEHHA, 2013; O'Flaherty, 1998), (b) the model structure was incompatible with the Leggett model, so the transfer parameters could not be directly compared, and/or (c) the description of bone turnover and skeletal mass did not reflect well known changes in bone mineral metabolism associated with aging (all except O'Flaherty, 1998).

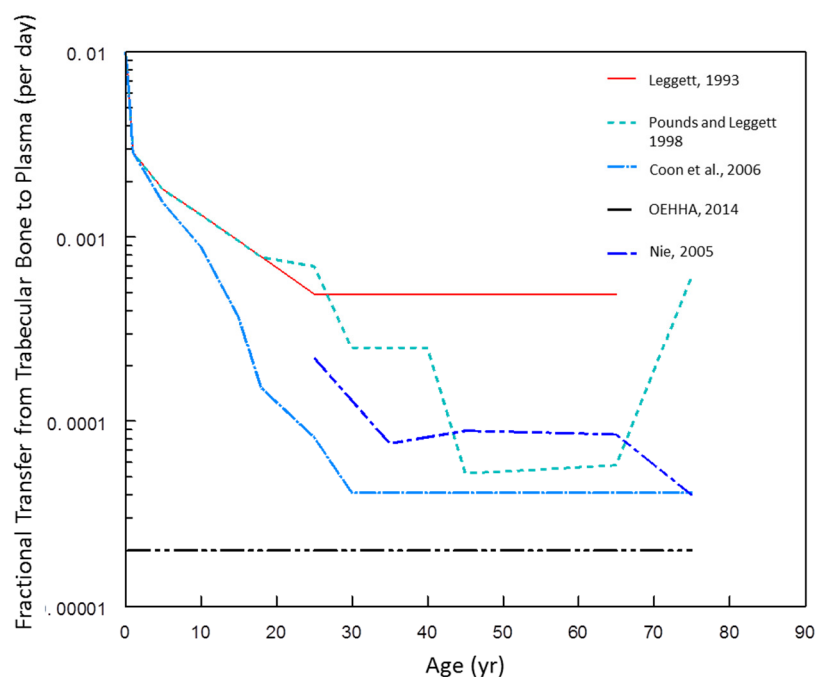


Figure M-3. Bone Transfer Rates Used in Different PBPK Models Since 1993.

Table M-3. Bone Transfer Rates Used in the Model

Age	Cortical Bone Transfer Rates	Trabecular Bone Transfer Rates
0	0.0102	0.0102
0.27	0.00822	0.00822
1	0.00288	0.00288
5	0.00154	0.00181
10	0.00089	0.00132
15	0.000512	0.000956
18	0.000370	0.000781
24	0.000082	0.000493
30	0.000041	0.000247
40	0.000041	0.000247
45	0.000041	0.000274
55	0.000041	0.000301
65	0.000041	0.000329
75	0.000041	0.000356

M.3. Evaluation and Calibration of the Updated Model

Two different exercises were conducted to compare the simulated blood lead values with literature data and to calibrate the model to provide adequate agreement. These two separate exercises, one for children and one for adults, are described below.

M.3.1. Comparison for Children

The childhood portion of the updated Leggett model was compared to NHANES data from the 2007-2008 survey (CDC, 2012). This particular survey was selected as the best match to the available intake estimates. The NHANES values were the average values across each different age bin (0-<1, 1-<2, 2-<3, 3-<4, 4-<5, 5-<6, and 6-<7), as shown in

Table M-4. Media intake rates were based on values in the Exposure Factors Handbook (EPA, 2011) while media concentrations were set to likely background values, as shown in

Table M-4. The concentrations and intake rates were used to calculate the daily lead intakes by inhalation and ingestion. Then, the Leggett model was run from birth to age 7 yr. The IEUBK model was also run to provide a comparison. The original Leggett model predicted blood lead values a factor of 2 to 3 higher than those predicted by the IEUBK or reported by NHANES; however, after adjusting the RBC deposition fraction and performing the scaling of model parameters, the adjusted Leggett model agrees very closely to the NHANES data. **Figure M-4** compares the blood lead concentrations from NHANES and model simulations using IEUBK, Leggett (version 4) and Leggett (version 5). The decrease in blood lead between ages 0.5 to 1 year is because the intestinal absorption fraction gradually decreases from 45 to 30 percent by age 1 yr. The rapid increase in blood lead at age 1 yr is due to the substantial and abrupt 67% increase in lead intake (see

Table M-4). Version 5 of the Leggett model agrees well with the NHANES data. It should be noted, however, that this calibration only applies to chronic exposures; no data were available to perform analysis on shorter-term exposures such as those experienced during a renovation event.

Table M-4. Background Media Concentrations and Intake Rates Used for the Childhood Model Calibration

Parameter	Source	Age 0-<1	Age 1-<2	Age 2-<3	Age 3-<4	Age 4-<5	Age 5-<6	Age 6-<7
Soil and Dust Ingestion Rate (g/day)	Exposure Factors Handbook (US EPA, 2011)	0.06	0.1	0.1	0.1	0.1	0.1	0.1
Fraction of soil and dust ingestion that is soil	Exposure Factors Handbook (US EPA, 2011)	0.45						
Background Residential Dust Concentration (µg/g)	HUD (2002), averaged across vintages and converted to concentration	75.7						
Background Residential Soil Concentration (µg/g)	HUD (2002), averaged across vintages	44.6						
Dietary Lead Intake (µg/day)	Exposure Factors Handbook (US EPA, 2011) and Total Diet Survey (US FDA, 2007)	2.1	3.9	4.7	4.4	4.4	4.4	4.5
Water Intake (L/day)	Exposure Factors Handbook (US EPA, 2011)	0.32	0.27	0.32	0.33	0.33	0.33	0.41
Water Lead Concentration (µg/L)	Total Diet Survey (FDA, 2007)	1.0						
Ventilation Rate (m ³ /day)	Exposure Factors Handbook (US EPA, 2011)	5.4	8	9.5	10.9	10.9	10.9	12.4
Air Lead Concentration (µg/m ³)	EPA's Air Quality Systems (AQS) database (USEPA, 2010)	0.02						
Total Inhalation Intake (µg/day)		0.108	0.16	0.19	0.218	0.218	0.218	0.248
Total Gastrointestinal Intake (µg/day)		6.16	10.31	11.17	10.91	10.91	10.91	11.07
NHANES 2007-2008 blood lead values (µg/dL)		1.4	1.7	1.3	1.2	1.0	1.1	0.8

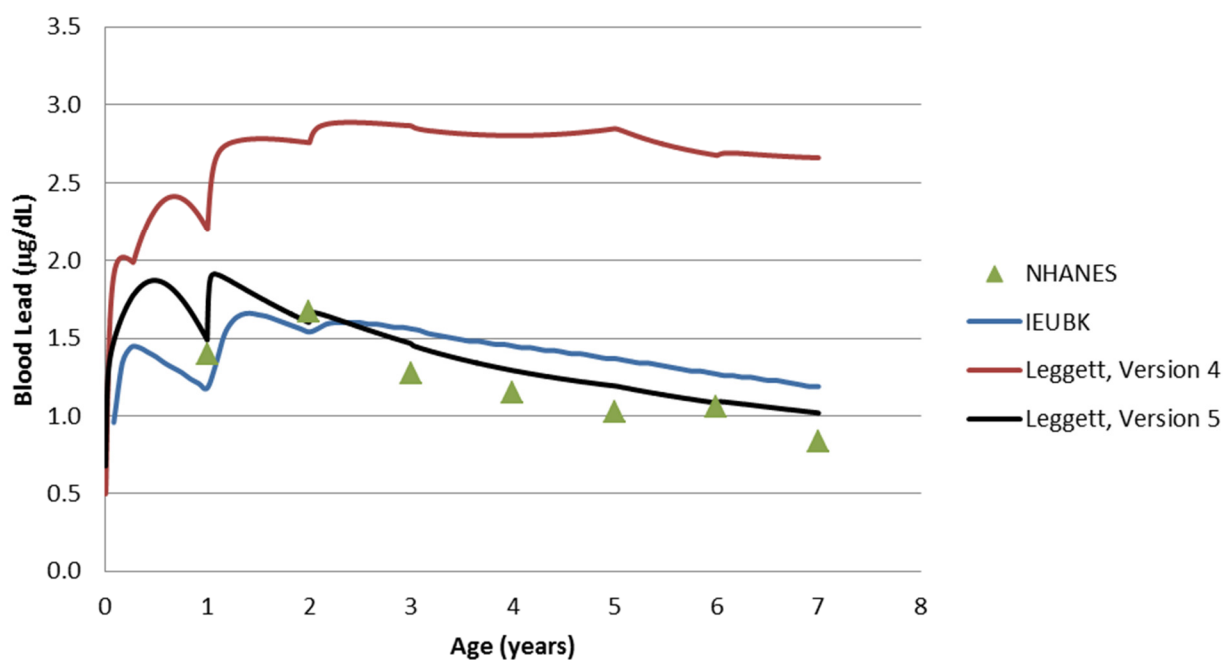


Figure M-4. Comparison of NHANES, IEUBK, Leggett (version 4) and Leggett (version 5) blood lead levels.

M.3.2. Evaluation of Updated Leggett Model in Occupationally Exposed Adults

In order to evaluate the performance of the Leggett model for adults, data were obtained from subjects in three longitudinal bone lead studies performed in 1994 (n = 381), 1999 (n = 313), and 2008 (n = 497) (Nie et al., 2005; 2008 data not yet published). In these studies, there were 209 subjects who participated in all three studies, so these subjects were used for the evaluation. For each participant, tibia (cortical bone) and calcaneus (trabecular bone) lead was measured *in vivo* using ^{109}Cd K X-ray fluorescence. Blood lead measurements and a cumulative blood lead index were also available. Finally, the study population was characterized by a discontinuity in lead exposure from July 1990 to May 1991 during a plant strike.

The dataset does not provide measures of lead exposure or intakes, so intake estimates were optimized iteratively using the Leggett model. An initial guess was made for each subject, and the intake was assumed to decrease in proportion to the blood lead decreases. The assumption is that an individual subject's work place habits, diet, personal workplace activity (job), personal hygiene and physiology (e.g. diet, age, gender) that modulate lead exposure, lead intake, and lead uptake were consistent within a subject. The biokinetic parameters of the model were not further adjusted. Thus, only lead intake was

adjusted was adjusted until the mean square error (MSE) between the simulated and actual blood lead and a bone lead measurements was minimized as shown below.

$$\text{MSE} = \frac{(((\text{cortical94} - \text{tibia94i}) * 3 + (\text{trabecular94} - \text{calcaneus94i}) * 2 + (\text{pbb94} - \text{pbb94i}))^2 + ((\text{cortical99} - \text{tibia99i}) * 3 + (\text{trabecular99} - \text{calcaneus99i}) * 2 + (\text{pbb99} - \text{pbb99i}))^2 + ((\text{cortical08} - \text{tibia08i}) * 3 + (\text{trabecular08} - \text{calcaneus08i}) * 2 + (\text{pbb08} - \text{pbb08i}))^2)}{3}$$

This error term gives more weight to cortical bone lead (as the most stable body store) and less to blood lead (as the most labile body compartment). This weighting is similar to that used by Coon et al. 2006.

Figure M-5. Comparison of Mean Square Error between Simulated and Actual Blood and Bone Lead both Before and After the Intake Optimization.

shows examples of the mean square error before and after optimization. In general, the mean square error was decreased by a factor of 10 during the optimization. After the optimization was performed, the data were examined for each subject. In general, inspection indicated that cortical bone lead levels were biased low while blood lead levels were biased high. The bone and RBC transfer rates were adjusted in order to provide the best overall fit in the different subjects.

Figure M-6 compares the blood lead, cortical bone lead, and trabecular bone lead estimates from Version 4 of the Leggett model, Version 5 of the Leggett model, and the actual data from one occupational worker. The model Version 5 was calibrated using the bone and blood lead data, and the cumulative blood lead index (CBLI) serves as an additional check of the model fit. For this individual, the model updates reduce the over prediction of blood lead and provide better fits to the data.

Original vs. final MSE

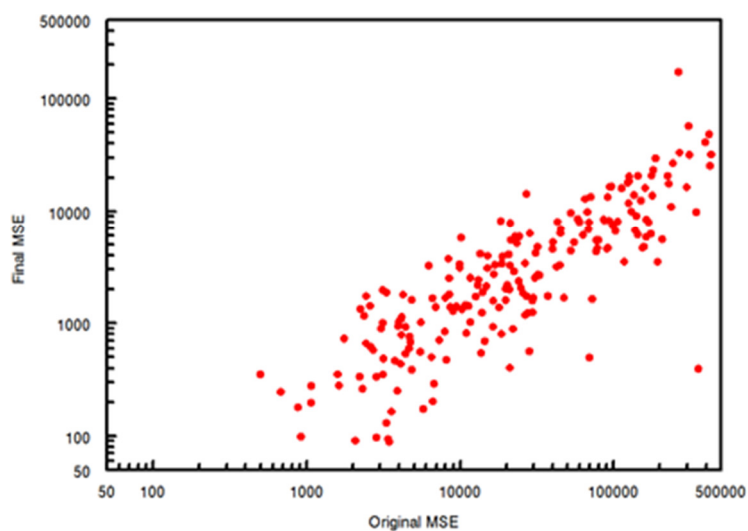


Figure M-5. Comparison of Mean Square Error between Simulated and Actual Blood and Bone Lead both Before and After the Intake Optimization.

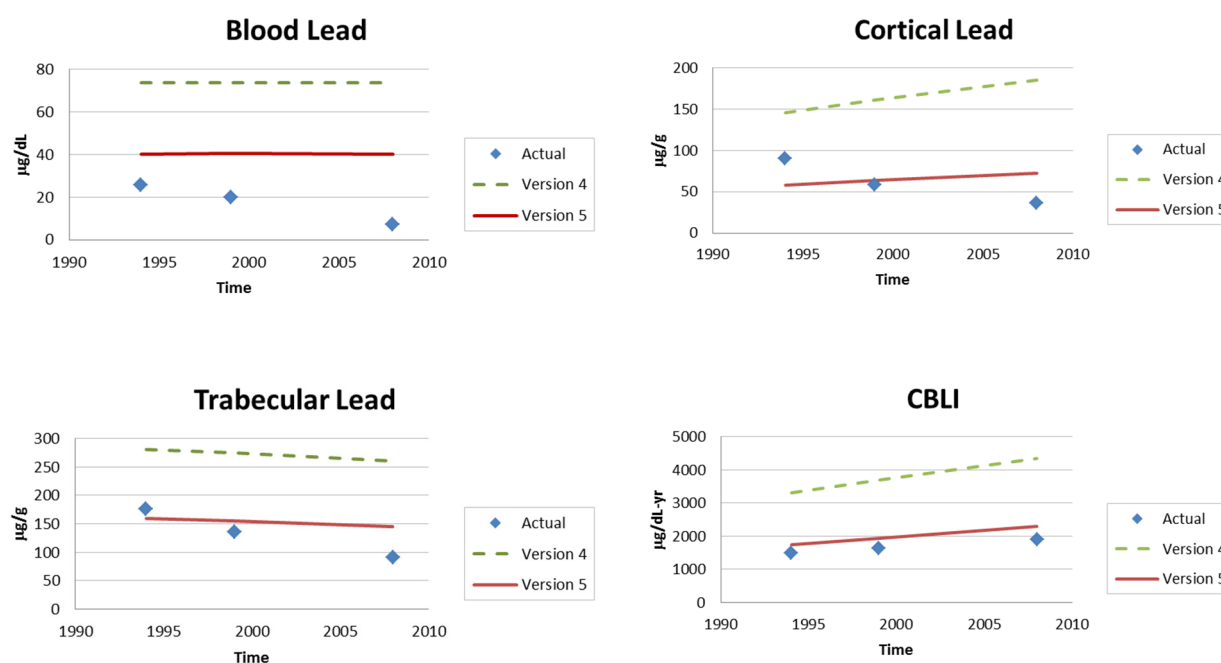


Figure M-6. Comparison of Blood and Bone Lead Predicted Values to Measured Values in One Occupationally Exposed Adult. CBLI = Cumulative Blood Lead Index

M.4. Issues to consider at future date

Additional activities can be undertaken in the future to further improve the model performance and reliability:

- The modifications resulting in Version 5 of the model should be published in a peer-reviewed journal to facilitate communication and critical review of the model modifications and updates.
- The age-dependent parameters newly included in the FORTRAN code should be moved to a revised input file. This revision will increase transparency for these parameters, and facilitate modification and further testing. Such revision will, of course, essentially decouple the input files used over the last twenty years from the current version of the Leggett model.
- Opportunities should be developed to use stable isotope tracers in humans to better define key age-dependent parameters of lead metabolism. Such an effort should be focused on gastrointestinal bioavailability and on skeletal processes.

- The clinical measures of bone mineral density and bone mass should continue to be monitored for data to inform the model's age-dependent skeletal description.
- The Health and Welfare has conducted a study measuring blood lead and bone lead (K-XRF) on non-occupationally exposed population in Toronto. This study population includes children and the aged (David Chettle, personal communication). This is a valuable data set to calibrate and validate the updated Leggett model.
- The Leggett model should be updated to consider gender.
- The model could be incorporated in EPA agency-wide efforts to create an All Ages Lead Model (AALM).

References for Appendix M

Brinckmann P; W Frobin; Gunnar Leivseth. Musculoskeletal biomechanics. 2002. Published by Stuttgart, New York). Centers for Disease Control and Prevention, (2012). National Health and Nutrition Examination Survey 2010-2012. U.S. Department of Health and Human Services, Centers for Disease Control and Prevention.

Coon, S, A Stark, E Peterson, A Gioi, G Kortsha, J Pounds, D. Cheattle, and J Gorrell. 2006. Whole-body lifetime occupational lead exposure and risk of Parkinson's Disease. Environmental Health Perspectives Vol. 114, No. 12, Dec., 2006.

Centers for Disease Control and Prevention. 2012. National Health and Nutrition Examination survey. Available at <http://www.cdc.gov/nchs/nhanes.htm>.

HUD, 2002. National Survey of Lead and Allergens in Homes. <http://www.niehs.nih.gov/research/atniehs/labs/lrb/enviro-cardio/studies/nslah/index.cfm>

Leggett RW. (1993). An age-specific kinetic model of lead metabolism in humans. Environmental Health Perspectives 101:598-616.

Nie, L, Chettle DR, Webber CE, Brito JA, O'Meara JM, McNeill FE. 2005. The study of age influence on human bone lead metabolism by using a simplified model and X-ray fluorescence data. J Environ Monit. 2005 Nov;7(11):1069-73.

OEHHA. 2013. Estimating Workplace Air and Worker Blood Lead Concentration Using an Updated Physiologically-based Pharmacokinetic (PBPK) Model. Available at http://oehha.ca.gov/air/risk_assess/PBPK2013.pdf.

O'Flaherty, E. 1998. A physiologically based kinetic model for lead in children and adults. *Environ Health Perspect.* Dec 1998; 106(Suppl 6): 1495–1503.

Rabinowitz, MB, G W Wetherill, and J D Kopple. 1976. Kinetic analysis of lead metabolism in healthy humans. *J Clin Invest.* Aug 1976; 58(2): 260–270.

Rowland, RE. Resorption and bone physiology. pp. 335-351 in H. M. Frost, ed., *Bone Biodynamics*, Boston:Little, Brown, and Company; 1964.

US EPA, 2010. EPA's Air Quality Systems (AQS) database. Available at <http://www.epa.gov/ttn/airs/airsaqs/detaildata/downloadaqsdta.htm>.

US EPA, 2011. Exposure Factors Handbook. Available at <http://www.epa.gov/ncea/efh/pdfs/efh-complete.pdf>.

US EPA. (2013). Integrated Science Assessment for Lead. U.S. Environmental Protection Agency, Washington, DC, EPA/600/R-10/075F.

US FDA, 2007. Total Diet Survey. Available at <http://www.fda.gov/Food/FoodScienceResearch/TotalDietStudy/default.htm>.

Valentin, 2002. Basic Anatomical and Physiological Data for Use in Radiological Protection Reference Values. ICRP Publication 89. *Ann. ICRP* 32 (3-4).

Appendix M Attachment 1. Leggett Version 5 Code

C UNITS: all times are in days, but ages are in years.
C Pb is in micrograms.
C INMODE is intake mode.
C INMODE=0 is injection (direct input) into diffusible plasma,
C 1 is inhalation, 2 is ingestion, 3 is any combination of 0, 1, and 2.
C IACUTE=1 is acute intake & 2 is chronic intake.
C The chronic intake rate may be varied with time in a stepwise fashion.
C The chronic injection rate is the variable CHR, which is later converted to CRONIC.
C The chronic inhalation rate is the variable BRETH, which is later converted
C to BRTCRN. The chronic ingestion rate is eat, later converted to EATCRN.
C ICRP.for received from Rich Leggett 9/93
C ICRPv001 (chelate.for) add line#53 for chelation 10/96; rwl
C ICRPv002 convert to crtconbm & trbconbm bone mineral density; jgp
C ICRPv003 convert output time from DAYS to YEARS; 6/97; jgp
C ICRPv004 add UPTAKEGI, UPTAKERI, UPTAKE; correct trbconbm conversion;
C add decimal to YEARS; 11/97 jgp & rwl
C ICRPv005 add age-dependent scaling for
RBCONC,RENCON,CRTCON,TRBCON,ASHCON,TORBC
c April 2014, JGP
C ICRPv005a adjust Pb distribution to cort-trab bone; fraction trab-cort bone
DIMENSION DELTA(10),ICYC(10),Q(50)
DIMENSION CHAGE(14),ENDPT(1000),CHR(1000),BRETH(1000),EAT(1000),
\$ AGSCAL(14),ARCORT(14),ARTRAB(14),ATBONE(14),ATFRAC(14),
\$ AF1(14),ARCS2B(14),ARTS2B(14),ARCSDF(14),ARTSDF(14),
\$ ARBLAD(14),ARLVR2(14),ARKDN2(14),ARBRAN(14),ARRBC(14),
\$ ARD2CS(14),ARD2TS(14),ARD2DC(14),ARD2DT(14),ATBRAN(14),
\$ ATSOFO(14),ATSOFO1(14),ATSOFO2(14),AAMTBL(14),RDIFF(14),
\$ FLONG(14),AKIDWT(14),ATSKELWT(14),ATTRABWT(14),ATCORTWT(14),
\$ FRTTRAB(14),ARBCVOL(14),APLSVOL(14),ABLDHCT(14),ATORBC(14)
REAL INTACT,LAMOUT
OPEN(30,FILE='POUNDS.DAT')
OPEN(50,FILE='TEMP.DAT')
READ(30,*) EXPAGE
READ(30,*) NDELTA,DELTA0,NCYCLE,ENDDAY
READ(30,*) (DELTA(I),I=1,NDELTA)
READ(30,*) (ICYC(I),I=1,NDELTA)
READ(30,*) ISKIP
READ(30,*) I1,I2,I3,I4,I5
READ(30,*) INMODE,IACUTE,LINPUT
C READ # CHRONIC INTAKE STEPS UP TO 50 AND CONSECUTIVE
C ENDPOINTS IN DAYS, STARTING WITH DAYS=0.0.

```
READ(30,*) NCHRON
IF (IACUTE .EQ. 2) READ(30,*) (ENDPT(I),I=1,NCHRON)
IF (IACUTE .EQ. 2) READ(30,*) (CHR(I),I=1,NCHRON)
IF (IACUTE .EQ. 2) READ(30,*) (BRETH(I),I=1,NCHRON)
IF (IACUTE .EQ. 2) READ(30,*) (EAT(I),I=1,NCHRON)
IF (IACUTE .NE. 2) READ(30,*) DUMMY
READ(30,*) NUMAGE,XXMAGE
READ(30,*) (CHAGE(I),I=1,NUMAGE)
READ(30,*) (AF1(I),I=1,NUMAGE)
READ(30,*) RDECAY
READ(30,*) IRBC,RBCNL,SATRAT,POWER
READ(30,*) IFETAL,BLDMOT,BRATIO
READ(30,*) SOFIN,RBCIN,BONIN,RENIN,HEPIN,BRANIN
READ(30,*) R1,R2,R3,R4,CILIAR
READ(30,*) BR1,BR2,BR3,BR4
READ(30,*) RSTMC,RSIC,RULL,RLLI
READ(30,*) (AGSCAL(I),I=1,NUMAGE)
READ(30,*) (ARCORT(I),I=1,NUMAGE)
READ(30,*) (ARTRAB(I),I=1,NUMAGE)
READ(30,*) (ARCS2B(I),I=1,NUMAGE)
READ(30,*) (ARTS2B(I),I=1,NUMAGE)
READ(30,*) (ARCSDF(I),I=1,NUMAGE)
READ(30,*) (ARTSDF(I),I=1,NUMAGE)
READ(30,*) (RDIFF(I),I=1,NUMAGE)
READ(30,*) (FLONG(I),I=1,NUMAGE)
READ(30,*) RLVR1,RKDN1
READ(30,*) (ARBLAD(I),I=1,NUMAGE)
READ(30,*) (ARLVR2(I),I=1,NUMAGE)
READ(30,*) (ARKDN2(I),I=1,NUMAGE)
READ(30,*) RSOF0,RSOF1,RSOF2
READ(30,*) (ARBRAN(I),I=1,NUMAGE)
READ(30,*) TOURIN,TOFECE,TOSWET,S2HAIR
READ(30,*) (ATBONE(I),I=1,NUMAGE)
READ(30,*) (ATFRAC(I),I=1,NUMAGE)
READ(30,*) TOLVR1,H1TOH2,H1TOSI,H1TOBL
READ(30,*) TOKDN1,TOKDN2
READ(30,*) (ATSOF0(I),I=1,NUMAGE)
READ(30,*) (ATSOF1(I),I=1,NUMAGE)
READ(30,*) (ATSOF2(I),I=1,NUMAGE)
READ(30,*) (ATBRAN(I),I=1,NUMAGE)
DO 6 I=1,NUMAGE
```

```
ARD2CS(I)=(1.-FLONG(I))*RDIFF(I)
ARD2TS(I)=(1.-FLONG(I))*RDIFF(I)
ARD2DC(I)=FLONG(I)*RDIFF(I)
ARD2DT(I)=FLONG(I)*RDIFF(I)
6 CONTINUE
READ(30,*) TORBC
READ(30,*) TOEVF,SIZEVF
READ(30,*) RPLAS,TOPROT,RPROT
READ(30,*) (ARRBC(I),I=1,NUMAGE)
READ(30,*) XRBCVOL,XPLSVOL
C   ADJRBC=RBCVOL/(RBCVOL+PLSVOL) moved to below
READ(30,*) (AAMTBL(I),I=1,NUMAGE)
READ(30,*) ICHEL,CHLEFF,CHEL1,CHEL2
IF (IACUTE .EQ. 1 .AND. LINPUT .EQ. 1) WRITE(*,11)
IF (IACUTE .EQ. 2 .AND. LINPUT .EQ. 1) WRITE(*,12)

C   Age-Dependent Kidney Mass from ICRP v89, p148
C   WHERE AGES 0,0.27,1,5,10,15,18,24,30,40,45,55,65 and 75 yr
AKIDWT (1) = 25.
AKIDWT (2) = 36.
AKIDWT (3) = 70.
AKIDWT (4) = 110.
AKIDWT (5) = 180.
AKIDWT (6) = 250.
AKIDWT (7) = 310.
AKIDWT (8) = 310.
AKIDWT (9) = 310.
AKIDWT (10) = 310.
AKIDWT (11) = 310.
AKIDWT (12) = 310.
AKIDWT (13) = 310.
AKIDWT (14) = 310.

C   AGE-DEPENDENT TOTAL SKELETAL MASS (g) from ICRP v89, page 170
C   WHERE AGES ARE 0,0.27,1,5,10,15,18,24,30,40,45,55,65 and 75 YEARS
ATSKELWT (1) = 370.
ATSKELWT (2) = 642.
ATSKELWT (3) = 1170.
ATSKELWT (4) = 2430.
ATSKELWT (5) = 4500.
ATSKELWT (6) = 7950.
ATSKELWT (7) = 10500.
ATSKELWT (8) = 10500.
ATSKELWT (9) = 10500.
```

ATSKELWT (10) = 10500.

ATSKELWT (11) = 10500.

ATSKELWT (12) = 10500.

ATSKELWT (13) = 10500.

ATSKELWT (14) = 10500.

C AGE-DEPENDENT Fraction of total skeletal mass comprised of trabecular bone

C WHERE AGES ARE 0,0.27,1,5,10,15,18,24,30,40,45,55,65 and 75 YEARS

C (changed from 99,96,87,)

FRTTRAB (1) = .95

FRTTRAB (2) = .90

FRTTRAB (3) = .85

FRTTRAB (4) = .50

FRTTRAB (5) = .34

FRTTRAB (6) = .23

FRTTRAB (7) = .20

FRTTRAB (8) = .20

FRTTRAB (9) = .20

FRTTRAB (10) = .20

FRTTRAB (11) = .20

FRTTRAB (12) = .20

FRTTRAB (13) = .20

FRTTRAB (14) = .20

C CALCULATE AGE-DEPENDENT MASS OF TRABECULAR AND SKELETAL BONE AT 14 AGES

ATTRABWT=ATSKELWT*FRTTRAB

ATCORTWT=ATSKELWT*(1-FRTTRAB)

C Age-dependent ARBCVOL and APLSVOL calculated from age-dependent hematocrit and total blood (7) .48->.42

ABLDHCT (1) = .575

ABLDHCT (2) = .37

ABLDHCT (3) = .35

ABLDHCT (4) = .38

ABLDHCT (5) = .38

ABLDHCT (6) = .40

ABLDHCT (7) = .42

ABLDHCT (8) = .45

ABLDHCT (9) = .45

ABLDHCT (10) = .45

ABLDHCT (11) = .45

ABLDHCT (12) = .45

ABLDHCT (13) = .45

```
ABLDHCT (14) = .45

ARBCVOL=AAMTBL*ABLDHCT
APLSVOL=AAMTBL*(1-ABLDHCT)
C  ADJRBC=RBCVOL/(RBCVOL+PLSVOL) Calculation replaced by BLDHCT

C  Age-dependent deposition fraction to RBC
ATORBC (1) = 0.20
ATORBC (2) = 0.20
ATORBC (3) = 0.20
ATORBC (4) = 0.20
ATORBC (5) = 0.21
ATORBC (6) = 0.22
ATORBC (7) = 0.22
ATORBC (8) = 0.22
ATORBC (9) = 0.22
ATORBC (10) = 0.22
ATORBC (11) = 0.22
ATORBC (12) = 0.22
ATORBC (13) = 0.22
ATORBC (14) = 0.22

11 FORMAT(' Enter acute input.')
12 FORMAT(' Enter chronic input to blood.')
   IF (IACUTE .EQ. 1 .AND. LINPUT .EQ. 1) READ(*,*)ACPLAS
   IF (IACUTE .EQ. 2 .AND. LINPUT .EQ. 1) READ(*,*)CHR(1)
   IF (IACUTE .EQ. 1 .AND. LINPUT .NE. 1) AACUTE=1.0
   IF (IACUTE .EQ. 1 .AND. LINPUT .EQ. 1) AACUTE=ACPLAS
C
   IF (IFETAL .NE. 1 .OR. EXPAGE .GT. 0.01 .OR.
$   IACUTE .NE. 2) GO TO 15
   YSOF2=SOFIN*(BLDMOT*BRATIO*3./RBCIN)
   YRBC=RBCIN*(BLDMOT*BRATIO*3./RBCIN)
   YCVOL=0.8*BONIN*(BLDMOT*BRATIO*3./RBCIN)
   YTVOL=0.2*BONIN*(BLDMOT*BRATIO*3./RBCIN)
   YKDN2=RENIN*(BLDMOT*BRATIO*3./RBCIN)
   YLVR2=HEPIN*(BLDMOT*BRATIO*3./RBCIN)
   YBRAN=BRANIN*(BLDMOT*BRATIO*3./RBCIN)
15 CONTINUE
   HOWOLD=EXPAGE
   DAYS=0.0
   BTEMP=0.0
C BEGIN CALCULATIONS.
   DO 1000 N=1,NCYCLE
```

```
C CHRONIC INTAKE SWITCH IS IACUTE.
  BRTCRN=0.0
  IF (IACUTE .NE. 2) GO TO 38
  DO 35 I=2,NCHRON+1
  IF (DAYS .GT. ENDPT(I-1)-1.0E-09) GO TO 35
  CRONIC=CHR(I-1)
  BRTCRN=BRETH(I-1)
  EATCRN=EAT(I-1)
  GO TO 38
35 CONTINUE
38 CONTINUE
  IF (DELTO .GT. 0.0) THEN
    DELT = DELTO
  ELSE
    DO 52 ISTEP = 1, NDELT
      IF (N .LE. ICYC(ISTEP)) THEN
        DELT = DELTA(ISTEP)
        GO TO 53
      END IF
    52 CONTINUE
    53 CONTINUE
  END IF
  HOWOLD=HOWOLD+DELT/365.
  DAYS=DAYS+DELT
  TMINS=1440.*DAYS
  XMINS=1440.*DAYS
  HOURS=24.*DAYS
  YEARS=DAYS/365.
  IF (DAYS .GT. 1.0) TMINS=DAYS
C IN THE FOLLOWING THE AGE-DEPENDENT VARIABLES ARE INTERPOLATED
C TO GET VALUES FOR AGE HOWOLD.
C SKIP THE FOLLOWING STEPS FOR PERSONS OLDER THAN XMXAGE YEARS.
  IF (HOWOLD .GE. XMXAGE) GO TO 500
C
  DO 200 JAGE=1,NUMAGE
  IF (HOWOLD .GE. CHAGE(JAGE)) GO TO 200
  K=JAGE-1
  GO TO 300
200 CONTINUE
C
300 CONTINUE
C
  L=K+1
  U=HOWOLD-CHAGE(K)
```

```
V=CHAGE(L)-HOWOLD
W=V/(U+V)
Z=U/(U+V)
C
  GO TO 600
C
C FOR THE CASE IN WHICH HOWOLD IS AT LEAST XMXAGE YEARS:
500 K=NUMAGE
  L=NUMAGE
  W=1.0
  Z=0.0
C
600 CONTINUE
C
C DETERMINE BY INTERPOLATION THE RATES AND FRACTIONS AT AGE HOWOLD.
C
  F1=W*AF1(K)+Z*AF1(L)
  AMTBLD=W*AAMTBL(K)+Z*AAMTBL(L)
  RCORT=W*ARCORT(K)+Z*ARCORT(L)
  RTRAB=W*ARTRAB(K)+Z*ARTRAB(L)
  TFRAC=W*ATFRAC(K)+Z*ATFRAC(L)
  TBONE=W*ATBONE(K)+Z*ATBONE(L)
  TOSOF0=W*ATSOF0(K)+Z*ATSOF0(L)
  TOSOF1=W*ATSOF1(K)+Z*ATSOF1(L)
  TOSOF2=W*ATSOF2(K)+Z*ATSOF2(L)
  TOBRAN=W*ATBRAN(K)+Z*ATBRAN(L)
  RCS2B=W*ARCS2B(K)+Z*ARCS2B(L)
  RTS2B=W*ARTS2B(K)+Z*ARTS2B(L)
  RCS2DF=W*ARCSDF(K)+Z*ARCSDF(L)
  RTS2DF=W*ARTSDF(K)+Z*ARTSDF(L)
  RDF2CS=W*ARD2CS(K)+Z*ARD2CS(L)
  RDF2TS=W*ARD2TS(K)+Z*ARD2TS(L)
  RDF2DC=W*ARD2DC(K)+Z*ARD2DC(L)
  RDF2DT=W*ARD2DT(K)+Z*ARD2DT(L)
  RLV2=W*ARLV2(K)+Z*ARLV2(L)
  RKDN2=W*ARKDN2(K)+Z*ARKDN2(L)
  RBLAD=W*ARBLAD(K)+Z*ARBLAD(L)
  RBRAN=W*ARBRAN(K)+Z*ARBRAN(L)
  RRBC=W*ARRBC(K)+Z*ARRBC(L)
  GSCALE=W*AGSCAL(K)+Z*AGSCAL(L)
  KIDWT=W*AKIDWT(K)+Z*AKIDWT(L)
  TSKELWT=W*ATSKELWT(K)+Z*ATSKELWT(L)
  TRABWT=W*ATTRABWT(K)+Z*ATTRABWT(L)
  CORTWT=W*ATCORTWT(K)+Z*ATCORTWT(L)
```

RBCVOL=W*ARBCVOL(K)+Z*ARBCVOL(L)
PLSVOL=W*APLSVOL(K)+Z*APLSVOL(L)
BLDHCT=w*ABLDHCT(K)+Z*ABLDHCT(L)
TORBC= w*ATORBC(K)+Z*ATORBC(L)

C ADJRBC=W*AADJRBC(K)+Z*AADJRBC(L)

C

TEVF=TOEVF
AGESCL=(1.0-TEVF-TBONE)/(1.0-TEVF-ATBONE(NUMAGE))
TURIN=AGESCL*TOURIN
TFECE=AGESCL*TOFECE
TSWET=AGESCL*TOSWET
TSOF0=AGESCL*TOSOF0
TSOF1=AGESCL*TOSOF1
TSOF2=AGESCL*TOSOF2
TBRAN=AGESCL*TOBRAN
TLVR1=AGESCL*TOLVR1
TKDN1=AGESCL*TOKDN1
TKDN2=AGESCL*TOKDN2
TRBC=AGESCL*TORBC
TPROT=AGESCL*TOPROT

C

DECRBC=YRBC/RBCVOL
DECPLS=YPLAS/PLSVOL
BLDVOL=RBCVOL+PLSVOL
DECLTR=YBLUD/BLDVOL
TOORBC=TRBC
IF (IRBC .NE. 1 .OR. RBCONC .LE. RBCNL) GO TO 610
TOORBC=TRBC*(1.-((RBCONC-RBCNL)/(SATRAT-RBCNL)))*POWER
IF (TOORBC .LT. 0.0) TOORBC=0.0

610 CONTINUE

TSUM=TOORBC+TEVF+TPROT+TBONE+TURIN+TFECE+TSWET+TLVR1
\$ +TKDN1+TKDN2+TSOF0+TSOF1+TSOF2+TBRAN
CF=(1.-TOORBC)/(1.-TRBC)
RPLS=TSUM*RPLAS
REVF=TEVF*RPLS/SIZEVF
IF (ICHEL. EQ. 1 .AND. DAYS .GE. CHEL1 .AND. DAYS .LE. CHEL2)
\$ THEN
TEVF=(1.-CHLEFF)*TEVF
TFECE=(1.-CHLEFF)*TFECE
TSWET=(1.-CHLEFF)*TSWET
TSOF0=(1.-CHLEFF)*TSOF0
TSOF1=(1.-CHLEFF)*TSOF1

```
TSOF2=(1.-CHLEFF)*TSOF2
TBRAN=(1.-CHLEFF)*TBRAN
TLVR1=(1.-CHLEFF)*TLVR1
TKDN1=(1.-CHLEFF)*TKDN1
TKDN2=(1.-CHLEFF)*TKDN2
TPROT=(1.-CHLEFF)*TPROT
TBONE=(1.-CHLEFF)*TBONE
TOORBC=(1.-CHLEFF)*TOORBC
TURIN=1.0-TOORBC-TEVF-TPROT-TBONE-TFECE-TSWET-TLVR1
$ -TKDN1-TKDN2-TSOF0-TSOF1-TSOF2-TBRAN
END IF
```

```
C
IF (INMODE .EQ. 0 .OR. INMODE .EQ. 2) GO TO 55
```

```
C
C LUNG 1 COMPARTMENT
Y0=YR1
IF (IACUTE .EQ. 1 .AND. N .EQ. 1) Y0=R1*AACUTE
P=0.0
IF (IACUTE .EQ. 2) P=R1*BRTCRN
LAMOUT=RDECAY+BR1
YR1=ACTVTY(Y0,P,LAMOUT,DELT)
YR1W=INTACT(Y0,P,LAMOUT,DELT)
```

```
C
C LUNG 2 COMPARTMENT
Y0=YR2
IF (IACUTE .EQ. 1 .AND. N .EQ. 1) Y0=R2*AACUTE
P=0.0
IF (IACUTE .EQ. 2) P=R2*BRTCRN
LAMOUT=RDECAY+BR2
YR2=ACTVTY(Y0,P,LAMOUT,DELT)
YR2W=INTACT(Y0,P,LAMOUT,DELT)
```

```
C
C LUNG 3 COMPARTMENT
Y0=YR3
IF (IACUTE .EQ. 1 .AND. N .EQ. 1) Y0=R3*AACUTE
P=0.0
IF (IACUTE .EQ. 2) P=R3*BRTCRN
LAMOUT=RDECAY+BR3
YR3=ACTVTY(Y0,P,LAMOUT,DELT)
YR3W=INTACT(Y0,P,LAMOUT,DELT)
```

```
C
C LUNG 4 COMPARTMENT
Y0=YR4
IF (IACUTE .EQ. 1 .AND. N .EQ. 1) Y0=R4*AACUTE
```

```
P=0.0
IF (IACUTE .EQ. 2) P=R4*BRTCRN
LAMOUT=RDECAY+BR4
YR4=ACTVTY(Y0,P,LAMOUT,DELT)
YR4W=INTACT(Y0,P,LAMOUT,DELT)
YLUNG=YR1+YR2+YR3+YR4
55 CONTINUE
C-----
IF (INMODE .EQ. 0) GO TO 65
C STOMACH CONTENTS (STMC) COMPARTMENT
Y0=YSTMC
IF (INMODE .EQ. 2 .AND. IACUTE .EQ. 1 .AND. N .EQ. 1)
$ Y0=AACTUTE
P=0.0
IF (INMODE .GT. 1 .AND. IACUTE .EQ. 2) P=EATCRN
IF (INMODE .EQ. 1 .OR. INMODE .EQ. 3) P=EATCRN+
$ CILIAR*(BR1*YR1W+BR2*YR2W+BR3*YR3W+BR4*YR4W)/DELT
LAMOUT=RDECAY+GSCALE*RSTMC
YSTMC=ACTVTY(Y0,P,LAMOUT,DELT)
YSTMCW=INTACT(Y0,P,LAMOUT,DELT)
65 CONTINUE
IF (INMODE .EQ. 0 .AND. N .EQ. 1) GO TO 66
C-----
C SMALL INTESTINE CONTENTS (SIC) COMPARTMENT
Y0=YSIC
P=(GSCALE*RSTMC*YSTMCW+H1TOSI*RLVR1*YLVR1W+TFECE*CF*BTEMP)/DELT
LAMOUT=RDECAY+GSCALE*RSIC
YSIC=ACTVTY(Y0,P,LAMOUT,DELT)
YSICW=INTACT(Y0,P,LAMOUT,DELT)
66 CONTINUE
C-----
C PLASMA (PLS); THIS IS DIFFUSIBLE PLASMA PB;
C DOES NOT INCLUDE RELATIVELY SLOWLY EXCHANGEABLE PLASMA-
C PROTEIN-BOUND PB, WHEN THE LATTER COMPARTMENT IS USED.
Y0=YPLS
IF (INMODE .EQ. 0 .AND. N .EQ. 1 .AND. IACUTE .EQ. 1)
$ Y0=AACTUTE
P1=(RPROT*YPROTW+RRBC*YRBCW+REVF*YEVFW+RSOF0*YSOF0W
$ +(1.0-S2HAIR)*RSOF1*YSOF1W+RSOF2*YSOF2W
$ +H1TOBL*RLVR1*YLVR1W+RLVR2*YLVR2W
$ +RKDN2*YKDN2W+RCS2B*YCSURW+RTS2B*YTSURW
$ +RCORT*YCVOLW+RTRAB*YTVOLW+RBRAN*YBRANW
$ +F1*GSCALE*RSIC*YSICW)/DELT
IF (IACUTE .EQ. 2) P1=P1+CRONIC
```

IF (INMODE .EQ. 1 .OR. INMODE .EQ. 3) P1=P1+
\$ (1.0-CILIAIR)*(BR1*YR1W+BR2*YR2W+BR3*YR3W+BR4*YR4W)/DELT
LAMOUT=RPLS+RDECAY
UPTAKEGI=(F1*GSCALE*RSIC*YSICW)/DELT
UPTAKERI=(1.0-CILIAIR)*(BR1*YR1W+BR2*YR2W+BR3*YR3W+BR4*YR4W)/DELT
UPTAKE=UPTAKEGI+UPTAKERI
C ACTIVITY AND INTEGRATED ACTIVITY
YPLS=ACTVTY(Y0,P1,LAMOUT,DELT)
YPLSW=INTACT(Y0,P1,LAMOUT,DELT)
BTEMP=RPLS*YPLSW
C
C PLASMA-PROTEIN BOUND PB (PROT)
Y0=YPROT
P=TPROT*CF*BTEMP/DELT
LAMOUT=RPROT+RDECAY
YPROT=ACTVTY(Y0,P,LAMOUT,DELT)
YPROTW=INTACT(Y0,P,LAMOUT,DELT)
YPLAS=YPLS+YPROT
YPLASW=YPLSW+YPROTW
C
C
C RED BLOOD CELLS (RBC)
Y0=YRBC
C NOTE THAT CF HAS BEEN REMOVED FROM FOLLOWING:
P=TOORBC*BTEMP/DELT
LAMOUT=RRBC+RDECAY
YRBC=ACTVTY(Y0,P,LAMOUT,DELT)
YRBCW=INTACT(Y0,P,LAMOUT,DELT)
YBLUD=YPLAS+YRBC
SUMRBC=SUMRBC+YRBCW
C
C EVF
Y0=YEVF
P=TEVF*CF*BTEMP/DELT
LAMOUT=REVF+RDECAY
YEVF=ACTVTY(Y0,P,LAMOUT,DELT)
YEVFW=INTACT(Y0,P,LAMOUT,DELT)
C
C FAST TURNOVER SOFT-TISSUE COMPARTMENT (SOF0)
Y0=YSOFO
P=TSOF0*CF*BTEMP/DELT
LAMOUT=RSOF0+RDECAY
YSOFO=ACTVTY(Y0,P,LAMOUT,DELT)
YSOFOW=INTACT(Y0,P,LAMOUT,DELT)

C
C INTERMEDIATE TURNOVER SOFT-TISSUE COMPARTMENT (SOF1)
Y0=YSO1
P=TSOF1*CF*BTEMP/DELTA
LAMOUT=RSOF1+RDECAY
YSO1=ACTVTY(Y0,P,LAMOUT,DELTA)
YSO1W=INTACT(Y0,P,LAMOUT,DELTA)

C
C SLOW TURNOVER SOFT-TISSUE COMPARTMENT (SOF2)
Y0=YSO2
P=TSOF2*CF*BTEMP/DELTA
LAMOUT=RSOF2+RDECAY
YSO2=ACTVTY(Y0,P,LAMOUT,DELTA)
YSO2W=INTACT(Y0,P,LAMOUT,DELTA)

C
C BRAIN (BRAN)
Y0=YBRAN
P=TBRAN*CF*BTEMP/DELTA
LAMOUT=RBRAN+RDECAY
YBRAN=ACTVTY(Y0,P,LAMOUT,DELTA)
YBRANW=INTACT(Y0,P,LAMOUT,DELTA)

C
C CORTICAL SURFACE (CSUR)
Y0=YCSUR
P=(TBONE*(1.0-TFRAC)*CF*BTEMP+RDF2CS*YCDIFW)/DELTA
LAMOUT=RCS2B+RCS2DF+RDECAY
YCSUR=ACTVTY(Y0,P,LAMOUT,DELTA)
YCSURW=INTACT(Y0,P,LAMOUT,DELTA)

C
C EXCHANGEABLE CORTICAL VOLUME (CDIF)
Y0=YCDIF
P=RCS2DF*YCSURW/DELTA
LAMOUT=RDF2CS+RDF2DC+RDECAY
YCDIF=ACTVTY(Y0,P,LAMOUT,DELTA)
YCDIFW=INTACT(Y0,P,LAMOUT,DELTA)

620 CONTINUE

C-----
C NONEXCHANGEABLE CORTICAL VOLUME (CVOL)
Y0=YCVOL
P=RDF2DC*YCDIFW/DELTA
LAMOUT=RCORT+RDECAY
YCVOL=ACTVTY(Y0,P,LAMOUT,DELTA)
YCVOLW=INTACT(Y0,P,LAMOUT,DELTA)

C-----

C TRABECULAR SURFACE (TSUR)
Y0=YTSUR
P=(TBONE*TFRAC*CF*BTEMP+RDF2TS*YTDIFW)/DELTA
LAMOUT=RTS2B+RTS2DF+RDECAY
YTSUR=ACTVTY(Y0,P,LAMOUT,DELTA)
YTSURW=INTACT(Y0,P,LAMOUT,DELTA)
C-----
C EXCHANGEABLE TRABECULAR VOLUME (CDIF)
Y0=YTDIF
P=RTS2DF*YTSURW/DELTA
LAMOUT=RDF2TS+RDF2DT+RDECAY
YTDIF=ACTVTY(Y0,P,LAMOUT,DELTA)
YTDIFW=INTACT(Y0,P,LAMOUT,DELTA)
630 CONTINUE
C-----
C NONEXCHANGEABLE TRABECULAR VOLUME (TVOL)
Y0=YTVOL
P=RDF2DT*YTDIFW/DELTA
LAMOUT=RTRAB+RDECAY
YTVOL=ACTVTY(Y0,P,LAMOUT,DELTA)
YTVOLW=INTACT(Y0,P,LAMOUT,DELTA)
C-----
C LIVER 1 (LVR1)
Y0=YLVR1
P=TLVR1*CF*BTEMP/DELTA
LAMOUT=RLVR1+RDECAY
YLVR1=ACTVTY(Y0,P,LAMOUT,DELTA)
YLVR1W=INTACT(Y0,P,LAMOUT,DELTA)
C-----
C LIVER 2 (LVR2)
Y0=YLVR2
P=H1TOH2*RLVR1*YLVR1W/DELTA
LAMOUT=RLVR2+RDECAY
YLVR2=ACTVTY(Y0,P,LAMOUT,DELTA)
YLVR2W=INTACT(Y0,P,LAMOUT,DELTA)
YLIVR=YLVR1+YLVR2
C-----
C KIDNEYS 1
Y0=YKDN1
P=TKDN1*CF*BTEMP/DELTA
LAMOUT=RKDN1+RDECAY
YKDN1=ACTVTY(Y0,P,LAMOUT,DELTA)
YKDN1W=INTACT(Y0,P,LAMOUT,DELTA)
C-----

C KIDNEYS 2

Y0=YKDN2
P=TKDN2*CF*BTEMP/DELT
LAMOUT=RKDN2+RDECAY
YKDN2=ACTVTY(Y0,P,LAMOUT,DELT)
YKDN2W=INTACT(Y0,P,LAMOUT,DELT)

C

YKDNE=YKDN1+YKDN2

C-----

C BLADDER

Y0=YBLAD
P=(TURIN*CF*BTEMP+RKDN1*YKDN1W)/DELT
LAMOUT=RBLAD+RDECAY
YBLAD=ACTVTY(Y0,P,LAMOUT,DELT)
YBLADW=INTACT(Y0,P,LAMOUT,DELT)

C-----

C UPPER LARGE INTESTINE CONTENTS

Y0=YULIC
P=(1.0-F1)*GSCALE*RSIC*YSICW/DELT
LAMOUT=GSCALE*RULI+RDECAY
YULIC=ACTVTY(Y0,P,LAMOUT,DELT)
YULICW=INTACT(Y0,P,LAMOUT,DELT)

C-----

C LOWER LARGE INTESTINE CONTENTS

Y0=YLLIC
P=GSCALE*RULI*YULICW/DELT
LAMOUT=GSCALE*RLLI+RDECAY
YLLIC=ACTVTY(Y0,P,LAMOUT,DELT)
YLLICW=INTACT(Y0,P,LAMOUT,DELT)

C-----

C URINE

U0=YURIN
Y0=YURIN
P=RBLAD*YBLADW/DELT
YURIN=Y0+P*DELT
UTEMP=P*DELT
URIN=YURIN-U0

C-----

C FECES

Y0=YFECE
P=GSCALE*RLLI*YLLICW/DELT
YFECE=Y0+P*DELT
FTEMP=P*DELT

C-----

C SWEAT
 $Y0=YSWET$
 $P=TSWET*CF*BTEMP/DELT$
 $YSWET=Y0+P*DELT$

C-----
C HAIR, NAILS, DESQUAMATED SKIN
 $Y0=YHAIR$
 $P=S2HAIR*RSOF1*YSOF1W/DELT$
 $YHAIR=Y0+P*DELT$

C-----
C
 $SIGMA=YPLAS+YRBC+YEVF+YSOF0+YSOF1+YSOF2+YBRAN$
 $\$ +YCVOL+YTVOL+YCSUR+YTSUR+YCDIF+YTDIF+YKDNE+YBLAD+YLIVR$
 $\$ +YR1+YR2+YR3+YR4+YSTMC+YSIC+YULIC+YLLIC$
 $\$ +YURIN+YFECE+YSWET+YHAIR$
 $TBODY1=YPLAS+YRBC+YEVF+YSOF0+YSOF1+YSOF2+YBRAN$
 $\$ +YCVOL+YTVOL+YCSUR+YTSUR+YCDIF+YTDIF+YKDNE+YLIVR$
 $TBODY2=TBODY1+YR1+YR2+YR3+YR4+YBLAD$
 $\$ +YSTMC+YSIC+YULIC+YLLIC$
 $TOTEXC=YURIN+YFECE+YSWET+YHAIR$
 $YSKEL=YCVOL+YTVOL+YCSUR+YTSUR+YCDIF+YTDIF$
 $YTRAB=YTSUR+YTDIF+YTVOL$
 $YCORT=YCSUR+YCDIF+YCVOL$
 $YSOFT=YSOF0+YSOF1+YSOF2$
IF (TBODY1 .NE. 0.0) BONFRC=YSKEL/TBODY1
IF (TBODY1 .NE. 0.0) BRNFRC=YBRAN/TBODY1
IF (TBODY1 .NE. 0.0) HEPFRC=YLIVR/TBODY1
IF (TBODY1 .NE. 0.0) BLDFRC=YBLUD/TBODY1
IF (TBODY1 .NE. 0.0) RENFRC=YKDNE/TBODY1
IF (TBODY1 .NE. 0.0) OTHFRC=YSOFT/TBODY1
IF (YBLUD .NE. 0.0) PLSRBC=YPLAS/YBLUD
IF (AMTBLD .NE. 0.0) BLCONC=YBLUD/AMTBLD
C IF (RBCVOL .NE. 0.0) RBCONC=YRBC/(ADJRBC*AMTBLD) replaced by next line
IF (RBCVOL .NE. 0.0) RBCONC=YRBC/(BLDHCT*AMTBLD)

$RENCON=YKDNE/KIDWT$
 $CRTCON=YCORT/CORTWT$
 $TRBCON=YTRAB/TRABWT$
 $ASHCON=YSKEL/TSKELWT$
 $CRTCONBM=CRTCON*1.8$
 $TRBCONBM=TRBCON*3.*1.8$

IF (N .GT. 1) CLEAR=(URIN/DELT)/YPLAS
IF (N .GT. 1) BCLEAR=100.*(URIN/DELT)/YBLUD

```
IF (YBLUD .NE. 0.0) PCENT=100.*YPLAS/YBLUD
Q(1)=YPLAS
Q(2)=YRBC
Q(3)=YBLUD
Q(4)=YSKEL
Q(5)=YCORT
Q(6)=YTRAB
Q(7)=YLIVR
Q(8)=YKDNE
Q(9)=YSOFT
Q(10)=YBRAN
Q(11)=YURIN
Q(12)=YFECE
Q(13)=TBODY2
Q(14)=TOTEXC
Q(15)=BONFRC
Q(16)=BRNFRC
Q(17)=HEPFRC
Q(18)=BLDFRC
Q(19)=RENFRC
Q(20)=OTHFRC
Q(21)=BLCONC
Q(22)=RBCONC
Q(23)=RENCON
Q(24)=CRTCON
Q(25)=TRBCON
Q(26)=ASHCON
Q(27)=CLEAR
Q(28)=BCLEAR
Q(29)=PCENT
Q(30)=YLUNG
Q(31)=Q(28)*Q(3)/100.
Q(32)=CRTCONBM
Q(33)=TRBCONBM
Q(34)=UPTAKEGI
Q(35)=UPTAKERI
Q(36)=UPTAKE
IF (MOD(N,ISKIP) .NE. 0) GO TO 1000
C   WRITE(*,991)YEARS,SIGMA,Q(I1),Q(I2),Q(I3),Q(I4),Q(I5)
   WRITE(50,991)YEARS,SIGMA,Q(I1),Q(I2),Q(I3),Q(I4),Q(I5)
   IF (DAYS .GT. ENDDAY) GO TO 1001
991 format(' ',1p7e10.3)
1000 CONTINUE
1001 CONTINUE
```

```
STOP
END
C
REAL FUNCTION INTACT(Y,P,X,D)
DX=D*X
IF (DX .GT. 50.0) GO TO 10
INTACT=((1.0-DEXP(-DBLE(X*D)))/X)*(Y-(P/X))+P*D/X
GO TO 20
10 INTACT=(1.0/X)*(Y-P/X)+P*D/X
20 CONTINUE
RETURN
END
C
FUNCTION ACTVTY(Y,P,X,D)
DX=D*X
IF (DX .GT. 50.0) GO TO 10
ACTVTY=(Y-(P/X))*DEXP(-DBLE(X*D))+P/X
GO TO 20
10 ACTVTY=P/X
20 CONTINUE
RETURN
```

Appendix M Attachment 2: Sample Input File for Model Version 5

Based on the model updates and the updated maternal blood lead value, an input file template was generated for the analysis and is reproduced below. All the parameter values in italics vary according to the specific iteration and when the renovation begins; the other values remain constant across all the different renovation and background intake simulations. These inputs include the age-dependent absorption rates, transfer rates, and deposition rates used in the model. They are listed in a series of 14 numbers on each input line of the file, where the 14 numbers correspond to the ages 0.27, 1, 5, 10, 15, 18, 24, 30, 40, 45, 55, 65, and 75 years old.

Table M-5. Input File Template for Analysis

0. LINE	# 1 Template for PnCB exposure analysis simulations
0.05,0,10000000,25550	# 2 # DIFF STEP LENGTHS; USE FIXED STEP LENGTH? MAXIMUM # STEPS; LAST DAY
0.01	# 3 DELTi; CALCULATIONS FIRST BASED ON STEP LENGTHS DELT1, THEN DELT2, ETC
1000,1900,2800,6700,1000000	# 4 ICYCi; USE TIME STEP DELT1 UP TO STEP ICYC1, DELT2 UP TO ICYC2, ETC
1	# 5 WRITE TO SCREEN ONLY ON THESE STEPS (E.G., EVERY 100TH TIME STEP)
21,24,25,22,23	# 6 FIVE SELECTED OUTPUTS
3,2,0	# 7 MODE OF INTAKE; SWITCH FOR ACUTE/CHRONIC; SWITCH FOR MANUAL INPUT (1)
7	# 8 NCHRON, # TIME STEPS IN CHRONIC INTAKE FUNCTION (UP TO 50)
365,730,1095,1460,1825,2190,10950,18250,25550	# 9 ENDPT, ENDPOINTS OF THE CHRONIC INTAKE TIME STEPS
7*0.0	# 10 UP TO 1000 CHRONIC INTAKE RATES DIRECTLY TO BLD ON STEPS,
0.108,0.16,0.19,0.218,0.218,0.218,0.248	# 11 UP TO 1000 CHRONIC LUNG DEPOSITION RATES (PER DAY)
6.16,10.31,11.17,10.91,10.91,10.91,11.07	# 12 UP TO 1000 CHRONIC INGESTION INTAKE RATES (PER DAY)
14,75.	# 13 NUMBER OF AGES AT WHICH PARAM VALUES ARE SPECIFIED & MAX OF THESE
0.,0.274,1.,5.,10.,15.,18.,24.,30.,40.,45.,55.,65.,75.	# 14 AGES (Y) AT WHICH PARAMETER VALUES ARE GIVEN EXPLICITLY
2*0.45,4*0.3,8*0.15,	# 15 GASTROINTESTINAL ABSORPTION FRACTION (F1)
0.0	# 16 RADIOLOGICAL DECAY RATE OF PB PER DAY
1,0.0,270.,1.5,	# 17 1 FOR NONLINEAR MODEL; 3 NONLINEAR PARAMETER VALUES
1,0.7,0.85	# 18 1 FOR FETAL EXPOSURE; MOTHER'S BLOOD CONC; FETUS:MOTHER BLD RATIO (10-->0.7)
0.50,0.07,0.32,0.01,0.055,0.045,	# 19 FRACS OF BODY PB AT BIRTH IN SOFT TISS, RBC, BONE, KIDNEY, LIVER, BRAIN
0.25,0.35,0.30,0.10,0.04,	# 20 FRACS OF DEPOSITED AMT ASSIGNED TO 4 LUNG COMPS; FRAC MOVEMENT TO GI
16.6,5.54,1.66,0.347,	# 21 BR1,BR2,BR3,BR4
24.,6.,1.85,1.0,	# 22 ADULT TRANSFER RATES FROM STOMACH AND INTESTINAL SEGMENTS
4*1.66667,1.33333,9*1.0	# 23 SCALES RATE OF MOVEMENT THRU GI TRACT AT 10 AGES
0.0102,0.00822,0.00288,0.00154,0.00089,0.000512,0.000370,0.000082,6*0.000041	# 24 CORT BONE from Rowland
0.0102,0.00822,0.00288,0.00181,0.00132,0.000956,0.000781,0.000493,2*0.000247,0.000274,0.000301,0.000329,0.000356	# 25 TRAB BONE
5*0.40,9*0.35	# 26 FRAC TRANSFER CORT SURF TO BLOOD
5*0.60,9*0.55	# 27 FRAC TRANSFER TRABECULAR SURFACE TO BLOOD

5*0.55,9*0.60	# 28 FRAC TRANSFER CORT SURFACE TO VOLUME
5*0.40,9*0.40	# 29 FRAC TRANSFER TRAB SURFACE TO VOLUME
14*0.023105	# 30 TOTAL TRANSFER RATE FROM EXCH BONE VOLUME
14*0.2	# 31 FRAC TRANSFER FROM EXCH VOL TO NONEXCH
0.0693,0.139	# 32 TRANSFER RATES FROM LIVER 1 AND KIDNEY 1
2*12.,15.,11.,8.,9*7.	# 33 TRANSFER RATE FROM U BLADDER TO URINE
4*0.00693,10*0.0019	# 34 TRANSFER RATE FROM LIVER 2
4*0.00693,10*0.0019	# 35 TRANSFER RATE FROM KIDNEY 2
2.079,0.00693,0.00038	# 36 TRANSFER RATES FROM 3 SOFT TISS COMPS
14*0.00095,	# 37 TRANSFER RATE FROM BRAIN
0.15,0.006,0.0035,0.4	# 38 DEP FRACS IN URINE,FECES,SWEAT; FRAC TRANS ST1 TO EXCRETION
2*0.24,0.144,0.128,0.179,0.237,8*0.08	# 39 DEPOSITION FRACTION IN BONE
0.2,0.2,0.2,0.222,0.25,0.279,8*0.556	# 40 FRACTION OF BONE DEPOSITION GOING TO TRABECULAR
0.04,0.1,0.45,0.45	# 41 DEP FRAC IN LIVER 1; FRACS LIVER 1 TO LIVER 2, SI, & PLASMA
0.02,0.0002	# 42 DEP FRACS IN KIDNEY 1 AND KIDNEY 2
3*0.08345,3*0.08375,8*0.08875	# 43 DEPOSITION FRACTION IN STO
3*0.01,3*0.01,8*0.005	# 44 DEPOSITION FRACTION IN ST1
3*0.001,3*0.001,8*0.001	# 45 DEPOSITION FRACTION IN ST2
3*0.00045,11*0.00015,	# 46 DEPOSITION FRACTION IN BRAIN
0.20,	# 47 DEPOSITION FRACTION IN RBC (superceded by age-dependent data in code)
0.5000,3.	# 48 DEPOSITION FRACTION IN EVF; SIZE OF EVF RELATIVE TO PLASMA
2000.,0.0004,0.139,	# 49 TRANSFER RATE FROM PLASMA; DEP FRAC & RATE OF LOSS FOR PLASMA PROTEINS
3*0.562,2*0.277,9*0.139	# 50 TRANSFER RATE FROM RRBC
22.,30.	# 51 AMOUNT OF RBC AND PLASMA (DL) IN REFERENCE ADULT MALE (superceded by code)
2.7,3.1,5.0,14.0,24.0,45.0,8*53.0	# 52 AMOUNT OF BLOOD (DL) AT 14 AGES
0,0.4,1243.,1250.	# 53 ICHEL, CHLEFF, CHEL1, CHEL2

Appendix N. Background Media Concentrations and Intakes

N.1. Dust

Background lead-dust loading estimates were found separately for public and commercial buildings (as a whole) and for residences. This section provides an overview of the data used to define the lognormal distributions used for each.

N.1.1. Public and Commercial Buildings

Little information is available about the levels of lead in dust in public and commercial buildings. A literature search was conducted but few sources were found. The data source found was the First National Health Survey of Child Care Centers (hereafter the CCC Report; Westat, 2003). The survey provides information on the geometric mean and geometric standard deviation from 336 samples of lead floor loading. Because of the relatively low number of samples in each vintage bin when the data were separated into the different bins, an overall distribution across all bins was used. The geometric mean and geometric standard deviation were taken from Table 5-5 from the Westat report, giving values of 0.8 $\mu\text{g}/\text{ft}^2$ and 2.25, respectively.

Table N-1. Public/Commerical Background Lead Dust Loadings

Vintage	Geometric Mean ($\mu\text{g}/\text{ft}^2$)	Geometric Standard Deviation
All	0.8	2.25

N.1.2. Residences

For residences, the background dust loading values were estimated using the American Healthy Homes Survey (AHHS) (HUD, 2011). AHHS is a follow-up to the National Survey of Lead and Allergens in Housing (NSLAH) conducted from 1997 through 2000 and monitored lead dust levels in homes. These data were favored over other sources (e.g., NHANES) because the raw survey data with vintage data were available so that different background dust distributions could be developed for each Approach housing vintage.

The raw survey data were obtained from HUD, and samples taken within a single home were averaged to provide one estimate per residence. If vintage information was not available for a given home, it was assigned to the home using random sampling from the overall distribution in the dataset. Then, the geometric mean and geometric standard deviation across the dataset was estimated in the SAS software

package, utilizing the sample weights in the data so that the estimates were nationally representative. The final distributions by vintage are shown in Table N-2.

Table N-2. Residential Background Lead Dust Loadings by Vintage.

Vintage	Geometric Mean ($\mu\text{g}/\text{ft}^2$)	Geometric Standard Deviation
Pre 1930	3.97	4.76
1930-1949	1.94	7.76
1950-1959	1.14	2.65
1960-1979	0.79	4.25
Post 1979	0.49	3.38

N.2. Soil

Similar to dust, background soil lead concentration estimates were found separately for public and commercial buildings (as a whole) and for residences. This section provides an overview of the data used to define the lognormal distributions used for each.

N.2.1. Public and Commercial Buildings

As with dust, limited information was available about soil lead concentrations around public and commercial buildings. This section provides a summary of data used for each building type. A summary of the input values is provided in Table N-3.

Table N-3. Public/Commercial Background Lead Soil Concentrations

Building Type	Point Estimate ($\mu\text{g}/\text{g}$)	Geometric Mean ($\mu\text{g}/\text{g}$)	Geometric Standard Deviation
Industrial	197.3	N/A	N/A
Commercial	49.97	N/A	N/A
Agricultural	N/A	17.1	1.75
Schools	N/A	28.0	3.00

Government/Commercial Buildings and Industrial Buildings

For government/commercial and industrial soils, a meta-analysis study of soil samples from 1970 to 2012 in different land use areas was used (Datko-Williams, 2013). The data were limited to measurements within the last 15 years based temporal trends in the Datko-Williams analysis, which

indicated an approximately 25-75% decrease in soil lead levels every 10-20 years. The studies were further limited to those in the “commercial” and “industrial” land use categories. The resulting 9 studies were from Florida, NY, Ohio, and Maryland. For each, the average was estimated and then the weighted average across studies using the number of samples in the study was estimated. These averages resulted in soil concentration estimates of 50 µg/g for government/commercial buildings and 197 µg/g for industrial buildings. Owing to the aggregated presentation of data in the meta-analysis study, the results were not further parsed into distributions, and a single point estimate was used for background soil.

Agricultural Buildings

For agricultural soils, the USGS background soil survey (<http://www.epa.gov/superfund/lead/background.htm#background>) provides estimates from 2004-2007, and, while not a structured survey like NSLAH or NHANES, is relatively nationally representative. Lead statistics based on 1,556 soil samples collected from the top 5 cm of soil that was “planted/cultivated” were calculated, resulting in a geometric mean of 17.1 µg/g and a geometric standard deviation of 1.75.

Schools

For schools, the same data source used for public and commercial building background dust (the CCC Survey) was used for soil as well. Values presented in Table 6-5 of that survey indicated a geometric mean of 28 µg/g and a geometric standard deviation of 3.

N.2.2. Residences

Background soil values were estimated using the National Survey of Lead and Allergens in Housing (NSLAH) survey data (HUD, 2002). The NSLAH survey examined allergen and contaminant levels in 831 housing units and was designed to be nationally representative. The data were binned into the different Approach building vintages, and survey weights were incorporated to estimate the geometric mean and geometric standard deviation, as shown in

Appendices to the Approach for Estimating Exposures and Incremental Health Effects from Lead due to Renovation, Repair, and Painting Activities in Public and Commercial Buildings

Table N-4.

Table N-4. Residential Background Lead Soil Concentrations by Vintage.

Vintage	Geometric Mean ($\mu\text{g}/\text{ft}^2$)	Geometric Standard Deviation
Pre 1930	367.4	3.53
1930-1949	144.1	3.69
1950-1959	79.6	3.77
1960-1979	24.2	3.29
Post 1979	15.8	2.32

N.3. Air

The background lead concentration data for ambient and indoor air used in this approach are based on a review of the 2009 annual average total suspended particulate (TSP) monitoring data for lead contained in EPA's Air Quality Systems (AQS) database (USEPA, 2010b,c).

The range of concentrations reported in this database was large, with a 10th percentile concentration of 0.01 $\mu\text{g}/\text{m}^3$ and a 90th percentile concentration of 0.18 $\mu\text{g}/\text{m}^3$. Based on these data, the geometric mean (0.02 $\mu\text{g}/\text{m}^3$) and geometric standard deviation (5.52) were selected to represent the range of background ambient air concentrations. Note, however, that this value may overestimate the ambient air concentration because lead monitors are often located in areas with nearby lead emission sources.

N.4. Intake, Blood Lead, and Bone Lead

The Approach estimates health effects for both children and adults. Because of historical changes in blood lead after changes in the lead content of gasoline and paint, population blood lead levels have been declining over the last few decades. Thus, the approach must take into account the blood lead history of the individual and simulate different 2014 background intakes, blood leads, and bone leads for different ages of adults.

To make these estimates, the NHANES survey estimates were compiled, starting with NHANES II and continuing through the latest measurements in 2012 (CDC, 2012). The population-average estimates of blood lead for each age and for each survey were estimated and compiled, as shown in Table N-5.

Table N-5. Average Blood Lead Levels Estimated from NHANES II through NHANES 2011-2012.

Age	1976-1980	1988-1991	1991-1994	1999-2000	2001-2002	2003-2004	2005-2006	2007-2008	2009-2010	2011-2012
0	16.8									
1	17.3	5.3	4.3	3.5	2.7	2.6	2.0	2.4	1.7	1.4
2	16.9	5.2	4.0	2.8	2.5	2.5	2.1	1.9	1.5	1.7
3	16.9	4.4	3.5	3.1	2.1	2.3	1.6	2.1	1.3	1.3
4	15.8	4.6	3.5	2.5	1.8	2.0	1.7	1.6	1.4	1.2
5	15.8	4.1	2.9	2.3	1.9	1.7	1.6	1.5	1.4	1.0
6	14.5	3.5	3.4	2.1	1.7	1.7	1.6	1.5	1.2	1.1
7	14.8	3.5	2.7	1.8	1.7	1.7	1.3	1.1	1.0	0.8
8	12.8	3.4	2.4	2.1	1.5	1.5	1.2	1.2	1.0	0.9
9	13.1	3.0	2.3	1.5	1.5	1.4	1.1	1.1	0.9	0.8
10	13.4	2.8	2.3	1.8	1.4	1.4	1.1	1.1	0.9	0.7
11	12.5	2.8	2.2	1.6	1.5	1.2	1.1	1.0	0.8	0.7
12	11.7	2.8	2.6	1.8	1.3	1.3	1.1	1.1	0.8	0.7
13	11.6	2.7	1.9	1.5	1.3	1.1	1.0	1.1	0.8	0.7
14	11.2	2.3	2.2	1.2	1.1	1.1	1.0	0.9	0.8	0.6
15	11.8	2.4	1.8	1.3	1.0	1.0	0.9	0.9	0.7	0.6
16	11.7	2.1	1.7	1.2	1.0	1.1	0.9	0.8	0.7	0.6
17	12.9	2.2	1.5	1.1	1.0	1.3	0.9	0.8	0.8	0.7
18	13.1	2.9	1.8	1.4	1.1	1.1	1.1	0.8	1.0	0.7
19	12.7	2.2	2.1	1.4	1.3	1.2	0.9	1.1	0.9	0.7
20	12.8	3.3	2.0	1.5	1.1	1.1	1.1	1.1	0.9	0.8
21	13.4	2.9	2.4	1.5	1.6	1.6	1.2	1.1	1.0	1.1
22	13.2	2.7	1.9	1.3	1.4	1.3	1.1	1.0	1.1	0.8
23	13.6	3.3	1.8	1.5	1.2	1.4	1.1	1.0	1.0	0.8
24	13.6	3.0	2.3	2.0	1.3	1.2	1.0	1.3	1.1	0.8
25	13.7	2.9	2.8	1.5	1.5	1.3	1.1	1.0	0.9	1.1
26	14.9	2.9	2.1	1.6	1.6	1.4	1.2	1.3	1.1	1.2
27	13.0	3.2	2.6	1.7	1.3	1.2	1.2	1.4	1.2	1.1
28	12.9	3.5	2.2	1.8	1.6	1.4	1.2	1.2	1.3	0.9
29	12.9	3.2	2.0	1.8	1.3	1.5	1.1	1.1	1.1	1.0
30	13.4	3.4	2.7	1.8	1.3	1.5	1.4	1.4	1.7	0.8
31	14.0	3.0	3.0	1.8	1.4	1.7	1.1	1.4	1.1	0.8
32	14.6	3.6	2.6	1.4	1.9	1.9	1.3	1.5	1.1	0.8

Appendices to the Approach for Estimating Exposures and Incremental Health Effects from Lead due to Renovation, Repair, and Painting Activities in Public and Commercial Buildings

Age	1976-1980	1988-1991	1991-1994	1999-2000	2001-2002	2003-2004	2005-2006	2007-2008	2009-2010	2011-2012
33	13.8	3.8	2.4	1.9	1.5	1.4	1.8	1.3	1.1	1.2
34	14.6	3.3	2.7	2.9	1.6	1.5	1.3	1.4	1.2	1.0
35	14.5	5.1	3.5	1.4	1.4	1.5	1.4	1.3	1.4	1.0
36	14.8	4.5	2.7	2.0	1.7	1.7	1.4	1.4	1.1	1.1
37	15.0	4.0	2.7	2.2	1.8	1.5	1.3	1.4	1.3	1.0
38	14.2	4.0	3.0	2.1	2.6	1.6	1.4	1.2	1.2	1.8
39	15.7	3.7	2.4	1.7	1.9	2.0	1.4	1.7	1.1	1.1
40	13.6	3.5	2.8	2.0	2.2	1.5	1.5	1.2	1.3	1.5
41	16.1	3.8	2.9	2.2	1.6	1.6	1.6	1.3	1.3	1.0
42	14.8	3.6	3.3	1.8	1.7	1.7	1.4	1.4	1.3	1.3
43	14.1	3.6	2.9	2.1	2.3	2.0	1.4	1.6	1.3	1.1
44	13.8	3.4	2.7	2.1	2.4	1.9	1.6	1.6	1.2	1.4
45	15.8	3.6	3.1	2.0	2.1	2.1	1.7	1.4	1.6	1.3
46	14.1	3.6	3.3	2.3	2.1	1.8	1.5	1.7	1.7	1.6
47	14.6	4.5	3.6	2.6	2.2	1.7	1.9	1.6	1.6	1.7
48	14.9	5.1	3.5	2.4	2.0	2.0	2.1	2.0	1.7	1.5
49	15.6	4.6	3.4	2.1	2.3	2.0	2.1	1.7	1.7	1.4
50	16.1	4.4	3.0	2.6	2.3	2.1	1.6	1.7	2.1	1.5
51	14.9	4.5	3.5	2.5	2.1	1.9	1.9	1.8	1.7	2.0
52	15.9	5.8	3.2	2.3	2.2	2.1	2.0	2.0	1.6	2.4
53	14.9	4.7	4.1	2.4	2.2	2.1	2.1	2.4	1.7	1.7
54	15.6	5.9	3.3	2.5	2.1	2.5	2.1	2.3	2.1	1.6
55	14.4	4.4	3.7	2.7	2.3	2.1	2.1	2.3	1.9	1.5
56	15.1	5.6	3.8	2.2	2.2	2.0	2.3	2.1	1.8	1.6
57	14.4	5.4	3.5	3.2	2.1	1.9	2.3	2.2	2.4	1.7
58	16.0	4.2	3.7	2.8	2.2	2.2	2.0	1.9	2.1	1.7
59	15.3	4.4	3.1	2.4	2.3	1.9	2.3	2.1	1.6	2.2
60	14.4	6.1	4.0	2.7	2.5	2.2	2.0	2.0	1.9	2.0
61	14.7	4.3	3.3	5.2	2.2	2.3	2.6	2.0	1.8	1.6
62	14.3	4.3	3.9	2.4	2.5	2.3	2.3	1.8	1.8	1.5
63	13.9	4.9	3.6	2.5	2.1	2.6	2.2	2.2	1.9	1.8
64	14.6	4.2	4.5	2.6	2.2	2.2	2.4	2.0	1.7	1.8
65	15.3	4.7	3.8	2.7	2.3	2.3	2.7	1.9	1.9	1.5
66	14.7	5.0	3.9	3.0	2.3	2.2	2.2	1.9	1.9	2.0

Appendices to the Approach for Estimating Exposures and Incremental Health Effects from Lead due to Renovation, Repair, and Painting Activities in Public and Commercial Buildings

Age	1976-1980	1988-1991	1991-1994	1999-2000	2001-2002	2003-2004	2005-2006	2007-2008	2009-2010	2011-2012
67	14.1	4.7	4.1	2.8	2.4	2.1	2.4	1.9	1.8	2.0
68	14.7	5.0	4.1	2.5	2.2	2.2	1.9	2.0	1.9	3.2
69	14.4	4.8	4.4	3.1	2.1	2.4	2.5	1.8	1.8	1.9
70	15.5	4.1	3.6	3.0	2.8	2.3	2.2	2.2	2.3	1.6
71	13.4	4.3	4.6	2.4	2.6	2.8	2.3	2.1	1.9	1.6
72	14.0	4.3	4.5	3.0	3.7	2.2	2.7	2.4	2.0	2.0
73	12.4	5.7	3.6	2.5	2.5	2.9	2.2	2.0	1.8	2.0
74	13.9	4.6	4.3	2.7	2.8	2.4	2.2	2.3	1.9	1.7
75	13.1	5.3	4.5	2.7	2.4	2.1	2.4	2.5	2.0	1.9
76		4.5	4.0	2.5	2.7	2.3	2.7	2.4	1.7	1.8
77		4.7	3.0	2.6	2.2	2.2	2.2	2.1	2.0	1.8
78		4.8	4.2	3.8	2.6	3.1	2.1	2.8	2.1	1.7
79		5.8	5.2	3.1	2.5	2.3	2.8	2.5	2.2	1.9
80		4.7	3.8	2.5	2.6	2.7	2.9	2.4	2.2	2.1
81		4.8	4.3	2.8	2.6	2.2	2.7			
82		4.6	4.6	3.1	2.4	3.1	2.7			
83		5.4	3.9	2.5	2.4	2.7	2.5			
84		4.8	4.5	2.8	2.5	2.6	2.8			
85		4.0	4.0	3.2	3.0	3.1	2.8			
86		5.3	4.9							
87		5.0	4.4							
88		5.0	4.7							
89		5.5	4.5							
90		5.0	3.6							

The different age groups were then grouped by taking the following into account:

- Childhood blood leads tend to be higher than adults, so age ranges cannot be so broad that they span children and adults,
- Legislation that limited lead in gasoline lead to a rapid decline in blood lead during the 1980's and 1990's, and
- Blood lead levels have continued to decline through the 2000's through today, although at a slower rate.

Because biokinetics vary with age and media concentrations have varied with calendar year, birth year is used to track different individuals and their intake values. Their biokinetics will then vary in the Leggett model with their age, but intake changes related to changes in media concentrations will happen in fixed calendar years.

Based on these observations, six different age ranges were defined based on birth year. Then, the average NHANES predictions for each survey and for each defined age range were estimated. The values are shown in Table N-6. Next, intake rates were assumed to be constant but then allowed to change at pre-defined years based on inspection of the rate of change of blood leads. The years selected include: 1984, 1993, 2000, and 2005. An initial guess at lead intake was arbitrarily set to 100 $\mu\text{g}/\text{day}$ for the first of these intake year ranges. Then, the initial guess was scaled during the subsequent years using the ratio of the blood lead in the first year range and the year range in question. For example, for the oldest individuals assumed to be born between 1930 and 1954, their intake from birth to 1984 was set to 100 mg/day . Then, their intake from 1984 to 1993 was scaled using the ratio of NHANES blood leads in 1992 (the closest survey year to 1993) and the NHANES measurements in closest to 1984 (1978). Looking at Table N-6, this ratio is $3.3/14.3 = 0.23$. Multiplying by the original guess of 100 $\mu\text{g}/\text{day}$ gives an intake guess from 1984 to 1993 of 23 $\mu\text{g}/\text{day}$. This scaling assumes that the intake will scale approximately linearly with blood lead; although this assumption is not strictly true, blood lead tends to trend linearly with intake over narrow regions of intake levels, and this assumption allows the initial guesses to incorporate information known about blood lead trends.

Next, the Leggett model was used to back-calculate the intake levels for each age using the initial guesses in Table N-6. The blood leads resulting from running the initial guesses were compared to the NHANES values by calculating the mean squared error (MSE) between the predicted (Leggett) and actual (NHANES) values. Lead intakes were optimized based on a gradient-descent method by iteratively adjusting the initial lead intakes by a factor until the MSE was minimized. The intakes corresponding to the minimized MSE were selected as the representative intakes for the selected birth year. This process was repeated for each birth year within each age range.

Table N-6. Age Ranges, Years When Intakes Change, Initial Intake Guesses, and Blood Lead Levels Used in Intake Optimization Calculation

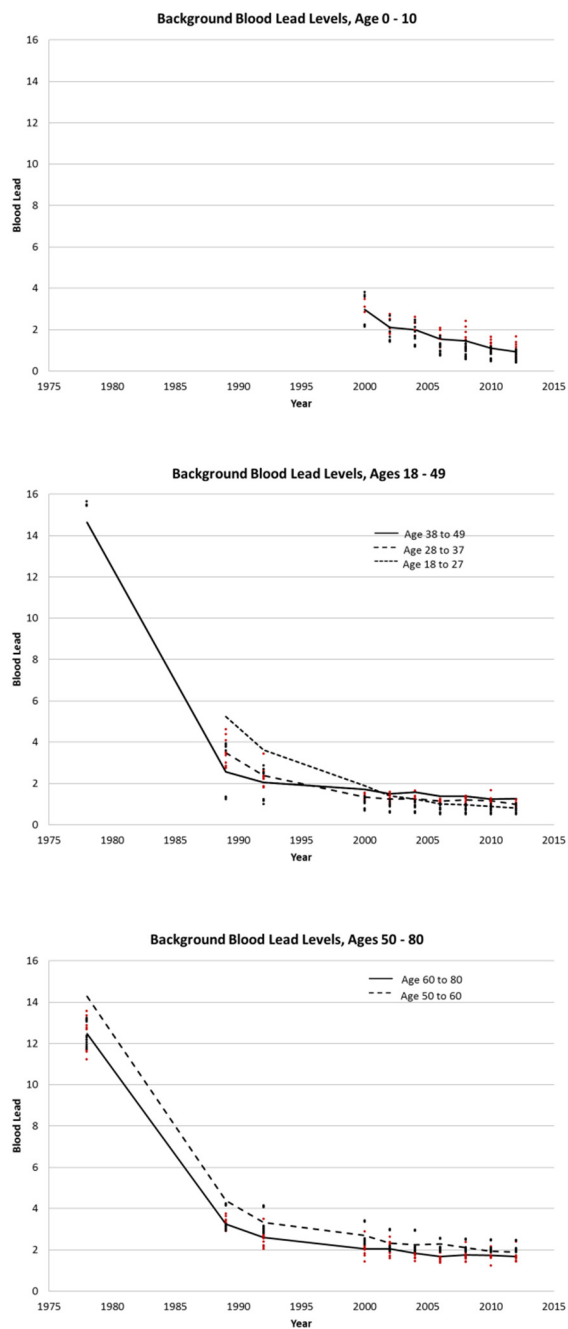
Birth Year: 1930-1954				Birth Year: 1955-1966				Birth Year: 1967-1976			
Year Intake Changes	Initial Intake Estimate (µg/day)	Blood Lead Year	NHANES Blood Lead (µg/dL)	Year Intake Changes	Initial Intake Estimate (µg/day)	Blood Lead Year	NHANES Blood Lead (µg/dL)	Year Intake Changes	Initial Intake Estimate (µg/day)	Blood Lead Year	NHANES Blood Lead (µg/dL)
1984	100	1978	14.3	1984	100	1978	12.5	1984	100	1978	14.6
1993	23	1989	4.4	1993	21	1989	3.3	1993	14	1989	2.6
2000	19	1992	3.3	2000	16	1992	2.6	2000	12	1992	2.0
2005	16	2000	2.7	2005	14	2000	2.1	2005	9	2000	1.7
2014	13	2002	2.3	2014	13	2002	2.1	2014	9	2002	1.5
		2004	2.2			2004	1.8			2004	1.6
		2006	2.3			2006	1.7			2006	1.4
		2008	2.1			2008	1.7			2008	1.4
		2010	1.9			2010	1.7			2010	1.3
		2012	1.9			2012	1.7			2012	1.3
Birth Year: 1977-1986				Birth Year: 1987-1996				Birth Year: Post 1996			
Year Intake Changes	Initial Intake Estimate (µg/day)	Blood Lead Year	NHANES Blood Lead (µg/dL)	Year Intake Changes	Initial Intake Estimate (µg/day)	Blood Lead Year	NHANES Blood Lead (µg/dL)	Year Intake Changes	Initial Intake Estimate (µg/day)	Blood Lead Year	NHANES Blood Lead (µg/dL)
1984	100										
1993	68	1989	3.5	1993	100	1989	5.2				
2000	38	1992	2.4	2000	39	1992	3.6	2000	100		
2005	33	2000	1.3	2005	28	2000	1.9	2005	52	2000	3.0
2014	28	2002	1.2	2014	22	2002	1.4	2014	31	2002	2.1
		2004	1.3			2004	1.2			2004	2.0
		2006	1.1			2006	1.0			2006	1.5
		2008	1.2			2008	1.0			2008	1.5
		2010	1.2			2010	0.9			2010	1.1
		2012	1.0			2012	0.8			2012	0.9

Figure N-1 shows an overview of the consolidated average NHANES data used for each age range, the individual NHANES estimates for each age within the age range, and the fit data. Overall, the optimization routine provided good fits between the predicted and actual blood lead estimates.

The optimized intakes were used to estimate the background bone lead and blood lead values in the year 2014 and then projected forward with constant intake 5 additional years. The renovation was then assumed to occur in 2014 and the blood lead with renovation was simulated and compared to the background-only blood lead. A summary of select intake, blood lead, and bone lead estimates is provided in Table N-7. The full table was not included owing to the length of the table.

This approach assumes that intake is constant from the year of birth until 1984, which means that intakes for both children and adults are similar.

Appendices to the Approach for Estimating Exposures and Incremental Health Effects from Lead due to Renovation, Repair, and Painting Activities in Public and Commercial Buildings



Line = Data Used for Optimization; Red = Actual NHANES Data; Black = Fit Model Data

Figure N-1. NHANES Data and Fit Background Blood Lead Estimates

Table N-7. Estimated Intake Rates for Select Birth Years

Birth Year: 1930-1954			Birth Year: 1955-1966			Birth Year: 1967-1976		
Year Intake Changes	Intake for BY 1930 (µg/day)	Intake for BY 1942 (µg/day)	Year Intake Changes	Intake for BY 1955 (µg/day)	Intake for BY 1960 (µg/day)	Year Intake Changes	Intake for BY 1967 (µg/day)	Intake for BY 1972 (µg/day)
1984	44.48666	45.82987	1984	39.46613	35.15088	1984	61.88535	46.47278
1993	10.36069	10.67351	1993	8.242491	7.341253	1993	8.619557	6.472853
2000	8.40406	8.657807	2000	6.501917	5.790994	2000	7.267323	5.457393
2005	7.114232	7.329035	2005	5.332247	4.749217	2005	5.857615	4.398774
2014	5.891762	6.069654	2014	5.323517	4.741441	2014	5.330255	4.002753
Birth Year: 1977-1986			Birth Year: 1987-1996			Birth Year: Post 1996		
Year Intake Changes	Intake for BY 1977 (µg/day)	Intake for BY 1982 (µg/day)	Year Intake Changes	Intake for BY 1987 (µg/day)	Intake for BY 1990 (µg/day)	Year Intake Changes	Intake for BY 1996 (µg/day)	Intake for BY 2000 (µg/day)
1984	13.22644	12.2373						
1993	9.055472	8.378259	1993	9.139481				
2000	5.085096	4.704807	2000	3.519678	2.752592	2000	12.22738	
2005	4.323468	4.000137	2005	2.526356	1.975756	2005	6.312934	4.290547
2014	3.73722	3.457732	2014	2.027376	1.585525	2014	3.796646	2.580367

N.5. References for Appendix N

Centers for Disease Control and Prevention. 2012. National Health and Nutrition Examination survey. Available at <http://www.cdc.gov/nchs/nhanes.htm>.

Datko-Williams, L et al 2014. Analysis of U.S. soil lead (Pb) studies from 1970 to 2012. Science of the Total Environment. 854-63 (468-469).

HUD 2011. American Healthy Homes Survey.

HUD, 2002. National Survey of Lead and Allergens in Homes. <http://www.niehs.nih.gov/research/atniehs/labs/lrb/enviro-cardio/studies/nslah/index.cfm>

U.S. Environmental Protection Agency (U.S. EPA). 2010c. Air Quality System (AQS) Database. Available online at: <http://www.epa.gov/ttn/airs/airsaqs/aqsweb/aqswebwarning.htm>.

USGS 2011. Background soil survey. Available online at <http://www.epa.gov/superfund/lead/background.htm#background>

Westat. 2003. First National Environmental Health Survey of Child Care Centers. Final Report, Rockville, MD, www.hud.gov/offices/lead/techstudies/survey.cfm.

Appendix O. Population Biokinetic Variability

In the Approach, numerous variables are sampled in order to capture the expected range in the U.S. population. However, the biokinetic parameters in the Leggett model (e.g., transfer rates from blood to bone and total mass of bone) are not sampled. Data are not available in the literature to accurately develop distributions of these parameters for the U.S. population.

Instead, biokinetic variability is included after the blood lead is estimated from the Leggett model. This modeled blood lead is treated as a central tendency estimate (geometric mean), and a population-level geometric standard deviation (GSD) is assigned. Then, the lognormal distribution defined by the geometric mean Leggett blood lead prediction and GSD is sampled twenty five times to estimate the variability in the blood lead arising from biokinetic variability.

To determine the appropriate GSD to use, several factors were considered. The NHANES survey represents the most nationally-representative survey of blood lead across all age groups (CDC, 2012). Table O-1 shows the GSD estimated for each NHANES survey since the year 2000. The GSD values are consistent across the different surveys in spite of an overall decrease in blood lead over this period. For the Approach, a value of 1.9 was selected. The NHANES GSD represents variability associated with both the biokinetic differences in individuals as well as their differences in environmental media concentrations and intakes. For that reason, the lower of the two GSDs represented in NHANES was selected to represent the biokinetic variability.

Table O-1. NHANES Survey Population-level Blood Lead Geometric Standard Deviations

NHANES Survey Year	Population GSD
1999-2000	1.9
2001-2002	2.0
2003-2004	1.9
2005-2006	1.9
2007-2008	1.9
2009-2010	1.9
2011-2012	2.0

The selected GSD is larger than the recommended agency default in the IEUBK model (1.6). The IEUBK model is intended for use at contaminated sites, where the exposed population may be more

homogeneous. (US EPA 2010) NHANES is expected to give the best national-level estimate of the population-level GSD, so these values were preferred over the IEUBK default value.

O.1. References for Appendix O

Centers for Disease Control and Prevention. 2012. National Health and Nutrition Examination survey. Available at <http://www.cdc.gov/nchs/nhanes.htm>.

U.S. Environmental Protection Agency (U.S. EPA). 2010. Integrated Exposure Uptake Biokinetic Model for Lead in Children, IEUBKwin version 1.1, build 264. <http://www.epa.gov/superfund/health/contaminants/lead/products.htm#ieubk>.

Appendix P. Concentration-Response Curves Supporting Information

P.1. IQ (Lanphear et al. (2005) Pooled Analysis)

Lanphear et al. (2005) reported the results of seven studies that measured full-scale IQ in school age children (mean age at IQ testing was 6.9 years) in four U.S. cities (Boston, Cincinnati, Cleveland, and Rochester), as well as in Australia, Mexico, and Yugoslavia. All children were assessed using age-appropriate versions of the Wechsler scales. Four measures of lead exposure were examined: concurrent blood lead (PbB closest in time to the IQ test), maximum blood lead level (highest PbB measured at any time prior to the IQ test), average lifetime blood lead (time-weighted mean PbB incorporating the results of all blood lead measurements from 6 months to the concurrent sample), and early childhood blood average (mean PbB across all samples taken between ages 6 to 24 months). A pooled analysis of the relationship between cord blood lead levels and IQ also was conducted in the subsample for which cord blood samples were available.

Lanphear et al. explored regression models that adjusted for the effect of blood lead for site, as well as 10 common potential confounders. These included HOME Inventory scores, birth weight, maternal education and IQ, and prenatal substance abuse. Statistical testing was employed to assess the linearity or nonlinearity of the relationship between blood lead levels and FSIQ. Regression diagnostics also were performed to ascertain whether lead coefficients were affected by co-linearity or influential observations. The fits of all four measures of postnatal blood lead levels were compared based on R^2 values. The blood lead measure with the largest R^2 (adjusted for the same covariates) was nominated *a priori* as the preferred blood lead index relating lead exposure to IQ in subsequent inspections of the relationships. The primary analysis used a fixed-effects model, although a mixed model treating sites as random effects was also examined.

The median lifetime average blood Pb concentration in the seven cohorts that were studied was 12.4 $\mu\text{g}/\text{dL}$ (5th to 95th percentile, 4.1 to 34.8 $\mu\text{g}/\text{dL}$), with about 18 percent of the children having peak blood Pb levels below 10 $\mu\text{g}/\text{dL}$. The 5th to 95th percentile concurrent blood Pb levels ranged from 2.4 to 30 $\mu\text{g}/\text{dL}$. The mean IQ of all children was 93.2 [Standard Deviation (SD) 19.2] but this varied greatly between studies. All four measures of postnatal exposure were highly correlated. However, the concurrent blood Pb level exhibited the strongest association with IQ, as estimated by R^2 . Nevertheless, the results of the regression analyses for all blood Pb measures were very similar. The best-fitting model included the log of concurrent blood Pb, study site, maternal IQ, HOME Inventory scores, birth

weight, and maternal education. No significant interactions were observed between PbB and study site or other covariates.

Various models, including a linear model, a cubic spline function, a log-linear model, and a piecewise linear model, were investigated in Lanphear et al. (2005). The shape of the concentration-response relationship was determined to be non-linear; the log-linear model was found to best fit to the data, based on R² values. Using the log-linear models, the authors estimated a decrement of 1.9 points (95 percent CI: 1.2, 2.6) in FSIQ for a doubling of concurrent blood lead. Thus, the IQ point decrements associated with an increase in blood lead from below 1 to 10 µg/dL compared to 10 to 20 µg/dL were 6.2 points (95 percent CI: 3.8, 8.6) versus 1.9 points (95 percent CI: 1.2, 2.6). The individual effect estimates for the seven studies used in the pooled analysis also generally indicate steeper slopes in studies with lower blood lead levels compared to those with higher blood lead.

Table P-1. Log-Linear Regression Coefficients Estimated by Lanphear et al. (2005) and Recalculated by Crump et al. (2013)

Blood Lead Metric	Lanphear et al. (2005)	Crump et al. (2013) Estimates Derived Using Corrected Data
Early Life	-2.04 (-3.27, -0.81)	-2.21 (-3.38, -1.03)
Peak	-2.85 (-4.1, -1.6)	-2.86 (-4.10, -1.61)
Lifetime	-3.04 (-4.33, -1.75)	-3.19 (-4.45, -1.94)
Concurrent	-2.70 (-3.74, -1.66)	-2.65 (-3.69, -1.61) ¹

Lanphear et al. also estimated piecewise linear models relating the concurrent blood lead to IQ changes above and below “cutpoints” of 7.5 and 10 µg/dL. They found that the coefficients for IQ change below and above 7.5 µg/dL (-2.95 and -0.16, respectively) were both significantly negative and significantly different from one another (p = 0.015.) The coefficients for concurrent PbB below and above 10 µg/dL PbB were also reported to both be significantly negative (-0.80 and -0.13) but not significantly different from one another (p = 0.103.)

P.2. IQ (Crump et al. (2013) Reanalysis of Lanphear et al. Data)

Crump et al. (2013) subsequently obtained the raw data set supporting the Lanphear et al. pooled analysis, attempted to replicate the results of the original study, and sought to identify problems with the data and statistical methods that were used to analyze them, and to “evaluate the robustness of their conclusions.”

In their analysis, Crump et al. implemented several adjustments to the treatment of the data:

- They developed a revised site-specific scheme for linking specific blood lead sampling rounds to specific IQ measurements.
- Derived time-weighted average blood lead metrics to substitute for the unweighted metrics used by Lanphear et al., and added PbB measurements at 24 months into the calculation of the averages.
- Corrected the equation used in the log transformation of blood lead data from the Boston cohort.
- Substituted the McCarthy Scales of Children's Abilities General Cognitive Index measured at 57 months for the Wexler full-scale IQ at 120 months that had been used as the "concurrent" IQ measure for blood lead measured in the Boston cohort at 57 months (see Section 7.3.1.) For all other groups, Wexler full-scale IQ measurements were selected.
- Identified IQ measurement in 10 children from the Mexican Cohort where the closest "concurrent" measurement was at age 78 months rather than 72 months.

Crump et al. then attempted to replicate the earlier regression estimates derived by Lanphear et al., using the original data and the data that had been "corrected" based on the adjustments noted above. When estimating the log-linear models, they obtained the same results as seen in the earlier analysis. When models were fit to the "corrected" data (adjusted as described above), they obtained slightly different coefficient values from those derived Lanphear et al. (Table P-1), but the differences in coefficients were not significant, and the basic results of the analysis (negative and highly significant log-linear coefficients in the range from -2.2 to -3.2 for all blood lead metrics) were unchanged.

Crump et al. also estimated piecewise regressions for concurrent PbB values above and below the 7.5 and 10 ug/dL cutoff values. For these models, they obtained different results from the earlier analysis. Their slope coefficient for PbB < 7.5 ug/dL (2.54 IQ points/dL) was slightly smaller than that estimated by Lanphear et al. (-2.94), but both estimates were significantly less than zero. The estimated slope coefficient above 7.5 ug/dL (-0.15 ug/dL) was very close to that estimated by Lanphear (-0.16), and confidence intervals indicated that both values were significantly negative.

Crump et al. found that the piecewise linear regression coefficient for subjects with concurrent blood lead levels below 10 µg/dL were not significant, in contrast to the results reported by Lanphear et al., and that the difference between slope coefficients for subjects above and below this cutoff was likewise not significant. Using the "corrected" data, they estimated a blood lead-IQ slope of -1.06 (C.I. = 2.25, 0.118) below 10 µg/dL, compared to Lanphear et al.'s original -0.88 (C.I. = -2.13, 0.38.) While the value from the revised analysis becomes more negative, the confidence interval still includes zero; Crump et al. calculated a marginally significant p-value of 0.078.

Crump et al. also experimented with different cutpoints (i.e., the blood lead at which the slope of the IQ-blood lead relationship changes) and blood lead metrics in an attempt to identify the lowest blood lead concentrations at which slope coefficients retained significance. They found a generally consistent pattern of most slope coefficients remaining negative down to the lowest cutoff point analyzed (2 µg/dL.) However, the coefficients for blood lead cutoffs less than 5-7 µg/dL lost statistical significance, consistent with the decreasing numbers of subjects involved.

Crump et al. indicated “Although we found some small errors and questionable decisions by Lanphear et al. that, taken alone, could cause doubt in their conclusions, our reanalysis tended to support their conclusions. We concluded that there was statistical evidence that the exposure-response is non-linear over the full range of BPb evaluated in these studies, which implies that, for a given increase in blood lead, the associated IQ decrement is greater at lower BPb levels.” They noted, however, after fitting piecewise models to the various blood lead metrics, that the IQ loss could be “adequately modeled” at PbB levels less than 10 ug/dL. In addition, they concluded that the evidence support the existence of exposure-response relationship for IQ loss at peak PbB values as low as 7 ug/dL, and for concurrent PbB at 5 ug/dL. As noted above, however, these latter conclusions were based on linear regressions incorporating only small proportions of the data, and thus had less power to detect significant relationships.

As noted in Section 6.3, after reviewing the Crump et al. (2013) reanalysis of the Lanphear et al. (2005) study, EPA is retaining the basic log-linear regression approach to the prediction of IQ loss after renovation, while using the revised regression coefficients calculated by Crump et al.

P.3. IQ (Budtz-Jørgensen et al. (2013) Estimation of BMDs and BMDLs)

Budtz-Jørgensen et al. (2013) estimated blood lead-IQ relationships from the Lanphear et al. (2005) data using a set of linear mixed models of the general form:

$$IQ_{ij} = \alpha_j - f(d_{i,j}) + \gamma^1 x^1_{i,j} + \dots + \gamma^p x^p_{i,j} + \varepsilon_{ij}$$

This approach allows for the intercept of the model (α_j) to vary across the studies, whereas the effects of covariates (γ^1 - γ^p) are assumed to be constant across the studies. The expression $f(d_{i,j})$ captures the form of the blood lead-IQ dependence; both linear and log-linear transformations were used. It is not clear to what extent the form of the models used in this analysis differed from those used in the Lanphear 2005 study; the covariates were the same and there was no discussion of whether the problems with the data identified by Crump et al. were addressed.

An important difference from the previous analysis was that likelihood methods (rather than linear regression) were used to optimize the models. This allowed relative goodness of fits and model parsimony to be compared using differences in AIC (Akaike Information Criteria.) Another important difference was that Budtz-Jørgensen et al. applied the results of their models to derive BMD and BMDL estimates for a change of 1.0 IQ points for each blood lead metric. They also employed the “hybrid method” to estimate BMD and BMDL values for changes of 1, 2.5, and 5 percent changes in IQ assuming a background incidence of 5 percent. Finally, they compared the fits of linear and log-linear models (using AIC values), as well as estimating the same piecewise linear models (cutoffs at 10 and 7.5 $\mu\text{g}/\text{dL}$) fitted in the original analysis.

For concurrent blood lead, the log-linear model again provided a superior fit to both the linear and breakpoint models (lower AIC value.) For the other blood lead metrics, the log-linear model provided superior fits to the linear models and comparable or slightly inferior fits to data in the low-exposure range (below the cutoffs.) The BMD values for a 1.0 point change in IQ score derived from the log-linear models for different blood lead metrics fell into a relatively narrow range (0.355-0.558 $\mu\text{g}/\text{dL}$), and the BMDLs ranged from 0.260 to 0.343 $\mu\text{g}/\text{dL}$. The lowest values were estimated from concurrent blood lead and the highest for early childhood blood lead concentrations. BMDs/ BMDLs for piecewise linear models with breakpoints at 7.5 $\mu\text{g}/\text{dL}$ ranged from 0.712/0.434 $\mu\text{g}/\text{dL}$ for peak blood lead to 1.647/0.980 $\mu\text{g}/\text{dL}$ for concurrent lead. BMDs/ BMDLs for models with breakpoints at 10 $\mu\text{g}/\text{dL}$ are somewhat higher ranging from 1.034/0.689 (concurrent) to 3.769/1.610 (early childhood.)

EPA has decided not to employ the Budtz-Jørgensen et al. results in estimating IQ loss associated with renovation, for several reasons. First, use of the continuous regression models from the Lanphear/Crump et al. analysis does not require that selection of a cutoff value for reduced IQ and will produce a continuous distribution of IQ loss as a function of exposure. In contrast, the Budtz-Jørgensen BMDs and BMDLs are calculated for specified values of IQ loss (1 point, 1 percent, etc.), so the output of a risk assessment using these values would be an estimate of what proportion of the exposed population exceeds the selected cutoff values. EPA believes that the regression approach will provide more useful information about the distribution of outcomes (predicted IQ changes) than would be obtainable using the BMDs/BMDLs from the Budtz-Jørgensen et al. study without considerable adaptation. In addition, the Lanphear et al. (2005) and Crump et al. (2013) analyses directly provide well-documented regression coefficients that have been subject to extensive quality assurance and peer review, while the equations and model fits from the Budtz-Jørgensen et al. study have not been made publically available and would require independent review by EPA scientists for use in regulatory analysis. Finally, many of the BMDL values estimated by Budtz-Jørgensen et al. are less than 1 $\mu\text{g}/\text{dL}$,

and EPA is reluctant to predict risks in this range because there are so few observations below 1 ug/dL in the Lanphear et al. data set.

P.4. Estimation of Birthweight Reductions from Zhu et al. (2010) Model

As discussed in Section 6.4, Zhu et al. (2010) tested a number of fractional polynomial models relating observed variations in birthweight to maternal blood lead concentrations and multiple covariates, including gestational age, maternal age, race, Hispanic ethnicity, education, smoking, alcohol drinking, drug abuse, in wedlock, participation in special financial assistant program, parity, infant sex, and timing of the blood lead test relative to birth. They found that a model incorporating a square root transformation of maternal blood lead provided the best fit to the data. While they did not provide the coefficients and standard errors for their model, the article includes estimates of the mean and 95% upper and lower confidence limits on the predicted body weight reductions at blood lead concentrations up to 10 ug/dL (Table P-2).

Table P-2. Predicted Birthweight Reductions Based on Fractional Polynomial Model from Zhu et al. (2010)

PbB	BWR (gms)	95% UCL	95% LCL	Mean-LCL	UCL-Mean	Effective Std. Dev. ¹
0	--	--	--	--	--	--
1	-27.4	-17.1	-37.8	10.4	10.3	5.28
2	-38.8	-24.1	-53.4	14.6	14.7	7.47
3	-47.5	-29.6	-65.4	17.9	17.9	9.13
4	-54.8	-34.2	-75.5	20.7	20.6	10.54
5	-61.3	-38.2	-84.4	23.1	23.1	11.79
6	-67.2	-41.8	-92.5	25.3	25.4	12.93
7	-72.5	-45.2	-99.9	27.4	27.3	13.95
8	-77.6	-48.3	-106.8	29.2	29.3	14.92
9	-82.3	-51.2	-113.3	31.0	31.1	15.84
10	-86.7	-54.0	-119.4	32.7	32.7	16.68

¹. Estimated as (UCL-LCL)/3.92, assuming normal distribution

As shown in Figure P-1, the projected change in birthweight is linearly related to the square root PbB (this is inherent in the specified form of the model.) The slope of the relationship, as discussed in Section 7.4.1, is -27.4 grams per one unit change in the square root of maternal blood lead; this value is used in the estimation of mean change in body weight in Equation 7.1, repeated below.

$$\Delta BW = \Delta \text{sqrt}(PbB) * 27.4 + N(0, \Delta \text{sqrt}(PbB) * 5.28) \quad (7.1)$$

Variation in the predicted change around the mean was modeled as a normal distribution, based again on the inherent form of the Zhu et al. model, with an effective “standard deviation” modeled from the upper and lower confidence limits in Table P-2. It can be seen from the table that, at each PbB concentration, the confidence limits are symmetrical around the mean; assuming a normal distribution, and that the confidence limits are 1.96 standard deviations above and below the mean allows the estimation of the effective standard deviations as (UCL-LCL)/3.92, shown in the last column of Table P-2. As was the case for the mean birthweight reduction, the effective standard deviation also varies linearly with the square root of maternal PbB. As shown in Figure P-2, the slope of this relationship is 5.28 gm birthweight for each change of one unit in the square root of maternal PbB, this result provides the multiplicative coefficient used in the second term of Equation 7.1.

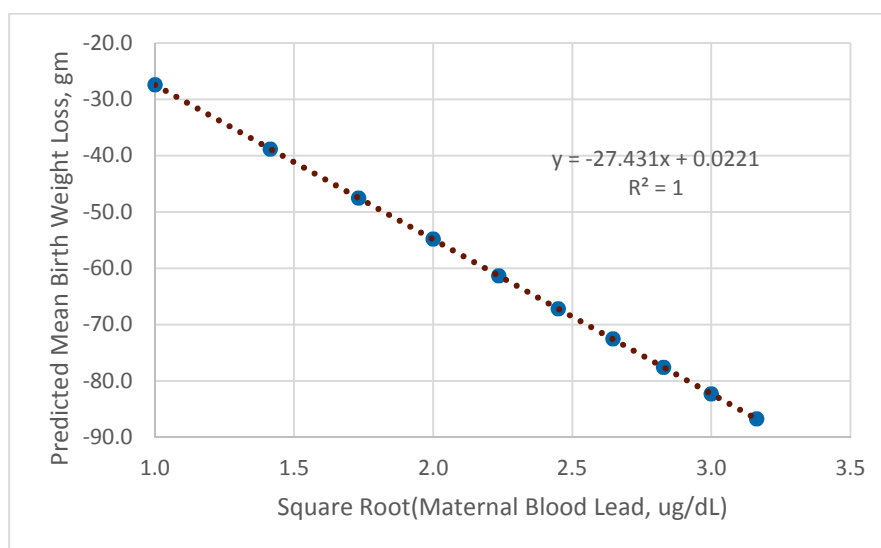


Figure P-1. Dependence of Predicted Mean Birth Weight Reduction on the Square Root of Maternal Blood Lead

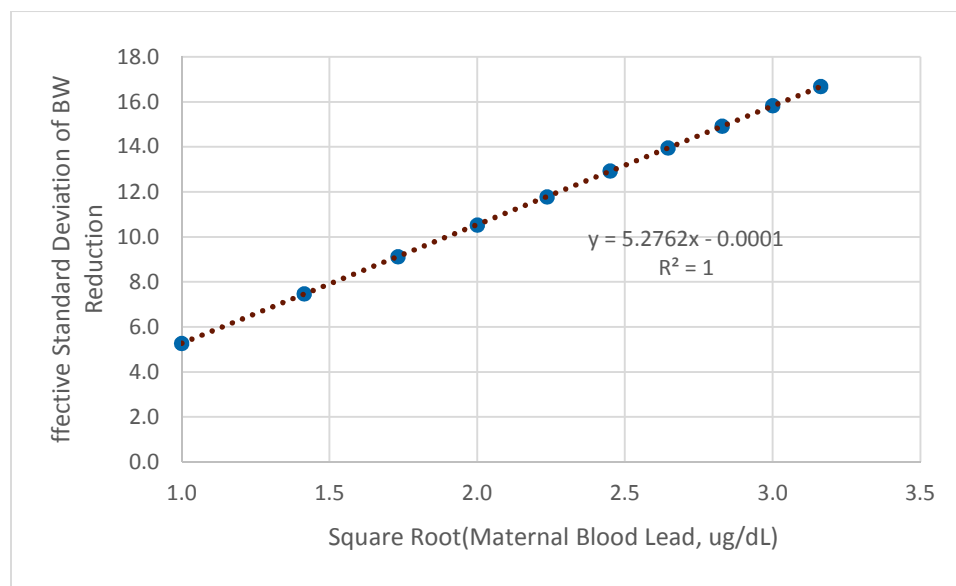


Figure P-2. Dependence of Variation in Prediction Birthweight Reduction on the Square Root of Maternal Blood Lead

Coefficients from the Zhu et al. model were estimated in models that included the large number of covariates listed above. Thus, the estimated changes in birthweight obtained using these coefficients reflect the observed characteristics of the study population, which may not precisely match the distribution of these characteristics of the pregnant population in the U.S. as a whole. By fixing the age distribution of the Monte Carlo model to be similar to that among the Zhu et al. study participants, that source of variation can at least be accounted for. The uncertainty associated with differences in distributions of the other covariates between the study population and the general U.S. population cannot be estimated directly.

P.5. Reduced Glomerular Filtration Rate (GFR) Based on Navas-Acien et al. (2009) Study

P.5.1. Estimation of Regression Coefficient and Standard Error

As discussed in Section 6.5, Navas-Acien et al. (2009) conducted an analysis of the relationship between risk of “category 3-5 kidney disease” (GFR < 60 ml/minute/1.73 M²) in a sample of almost 15,000 adult subjects from the 1999-2006 NHANES. In logistic regression models that included adjustments for a wide range of covariates (and for simultaneous exposures to cadmium), they found statistically significant elevations in the adjusted odds ratios (ORs) for low GFR in the upper quartile of the study population compared to the referent group, accompanied by a statistically significant positive trend in

OR across the quartiles. Using a model containing log-transformed blood lead as a continuous variable they estimated the odds ratios associated with an increase in PbB from 1.1 to 2.4 ug/dL (the 25th – 75th percentiles of the observed ranges, as shown in Table P-3. As discussed in Section 6.5, the models used to estimate the odds ratios also included urinary cadmium as a covariate, so the estimated association with lead exposure takes into account the effects on kidney function of simultaneous exposure to cadmium, which is also a known kidney toxin.

Table P-3. Navas-Acien et al. (2009) Regression Results, Estimated Coefficient Values, and Standard Errors

Gender-Specific Regression Results				
Group	PbB Range	OR	LCL	UCL
M	1.1-2.4	1.13	0.96	1.33
F	1.1-2.4	1.44	1.22	1.69
M+F	1.1-2.4	1.31	1.16	1.47

Because only the ORs were presented, it was necessary to back-calculate the β values and standard errors based on the ORs and changes in PbB, as illustrated in Table P-4.² Given the exponential form of the logistic regression, the β values for men and women can be estimated as $\ln(\text{OR})/\Delta\ln\text{PbB}$, where $\Delta\ln\text{PbB}$ is $\ln(2.4/1.1)$, the 75th/25th percentile blood lead values from the study.

Table P-4. Navas-Acien et al. (2009) Estimated β Values

Group	$\Delta\ln\text{PbB}$	$\ln(\text{RR})$	β
M	0.780	0.122	0.157
F	0.780	0.365	0.467
M+F	0.780	0.270	0.346

The standard errors were estimated for each of the coefficients based on the upper and lower confidence limits provided in the article as shown in

² The authors of study have been contacted to provide confirmation of the numerical derivations presented in this appendix.

Table P-5. Using a normal approximation (after confirming that the confidence limits were log-symmetrical), the standard errors were calculated as $\text{Standard Error} = \ln(\text{UCL/LCL}) / 3.92$. (The 95 percent upper and lower confidence limits are assumed to be 1.96 times larger or smaller than the estimated β values.) The standard errors were used to represent the variability in the β estimate as described below.

Table P-5. Estimation of Standard Errors Associated with the β Coefficients

Group	LCL	UCL	ln(UCL/LCL)	Std. Err.
Men	0.96	1.33	0.3260	0.083
Women	1.22	1.69	0.3259	0.083
Men+Women	1.16	1.47	0.2368	0.060

P.5.2. Estimation Low GFR Risk

As explained in Section 7.5, the absolute risk for a given individual in the Monte Carlo simulation was estimated to be:

$$LGFR = LGFR_0 * e^{(\beta+\varepsilon)*\Delta\ln PbB},$$

with $\Delta\ln PbB$ being the natural log of the ratio of the renovation and background blood lead estimates. As for birthweight, statistical uncertainty in the β variable was represented by adding an “ ε ” term, which takes the value of a normal distribution with a mean zero and standard deviation equal to the estimated standard errors from Table P-3. At each Monte Carlo iteration, an independent random sample is drawn from this distribution and added to the β estimate. As shown in the above equation, the risk of low GFR associated with renovation is calculated relative to background relative risks, which represent the average prevalences in different age groups and genders in the U.S. population. Background prevalence rates in the U.S. 2012 population provided by the Veterans Affairs Administration were obtained from the CDC (<http://nccd.cdc.gov/CKD/detail.aspx?QNum=Q391>) and are provided in Table P-6.

Table P-6. Prevalence of Chronic Kidney Disease (GFR <60 ml/minute/1.73 M²) in Adults, 2012 (percent)

Age	Female	Male
20-29 years	0.29	0.24
30-39 years	0.68	0.58
40-49 years	1.97	1.67
50-59 years	5.07	3.98
60-69 years	13.05	9.27
70+ years	25.6	21.06

P.6. Menke et al. (2006) Regression: Background Cardiovascular Mortality Risks

The risk of cardiovascular disease mortality will be estimated, as discussed in Section 6.6 and in US EPA 2014c as:

$$CVDM_{a,g} = CVDM_{0,a,g} * e^{(\beta+\varepsilon)*\Delta \ln PbB}$$

The exponential term on the right-hand side of the equation calculates the hazard ratio for a simulated subject of a given age and gender, while $CVDM_{0,a,g}$ represents that age- and gender-specific background risk of CVD mortality in the U.S. population. Values for $CVDM_{0,a,g}$ have been obtained from CDC-curated data (Centers for Disease Control 2010), as shown in Table P-7.

Table P-7. Background Cardiovascular Mortality Risks for the U.S. Population (CDC 2010)

Age (years)	Gender	Annual CVD Mortality
50-59	M	2.20E-03
	F	9.40E-04
60-69	M	4.60E-03
	F	2.30E-03
70-80	M	1.20E-02
	F	7.60E-03

P.7. References for Appendix P

Budtz-Jørgensen E, Bellinger D, Lanphear B, Grandjean P. (2013). An international pooled analysis for obtaining a benchmark dose for environmental lead exposure in children. *Risk Anal.* 2013;33:450–61.

Crump et al (2013). A statistical reevaluation of the data used in the Lanphear et al. (2005) pooled-analysis that related low levels of blood lead to intellectual deficits in children. *Critical Review Toxicology.* October:43 (9): 785-99.

Lanphear BP, Hornung R, Khoury J, et al. (2005). Low-level environmental lead exposure and children's intellectual function: an international pooled analysis. *Environ Health Perspect*, 113, 894–9.

Menke et al (2006). Blood lead below 0.48 micromol/L (10 microg/dL) and mortality among US adults. *Circulation*. 114:1388–1394.

Navas-Acien et al (2009). Blood Cadmium and Lead and Chronic Kidney Disease in US Adults: A Joint Analysis. *Am. J. Epidemiol.* (2009) 170 (9): 1156-1164.

Zhu et al (2010). Maternal Low-Level Lead Exposure and Fetal Growth. *Environmental Health Perspectives*. Volume 118. Number 10.

Appendix Q. Approach to estimate universe of P&CBs

National data on the universe of P&CBs and their spatial relationships both to each other and to residential buildings is limited. Due to this limitation, methods were developed to estimate the universe of P&CBs in the United States. These estimates were developed using the 2011 Maryland Department of Planning (MDP) MDProperty View dataset (MDP 2011). This appendix presents estimates for the number of P&CBs, as well as supplemental information about building types, and distances between P&CBs and all other building types.

The analysis used four general different building type categories: (1) agricultural, (2) commercial, (3) government, and (4) industrial. Agricultural, commercial, and industrial buildings generally included all buildings with the corresponding zoning designations on parcels that were not government owned. Government buildings generally included all buildings on government owned parcels that were zoned commercial or industrial.

Results are disaggregated according to the distance between a P&CB and other building categories, including residences. The distance categories considered in this analysis correspond to distances modeled and described in Section 3 of the Approach document. The universe of P&CBs and proximity analysis presents estimates of the number of residences located near P&CBs, and estimates of the number of non-residential buildings located near P&CBs.

There are no publically available sources of information on the national number of buildings for properties that are zoned industrial or agricultural. However, the U.S. Department of Energy's 2003 Commercial Building Energy Consumption Survey (CBECS) includes national estimates for the number of commercial buildings (DOE 2008). In addition, historical and current data on the national amount of commercial floor space are available from the U.S. Department of Energy, so these data are used to validate the corresponding estimates derived from the MDProperty View data.

The MDP (2011) data are particularly useful because they include geographical information (latitude and longitude coordinates) for each property. Therefore, these data can be used to estimate three critical elements of the analysis related to the proximity of P&CBs to residences and other P&CBs:

- (1) the number of buildings with at least one residence within a given distance from PnCBs,
- (2) the number of residences near PnCBs, and
- 3) the number of other PnCBs near PnCBs.

The MDP data have geographic and property information collected by the State Department of Assessments and Taxation (SDAT) for 2.2 million parcels in the state of Maryland, including parcel ownership and address information, and basic details about the parcel and structures associated with it. While the database does not contain information on the number of buildings on a parcel, it tracks other information that may indicate whether buildings may be present on the parcel.

The approach grouped the parcels into categories and then visually inspected a random sample of parcels. This visual inspection was used to estimate the average number of parcels with buildings and the average number of P&CBs per parcel. The number of P&CBs in Maryland was then calculated as the sum of the product of the number of parcels with buildings and the average number of P&CBs per parcel across the different parcel categories. National estimates are then extrapolated from the Maryland estimates based on the ratios of the total number of employer establishments in the United States to the total number in Maryland for the industries comprising the four building categories included in the analysis.

The number of buildings per parcel is not included in the MDProperty View dataset. Therefore, a random sample of parcels was drawn for each parcel type and the satellite images of the sampled parcels were visually examined using ArcGIS to identify the number of buildings on the parcel. The visual examination was complicated by the fact that parcel boundaries were not clearly delineated (parcels were denoted by centroids - single points representing the parcel's geometric center) and some parcels were obscured by tree cover or fuzzy satellite imagery. Best judgment was used to determine the parcel's boundaries, (e.g., physical landmarks, comparison of the parcel's acreage data to area measured by ArcGIS measurement tool, etc.), and the number of buildings on the parcel (cross-referencing with Google Maps). The methods used to estimate the average number of P&CBs per parcel varied for the different types of parcels. Another limitation of the analysis is the assumption that the Maryland data are representative of the number of buildings per parcel nationally.

For commercial, government, and industrial parcels, the average number of buildings per parcel was estimated by examining a sample of randomly selected parcels with buildings in each building category. Agricultural parcels were grouped into 1 of 13 size categories. Approximately 10 parcels were randomly selected for each size-residence category, with the exception of some of the smallest and largest size-

residence categories which had fewer than 10 parcels. The averages from the agricultural sample were then weighted by the proportion of parcels with buildings in each size-residence category.

The first building on an agricultural parcel with a residence is assumed to be the residence and all other buildings on that parcel are assumed to be agricultural buildings – only the agricultural buildings are included in the analysis since residential buildings are already regulated under the residential provisions of the LRRP program. For parcels with mixed commercial and residential use, it is assumed that all buildings are P&CBs. Buildings that were mixed-use were also identified. For example, a two story building with retail space on the first floor and apartments on the second floor.

The number of P&CBs in Maryland is estimated as the product of the total number of parcels with at least one building and the average number of buildings per parcel. National estimates are then extrapolated from the estimates for Maryland using the ratio of national employer establishments in the affected sectors to employer establishments in Maryland. Note that while other indicators could be used to extrapolate from Maryland to the U.S. (e.g., population, output, all employer and non-employer establishments), an important advantage of using employer establishments is that these data are available at the Zip Code level.

This allows for estimating the number of buildings by Zip Code, where the number of buildings can be combined with estimates for the proximity of the buildings to housing units. Note that the ratio of Maryland to U.S. commercial establishments was used to extrapolate from Maryland government P&CBs to the national number of P&CBs. This ratio is used because nearly all government parcels are zoned as commercial. It is also worth noting that the Maryland to United States ratio for both commercial establishments and population are both 1.87% (U.S. Census Bureau 2011a).

As indicated in Table O-1, there are an estimated 15.7 million P&CBs in the United States. Agricultural buildings account for approximately 50.3 percent (7.9 million) of the total, commercial buildings account for 28.4 percent (4.4 million), government buildings account for 6.0 percent (0.9 million), and industrial buildings account for 15.3 percent (2.4 million).

The steps used to combine the MDP data with Census data to develop national estimates of the proximity between P&CBs and residences are summarized as follows:

1. Use decennial Census data to group ZIP Code Tabulation Areas (ZCTAs) into *ZIP Code Groups*, so we can match those areas outside of Maryland with areas in Maryland that are likely to be similar in terms of the proximity between P&CBs and residences.
2. Use the MDP data to estimate the proximity of P&CBs to residences and other P&CBs within each Maryland ZIP Code Group.
3. Use Census County Business Patterns data compiled by ZIP Code on employer establishments to assign a weight to each Maryland ZIP Code Group, so that
4. Extrapolate from the Maryland data to national estimates for the parameters listed above.
5. Estimate the national parameters for proximity between P&CBs, residences, and other P&CBs as the weighted average of these parameters for the Maryland ZIP Code Groups.

Table O-1: Estimated Universe of P&CBs in Maryland and the United States

Building Category ¹	Ind. For Dwellings ^{2,3}	Structure Square Footage Reported	Class Code ⁴	Maryland				National		
				Total Parcels with P&CBs	P&CBs Per Parcel ⁵	Total Number of P&CBs	Number of Establish. ⁵	Number of Establish. ⁶	Ratio of MD to U.S. ⁶	Estimated Number of P&CBs
Agricultural	Yes	-	-	17,086	3.3	56,384	192	21,679	0.886%	6,363,883
	No	-	-	5,830	2.3	13,409				1,513,431
	<i>Subtotal</i>			22,916	3.0	69,793				7,877,314
Commercial	Yes	-	-	3,003	1.3	3,904	131,721	7,041,758	1.871%	208,658
	No	Yes	-	43,701		56,811				3,036,398
	-	No	-	17,174		22,326				1,193,266
	<i>Subtotal</i>			63,878		83,041				4,438,322
Government	-	Yes	-	2,888	1.4	4,043	-	-		216,088
	No	Yes	-	6,782		9,495				507,483
	-	-	Park/Rec	1,408		1,971				105,345
	-	-	Public Works	1,525		2,135				114,110
	<i>Subtotal</i>			12,603		17,644				943,026
Industrial	-	Yes	-	11,962	1.6	19,139	3,506	353,143	0.993%	1,927,392
	-	No	-	2,937		4,699				473,212
	<i>Subtotal</i>			14,899		23,838				2,400,604
Total				114,296		194,316				15,659,266

Notes: 1. The “Agricultural” land use category used in the Maryland database includes some parcels that would be considered residential under the LRRP program. To account for this, the agricultural parcel counts have been adjusted by 66.5 percent to account for the difference between the total area of farmland in Maryland according to the Census of Agriculture (2,051,756 acres) and the total area of the parcels classified as agricultural in the Maryland dataset (3,084,052 acres).

2. Agricultural and commercial parcels were broken out by whether they contain residential structures because these structures are already covered under the LRRP program under the residential rule. There were only three industrial parcels with records indicating there were residential structures and all of them appear to be categorized incorrectly. Thus, industrial parcel counts are not broken out by the presence of residential dwellings.

3. A parcel is assumed to have a residence if it has a nonzero value in the total number of dwellings field.

4. Class codes provide detail on the parcel’s ownership type (public, state, private, etc.) and use (hospital, park, school). Parcels without housing and/or building data were grouped by class code and examined separately. Government parcels in the (1) Parks and Recreation and (2) Public Works class codes were identified as potentially different from other parcel types with respect to the likelihood of having a building on the parcel.

5. Estimated from a sample of parcels that were visually inspected to obtain information not contained in the original MDP dataset. See Appendix 1 for a description of how these parameters were estimated and the estimated confidence intervals.

6. “Agricultural” establishments include those from NAICS 11; “Commercial” establishments include those from NAICS 23, 42, 44, 48, 51, 52, 53, 54, 55, 56, 61, 62, 71, 72, and 81; “Industrial” establishments include those from NAICS “21, 22, and 31.

Sources: MDP 2011, USDA 2009, U.S. Census Bureau 2011a, b

Q.1. References for Appendix Q

Maryland Department of Planning and Maryland State Department of Assessments and Taxation (MDP). 2011. *MdProperty View 2011 Edition*. Maryland Department of Planning is the owner of the MDProperty View Product, parcel x,y reference points, property maps and land use/land cover data. Maryland State Department of Assessments and Taxation owns the parcel dataset records in the MdProperty View Product.

U.S. Census Bureau. 2011a. *2010 Census of Population and Housing Summary Files for All States (Machine Readable Files)*.

U.S. Department of Energy (U.S. DOE). 2008. *2003 Commercial Buildings Energy Consumption Survey: Public Use Microdata Files*.